

# รายงานวิจัยฉบับสมบูรณ์

โครงการลำไอออนพลังงานต่ำกับงานทางด้านเทคโนโลยีชีวภาพ Low Energy Ion Beam in Biotechnology

โดย ศาสตราจารย์ ดร. ถิรพัฒน์ วิลัยทอง และคณะ

## รายงานวิจัยฉบับสมบูรณ์

# โครงการถำไอออนพลังงานต่ำกับงานทางด้านเทคโนโลยีชีวภาพ Low Energy Ion Beam in Biotechnology

ศาสตราจารย์ คร. ถึงพัฒน์ วิลัยทอง

Dr. Yu Liangdeng

รองศาสตราจารย์ คร. สมบูรณ์ อนันตลาโภชัย
รองศาสตราจารย์ คร. อดิศร กระแสชัย

ภาควิชาฟิสิกส์ คณะวิทยาศาสตร์ มหาวิทยาลัยเชียงใหม่ ภาควิชาฟิสิกส์ คณะวิทยาศาสตร์ มหาวิทยาลัยเชียงใหม่ ภาควิชาชีววิทยา คณะวิทยาศาสตร์ มหาวิทยาลัยเชียงใหม่ และคณะ ภาควิชาพืชสวน คณะวิทยาศาสตร์ มหาวิทยาลัยเชียงใหม่ และคณะ

#### กิตติกรรมประกาศ

งานวิจัยที่ได้ดำเนินการภายใต้ทุนส่งเสริมกลุ่มวิจัยนี้ เป็นผลงานที่ได้ทำร่วมกันระหว่าง
บุคลากรในแขนงวิชาต่างๆ ได้แก่ ฟิสิกส์ วิศวกรรม วัสคุศาสตร์ ชีววิทยา พืชสวน ทั้งในและนอก
ประเทศมีบุคลลที่เกี่ยวข้องโดยตรงหลายสิบคนทุกระดับชั้น มืองค์กรหลายองค์กรทั้งในและนอก
ประเทศที่มีส่วนสนับสนุนการดำเนินงานในส่วนต่างๆ ทำให้ "เรา" ได้ความรู้อีกระดับหนึ่งและได้
ก้าวสู่อนาคตอีกก้าวหนึ่ง อย่างมั่นคง

โครงการนี้จึงขอบันทึกถึงบุคคลและองค์กรต่างๆ ไว้ค้วยความขอบคุณยิ่ง

Dr. Ian G. Brown แห่ง Lawrence Berkeley National Laboratory (LBNL) ที่ได้ช่วยดูแล โครงการนี้ตั้งแต่ต้นจนจบ รวมทั้งกำกับดูแลการทดลองระดมยิงเซลล์พืชที่ LBNL ทำให้เราได้ ภาพถ่าย AFM ของเซลล์ที่ถูกระดมยิงด้วยไอออนเป็นภาพแรกๆ ของโลก

Dr. I. Ratera, Dr. D. F. Ogletree และ Dr. O. R. Monteiro แห่ง Lawrence Berkeley National Laboratory ที่ได้ให้คำแนะนำและฝึกบุคลากรของเราในการถ่ายภาพด้วยกล้อง AFM รวมถึง การถ่ายและประมวลภาพ AFM ของเซลล์หลังจากถูกระคมยิงด้วยไอออนมวลหนัก ทำให้เราได้ ภาพถ่ายที่ยอดเยี่ยมที่สุด

ผู้ช่วยศาสตราจารย์ คร. รัตติกร ยิ้มนิรัญ แห่งภาควิชาฟิสิกส์ มหาวิทยาลัยเชียงใหม่ที่ได้ กรุณาให้คำแนะนำการออกแบบติคตั้งระบบกันกระเทือนของกล้อง AFM ที่ติคตั้งในแชมเบอร์ สุญญากาศ

- คร. พิศิษฐ์ สิงห์ใจ แห่งภาควิชาฟิสิกส์ มหาวิทยาลัยเชียงใหม่ ที่ได้ให้คำแนะนำในการใช้ งานกล้อง AFM อย่างต่อเนื่อง
- คร. วรรณจันทร์ แสงหิรัญ ถี และ คร. ปียะรัตน์ นิมมานพิภักดิ์ แห่งภาควิชาเคมี มหาวิทยาลัยเชียงใหม่ ที่ได้สละเวลาให้คำแนะนำบุคลากรของเราได้เรียนรู้เทคนิคการคำนวนแบบ molecular dynamics ในการจำลองการระคมยิงผนังเซลล์ด้วยลำไอออนมวลหนัก

กุณสมกิด แช่นั่ง และบริษัทพาราวินเซอร์ จำกัด ที่ได้กรุณาดูแลการซ่อมเครื่อง AFM จน สามารถใช้งานได้ ทำให้เราสามารถถ่ายภาพ AFM ของเซลล์ที่ถูกระคมยิงด้วยลำไอออนภายในห้อง สญญากาศได้เป็นแห่งแรกๆ ของโลก

Prof. Zengliang Yu แห่ง Key Laboratory for Ion Bioengineering, Hefei ที่ได้ให้ข้อมูล เบื้องค้นเกี่ยวกับการปรับปรุงพันธุ์ข้าวในประเทศจีนโดยใช้ลำไอออน และได้เอื้อเฟื้อให้เราแปล หนังสือชื่อ Introduction to Ion Beam Biotechnology จากภาษาจีนเป็นภาษาอังกฤษ

ศูนย์เทคโนโลยีโลหะและวัสคุแห่งชาติ ที่ได้ให้ทุนสนับสนุนการคำเนินงานของหน่วย เทคโนโลยีไอออนบีมอย่างต่อเนื่อง ทำให้เราสามารถเดินเครื่องยิงไอออนชนิคต่างๆ ได้ตลอดทั้งปี International Program in Physical Science ที่ได้สนับสนุนเราอย่างต่อเนื่องตลอดระยะเวลา สองปีที่ผ่านมา รวมทั้งได้สนับสนุนการจัดสัมมนาเชิงปฏิบัติการนานาชาติ PIM04 ที่เชียงใหม่

เราขอขอบคุณสำนักงานกองทุนสนับสนุนการวิจัย (สกว.) ที่ได้จัดสรรทุนปริญญาเอก กาญจนาภิเษก สำหรับนักศึกษาในโครงการ 1 คน ทำให้เธอสำเร็จปริญญาเอกอย่างเต็มภาคภูมิ และ งานของเราในส่วนงานวิจัยพื้นฐานก็เดินหน้าต่อไปอย่างมั่นคง ขอขอบคุณที่ได้จัดสรรทุนเมธีวิจัย อาวุโสให้แก่พวกเราเป็นครั้งที่สาม ทำให้เราเข้าใจอันตรกิริยาระหว่างไอออนกับเซลส์สิ่งมีชีวิตได้ดี ยิ่งขึ้น และสามารถประยุกต์แนวคิดพื้นฐานกับงานด้านการปรับปรุงพันธุ์พืชได้อย่างแยบยล

ท้ายสุคนี้ ค้วยความสำนึกในพระมหากรุณาธิคุณของสมเด็จพระบูรพกษัตริยาธิราชที่ทรงคล บันคาลให้เราได้ก้าวเดินอย่างสมศักดิ์ศรีอีกก้าวหนึ่งสู่อนาคต

#### **ABTRACT**

Project Code

: RTA4680016

Investigator

Professor Dr. Thiraphat Vilaithong Senior Thailand Research Fund Scholar

Fast Neutron Research Facility

Department of Physics Faculty of Science Chiang Mai University Chiang Mai 50200, Thailand

E-mail Address

thirapat@fnrf.science.cmu.ac.th

Project Period

3 years

Objectives

: To understand the fundamental mechanisms involved in ion

interaction with living organisms.

To apply low energy ion beam to induce mutation in Thai

jasmine rice and flower crops.

Methodology

Low energy bombardment of onion skin cells with both metallic and gaseous ion species, such as N, Ar, Mg, Ti, Fe, Ni, Cu at fluences of  $1 - 5 \times 10^{15}$  ions / cm<sup>2</sup> and energies of 25 - 30keV were carried out. A scanning electron microscope and atomic force microscope (AFM) were used to observe the microcrater structure. Three different computer codes that provide a simulation of ion penetration in matter TRIM, T-Dvn and PROFILE have been used to investigate the expected depth profiles for the case of Ti bombardment, and compare with the experimental RBS results. The work also included the design and installation of an in-situ AFM system to the beam line of our bioengineering ion implantation facility and ongoing relevant experiments. The molecular dynamic simulations of Fe ion bombardment of onion skin cell wall were carried out. Cellular I - Beta surface was used as a model material for the cell wall.

Seeds of Thai purple rice and jasmine rice (Oryza sativa incida var purple rice and KDML 105, respectively) were bombarded with nitrogen ions at fluence of 2 – 8 x 10<sup>16</sup> ions / cm<sup>2</sup> and energy of 60 keV number of rice mutants were obtained and characterized for 5 generations (MS). HAT – RAPD (high annealing temperature – RAPD) were used to determine genetic modification in the mutant genomes.

Rose, petunia and chrysanthemum were used in the studies of low energy ion beam induced mutation in flower crops. As for rose, nodal buds along the open flower stem were exposed to  $60 \, \text{keV}$  nitrogen ions at a fluence of  $1 \times 10^{16} \, \text{ions} / \, \text{cm}^2$ . In petunia, seeds were bombarded with  $60 \, \text{keV}$  nitrogen ions at fluences  $1 - 10 \times 10^{16} \, \text{ions} / \, \text{cm}^2$ . As for chrysanthemum, the variety Reagan Dark was used. The flower receptacle part was as optically precultured for 5 days to induce cell division before bombarding with  $60 \, \text{keV}$  nitrogen ions and culturing in-vitro again.

Results

Ex-situ and in-situ Atomic Force Microscopy revealed the formation of microcrater – like structures with rim dimension

typically several several hundred nanometers; we speculate that micrometers might provide channels for the transfer of exogenous macromolecules (such as DNA) through the cell wall into the cell interior. The RBS – measured implanted ion depth profile was compared to several computer simulations, and the similarities and difference seen can be interpreted as being due to severe sputtering of the cell wall material. The molecular dynamic calculations indicate that ion – bombarded cellulose molecules are broken into fragments by the collision, which fragments then initiate molecular collision cascades, leading to the ejection of intact molecules and molecular fragments from the surface.

Five ion bombarded KDML 105 rice mutants were obtained and characterized for 5 generations as listed below.

Rice Mutant	Phenotypic variation	Genotypic variation (HAT-RAPD)
BKOS6	- Photoperiod insensitive - Early flowering - Short in stature - Reddish- dark brown to black in leaf sheath - Dark brown to black in seed coat (hull) - Black rice seeds (brown rice)	Additional DNA band
TKOS4	<ul> <li>Photoperiod insensitive</li> <li>Early flowering</li> <li>Low tillering capacity</li> <li>Low % filled-spikelets</li> <li>Low number panicles/plant</li> <li>Tall variety</li> </ul>	Additional DNA band
PKOS1	<ul> <li>Photoperiod insensitive</li> <li>Big and long panicles</li> <li>high % filled spikelets</li> <li>High number of seeds in panicle</li> <li>Short in stature</li> </ul>	Additional DNA band
PKOS2	<ul> <li>Photoperiod insensitive</li> <li>Big and long panicles</li> <li>high % filled spikelets</li> <li>High number of seeds in panicle</li> <li>Short in stature</li> </ul>	Additional DNA band
PKOS3	- Photoperiod insensitive - Big and long panicles - high % filled spikelets - High number of seeds in panicle - Short in stature	Additional DNA band

In the studies on low energy nitrogen ion induced mutation of rose, petunia and chrysanthemum, following results were obtained. One rose variety, Ingrid Bergman shows changes in flower colour as well as wrinkle petal. The viability of the treated buds was 58.9 % in petunia. Wide arrays of mutated characteristics were obtained both in vegetative and reproductive parts. Various leaf changes were found, i.e. slim leaf, rolled leaf, large leaf, rough leaf surface, yellow leaf, and albino leaf. Up to 13-15% stunt growth were found in some doses. Concerning the flower, different patterns of changes were found on the petal, i.e. white strip, white spot, ununiformed colour, pale colour, and variegated flower. The changing percentage were interestingly high; especially the petal colour e.g. the variegated colour was 61.1 %. The ion beam 1-4 x10<sup>16</sup> ions / cm<sup>2</sup> could change the anther into small petal. The ion beam could also change the flower shape into round shape star shape as well as reduce in flower size. Fourteen attractive mutants were tissued cultured using shoot tip and propagated to test for their permanent characters. The tissue culture-derived plantlets appeared to be true to type, proving the mutants were caused by the change in the chromosome. Twenty four mutants were also selected for the identification at the molecular level using RAPD technique. Four (OPA 04,OPA 07,OPA 09 and OPA 10) out of eleven primers demonstrated bands in the range of 550-3120 base pairs. RAPD technique can be used to identify different banding patterns among petunia mutants result from ion beam bombardment. Each of the primers, however, was not able to set each mutant apart. Therefore, several primers were required. As for chrysanthemum: Nitrogen ion beam at 4x10 ions/cm<sup>2</sup> reduced survival percentage of the explants. The rooted shoot lets derived from the cultured explants were grown and forced to flower in a nursery. Flower colour changes in its intensity, paler (1.1-2.2%) and darker (20-33.3%) colour as well as variegated colour (1.5-5.6%) were observed. Only 1 plant (0.6%) changed the colour from pink to bronze. Low energy bombardment of onion skin cell with both metallic and gaseous ion species can induce the formation of microcrater – like structures on the onion skin cell walls.

Conclusion

Ex – situ and in – situ Atomic Force Microscopy revealed the formation of microcrater – like structures with rim dimension typically several hundred nanometers; we speculate that the microcraters might provide channels for the transfer of exogenous macromolecules (such as DNA) through the cell wall into the cell interior.

Low energy nitrogen ions at a certain range of energy and fluence can induce mutation in Thai purple and jasmine rice and flower crops such as rose, petunia and chrysanthemum.

Recommendation:

Understanding of the fundamental mechanisms involved in ion interaction with living cells is not yet well developed. A fundamental question about the mechanism is the possible formation of pathways due to ion bombardment that are responsible for the gene transfer.

This aspect of ion-biological cell interactions need further investigation.

This application of low energy ion beam to induce mutation in rice and other energy crops should be further explored to obtain mutants with specified phenotypes.

Keywords

: ion bombardment; micro-crater; plant cell envelope; included mutation, purple rice, jasmine rice, rose, petunia, chrysanthemum.

#### **EXECUTIVE SUMMARY**

Ion beam bombardment of biological material has been recently applied for gene transfer in both plant and bacterial cells. Understanding of the fundamental mechanisms involved in ion interaction with living cells is not yet well developed. A fundamental question about the mechanism is the possible formation of pathways due to ion bombardment that are responsible for the gene transfer. Low energy bombardment of onion skin cells with both metallic and gaseous ion species, such as N, Ar, Cl, Xe, Fe, Mg, Ti, and Cu at fluences of 1-5 x 10<sup>15</sup> ion/cm<sup>2</sup>, can induce the formation of microcrater-like structures on the onion skin cell walls. A scanning electron microscope and an atomic force microscope (AFM) were used to observe these microcrater structures. Mass loss measurements indicate dehydration of the onion skin samples of up to 85% over a period of 5 minutes. Ex-situ AFM subsequent to Fe ion bombardment reveal an average microcrater depth of 60 nm, which compares with a penetration depth for Ti ions as determined experimentally using RBS characterization, of approximately 15 nm. Three different computer codes that provide a simulation of ion penetration in matter TRIM, T-Dyn and PROFILE have been used to investigate the expected depth profiles for the case of Ti bombardment, and compared with the experimental RBS results; it was found that the PROFILE code shows the best correspondence to the RBS. The work reported here has also included the design and installation of an in-situ AFM system to the beam line of our bioengineering ion implantation facility, and ongoing relevant experiments. Work todate has shown clear evidence of microcraters formed on onion skin cells bombarded by 25 keV Ar ion with fluence 1-2 x 10<sup>15</sup> ion/cm<sup>2</sup>, allowing comparison of observations made in-situ (in the vacuum chamber of the bio-implanter) and observations made in atmosphere some time after removal of the samples from the implanter.

The molecular dynamics simulations of Fe ion bombardment of onion skin cell wall have been carried out. A study of the interaction of energetic Fe ions with cellulose I-Beta surface which was used as a model material for the cell wall is reported, including results for ion penetration depth as a function of location, ion energy, and ion fluence. The calculations indicate that ion-bombarded cellulose molecules are broken into fragments by the collision, which fragments then initiate molecular collision cascades, leading to the ejection of intact molecules and molecular fragments from the surface.

Low energy ion beam has been applied to induced to induced mutation in Thai purple rice and Thai jasmine rice (*Oryza sativa indica* var. purple rice and KDML 105 respectively) under certain condition.

About 1200 seeds of Thai purple rice were bombarded by low – energy nitrogen ions accelerated by 60 kV with ion fluences of 1, 4 and 8 x 10 <sup>16</sup> ions/cm<sup>2</sup>, Consequently, the bombarded seeds were germinated for 5 days, and then rice seedlings were transferred to grow in soil until ripening stage. Two mutants were observed only in rice plants bombarded with the fluence of 1 x 10 <sup>16</sup> ions/cm<sup>2</sup>. Leaf blade and stem sheath of the mutants were green. In order to determine genetic modification in the mutant genomes, HAT – RAPD (High Annealing Temperature–RAPD) was chosen for DNA investigation. Of 10 primers three primers named OPK14, OPH15 and OPL01 detected genetic variation between the mutant and control. An additional DNA band

was detected by OPK14 at the molecular weight of 600 bp in both mutants. The DNA fragment was subcloned and sequenced. The analysis revealed that the DNA fragment encoding partial sequence of protein (designated OSP450) belonging to members of P450 plant protein family. Low energy ion beam has been applied to induced mutation in Thai purple rice and Thai jasmine rice (*Oryza Sativa indica* var. purple rice and KDML 105 respectively) under certain condition.

Number of rice mutants were obtained and characterized for 5 generations (M5) as mentioned in this report. Our aim in the research proposal was to investigate rice mutants with dwarf and photoperiod insensitive properties. The rice mutant line, PKOS1, PKOS2, and PKOS3, provided these characters. Although the line, TKOS4, its height is taller than the origin variety (KDML 105), it contained early flower flowering and photoperiod insensitive phenotypes.

In the studies on low energy ion beam induced mutation in flower crops, three important crops. i.e. rose, petunia and chrysanthemum were used. Various attempts were made to obtain suitable conditions and techniques for each floral crop mutation induced by the novel means of low energy ion beam. As for rose, nodal buds along the opened-flower stem were used. Parafilm was used as stem wrapping material to prevent the loss of water content, leaving only the bud exposed to the ion beam. The treated buds were there after grafted onto Rosa multiflora rootstock. One rose variety. Ingrid Bergman out of the three varieties investigated after exposing to the nitrogen ion beams at  $1x10^{16}$  ions/cm<sup>2</sup>, 60 keV showed changes in flower colour as well as wrinkle petal. The viability of the treated buds was 58.9%.

In petunia (a seed propagated crop), seeds with and without seed coat were investigated both in vivo and in vitro. Ion beam did not affect germination percentage of the seeds sown under aseptic conditions, but the seedlings showed abnormalities after wide arrays exposing the seeds to the nitrogen beam (1-10x10" ions/cm<sup>2</sup>, 60 keV). Wide arrays of mutated characteristics were obtained both in vegetative and reproductive parts. Various leaf changes were found, i.e. slim leaf, rolled leaf, large leaf, rough leaf surface, yellow leaf, and albino leaf. Up to 13-15% stunt growth were found in some doses. Concerning the flower, different patterns of changes were found on the petal, i.e. white strip, white spot, ununiformed colour, pale colour, and variegated flower. The changing percentage were interestingly high; especially the petal colour e.g. the variegated colour was 61.1 %. The ion beam 1-4 x10<sup>16</sup> ions / cm<sup>2</sup> could change the anther into small petal. The ion beam could also change the flower shape into round shape star shape as well as reduce in flower size. Fourteen attractive mutants were tissued cultured using shoot tip and propagated to test for their permanent characters. The tissue culture-derived plantlets appeared to be true to type, proving the mutants were caused by the change in the chromosome. Twenty four mutants were also selected for the identification at the molecular level using RAPD technique. Four (OPA 04,OPA 07,OPA 09 and OPA 10) out of eleven primers demonstrated bands in the range of 550-3120 base pairs. RAPD technique can be used to identify different banding patterns among petunia mutants result from ion beam bombardment. Each of the primers, however, was not able to set each mutant apart. Therefore, several primers were required.

As for chrysanthemum, the variety Reagan Dark was used. The flower receptacle part was aseptically precultured for 5 days to induce cell division before bombarding with nitrogen ion beam and culturing *in vitro* again. Nitrogen ion beam at 4x10 ions/cm<sup>2</sup> reduced survival percentage of the explants. The rooted shootlets derived from the cultured explants were grown and forced to flower in a nursery. Flower colour changes in its intensity, paler (1.1-2.2%) and darker (20-33.3%) colour as well as variegated colour (1.5-5.6%) were observed. Only 1 plant (0.6%) changed the colour from pink to bronze.

## Chapter I

## Subproject I: Basic Studies on Ion-Cell Interactions

#### 1.1 Introduction

In order to understand mechanisms involved in ion-beam-induced biological effects such as gene transfer and mutation, basic studies on ion-cell interactions have been carried out in the project. The objectives of the project include

- Development of specialized ion beam lines for bioengineering research and applications
- Investigation on ion-bombardment induced formation of microcraters in the cell envelopes, which may act as pathways for exogenous molecule transfer into the cells
- Development of *in-situ* atomic force microscopy (AFM) for real time observation of the formation of microcraters
- Study of the interaction between ions and cell envelope at the molecular level using molecular dynamics simulation
- Cooperation with biological teams for ion beam bombardment of biological samples.

Under the support of the Thailand Research Fund, through three years of great efforts in implementing the project, we have achieved tremendous attainments:

- Completion of the specialized bioengineering ion beam line.
- Completion of the *in-situ* atomic force microscope system.
- Completion of modification of the industrial ion implanter for bioengineering applications.
- Discovery of ion-beam-bombardment induced formation of micro/nano-crater-like structure on the biological cell envelope.
- Initiation of molecule-level study of interaction between ions and biological cell envelopes using molecular dynamics simulation.
- Collaboration with biological teams in ion beam facility and experiment operations.
- Fostering of two Ph.D.s, two Masters, and four Bachelors.
- Outputs of 16 international and national publications and presentations, and a national award.

These achievements have won our recognition in the international society. This honor not only belongs to our research group but also Thailand. Details of the achievements are reported below.

## 1.2 Bioengineering-specialized Ion Beam Line

The ion beam line specialized in bioengineering experiments and applications, named CMU3, has been constructed, installed and totally completed at the laboratory of Fast Neutron Research Facility (FNRF), Chiang Mai University (CMU), as shown in Figure 1. The beam line has following special features:

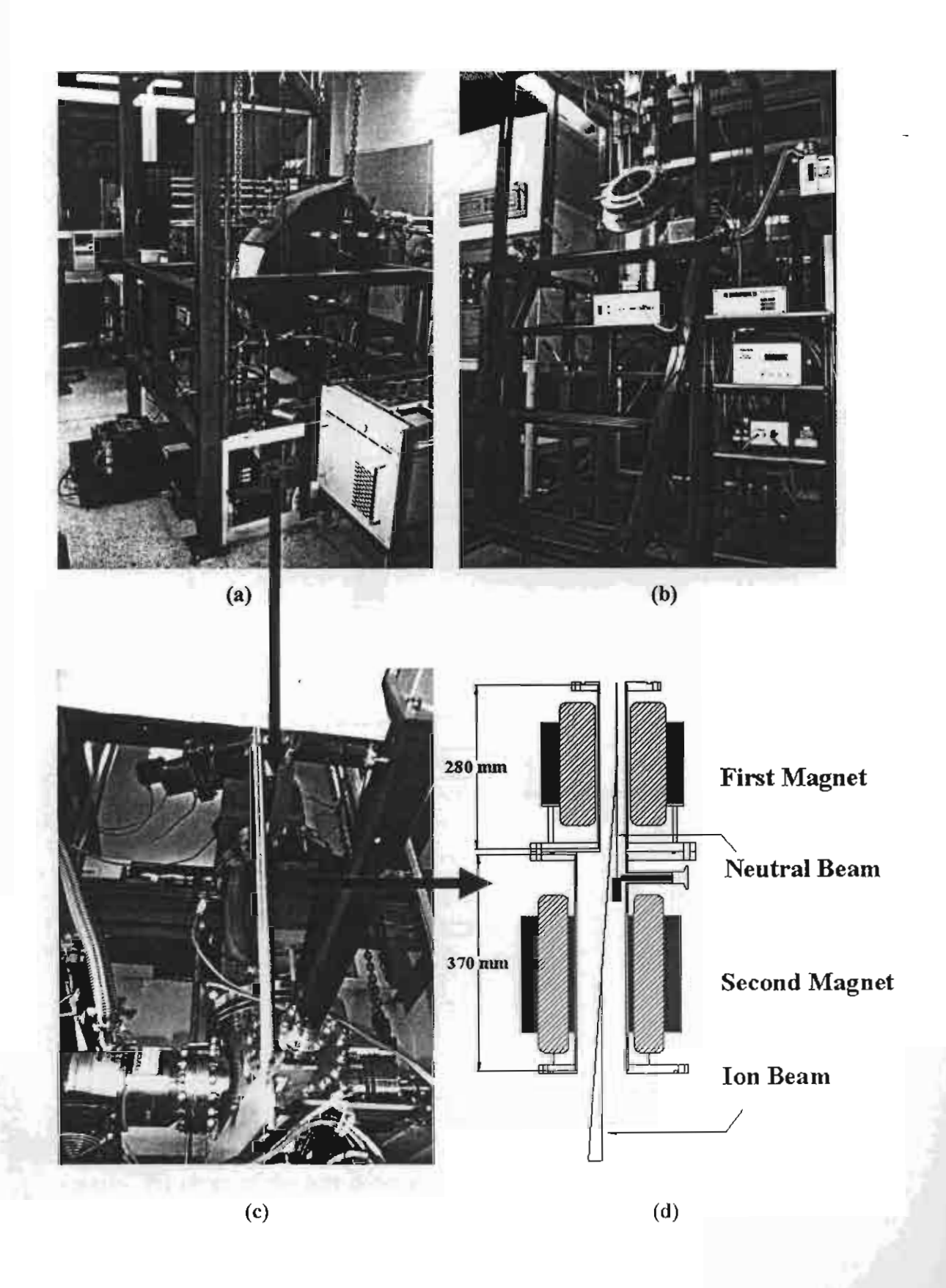
- 1. Vertical beam line
- 2. Low energy (30 keV)
- 3. Versatile beam
- 4. High beam quality and manipulation
- 5. Double beam swerve eliminating neutral particle
- 6. Fast pumped target chamber
- 7. Bio-environment in the target chamber
- 8. In-situ AFM
- 9. Bio-clean housing and biological supports.

This ion beam line is unique in the world for ion beam bioengineering research. Ion beam bioengineering or biotechnology research and application experiments have actively been carried out with the bioengineering ion beam line. Plentiful results have been obtained in mutation, gene transfer and observation of ion-bombarded cell envelopes (some results are shown in following sections).

# 1.3 Modification of the Industrial Ion Implanter for Bioengineering Applications

Modification of the high-current industrial-service ion implanter, CMU2, for large-area ion beam mutation of plants has been completed, as shown in Figure 2. The modifications include

- A new smaller chamber has been installed into the beam line to replace the quadrupole focusing magnet doublet at the old beam line for fast processing;
- Special biosample holders and stage have been constructed for ion beam mutation of a large number of samples;
- Special beam operation measures have been developed for living biosamples survival and safety.



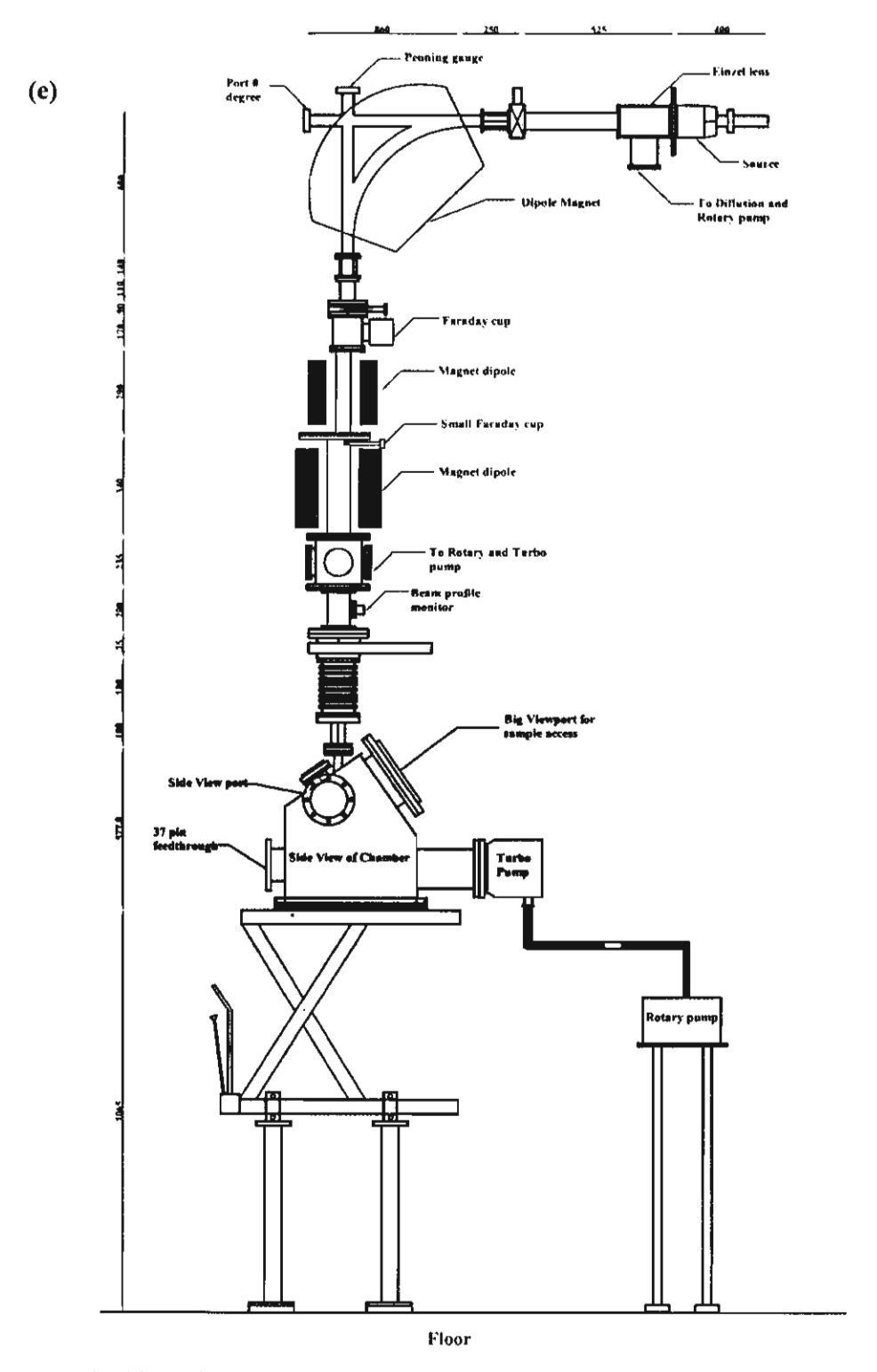


Figure 1. The bioengineering-specialized ion beam line system. (a) Photo of the part upstairs, (b) photo of the part downstairs, (c) and (d) photo and schematic of the double-magnet beam steering system, respectively (the arrow shows where the system is and zoomed), and (e) schematic of the entire beam line.

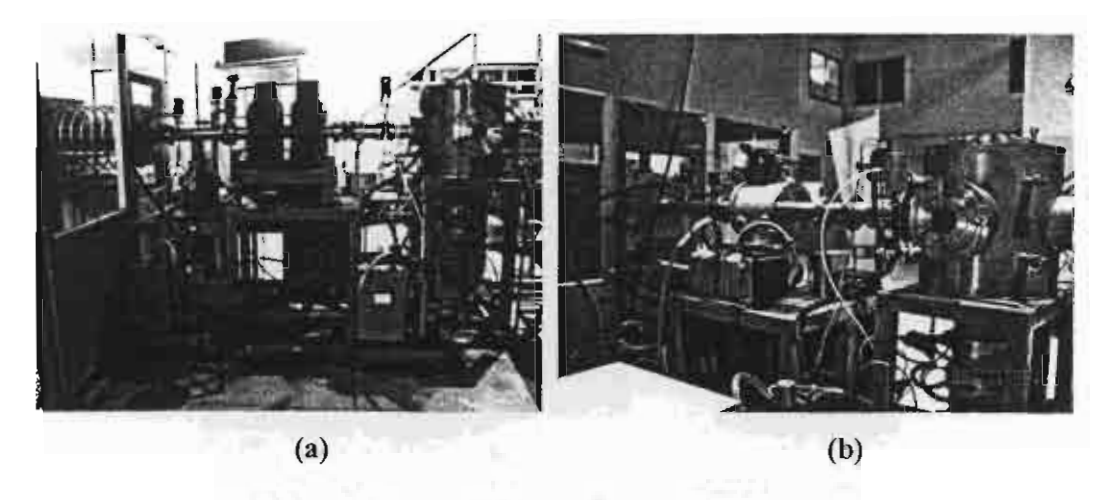


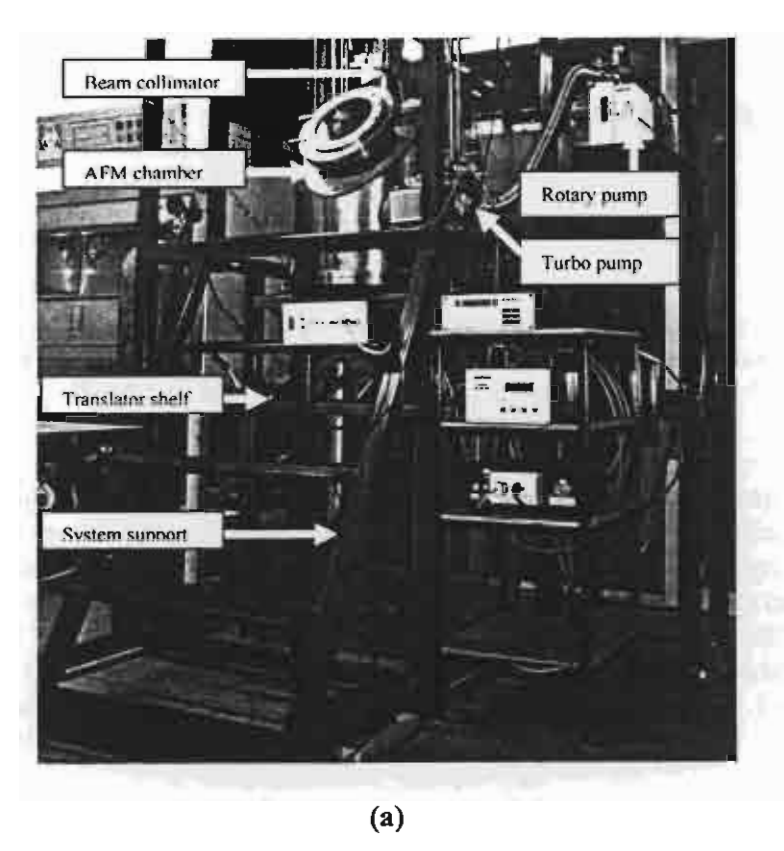
Figure 2. Photo of the high-current ion implanter, CMU2. (a) Before modification, and (b) after modification. In both photos, left side is the ion source and high-voltage terminal, and right side the target chambers.

## 1.4 In-situ Atomic Force Microscope (AFM)

In order to investigate ion beam interaction with biological cell envelope for understanding mechanisms involved in ion beam induced gene transfer and mutation, we designed, constructed and installed an *in-situ* atomic force microscope (AFM) system for the bioengineering ion beam line, CMU3. As shown in Figure 3, the *in-situ* AFM system includes

- In-situ AFM chamber at the beam line terminal
- Commercial AFM (SPM 9500-J2, Shimadzu) inside the chamber
- Tilting superlene seat supporting the AFM
- Damping system of 7-stage stack beneath the seat
- Feed-through connects at the chamber ports
- Data processing computer and AFM controller outside the chamber
- Beam collimator system above the chamber
- · Beam shutter system above the AFM
- Pumping system connected to the chamber
- Support shelf, vertically translateable, supporting the whole chamber system
- Support frame supporting the entire system at the beam line.

This *in-situ* AFM system is unique in the world. Challenges have been always with us. Now, the system has been started to work on experiments and preliminary results have been obtained (reported in next sections).



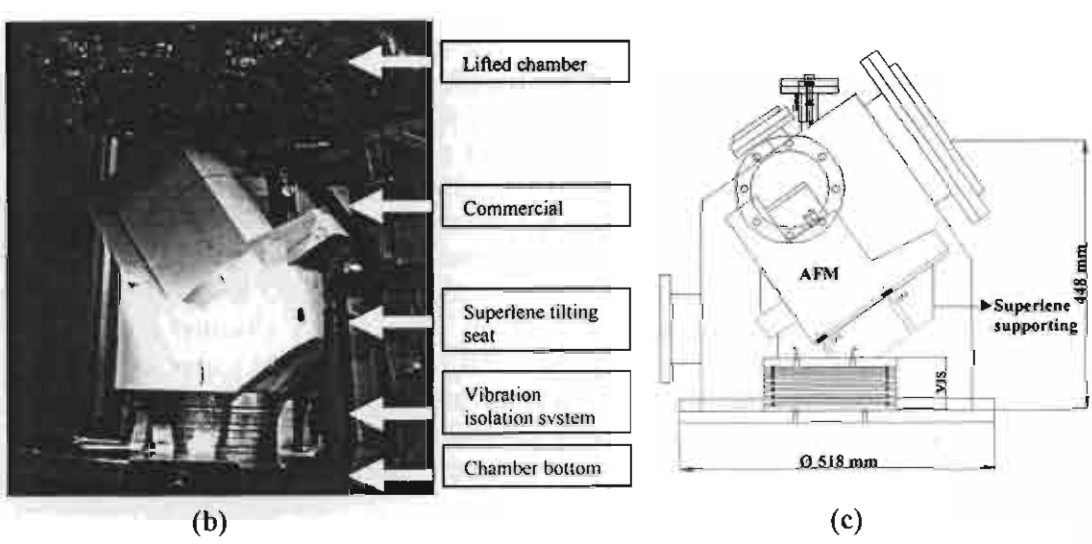


Figure 3. The *in-situ* AFM system at the bioengineering ion beam line. (a) Over view photo. (b) Photo of the *in-situ* AFM with its superlene tilting seat sitting on the vibration isolation system, a stack of 7 metallic plates separated by 3 pieces of tiny Orings between each pair of the plates, inside the AFM chamber. In the photo, the chamber cover is lifted now. (c) Schematic of the *in-situ* chamber and the AFM inside, side view.

# 1.5 Ion-beam-bombardment Induced Formation of Micro/Nano-crater-like Structure on the Biological Cell Envelope

#### 1.5.1 Introduction

Ion beam bombardment of biological organisms has been recently applied for gene transfer in both plant and bacterial cells. In this application, a low-energy ion beam, typically in tens of keV range, bombards biological cells to perforate the cell wall, through which exogenous macromolecules can be introduced into the cell interior in a subsequent post-bombardment biological processing step. However, a consistent physical mechanism for this significant result has not yet been developed. Questions to be understood include how the exogenous DNA macromolecules enter the cell, whether the molecules are directly transferred through pathways in the cell envelope, whether and how ion bombardment creates the pathways, and the nature of the pathway structure and geometry. Thus, we have investigated the effects of ion bombardment on plant cell envelopes from a more fundamental perspective and finally found that ion beam bombardment can generally induce formation of micro/nano-crater-like structure on the cell envelope.

#### 1.5.2 Experiment

Thin layers of onion epidermis were prepared from ordinary fresh yellow onions. The onion was cut and the third layer from the outer shell removed. From the middle part of this layer, a thin skin of onion epidermis was peeled and attached to a flat holder using carbon tape. Ion bombardment was carried out using either the bioengineering ion beam line, CMU3, at Chiang Mai University, or the metal vapor vacuum arc (MEVVA) ion source metal ion implanter at Berkeley. A broad range of ion species was used for bombardment, including gaseous N, Cl, Ar and Xe, metals Mg, Ti, Fe, Ni and Cu. The average ion energy was about 20 - 30 keV, and the ion fluence was typically 1 to  $2 \times 10^{15}$  ions/cm<sup>2</sup>; for some ion species (such as Ar) the fluence was varied from  $1 \times 10^{13}$  to  $2.5 \times 10^{15}$  ions/cm<sup>2</sup>. Cellulose and very dry onion skin were also used as targets for investigating relevant mechanisms. After ion bombardment, the samples were removed from the vacuum chamber and promptly observed microscopically using scanning electron microscopy (SEM) and atomic force microscopy (AFM).

#### 1.5.3 Results and Preliminary Conclusions

SEM and AFM observations of the ion-bombarded samples found formation of micro/nano-crater-like structures on the cell envelopes (Figures 4 and 5). Some characteristics of the craters were also investigated, such as the size, depth, beam condition dependence, and possible causes.

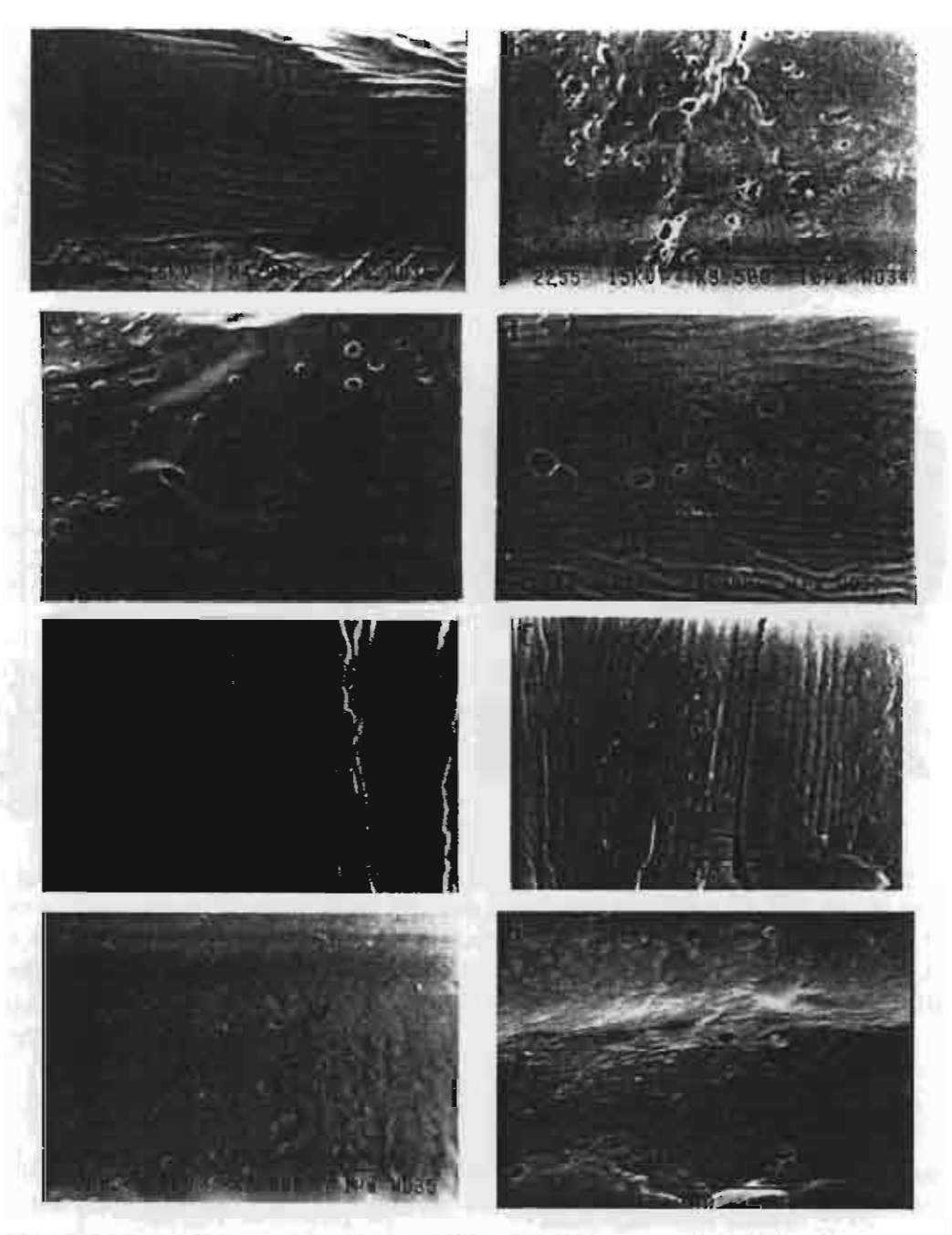


Figure 4. SEM photographs of onion cell surface bombarded by various ion species, compared with that of the control. (a) vacuum (unbombarded) control, and bombarded by ions of (b) Mg (20 keV), (c) Xe (30 keV), (d) Cl (25 keV), (e) Fe (25 keV), (f) Au (25 keV), (g) N (25 keV), (h) Ar (25 keV), with fluences of 1 × 10<sup>15</sup> ions/cm<sup>2</sup>.

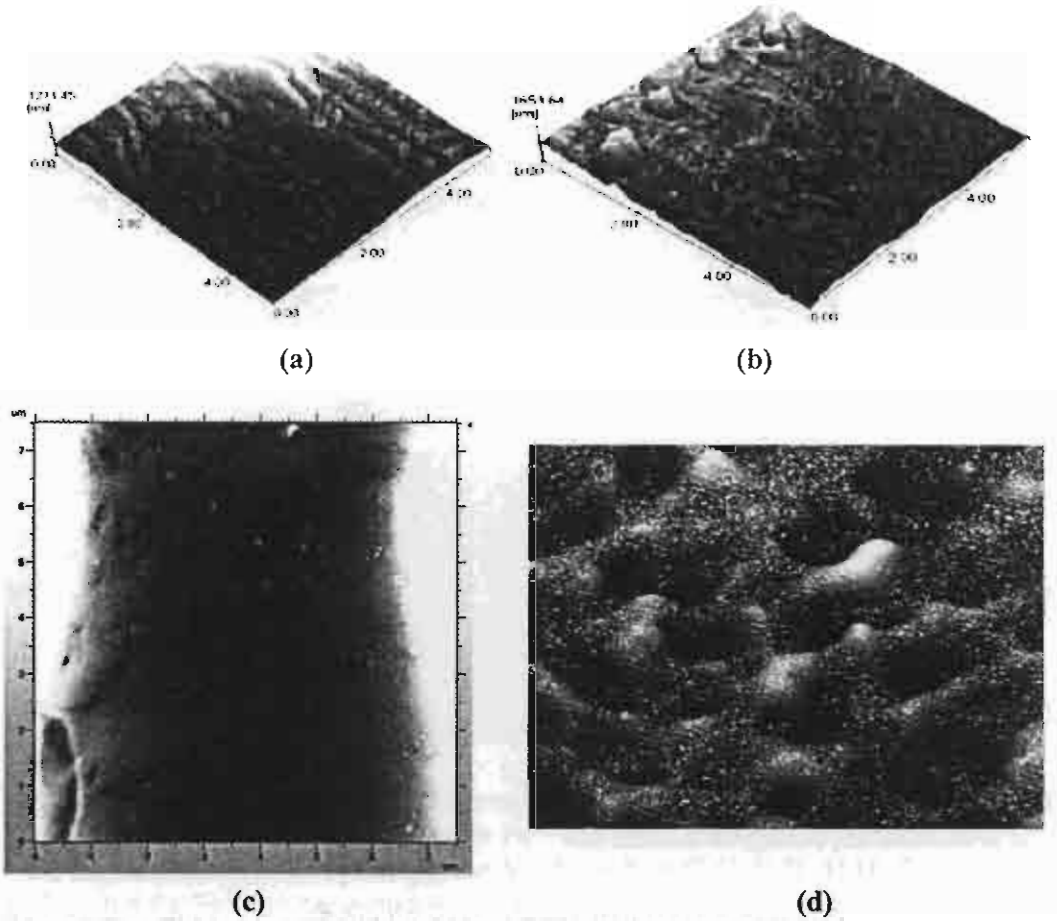


Figure 5. AFM images of onion skin surface. (a) Vacuum control, (b) 3-D image of the surface scanned in atmosphere after ion bombardment with a 25-keV Ar-ion beam to a fluence of  $1 \times 10^{15}$ /cm<sup>2</sup>, (c) 2-D image of the ion bombarded surface with the same condition as that of (b) but scanned in a near-in-situ condition, and (d) 3-D image of the cell surface bombarded by Fe ions at 25 keV with a fluence of  $1 \times 10^{15}$  ions/cm<sup>2</sup>.

This is the first time in the world to observe micro/nano-crater-like structures in the plant cell envelopes induced by ion beam bombardment. We preliminarily conclude

- The formation of microcrater-like structures in the plant cell envelope is a general phenomenon induced only by ion bombardment.
- The reason for microcrater formation seems related to the special microstructure of the cell wall.
- Further studies are needed for whether the craters are indeed the pathways for exogenous DNA transfer into biological cells, and if they are, how DNA is transferred through these channels.

### 1.6 Molecular Dynamics Simulation

We have initiated molecular dynamics simulation of ion interaction with plant cell envelope for understanding the mechanisms at the molecular level. As actually starting from zero, we have commanded some knowledge and skill on the method and obtained some preliminary results (Figure 6).



Figure 6. The MD simulated cellulose structure after Fe<sup>2+</sup> bombardment for 0.01024 ps. From the figure, it is seen that after Fe<sup>2+</sup> ion bombardment on cellulose structure with the velocity 6013.19726 Å/ps, the bonds such as C-C, C-H, H-H, C-O, etc. are broken and the Fe<sup>2+</sup> ion can penetrate the top surface of cellulose structure.

#### 1.7 Mechanisms for Ion Beam Induced Mutation

#### 1.7.1 Introduction

Ion beam induced mutation breeding of crops including rice, flowers and vegetables has been achieved at Chiang Mai University. However, physics mechanisms involved in the ion beam induced mutation have not yet been understood. The major question is how a low-energy ion beam is able to penetrate fairly thick substance layers of a seed including the seed coat or embryo coat before interacting with the embryo to induce mutation of DNA in the cells. In order to find solutions, we have done some preliminary investigations.

#### 1.7.2 Experiment

In the same conditions as those used in ion-beam mutation experiments, seeds with coats or without coats of rice, vegetable, flower and bean were bombarded in vacuum by nitrogen ions accelerated by 30 kV and 60 kV to fluences of 1, 2 and 4 ×  $10^{16}$ /cm² using CMU2 ion implanter. For some of the seeds, the seed coats were removed to expose the embryos directly to the ion beam. For other seeds that had the coats, the seed orientations were random as knowledge lacked on where the embryo was. After ion bombardment, the morphology of the seed surface was examined using scanning electron microscopy (SEM). It should be noted that the ion beam conditions applied for SEM observation were the same as those for ion beam mutation experiments. For example, green bean seeds were N-ion bombarded with the similar conditions and afterwards grown in soil. Mutations were found as shown in Figure 7.

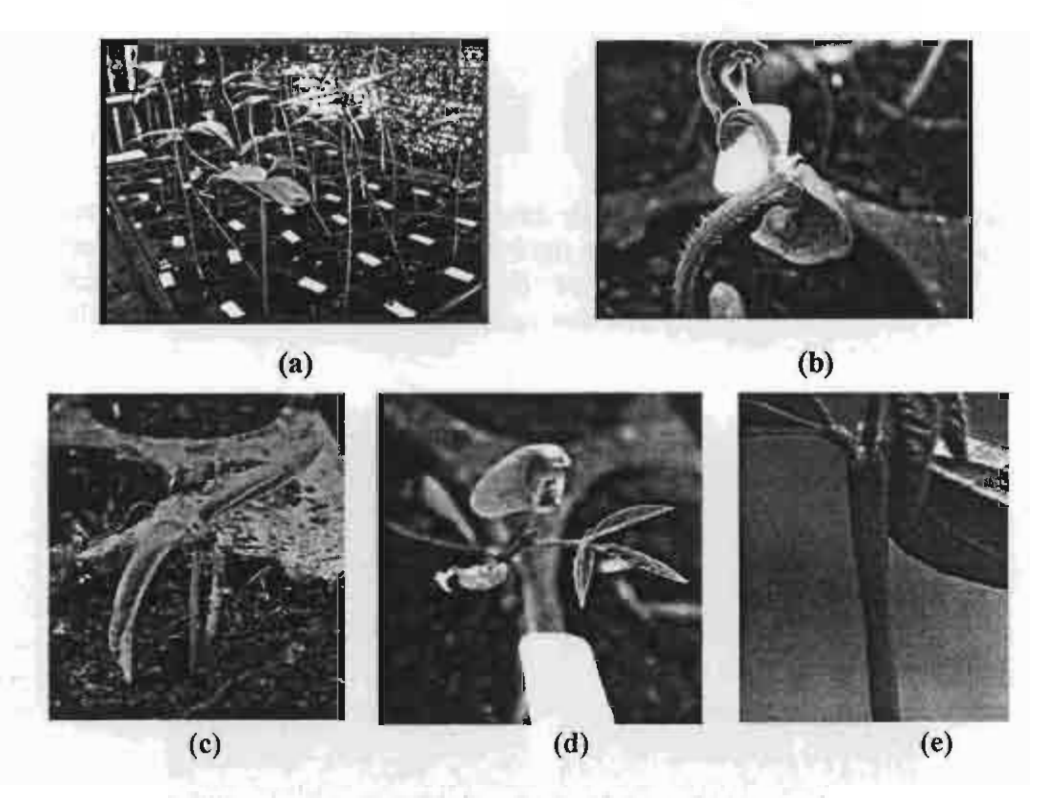


Figure 7. Germination and growth of the Mung bean seeds after ion beam bombardment with nitrogen ion beam with an energy of 30 keV and a fluence of  $1 \times 10^{16}$ /cm<sup>2</sup>. Mutations can be observed. (a) Control in vacuum, and (b) – (e) ion bombarded. Compared with the control (a), it is seen that in (b), the leaves are rolled up and shrunk (observed in 30% of the total seedlings), and the stem bent; in (c) there grow double stems, observed at only one seedling among 100 (it should be only a single stem); in (d) there grow a branch (it should not have a branch) as well as rolled and shrunk leaves; in (e) the stem becomes fairly thick, observed at only one seedling among 100 (it should be thin as shown by the control).

#### 1.7.3 Results and discussion

The SEM results are shown in Figures 8 - 11.

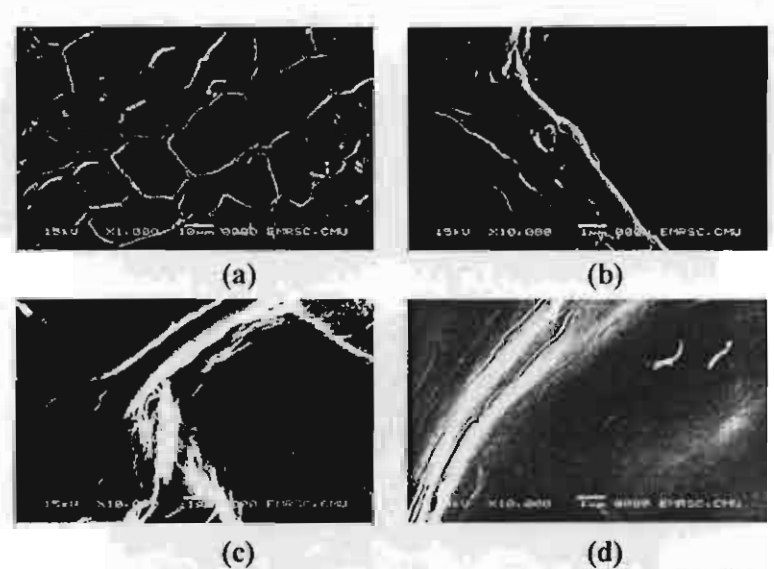


Figure 8. Jasmine rice KDML seeds with the coat removed from the embryo. (a) Control, low magnification, (b) control, high magnification, (c) bombarded with  $2 \times 10^{16}/\text{cm}^2$ , high magnification, and (d) bombarded with  $4 \times 10^{16}/\text{cm}^2$ , high magnification. The ion acceleration voltage was 60 kV.

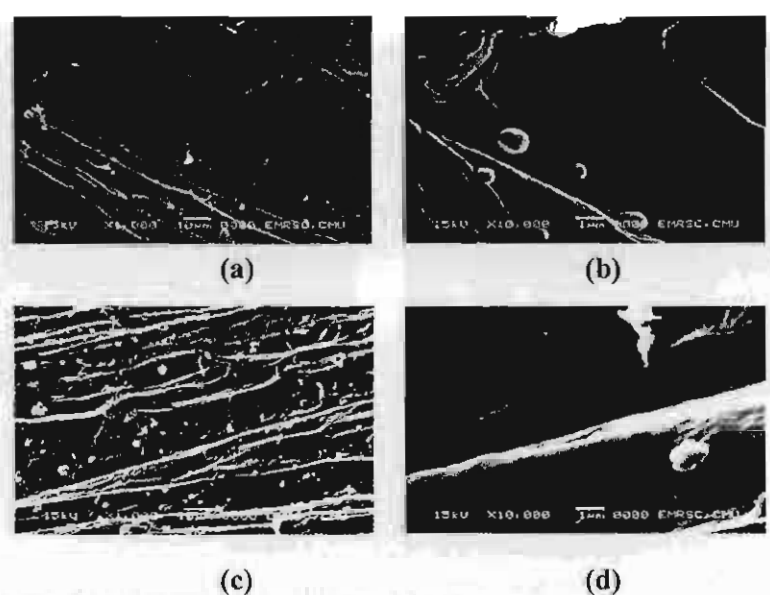


Figure 9. Vegetable lettuce seeds. (a) Control, low magnification, (b) control, high magnification, (c) bombarded with  $4 \times 10^{16}/\text{cm}^2$ , low magnification, and (d) bombarded with  $4 \times 10^{16}/\text{cm}^2$ , high magnification. The ion acceleration voltage was 60 kV.

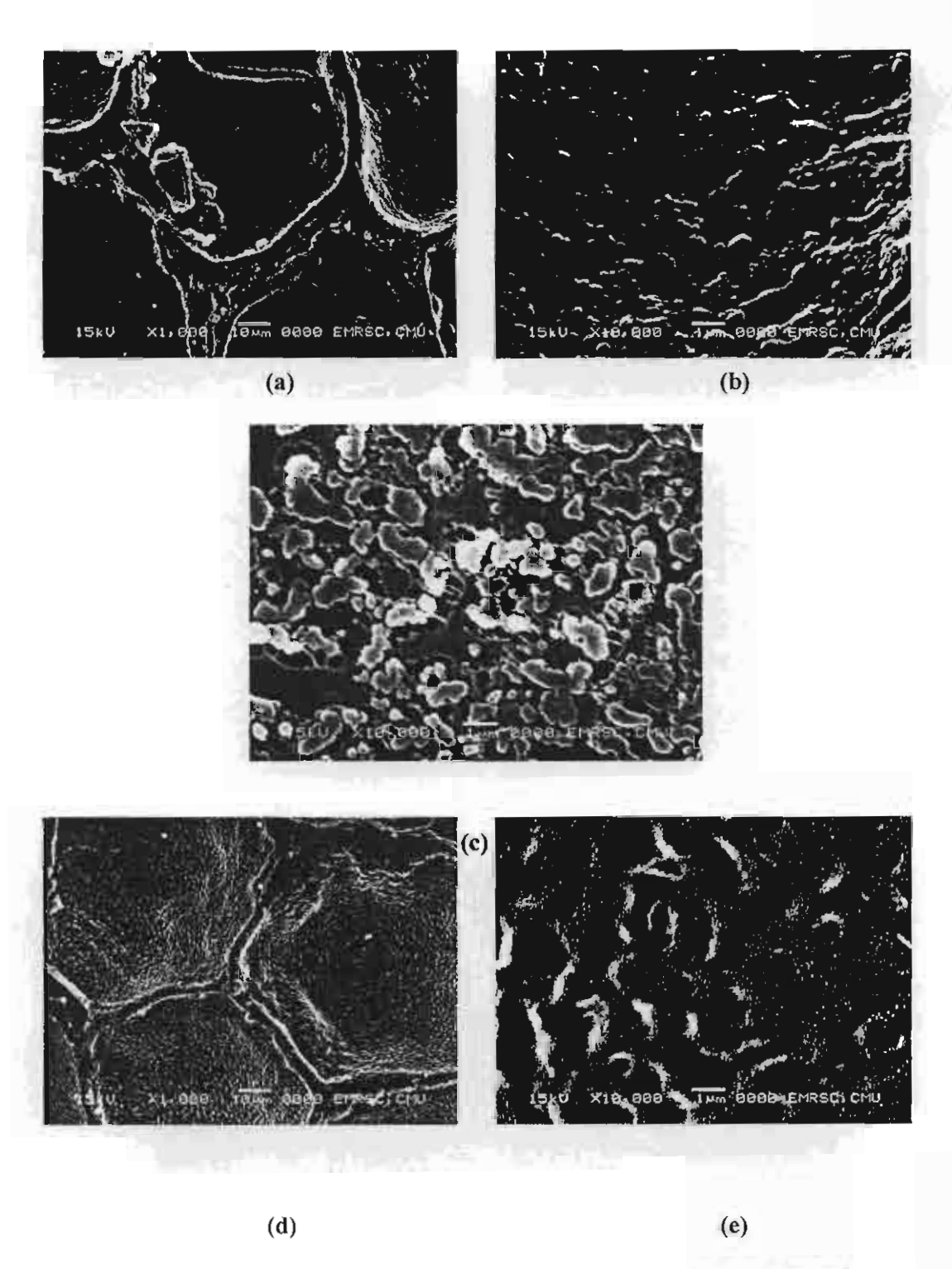
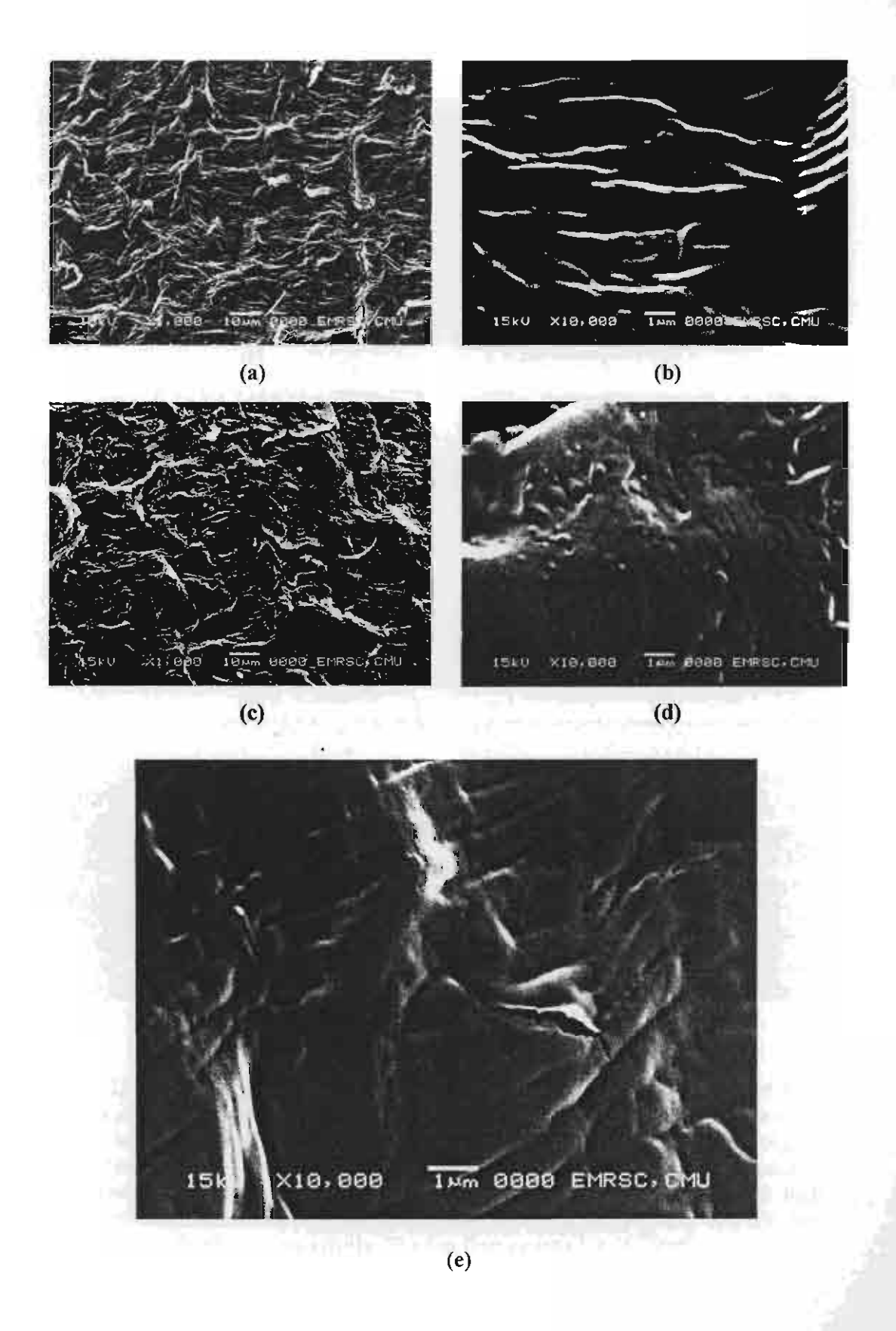


Figure 10. Flower petunia seeds. (a) Control, low magnification, (b) control, high magnification, (c) bombarded with  $2 \times 10^{16}/\text{cm}^2$ , high magnification, (d) bombarded with  $4 \times 10^{16}/\text{cm}^2$ , low magnification, and (e) bombarded with  $4 \times 10^{16}/\text{cm}^2$ , high magnification. The ion acceleration voltage was 60 kV.



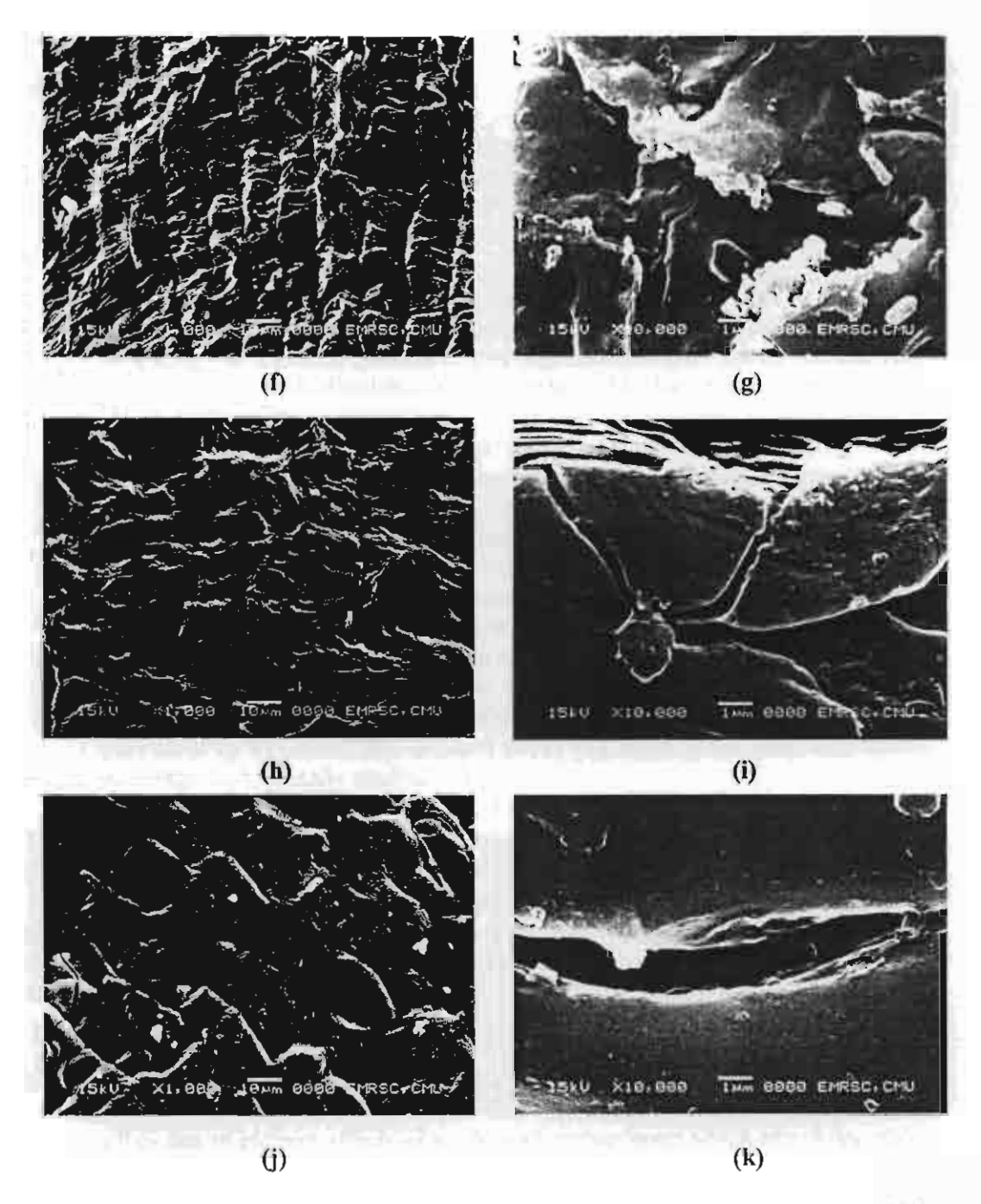


Figure 11. Mung bean (or green bean) seeds. (a) and (b) control, low and high magnifications, respectively; (c), (d) and (e) bombarded with an ion acceleration of 30 kV, low and high magnifications, respectively, different locations for (d) and (e); (f) bombarded with an ion acceleration of 60 kV, low and high magnifications, respectively; (h) bombarded with an ion acceleration of 80 kV, low and high magnifications, respectively; (j) bombarded with an ion acceleration of 100 kV, low and high magnifications, respectively. The ion fluence was  $1 \times 10^{16}$ /cm<sup>2</sup>.

Some observations from the SEM micrographs with their related discussions are summarized below.

- After ion bombardment, the surface of the seeds, at either the coat or the embryo, generally becomes smoother compared with that of the control. The smoothing increases as increasing of the fluence (e.g. as shown in Figures 8c and 8d). This demonstrates the ion sputtering effect on the material surface for thinning the material layer.
- After ion bombardment, at some locations, which are thought to be softer than
  others, material is sputtered out more than other locations that are thought to
  be harder, leaving deep grooves or pits (e.g. as shown in Figures 10c and 10e).
  The thinning and digging of the surface by ion beam may enhance
  subsequently coming ions penetrating deeper in the seed coat or envelope
  materials so that some ions may reach the genetic substance in the cell.
- Either before or after ion bombardment, some cracks are shown on the surface. And the cracks seem more after ion bombardment than before (e.g. as shown in most of the figures). It is the first time to see this phenomenon. This is considered to be very significant in leading to ion deep penetration. Some ions can go through the cracks to bombard much deeper locations. This is the very probable reason for ions to interact with genetic substance in the cell with a reasonable rate. Concerning how the cracks form, for the unbombarded seeds, they may originally exist or form by vacuum and vacuum-environmental low temperature induced deformation of the coat; for the bombarded seeds, they may form by implanted ions induced stress and strain in the coat. This should be further emphatically studied.

#### 1.7.4 Preliminary conclusion and comments

The bombarding ions that can probably interact with the genetic substance in the cell embryo to induce mutation may have the chance to pass through cracks formed in the seed coat or embryo coat to bombard the embryo. The cracks may be formed originally and by ion bombardment and sputtering induced stress as well.

Further work is very much needed to explore mechanisms involved in ion beam induced mutation. Is the induction due to direct effects of ion beam bombardment which may lead to energetic ions interacting with the genetic substance in the cell or due to indirect effects of ion beam bombardment which may bring about photon (such as X-ray) and/or electron emission, which can interact with the genetic substance, or due to biological effect (such as free radical formation) induced by ion beam bombardment? We should screen these effects and figure out answers.

## **Chapter II**

**Subproject II:** An application of low energy ion beam for KDML 105 (*Oryza sativa indica*) induced mutation

#### 1. Introduction

The objectives of the research works in the subproject II were aimed to study on the appropriate condition for ion beam bombardment such as ion energies, ion fluences, and ion species, to induce mutation in purple rice and Thai jasmine rice by using ion beam technique.

For the 1<sup>st</sup> to the 5<sup>th</sup> half yearly progress reports, the results of the series of intensive research activities showed the succeed of the research works that have been carried out since 2003 to the mid of 2006. Studied on the appropriate condition of the  $N_2^++N^+$  ions beam condition induced mutation in rice seeds; firstly, purple rice were used as indicator, showing the broad range of ion energies of 60-125 keV with the ion fluences ranges of  $1 \times 10^{16}$ - $5 \times 10^{17}$  ions/cm<sup>2</sup>. Consequently the chosen conditions were applied to induce mutation in Thai jasmine rice seeds. Eight rice mutants (M<sub>1</sub>) resulted from the ion bombardment on Thai jasmine rice (KDML 105) seeds have been reported. The mutants were cultivated for 6 generations (M<sub>6</sub>). Characterization of the rice mutants were carried out and discussed. Hereby we summarized our research work results, outcome, and the output of the subproject II.

# 2. <u>Description of experiments carried out since 2003 to the end of 2005</u>

# 2.1 Study on the appropriate condition of ion beam bombardment on purple rice (Oryza sativa indica)

#### Experiment

4800 rough seeds of purple rice were heated in hot-air oven, at 49 C for 5 days in order to break rice dormancy. The seeds were then husked one by one by hand to avoid any damage to the rice embryos and then put in the rice sample holders. The seeds were bombarded with N<sup>+</sup>+N<sub>2</sub><sup>+</sup> ions at the ion energies ranging from 60-125 keV with the ion fluences of 1x10<sup>16</sup>-5x10<sup>17</sup> ions/cm<sup>2</sup> generated by non-mass analyzed 150 kV ion implanter at Chiang Mai University. The seeds were then soaked in distilled water in plastic bags for 2-3 minutes and then the water was poured out of the bags. The seeds were further kept in the moisture condition overnight. The seeds were then directly cultured in soil, 0.5 cm beneath the soil surface, for 3-4 weeks. After 3-4 weeks, survive rice seedlings that were around 15 cm in height were then transferred to grow as transplanted rice in soil in plastic pot (13 inches in diameter) as 5 seedlings/pot adjusted the water level of 5-10 cm height for 2 months. The changing of phenotypic variation in rice plants as green leaves were observed, recorded. And genotypic variations were analyzed by HAT-RAPD method.

#### Results and Discussions

Table I showed the ion beam bombardment conditions that induced mutation in purple rice. The phenotypic and genotypic variations were shown in Fig I and Fig 2. The mutation was found as random phenomenon in most of the ion energies and ion fluences used in the experiment. Phenotypic and genotypic variations were found stable in M<sub>1</sub>-M<sub>4</sub> generation.

Table I. The ion beam bombardment conditions induced mutation in purple rice.

Energy (keV)	Ion fluences	Number of	Number of purple
Ziioigj (iio i )	(ions/cm <sup>2</sup> )	germination	rice plants showing
		(cultured from 400	phenotypic
		seeds)	variation
		,	(green leaves)
60	1x10 <sup>16</sup>	395	2
	$4x10^{16}$	394	0
	8x10 <sup>16</sup>	386	0
	$2x10^{17}$	244	0
	5x10 <sup>17</sup>	238	0
80	1x10 <sup>16</sup>	391	1
	i 4x10 <sup>16</sup>	385	2
	8x10 <sup>16</sup>	369	1
	$2x10^{17}$	198	0
	5x10 <sup>17</sup>	177	0
100	1x10 <sup>16</sup>	396	3
	$4x10^{16}$	390	0
	8x10 <sup>16</sup>	335	0
	2x10 <sup>17</sup>	125	0
	5x10 <sup>17</sup>	122	0
125	1x10 <sup>16</sup>	392	0
	$4 \times 10^{16}$	378	0
	8x10 <sup>16</sup>	292	0
	2x10 <sup>17</sup>	57	0
	5x10 <sup>17</sup>	40	0
Vacuum control		386	0

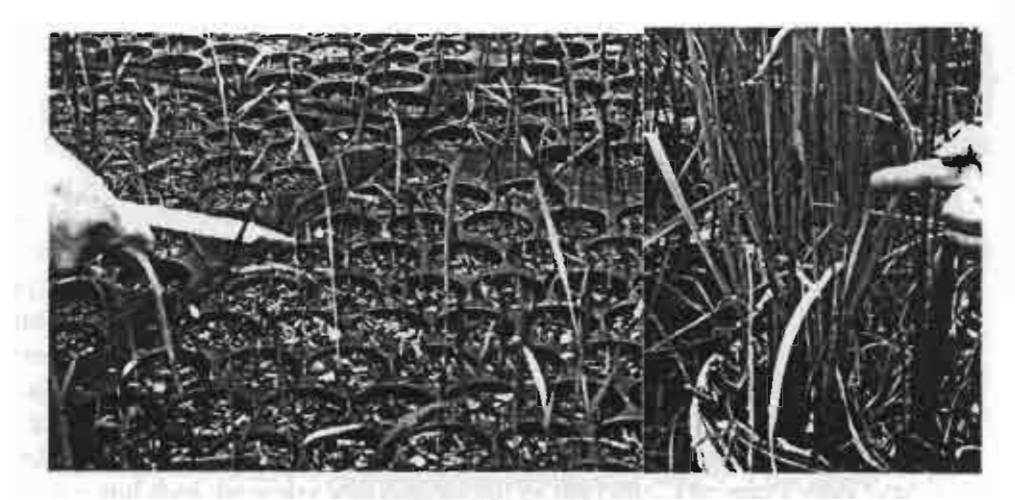


Figure 1. Phenotypic variation as green leaves found in purple rice plants cultured from purple rice seeds bombarded with the  $N^++N_2^+$  ions.

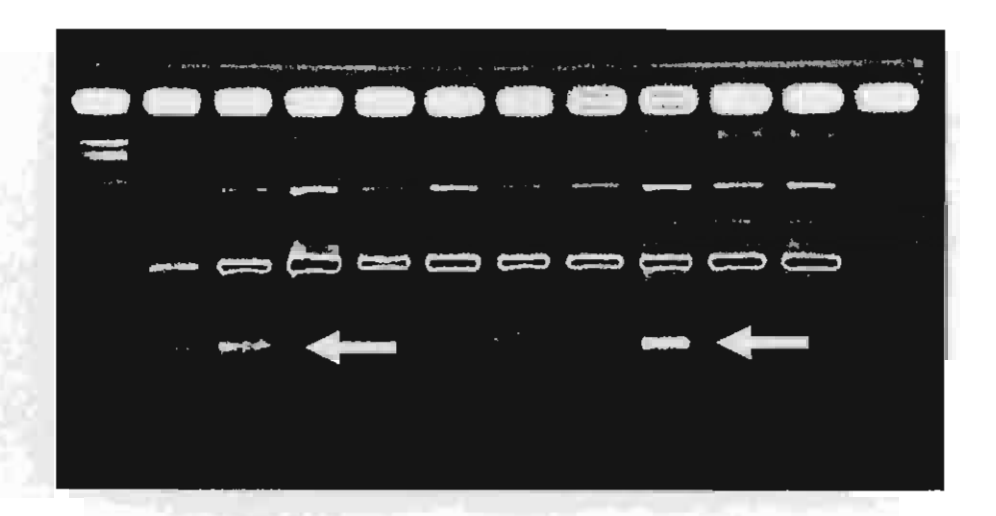


Figure 2. Additional DNA band at 600 bp found in purple rice mutant detected by OPH15 primer performed by HAT-RAPD method. Arrows indicate additional bands in the mutants.

# 2. 2. <u>Ion beam induced mutation on Thai jasmine rice</u> (*Oryza sativa indica*, KDML 105)

The aims of the experiment were to induced mutation in Thai jasmine rice by ion beam technique and to screen for short in stature and photoperiod insensitive characters in ion bombarded Thai jasmine rice seeds.

#### **Experiments**

Many ten series of ion bombardment were carried out from the beginning of 2003 to the end of 2005. Around 20,000 KDML 105 rice seeds were heated in the hot-air oven, at 49 C for 5 days to break rice dormancy as described above. The rice seeds were carefully husked one by one by hand to avoid any damage to embryo tissues. The brown rice seeds were placed in the target holders then put in target chamber. The seeds were ion bombarded with  $N_2^++N^+$  ion beam at the energy level of 60-100 keV with the ion fluences ranging from 1x10<sup>16</sup> to 5x10<sup>17</sup> ions/cm<sup>2</sup>. The control in the experiment were set as vacuum negative control (hushed seeds) and vacuum positive control (husked seeds put in target chamber, under experimental condition). After the ion bombardment the ion bombarded seeds and the controls were put in distilled water in sterile plastic bags for 2-3 minutes and then the water was poured out of the bags. The seeds were kept in such moisture condition overnight. The seeds were then directly cultured in soil. 0.5 cm beneath the soil surface, for 3-4 weeks. After 3-4 weeks all seedlings with around 15 cm in height were transferred to grow as transplanted rice in soil in plastic pot (1 seedling/pot) adjusted the water level of 5-10 cm height for 2 months. The mutation induction in the rice plant as short in stature and photoperiod insensitivity was carefully observed.

#### Results and discussions

Eight rice mutants were obtained (see Table II), showing the properties of short in stature, photoperiod insensitive, etc., as shown in Fig. 3-6. Genetic variations were found in all rice mutants. The examples of genetic variations detected by HAT-RAPD technique were shown in Fig 7-8.

Table II. Summarized data of the eight ion bombarded KDML 105 rice mutants.

Rice plants	lon bombardment condition	Phenotypic variation	Genotypic variation (HAT-RAPD)
BKOS6	N <sub>2</sub> + N <sup>+</sup> , 60 keV, 2x10 <sup>16</sup> ions/cm <sup>2</sup>	-Photoperiod insensitive -Early flowering -Short in stature - Reddish- dark brown to black in leaf sheath -Dark brown to black in seed coat (hull) -Black rice seeds (brown rice)	Additional DNA band
TKOS4	N <sub>2</sub> + +N <sup>+</sup> , 80 keV, 8x10 <sup>16</sup> ions/cm <sup>2</sup>	-Photoperiod insensitive -Early flowering -Low tillering capacity -Low % filled-spikelets -Low number panicles/plant -Tall variety	Additional DNA band
PKOS1	N <sub>2</sub> + N, 60 keV, 2x10 <sup>17</sup> ions/cm <sup>2</sup>	Photoperiod insensitive -Big and long panicles -high % filled spikelets -High number of seeds in panicle -Short in stature	Additional DNA band
PKOS2	N <sub>2</sub> + N, 60 keV, 5x10 <sup>17</sup> ions/cm <sup>2</sup>	Photoperiod insensitive -Big and long panicles -high % filled spikelets -High number of seeds in panicle -Short in stature	Additional DNA band
PKOS3	, N <sub>2</sub> +N, 60 keV, 8x10 <sup>16</sup> ions/cm <sup>2</sup>	Photoperiod insensitive -Big and long panicles -high % filled spikelets -High number of seeds in panicle -Short in stature	Additional DNA band



Figure 3. BKOS6 rice seeds were dark brown to black seed coat (hull) compared with that of the KDML 105 control.

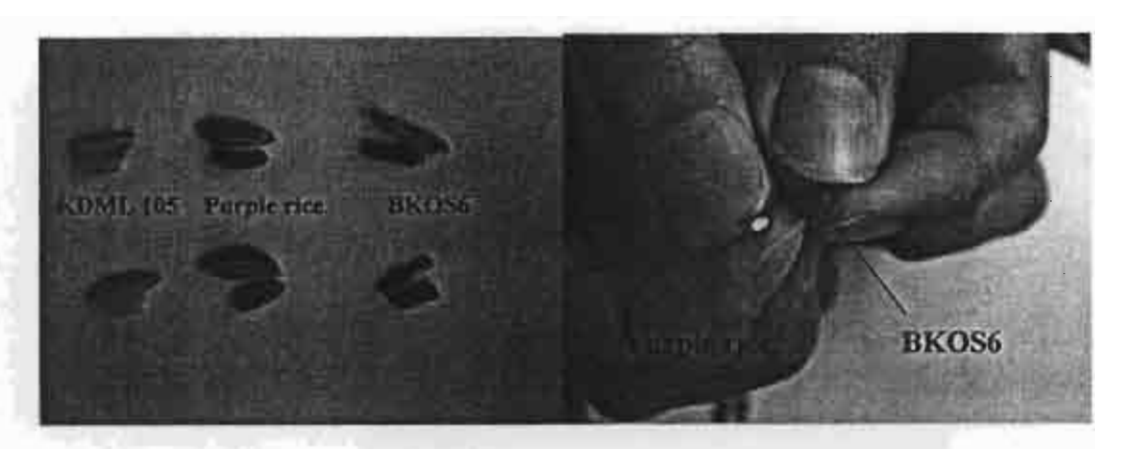


Figure 4. BKOS6 seeds compared with purple rice seeds and with of the KDML 105 control (left picture) and comparison between inner (cross section) color of BKOS6 grain and purple rice grain (right picture). Black color was only found in pericarp of purple brown rice but the black color was found in pericarp, tegmen, aleurone layer, and starchy endosperm, of BKOS6 brown rice.

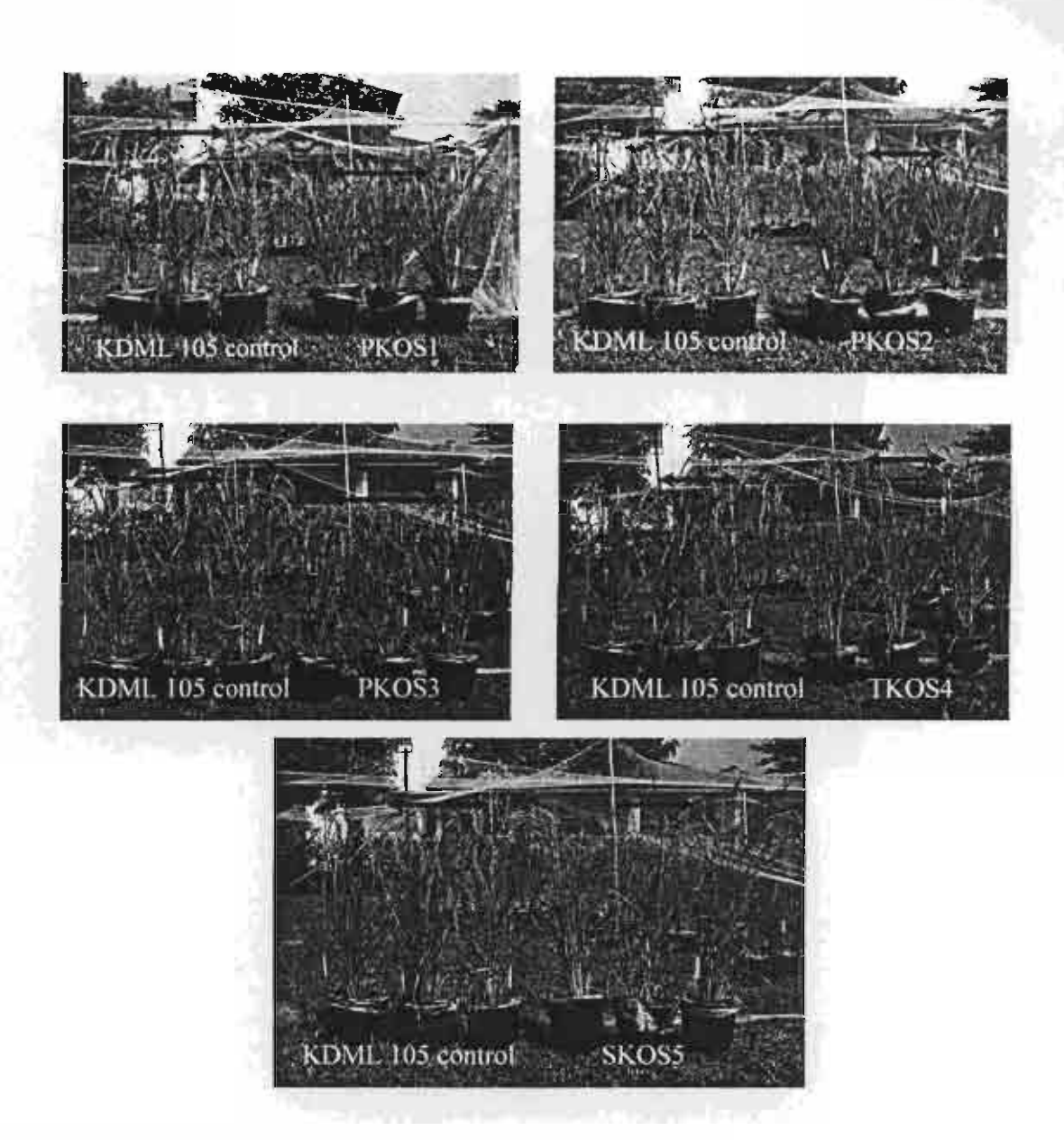
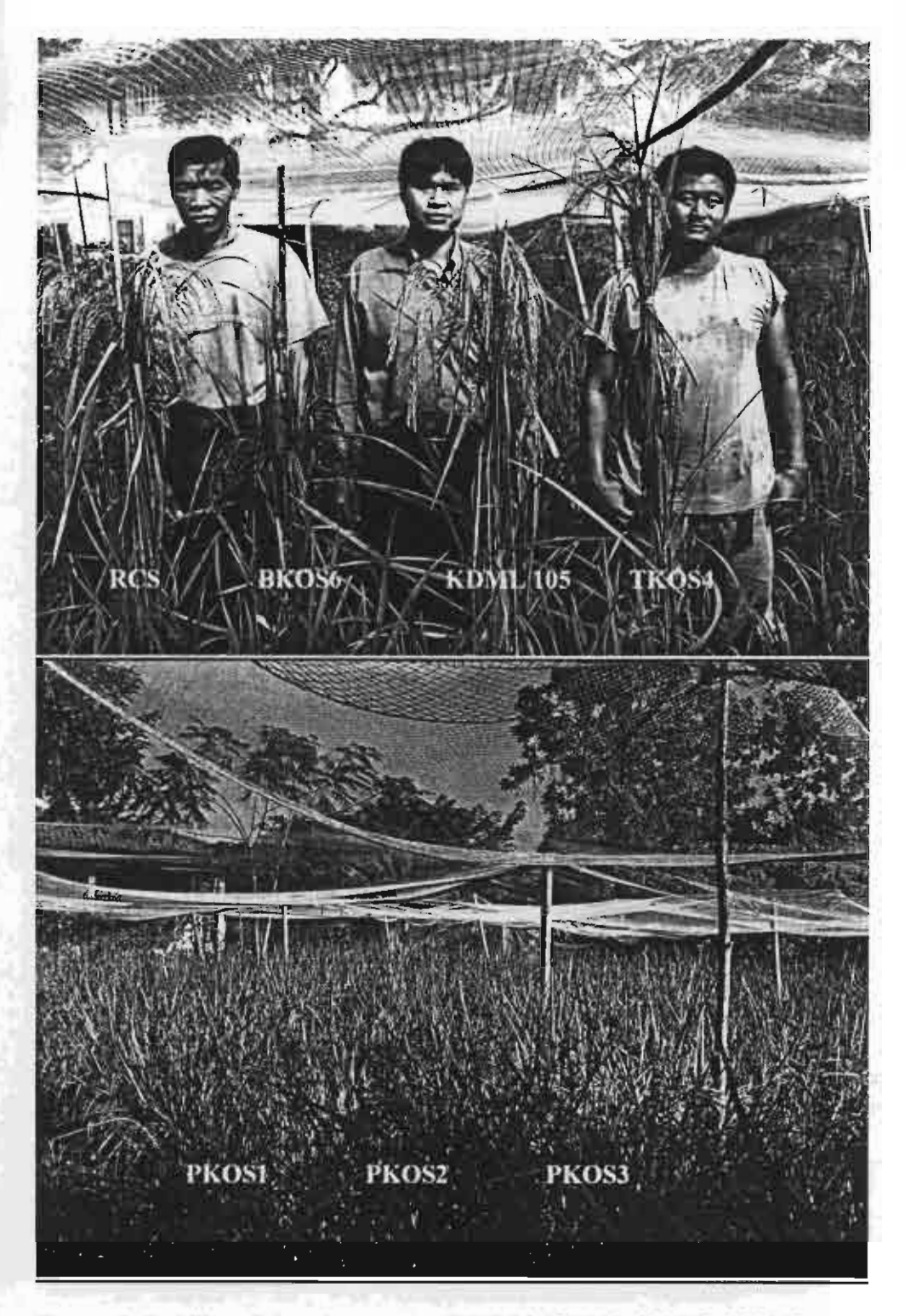


Figure 5. Appearance of mutants in height (arrows indicate the height of the rice plants, see data in table V) compared with of the KDML 105 control. PKOS1, PKOS2, and PKOS3, are short in stature and TKOS4 is tall variety.



**Figure 6.** Stability of short in stature of BKOS6, PKOS1, PKOS2, PKOS3 and tall variety property of TKOS4 was found in  $M_1$ - $M_5$  generation, and compared with RCS, KDML 105 control and Thai men with an average of 170 cm in tall.

## Primer OPD07

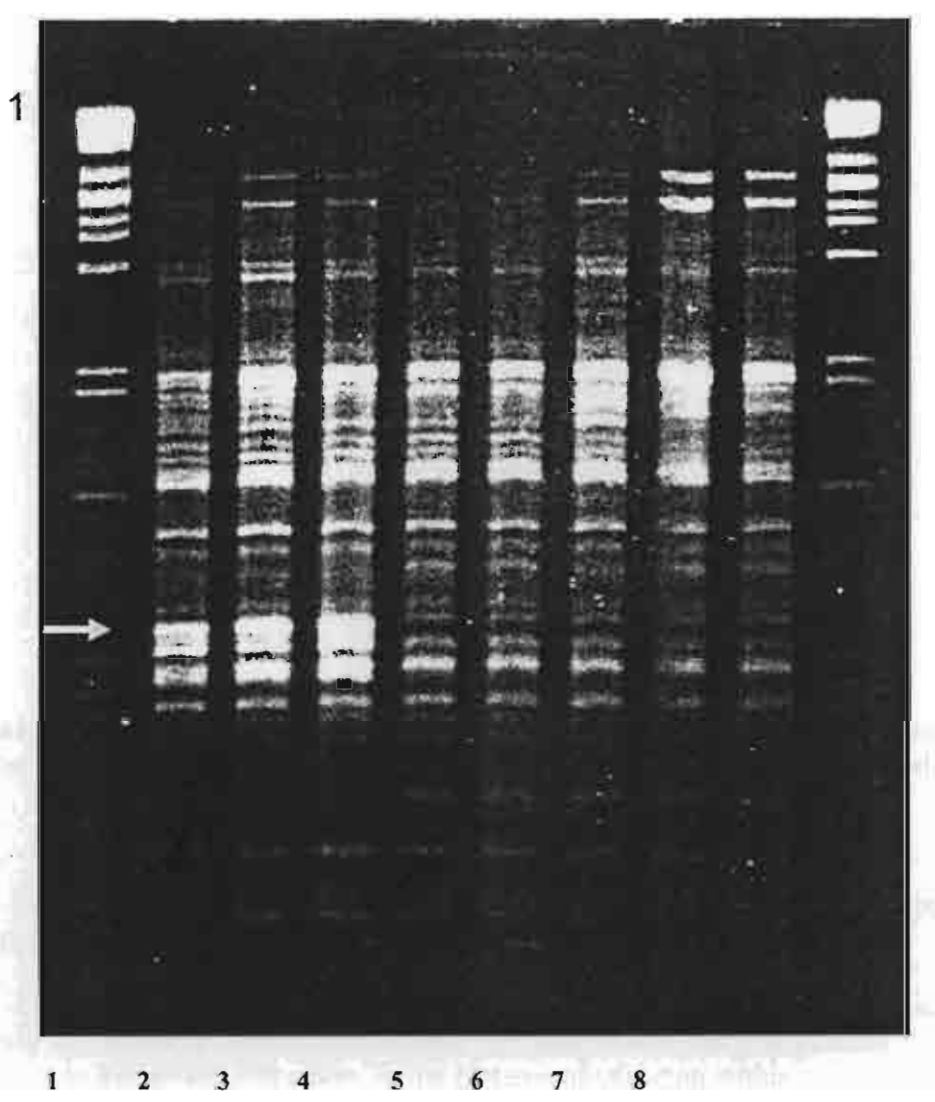


Figure 7. By using OPD07 primer in HAT-RAPD technique, genotypic variation as additional DNA band (arrow) was found in PKOS1, PKOS2 and PKOS3 compared with that of the KDML 105 control.

1= PKOS1, 2= PKOS2, 3= PKOS3, 4= vac+KDML 105, 5= vac-KDML 105, 6= TKOS4, 7= SKOS5, 8= vac-KDML 105

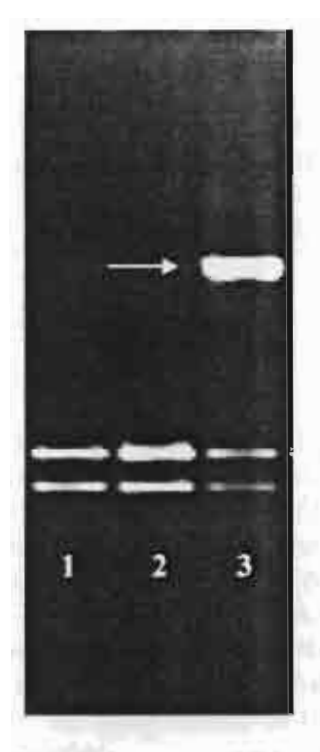


Figure 8. Utilizing HAT-RAPD technique, an additional DNA band (arrow) was found in BKOS6 (lane 3) compared with of the KDML 105 controls (lane 1 and lane 2).

# 2.3 Comparison of Oryza sativa KDML105 and its mutants by microsatellite markers

Our objectives were to use microsatellite markers to compare genetic variation among the wild type (*Oryza sativa* KDML105) and its mutants (BKOS6 and TKOS4), in order to determine differences in the patterns of variation within two rice mutants and control.

#### Experiment

Isolation of total genomic DNA for molecular marker analysis was carried out utilizing the cationic hexadecyl trimethyl ammonium bromide (CTAB) method of Weising et al.(1991) with small modifications. And amplification of DNA was performed by PCR method. Ten microsatellite primers were used in the experiment (see table III).

Table III. List of microsatellite markers used in the study. Marker designations are from Chen et al. (1997) and Temnykh et al. (2000)

Chromosome	Microsatellite Markers
	RM1
2	RM6, RM211
5	RM164, RM153
7	RM214, RM172
8	RM152, RM126, RM264

#### Results and discussions

The microsate primers (Table III) were used to amplify genomic DNA from control (KDML 105) and two mutants (BKOS6 and TKOS4) in order to determine their genetic variation. Figures 9-12 showed the amplification profiles generated by primers RM1, RM6, RM164 and RM211 across control plants and 2 population of rice mutants (BKOS6 and TKOS4), respectively. All ten microsatellite primers generated the reproducible and non-polymorphic DNA amplification patterns among the genomic DNA samples. The results showed the DNA patterns (molecular weights and number of bands) were not different between the control and the mutants, indicating that the mutants were the same variety as the control. They were not the contamination from other rice varieties.

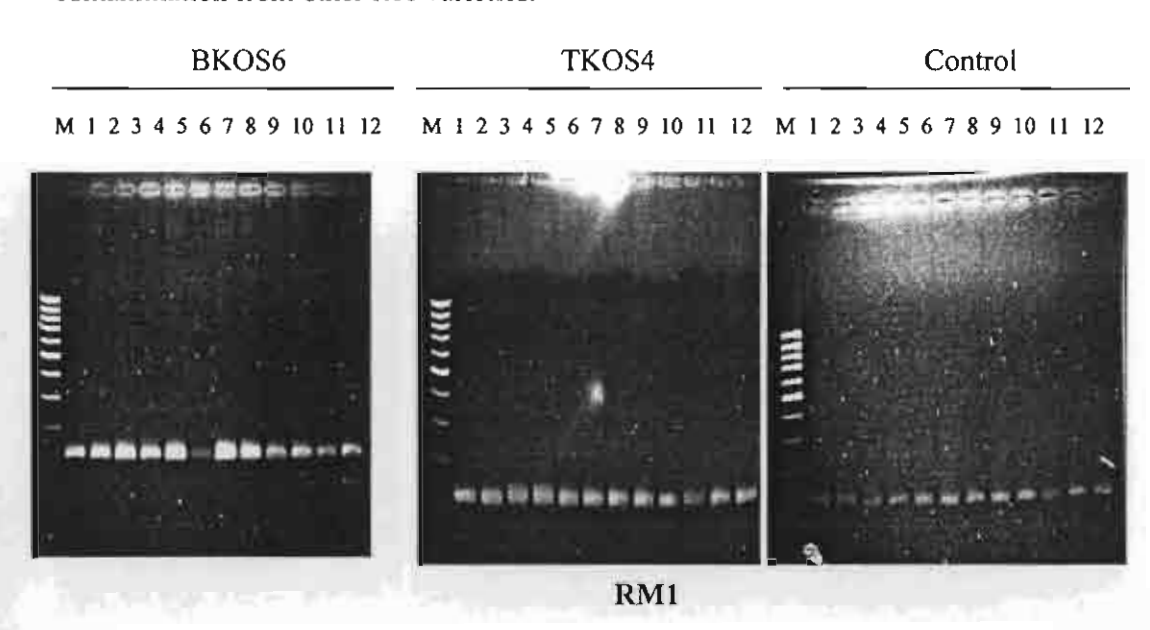
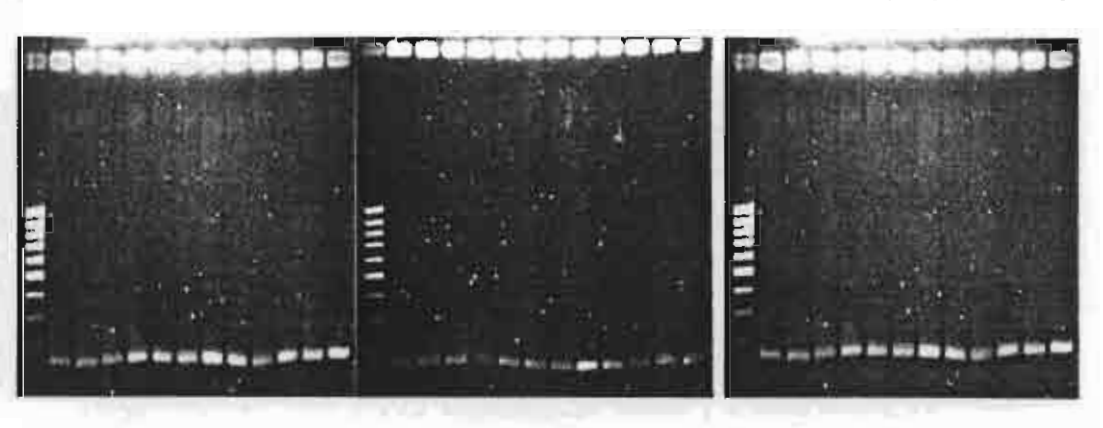


Figure 9. DNA fingerprinting pattern of *Oryza sativa* KDML105 generated by using the microsatellite primer RM1 (lane1-2: control, lane 3-12: mutant clones and lane M: 100 bp ladder)

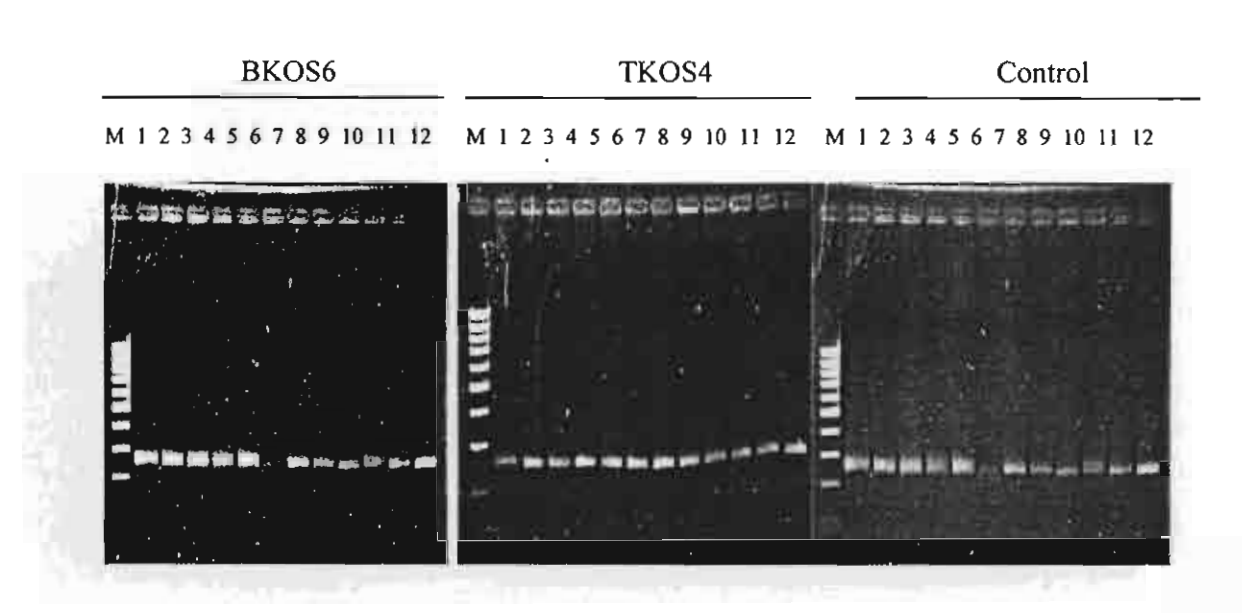
BKOS6 TKOS4 Control

M 1 2 3 4 5 6 7 8 9 10 11 12 M 1 2 3 4 5 6 7 8 9 10 11 12 M 1 2 3 4 5 6 7 8 9 10 11 12



#### RM6

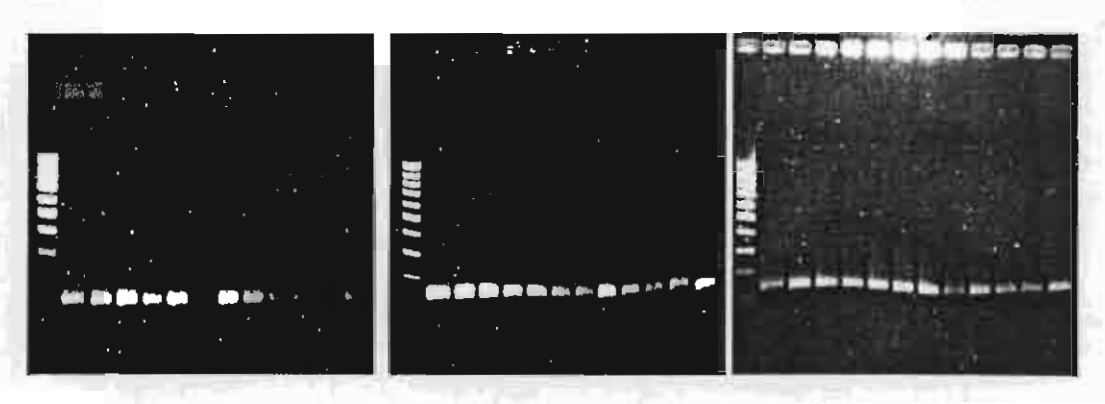
Figure 10. DNA fingerprinting pattern of *Oryza sativa* KDML105 generated by using the microsatellite primer RM6 (lane1-2: control, lane 3-12: mutant clones and lane M: 100 bp ladder)



#### RM164

**Figure 11.** DNA fingerprinting pattern of *Oryza sativa* KDML105 generated by using the microsatellite primer RM 164 (lane1-2: control, lane 3-12: mutant clones and lane M: 100 bp ladder)

M | 2 3 4 5 6 7 8 9 10 11 12 | M | 2 3 4 5 6 7 8 9 10 11 12 | M | 2 3 4 5 6 7 8 9 10 11 12



#### RM211

Figure 12. DNA fingerprinting pattern of *Oryza sativa* KDML105 generated by using the microsatellite primer RM 211 (lane1-2: control, lane 3-12: mutant clones and lane M: 100 bp ladder).

# 2.4 Investigation of characteristics of the mutants

Study on characteristics of the mutants such as gross appearance, culm length, seed size, etc., were carried out and discussed. The stability of the mutants in phenotypic and genotypic variations were tested in  $M_1$ - $M_5$  generations, in both inseason and off-season cultivations. Experimental results of the studies were shown in Table IV and Table V. The stability of the mutation was found in  $M_1$ - $M_5$  generations.

**Table IV.** Summarized data of the rice plants in  $M_4$  generation cultured in in-season cultivation. **Note:** Culm length was presented in centimeters, presented as an average value  $\pm SD$ .

Name	Date of seed cultivation (germination)	Date of Transplant Cultivation In plastic pot	Date of flowering	Date of harvesting	Culm length (at harvesting day)	Phenotypic variation
KDML 105 control	15/07/05	15/08/05	20/10/05	30/11/05	120.85±5.760	-
PKOS1	15/08/05	12/09/05	27/11/05	7/01/06	82.14±5.429	-Photoperiod insensitive -Short in stature
PKOS2	15/08/05	12/09/05	27/11/05	7/01/06	77.00±5.576	-Photoperiod insensitive -Short in stature
PKOS3	15/08/05	12/09/05	27/11/05	7/01/06	92.7±6.002	-Photoperiod insensitive -Short in stature
TKOS4	15/07/05	15/08/05	14/10/05	24/11/05	139.50±6.576	-Photoperiod insensitive -Early flowering -Tall variety
BKOS6	15/07/05	15/08/05	9/10/05	19/11/05	78.30±6.604	-Photoperiod insensitive -Early flowering -Short in stature

**Table V.** Data\* (Average value  $\pm$  SD) of panicle number, panicle length, branch number, spikelet number/panicle, culm length, and seed size, in M<sub>4</sub> generation of the mutants, "cm" refers to centimeters.

Rice plants	Panicle number/plant	Panicle length (cm)	Branch Number	Spikelet No./panicle	Seed size** (Width x
				·	Length x thickness)
Control	16±3	30.21	12±2	113±43	2.46±0.107
		±1.710			10.30±0.482 1.78±0.151
PKOS1	31±3	26.79 ±1.157	10±1	127±14	2.58±0.180 10.25±0.638
					2.14±0.084
PKOS2	30±5	27.02 ±1.095	10±1	132±11	2.50±0.162 9.79±0.661
PKOS3	23±3	27.465	10±1	134±18	2.05±0.113 2.48±0.179
		±1.469			9.84±0.572 1.98±0.161
TKOS4	11±2	28.72	10±1	120±17	2.22±0.141
		±1.724		_	10.08±0.359 1.91±0.061
BKOS6	18±3	25.26± 2.156	8±1	65±12	2.47±0.145 9.76±0.337
					1.87±0.107

<sup>\*</sup>Plants were cultured as 1 seedling/ plastic pot. Data was analyzed from 20 raw data. \*\*
Presented in millimeters.

# 3. Experiments carried out in 2006

#### 3.1 Detection of 2AP level and cooking quality in the mutants

After harvesting for 6-8 months, five rice mutants collected from M<sub>3</sub> generation (TKOS4, BKOS6, PKOS1, PKOS2, and PKOS3) as well as KDML 105 (M<sub>2</sub> generation) were tested for aromatic fragrance, softness, viscosity, and feature of rice seed. Score were set as 1,2,3,4, and 5, representing the degree of satisfaction ranging from the lowest to the highest scores, respectively. Random selection of 6 consumers from our lab were requested for cooking quality test. In order to compare to the KDML 105 the well cooked mutants rice were eaten and scored by the chosen consumers regarding to the indicated scored. 2AP (2-acethyl-1-pyrroline) was measured in the mutants and the control by GC technique using facilities at the Department of Chemistry, Faculty of Science, Chiang Mai University.

# Result and discussions

The results of the cooking quality in the rice mutants in M<sub>3</sub> generation (cultured in off-season period) compared with the KDML 105 in M<sub>2</sub> generation (cultured in in-season period) indicated that the satisfaction of consumers of the rice mutants was close to that of the KDML 105 control (Table VI).

Table VI. Score value in the cooking quality test in the mutants and KDML 105.

	TKOS4	BKOS6	PKOS2	PKOS3	KDML 105	PKOS1
Aromatic* fragrance	16	16	16	22	22	18
Softness	19	18	16	20	26	25
Viscosity*	20	26	23	20	21	20
Feature*	23	26	23	18	22	21
Total score	78	86	78	80	91	84

<sup>\*</sup> Data presented in the summation of six scores

The amount of 2AP in all rice seeds was shown in Table VII, indicating that PKOS1, PKOS2, PKOS3, TKOS4 and SKOS5 contain lower level of 2AP than that of the control and 2AP level was not detected in BKOS6.

**Table VII.** Comparison of 2AP concentration in rice seeds (kept in plastic back for around 6 months after harvesting) of the rice mutants and control measured by the GC method.

Sample	Amount (g)	Peak area of 2,6- DMP	Peak area of 2AP	Peak area ratio of 2AP/2,6- DMP	Average	SD	%RSD	Conc. of 2AP in rice sample
								(µg/g)
Control	100	1705.33	574.99	0.34	0.32	0.02	5.56	1.65
	100	1977.23	616.21	0.31				
PKOS1	100	1727.15	274.43	0.16	0.16	0.00	0.17	0.67
	100	1823.22	290.39	0.16				
PKOS2	100	1775.31	237.20	0.13	0.13	0.00	0.46	0.53
	100	1703.84	229.15	0.13				
PKOS3	100	1708.90	347.85	0.20	0.21	0.01	2.87	0.96
	100	1535.48	325.93	0.21				
TKOS4	100	2056.63	454.42	0.22	0.23	0.01	4.88	1.08
	100	2200.91	521.04	0.24				
BKOS6	100	1457.89	0.00	0.0000	0.0000	0.0000	0.0000	0.00
	100	1566.03	0.00	0.0000				

# 3.2 Effects of ion beam bombardment on KDML 105 cell surface and study on the accumulation of anthocyanins in BKOS6 plant tissues

The aims of the experiments were to study the effects of ion beam bombardment on the cell surface of KDML 105 rice seeds. And to study on the accumulation of anthocyanins in BKOS6 rice plants.

#### Materials

Seeds of *Oryza sativa* L cv. KDML105, BKOS6 rice plants, KDML 105 rice plants, and non mass-analyzed 150 kV ion implanter were used in the experiments.

#### **Experiments**

The seeds of KDML 105 were husked and fixed in the holders. The seeds were bombarded with N<sub>2</sub><sup>+</sup>+N<sup>+</sup> ions at the ion energy of 60 keV with the ion fluence of 2x10<sup>16</sup> ions/cm<sup>2</sup>. Bombarded-rice seeds were fixed on the holder. Seeds were sputter coated with gold particles in the Denton sputter coater and examined with a JEOL 5800 LV SEM operating at 15-kV accelerating voltage. Images were digitally recorded. Physiological changing on the cell surfaces of ion bombarded rice embryos was compared with that of the un-bombarded control.

BKOS6 and KDML 105 plant tissues such as root, leaves, leaf sheath, hull, husked seeds, etc., were observed.

#### Results and discussions

### Effect of ion beam bombardment on the rice embryo cell surface

Figure 13. A, B and C show a scanning electron micrograph image of the surface of untreated rice embryo cell. Figure 13, D, E and F shows another SEM image of a cell surface, which treated with an  $N^++N_2^+$  ion beam from an Advanced Energy Linear Ion Source. The treatment conditions were an applied voltage and dose of 60 keV and  $2x10^{16}ion/cm^2$ . From this image, it is clear that the surface topography has been significantly altered, the treated cell surface now much rougher and several surface features visible in the SEM. From the Figure 13E (arrow), the "channel" causing by ions was observed in the bombarded rice sample, this may be the entrance of the cascade ions to induce mutation in rice embryo.

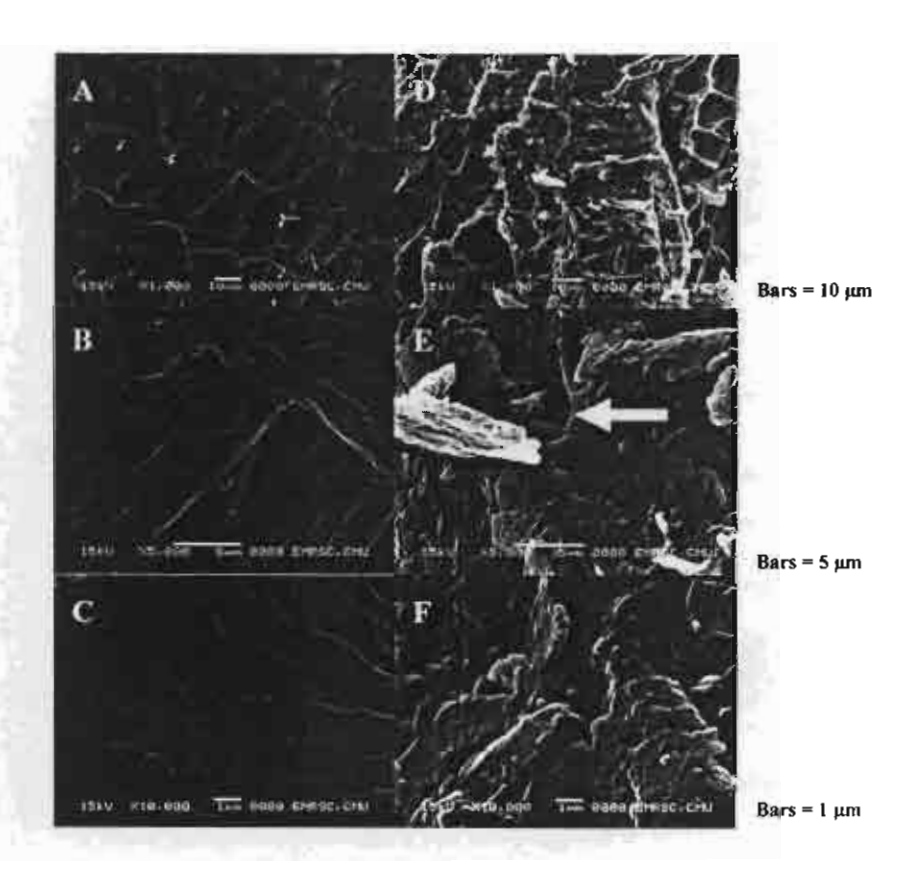


**Figure 13.** Effect of ion-beam bombardment on the morphology of seed embryo cells **A, B, C**; SEM images of untreated embryo cell surface of KDML105 at 1000, 5000 and 10000 times magnification, respectively.

D, E, F; SEM images of embryo cell surface treated with N<sup>+</sup>+N<sub>2</sub><sup>+</sup> ion at 1000X, 5000X and 10000X, respectively. Arrow indicates the "channel" caused by ion beam bombardment.

# Distribution of the accumulation of anthocyanins in BKOS6 rice tissues

Figure 14, A through C, illustrated the mutant (BKOS) phenotypes compared with the wild-type (WT, KDML 105) plant. The mutant has extremely purple color in immature-seed, auricle, stem, root, husked and de-husked mature seed. In addition, cross section of auricle of mutant showed the accumulation of anthocyanins inside the cells.

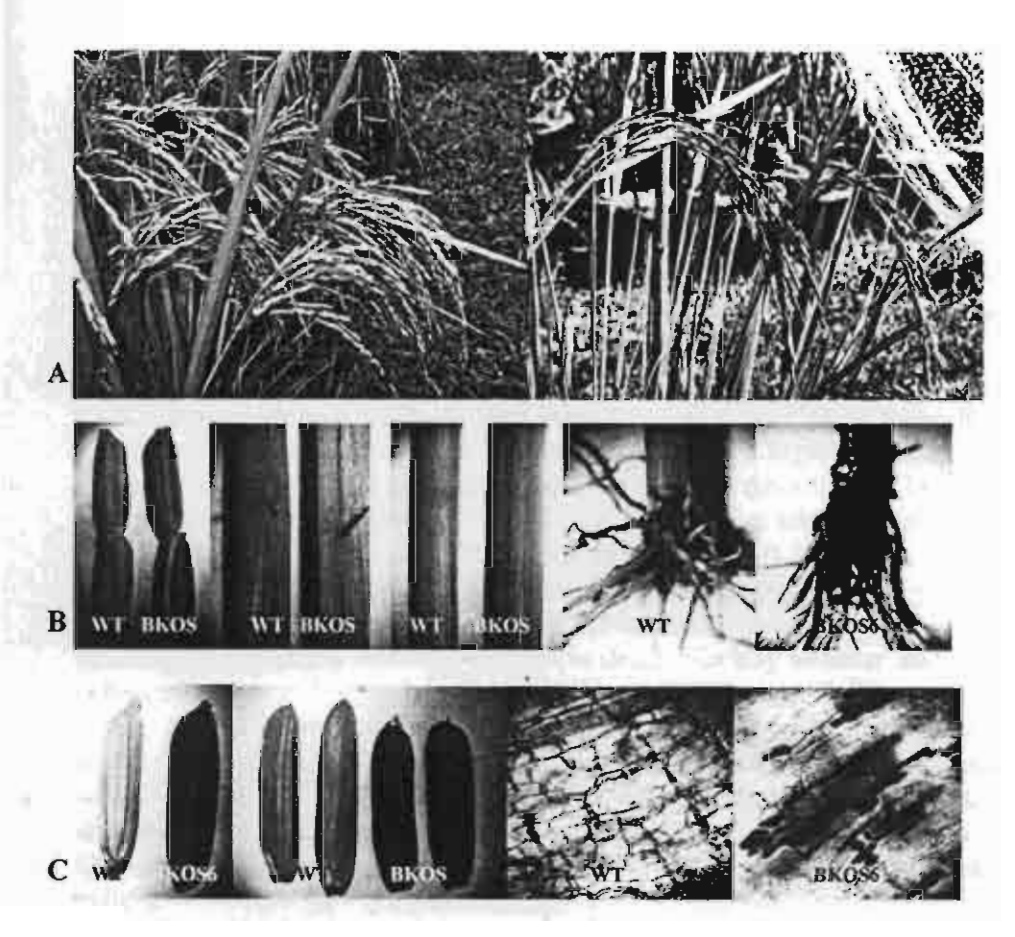


**Figure 14.** Comparison of gross appearance and accumulation of anthocyanins in rice plant tissues of KDML105 and BKOS6.

# **Chapter III**

# Subproject III: Low energy ion beam induced mutation in flower crops.

#### Final Report

In this final report the research team would like to describe the effect of low energy ion beam on three main flowering crops, i.e. petunia, chrysanthemum and rose.

#### Activities

#### 1. Rose

#### 1.1 Introduction

In our first and second progress reports, in February and August 2004, the research team reported the attempt to induce mutation in rose by using low energy ion beam. We used the variety "Black Magic" and the new hybrid of the Royal Project Foundation (RPF). The node section wrapping with small piece of parafilm exposed only the axillary bud used. The scale leaves were also removed from each bud. After bombardment the buds were grafted on the stock plants, Rosa multiflora. When the bud started to grow, the stock plants above the buds were removed to promote growth of the buds. Plants with well establishment were later on moved to Inthanon Research Station, 1,200 meters above sea level, as low temperature in the highlands enhanced plant growth and early blooming. The first flower which generated from the ion beam bombarded bud was observed for any kind of changes. The plants were later on cut back to induce new flush for further observation of the flower mutation.

In those experimental work the research team has learnt a lot about the sample preparation technique, the dose and the method to take good care of the plants eventhough mutations were not be able to detect visually whether leaf chimera or flower colour mutation.

However the research team still have the intention to research on rose plant and trying to improve the technique. Therefore in this last year of our research we aimed to work with the low land variety to avoid moving plants to the highlands. We decided to choose variety "Ingrid Bergman" (Figure 1) which was supplied by the nursery Ban Thor, Muang District, Chiangmai Province. The elevation where the plant was grown is 300 meters.



Figure 1 Rose variety Ingrid Bergman

#### 1.2 Material and method

In this last experiment, the nodal buds along the fully opened flower stem were once again used, but the scale leaves which cover the meristem of the buds were not removed as it was found out that it caused damage to the meristem region and reduced the successful rate of grafting. Parafilm was still used as wrapping material to prevent the lost of water content of the nodal bud sections. The samples were bombarded with nitrogen ion  $1\times10^{16}$  and  $4\times10^{16}$  ions/cm<sup>2</sup> at 60 KeV under vacuum condition (Figure 2). After bombardment the parafilm was removed from the sample and allowed them to return to their freshness by soaking them in water for several hours before the buds were removed from the nodal section and grafted on "Rosa multiflor" for further growth (Figure 3). The experimental plants were grown in the plastic open house in order to provide the best conditions for the plant growth (Figure 4).

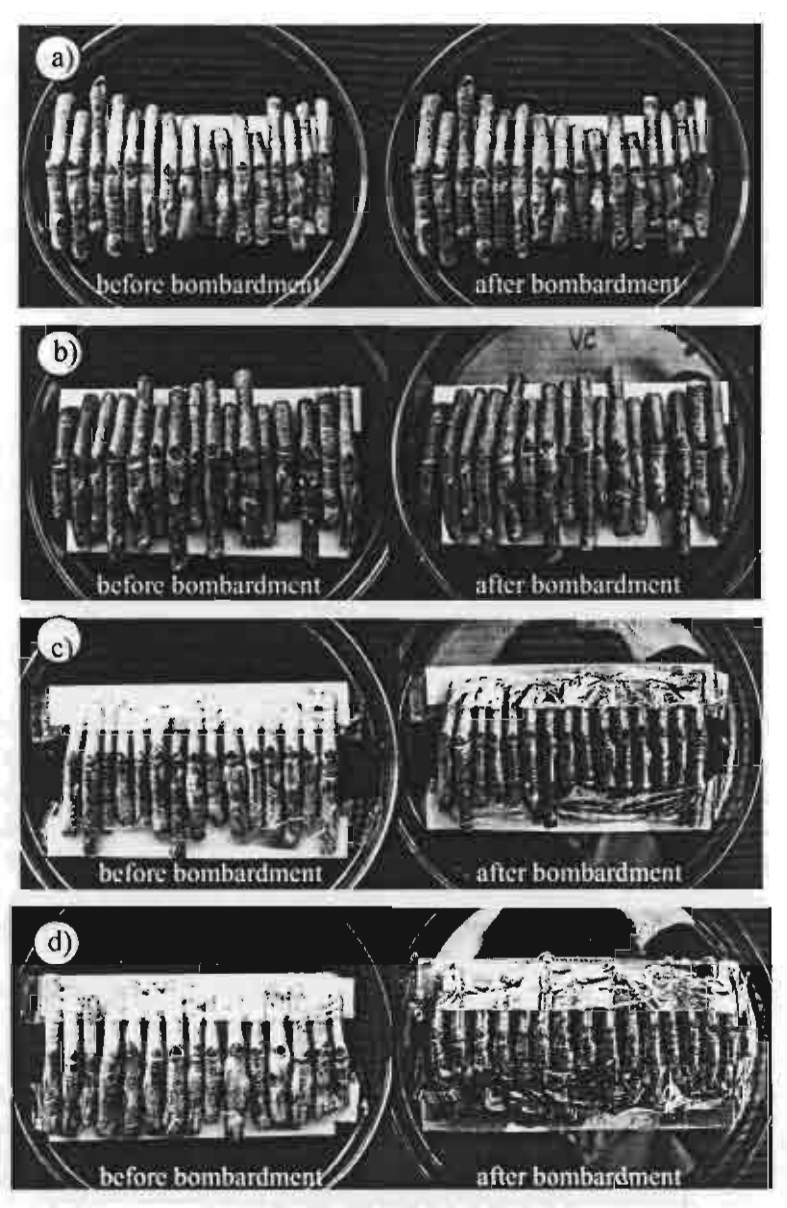


Figure 2 The preparation of rose buds for bombardment with nitrogen ion beam.

a) Natural control b) Vacuum control c) 1x10<sup>16</sup> ions/cm<sup>2</sup> d) 4x10<sup>16</sup> ions/cm<sup>2</sup>







Figure 3 Grafting of the treated bud onto the root stock.

a) remove the bud from the nodal section and the stock plants used b) after grafting c) growth of buds, 45 days after grafting

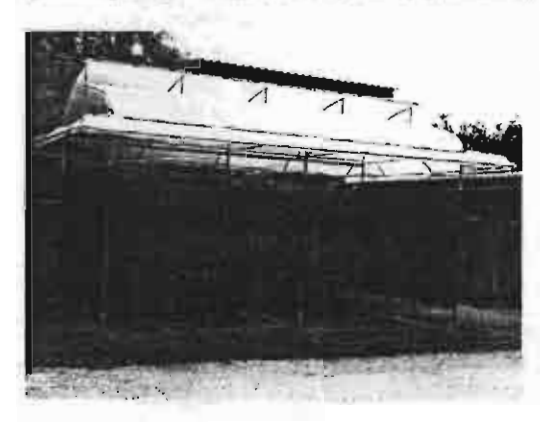


Figure 4 Experiment plastic open house.

#### 1.3 Results

#### 1.3.1 The effect of ion beams on the survival rate of bombarded

#### buds.

Five weeks after grafting the plastic strip that used to wind around the bud against the stock plants was removed in order to allow the bud to sprout. The colour of the bud was a good indicator to tell if the bud was still viable or not. According to our observation (Table1), buds under vacuum condition had less survival percentage than the controlled group (69.2 VS 96.2). Buds being bombarded with ion beams had also lower survival percentage than the controlled and also the vacuum controlled, the higher the dose the lesser the survival percentage.

Table 1 Viability of rose buds bombarded with nitrogen ion beams at various doses.

Treatment	Replication	Viability				
Treatment	Replication	Number	Percentage			
Natural Ctrl.	52	50	96.2			
Vacuum Ctrl.	65	45	69.2			
1x10 <sup>16</sup> ,60KeV	90	53	58.9			
4x10 <sup>Th</sup> ,60KeV	90	48	53.3			

#### 1.3.2 The effect of nitrogen ion beams on flower colour

The flowers which appeared at the terminal of the stem generated from the buds bombarded with ion beams did not show mutation, leaf chimera was also not found. In general plant growth from each treatment looked similar.

It is well known among the mutation breeders that "cutting back" technique could promote the appear once of mutation of vegetatively propagated plants. Therefore, the rose plants were cut back leaving 2-3 nodes at the base of each stem and the flower colour which appeared at the terminal of the new branches were continuously observed. It was found out that 1 branch from the plant receiving ion beam at 1x10<sup>16</sup> ions/cm<sup>2</sup> had paler colour than the controlled (Figure 5). The petals also showed wrinkle character (Figure 6).



Figure 5 Changing in flower colour of rose variety Ingrid Berman (left) control (right) plants generated from bud receiving nitrogen ion beam at 1x10<sup>16</sup> ions/cm<sup>2</sup>, 60 KeV.



Figure 6 The wrinkle petals of rose mutant receiving ion beam at 1x10<sup>16</sup> ions/cm<sup>2</sup>, 60 KeV.

#### 1.3.3 Conclusion

Ion beam could induce mutation in rose in terms of flower colour and petal characters. Though the percentage of the mutation was low, 1.1% (1 branch out of 90 branches), the mutated character can be vegetatively propagated. More work need to be done to increase higher more new characters and higher mutation rate.

#### 2. Petunia

#### 2.1. Introduction

In previous experiments reported in our 1 - 4 progress reports, we mainly emphasized on the finding for the proper techniques in order to bombard the seeds with nitrogen ion beams to induce mutation in both seeds with and without seed coat. We found that ion beams reduced the seed germination. Flowers with various shapes, leaves and petals were observed.

In this final report the research team would like to report on the culture of irradiated seed aseptically.

#### 2.2. Results

Seeds under aseptic conditions germinated within 3-7 days. Ion beam did not affect the germination percentage but the seedlings showed sign of abnormalities at the 4-6 leaf stage. The abnormal plants had abnormal leaf shape, rough leaf surface, pale green leaf and stunted growth (Table 2 and Figure 7).

**Table 2** Germination percentages and seedling abnormalities of petunia 3 weeks after seeds were bombarded with nitrogen ion beams at various doses, at 60 KeV.

<b>D</b>	Germination	Normal	Abnormal seedlings						
Dose	percentage	seedlings	Leaf shape and texture	Stunt in growth	Immature seedlings				
Control	83	83	-	-	-				
1x10 <sup>16</sup>	99	77	14	7	1				
2x10 <sup>16</sup>	94	<b>8</b> 7	4	0	3				
$4x10^{16}$	100	75	22	2	1				
6x10 <sup>16</sup>	97	82	8	6	1				
8x10 <sup>16</sup>	97	72	21	2	2				
10x10 <sup>16</sup>	100	89	11	0	1				

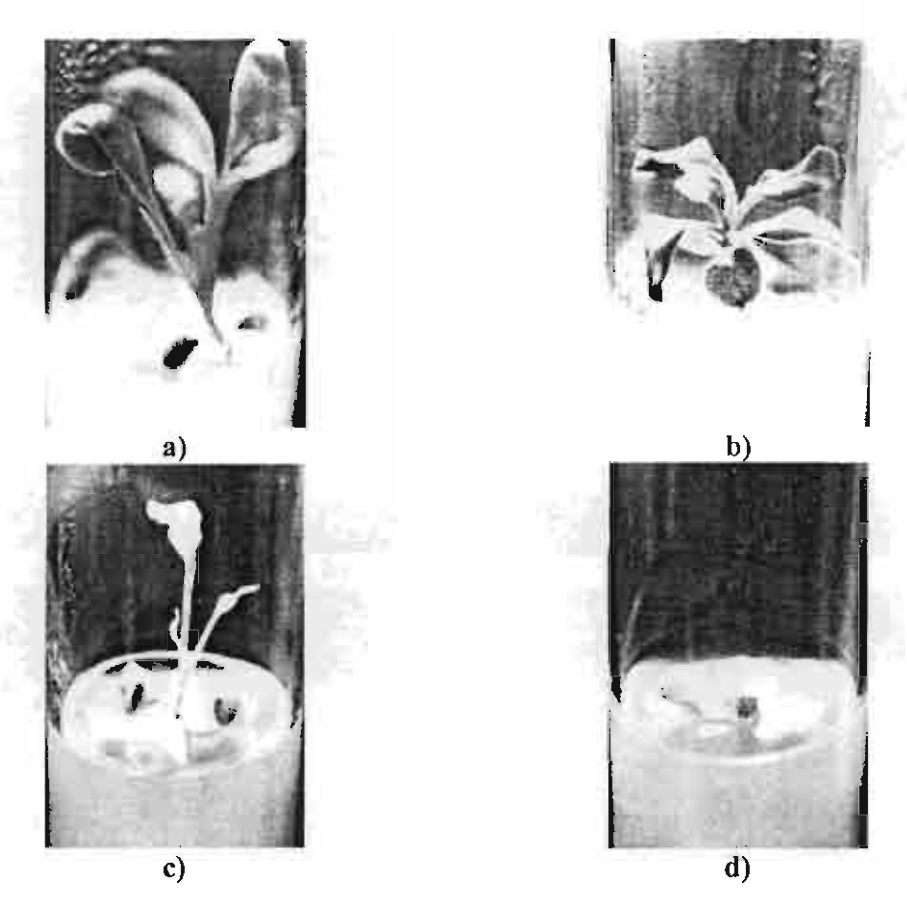


Figure 7 Abnormalities of seedlings.

a) abnormal leaf shape b) rolled leaf c) pale green leaf d) unhealthy seedlings

At the end of the cultural period under aseptic conditions (8weeks), the seedlings were potted. Though the survival percentages were satisfactory (Table 3), but the abnormal seedlings were still found (Figure8).

Table 3 Germination percentages and seedling abnormalities of petunia, 8 weeks after seeds were bombarded with nitrogen ion beams at various doses, 60 KeV.

_	Germination	Abnormal seedlings							
Dose	percentage	Leaf shape and texture	Stunt in growth	Immature seedlings					
Control	83	-	-	-					
$1x10^{16}$	99	9	13	1					
$2x10^{16}$	94	2	5	3					
$4x10^{16}$	100	11	15	1					
6x10 <sup>16</sup>	97	0	13	1					
$8x10^{16}$	97	1	9	2					
10x10 <sup>16</sup>	100	4	7	1					

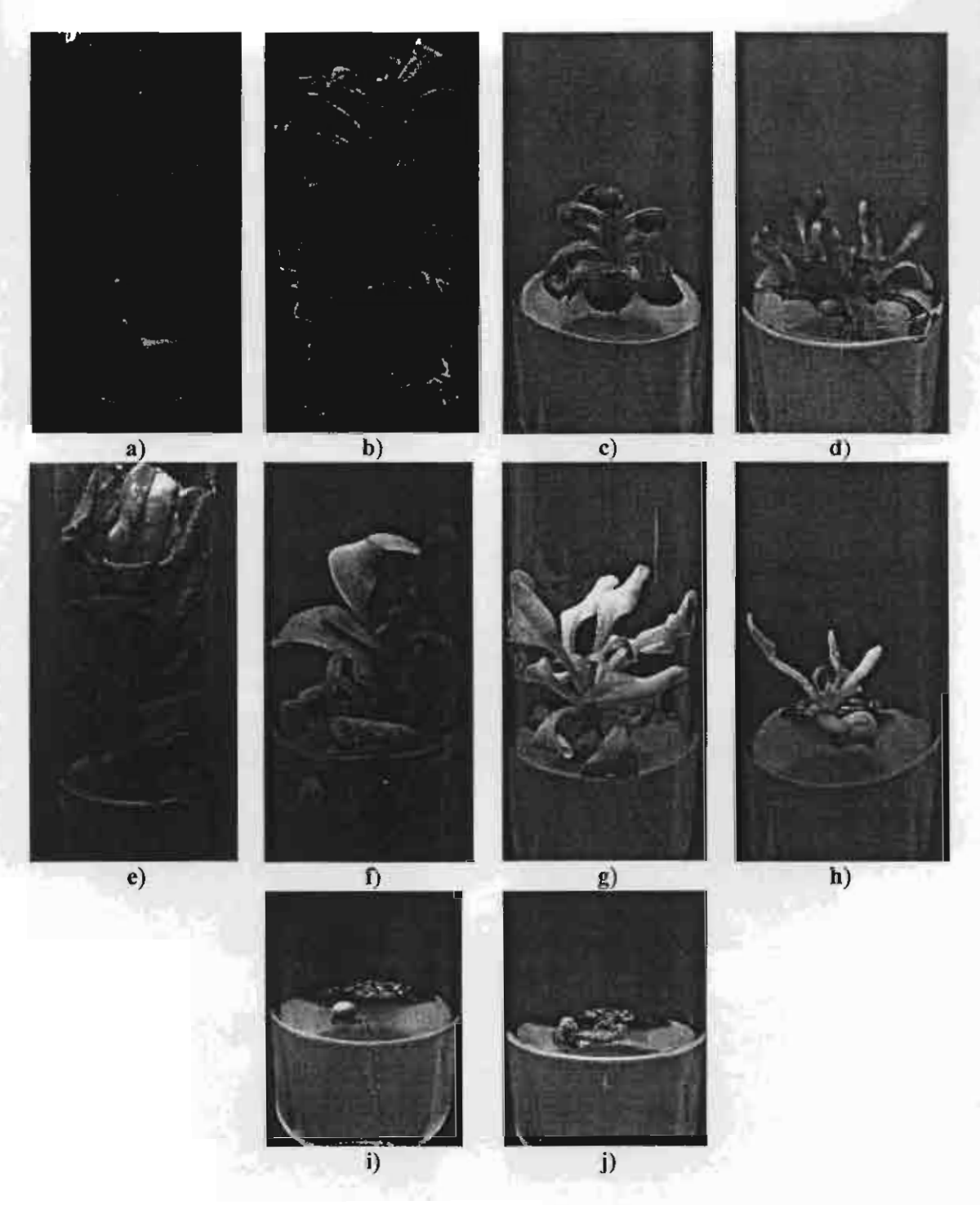


Figure 8 Conditions of the petunia seedlings 8 weeks after seed culturing.

a) normal seedling b) seedling with slim leaves c) rolled leaves d) dwarf seedling

e) large leaves f) rough surface g) yellow leaf h) lacking of chloroplast

i and j) unhealthy seedling

The potted seedlings were acclimatized and then transferred to the greenhouse for flowering. During acclimatization some plants died, however several mutations were received from plants receiving ion beams (Figure 9).

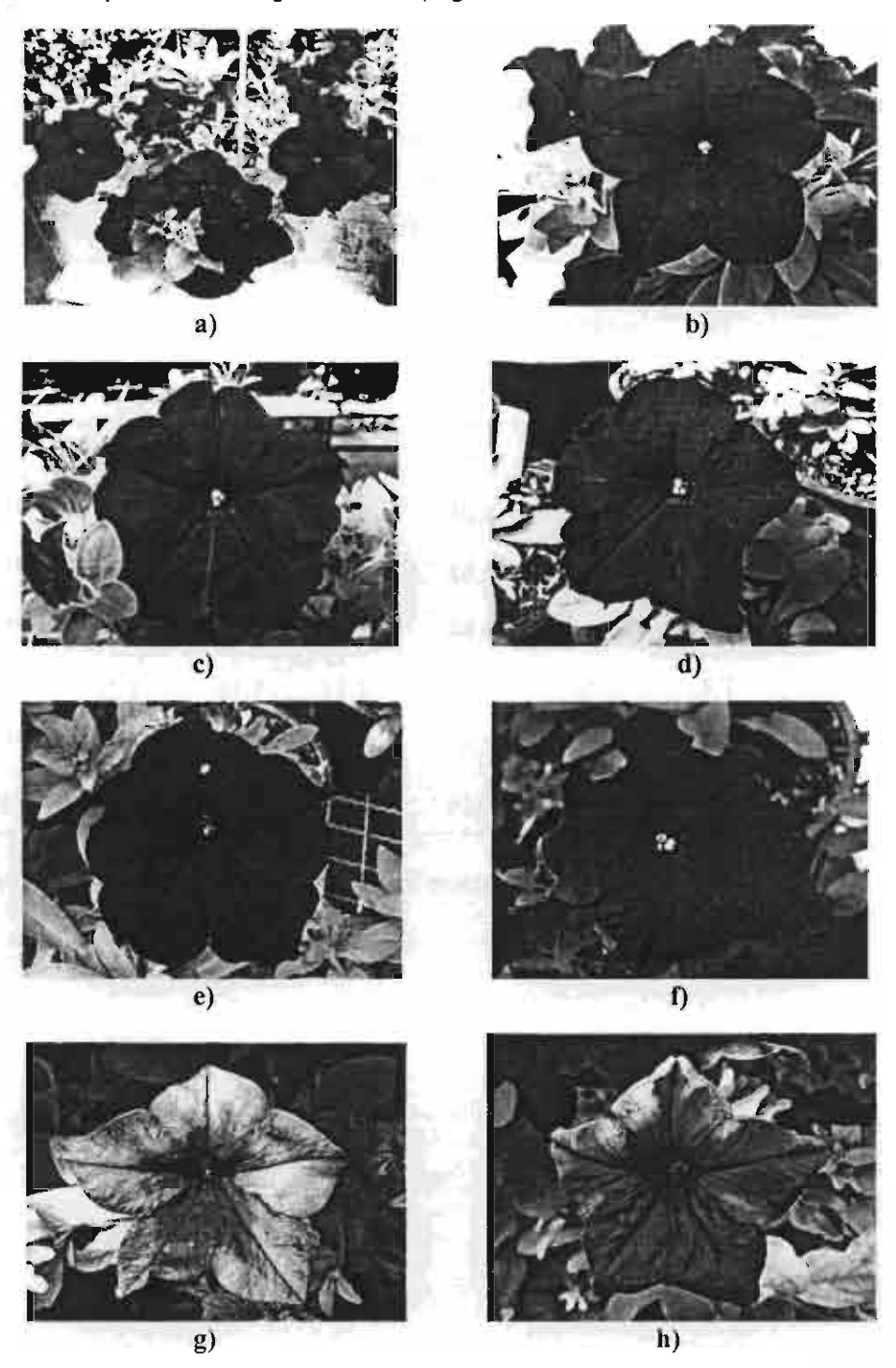


Figure 9 Characters of flower mutation petunia.

a) and b) controlled c) white strip on petal d) variegated flower e) white spot on petals

f) ununiform petal colour g and h) pale flower colour

Apart from colour mutation, mutants in terms of leaf shape were also found (Figure 10). It is worth mentioning that for the mutation characters some appeared only in certained branches some appeared only few flowers, and some flowers contained few characters. The details of the mutation were presented in Table 4.

**Table 4** Percentages of mutation types found in plants generated from seeds bombarded with ion beams under aseptic condition.

	Type of flower mutation *										
Dose	variegated strip		white dots	pale ununiform colour colour cut the rim		pale colouur	anther change into small petal	change in size			
Control	-	-	-	-	-	-	-	-			
1x10 <sup>16</sup>	53.8	43.6	10.2	56.4	33.3	12.8	2.6	2.6			
2x10 <sup>16</sup>	40.4	19.1	10.6	46.8	31.9	6.4	6.4	0			
4x10 <sup>16</sup>	44.4	22.2	8.3	44.4	25.0	8.3	2.8	2.8			
6x10 <sup>16</sup>	61.1	41.7	11.1	61.1	38.9	16.7	0	0			
8x10 <sup>16</sup>	59.0	41.0	28.2	48.7	20.5	7.7	0	2.6			
10x10 <sup>16</sup>	51.0	46.9	12.2	63.3	49.0	24.5	0	6.1			

<sup>\*</sup> one flower may contain several types of mutation.

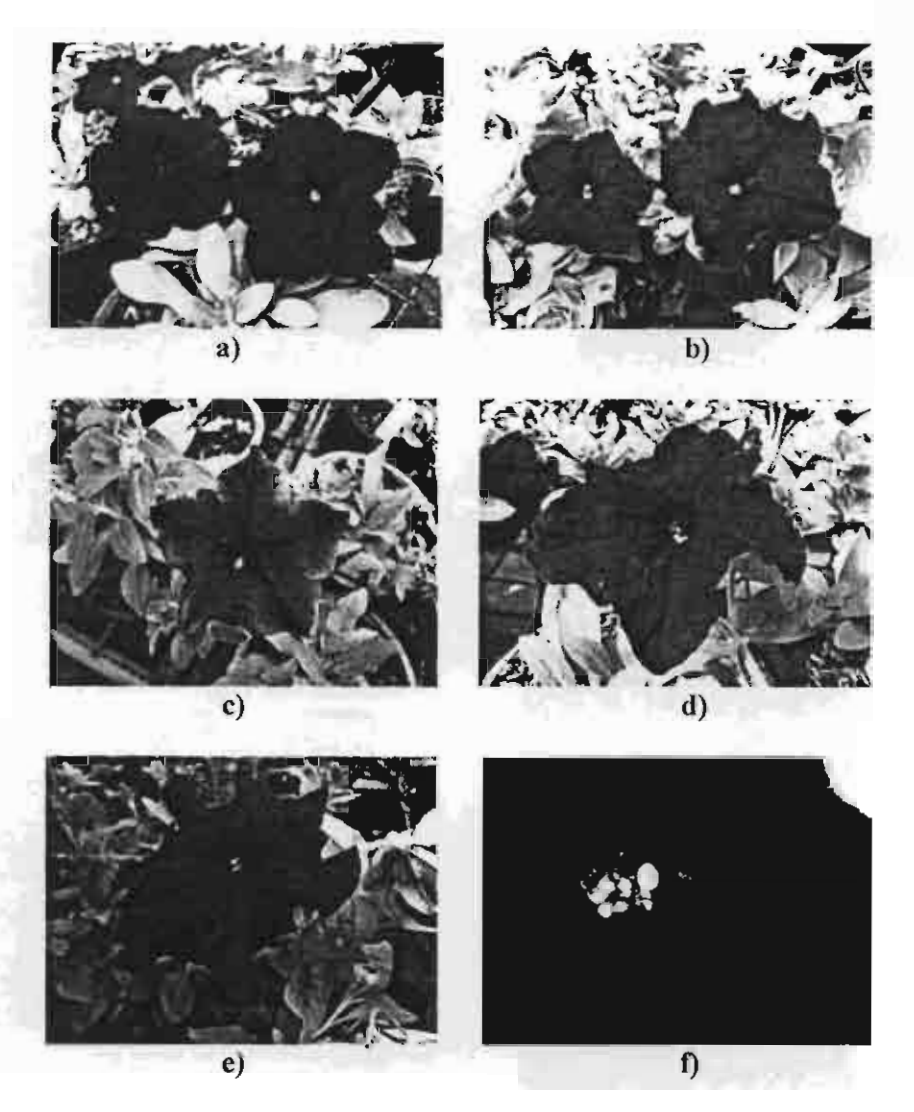


Figure 10 Various shapes of flowers derived from plants generated from the seeds bombarded with nitrogen ion beams.

a) round shape flower b) flower with small size c) star shape

d) long petal e) rolled petal f) anther change into petal

### 2.3. The study on the stability of the mutant

It is well known amongst the mutation breeders that mutated characters observed in the M1 generation can be induced through the malfunction of the physiological system on the genetical system of the plants. For the mutation caused by physiological system, e.g. the phyllotaxy or the leaf shape will be temporary and can soon turn back to normal during the plant development, and it is expected that the repair mechanism of the cell plays an important role. The changes in DNA whether they are due to chromosome aberration or gene mutation will be inherited which are wanted by the breeders.

During the course of this research, the research team selected the attractive mutants especially the flower shape, 14 mutants were finally selected and then tissue cultured using shoot tip. The plantlets were planted and observed in the same manner as mentioned above.

It was found out that the mutants vegetatively propagated by tissue culture appeared to be true to type which proved the mutants were caused by the change in the chromosome (Figure 11).

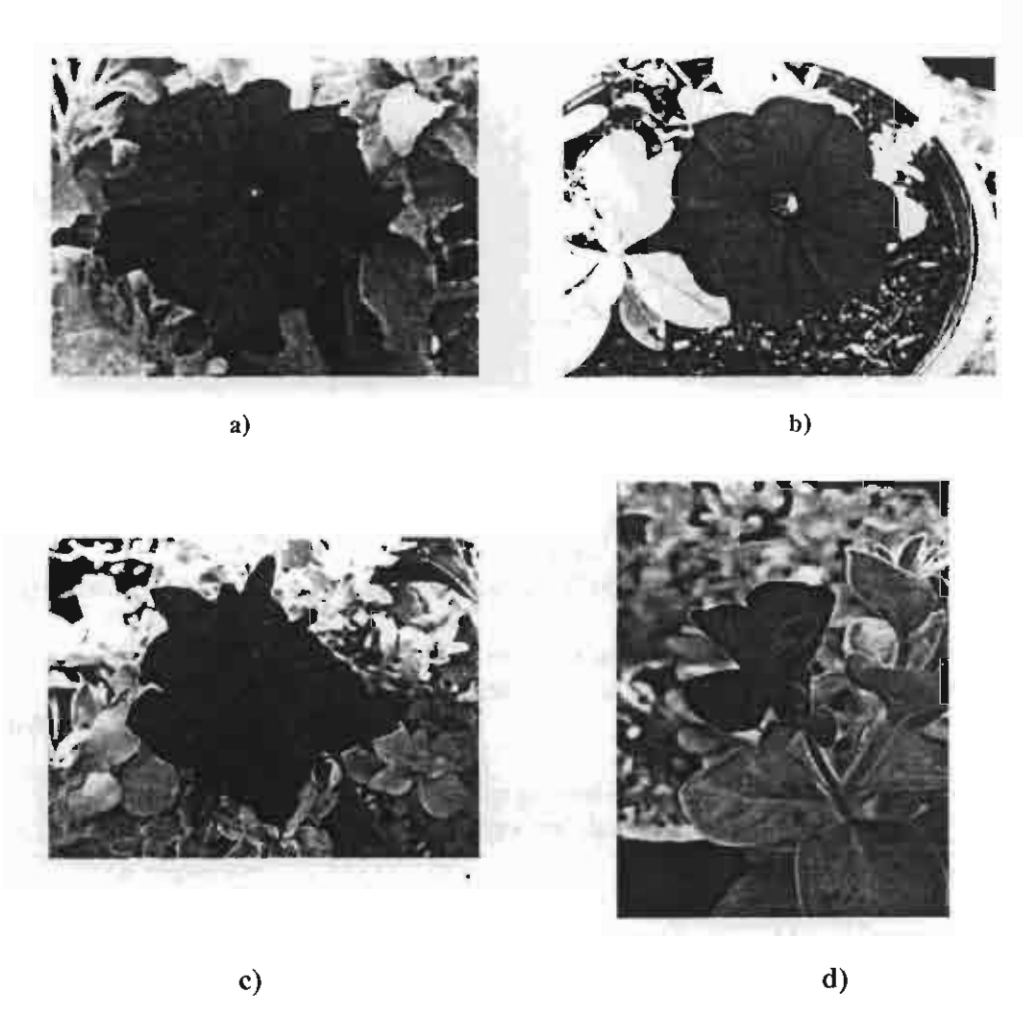


Figure 11 Vegetatively propagated of the mutation using tissue culture came true to type.

a) variegated flower b) round shape c) wrinkle petal d) pea shape flower

The research team was very much interested in the pea shape type of petunia flower mutants as they look quite attractive. The cause of the change in flower shape was investigated by the longitudinal section both the controlled and the mutants. After observation under under stereo microscope the research team found the shrinkening of the corolla (Figure 12).

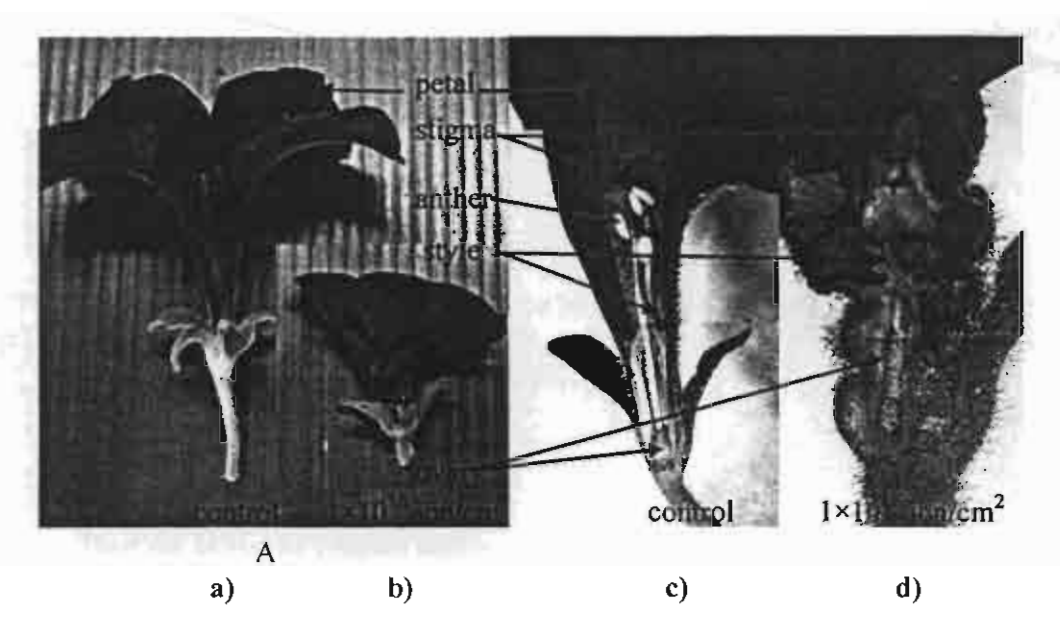


Figure 12 Flower mutants of petunia resulting from the bombardment of seeds by nitrogen ion beam at 1×10<sup>16</sup> ion/cm<sup>2</sup>

a) control b) mutant c) longitudinal section of control d) longitudinal section of mutant

# 2.4. The identification of the mutants by RAPD.

Twenty four mutants were selected for the identification at the molecular level as follows.

Leaf tissue (0.5 g.) was ground with mortar and pestle DNA was extracted using 2x CTAB

Eleven primers, which were OPA 01 OPA 04, OPA 05, OPA 07, OPA 08, OPA 09, OPA 10, OPA 11, OPA 14, OPA 15 and OPA 16 (Operon technology Alamada, USA), were used to characterize polymorphisms among the 24 petunia mutants

DNA amplification was performed in a DNA thermal cycle as follows: one cycle of 3 min at 94 °C; 28 cycles of 1 min at 94 °C. 1 min at 50 °C and 3 min at 74 °C; followed by one cycle of 1 min at 72 °C

The PCR-amplified products were separated by electrophoresis on 2.0% (w/v) agarose gel followed by staining in ethidium bromide, and visualized and photographed under UV light.

Four out of eleven primers demonstrated DNA polymorphic bands in the range of 550-3120 base pairs. Primer OPA 04 showed 13 bands, 7 of which were monomorphic bands and the others were polymorphic bands. Banding patterns of 8 mutants (lane 4, 6, 8, 10, 11, 12, 13, 14 and 17) were different from the control. Characters of plants and flowers were shown in figure 14.



Figure 13 DNA banding patterns of the controlled and the mutants of petunia using OPA 04 as a primer. Black arrows showed polymorphic bands and white arrows showed band from each mutant that were different from control. (Lane 1: control, Lanes 2-24: mutants)

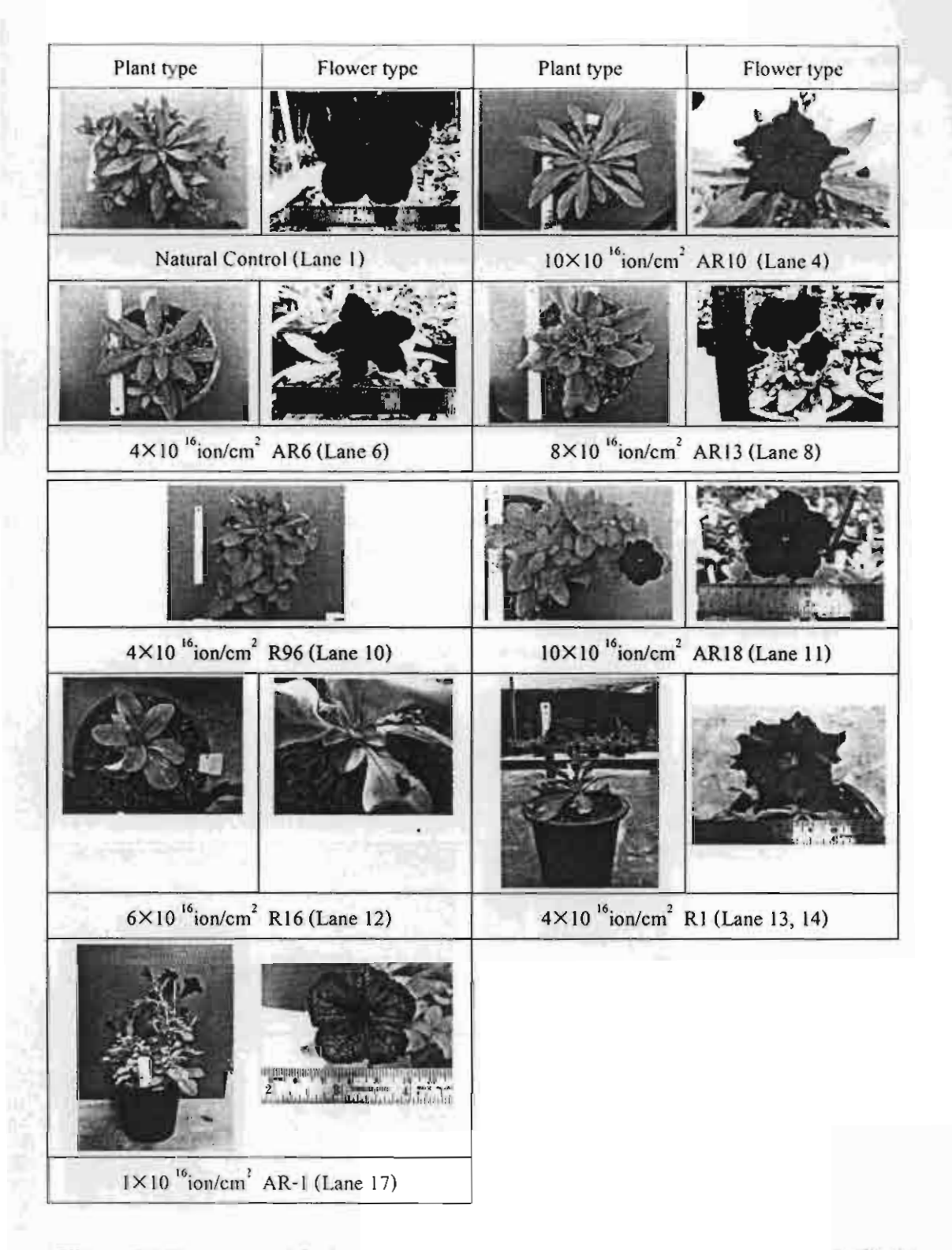


Figure 14 Characters of the indicated lanes in parenthesis refered to the mutants in figure 13.

DNA amplification using OPA 07 resulted in 7 bands, 5 monomorphic and 2 polymorphic, ranging from 700 to 3120 bp (figure 15). Five mutants that showed different patterns when compared to the control were lane 2, 6, 7, 12, 13 and 14.

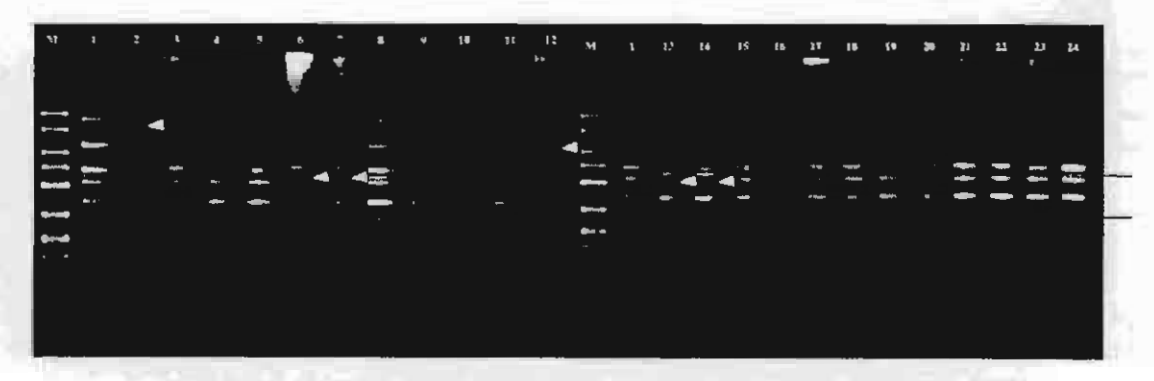


Figure 15 DNA banding patterns of the controlled and the mutants of petunia using OPA 07 as a primer. Black arrows showed polymorphic bands and white arrows showed band from each mutant that were different from control. (Lane 1: control, Lanes 2-24: mutants)

Plant type	Flower type	Plant type	Flower type
Natural Co	ntrol Lane 1	1×10 16 ion/cr	n <sup>2</sup> AR27 Lane 2
4×10 16 ion/cn	n <sup>2</sup> AR6 Lane 6	4×10 16 ion/c	m <sup>2</sup> AR26 Lane 7
6×10 16 ion/cm	<sup>2</sup> R16 Lane 12	4×10 16 ion/cm	n <sup>2</sup> R1 Lane 13, 14

Figure 16 Characters of the indicated lanes in parenthesis refered to the mutants in figure 15.

DNA banding patterns in the range of 320-2650 base pairs from primer OPA09 were presented in figure 17. Using this primer, the control plant showed only 1 band while several bands appeared on the mutants. Mutants characters represented DNA patterns in lanes 4, 6, 8, 12, 13, 14, 20, 21, 22 and 24 were shown in figure 18.

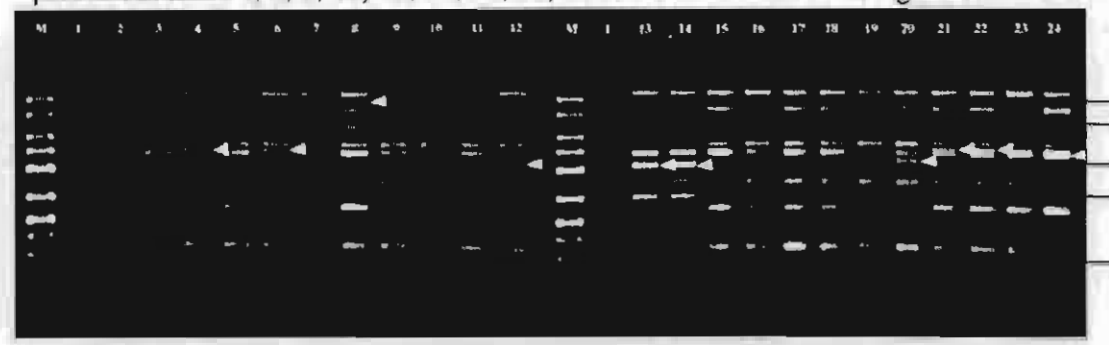


Figure 17 DNA banding patterns of the controlled and the mutants of petunia using OPA 09 as a primer. Black arrows showed polymorphic bands and white arrows showed band from each mutant that were different from control. (Lane 1: control, Lanes 2-24: mutants)



Figure 18 Characters of the indicated lanes in parenthesis referred to the mutants in figure 17.

The primer OPA 10 gave rise to 13 DNA bands where 10 were monomorphic and 3 were polymorphic with the DNA size between 250-2670 base pairs. Six types of mutation could be identified from lanes 6, 7, 12, 13 and 14 (Figure 19) and the characters of the mutants were shown in Figure 20.



Figure 19 DNA banding patterns of the controlled and the mutants of petunia using OPA 10 as a primer. Black arrows showed polymorphic bands and white arrows showed band from each mutant that were different from control. (Lane 1: control, Lanes 2-24: mutants)

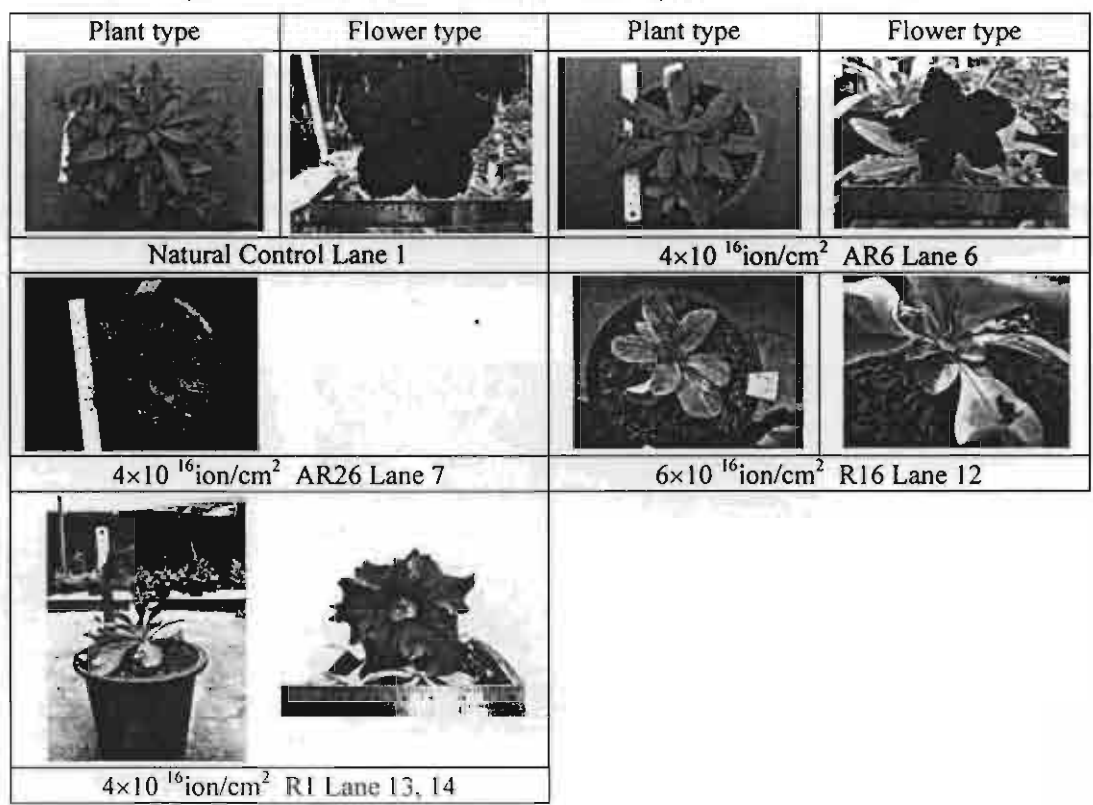


Figure 20 Characters of the indicated lanes in parenthesis referred to the mutants in figure 19.

In conclusion, RAPD technique can be used to identify different banding patterns among petunia mutants result from ion beam bombardment. Each of the primers, however, was not able to set each mutant apart. Therefore, several primers were required.

#### 3. Chrysanthemum

#### 3.1 Introduction

Chrysanthemum is one of the important crops in the oversea and also local markets. The advantage of this cut flower is that they can be produced year round by controlling light and dark period for the initiation and the development of the flower bud at the meristematic region of the stem. Both conventional and mutation breeding have been continuously done in order to induce new varieties. Those new varieties have more new colours, longer vase life and more disease resistance.

In our previous experiments we had tried to irradiate the meristematic region both at the active part, the shoot apex and the dormant one, the axillary bud. As mentioned in the previous reports, dehydration from the samples was the major problem. Parafilm was used to wind around the stem section whether they were the terminal section on the nodal section leaving only the small bombardment area but it was big enough for the water content in the stem went out to avoid rotting.

In this report the research team would like to report the results of the previous bombardment, the bombardment of the receptacles.

It is well worth mentioning here again that several methods were tried in order to prevent the dehydration and we finally found out that by dipping the receptacle in the liquid parafilm did help the dehydration of the sample.

#### 3.2. Material and method

The receptacles of variety Reagan Dark (Figure 21) were first cultured in the agar medium for 5 days to initiate the cell division. The samples were then bombarded with nitrogen ion beams at 5 doses 1, 2, 4, 6 and  $8 \times 10^{16}$  ions/cm<sup>2</sup> at 60 KeV under vacuum conditions. After bombardment the explants were sterilized and once again cultured. Shootlets generated on the explants were induced to root and then were acclimatized and planted individually in a 5 inch pot until they produced flowers by daylength control.



Figure 21 Chrysanthemum 'Reagan Dark' used in the experiment.

#### 3.3. Results

#### 3.3.1. The effect of nitrogen ion beam on the surface of the

#### receptacles.

The bombarded receptacles even though receiving the same dose from low to high doses showed various kinds of cell damage, Figure 22 show five categories of appearance in the receptacle after being cultured for 1 week.

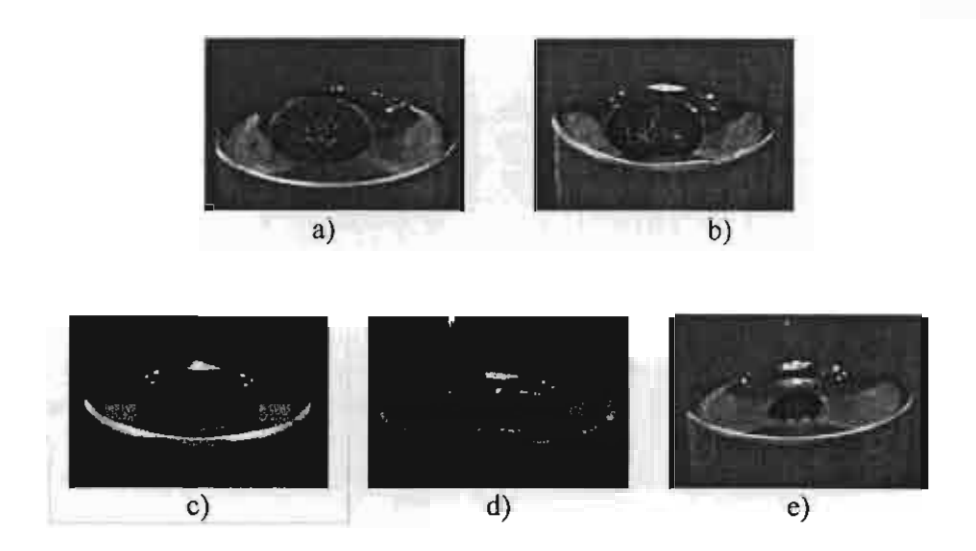


Figure 22 Various ion beam intensities affecting cell damage in chrysanthemum receptacle, I week after culturing.

a) no cell damage b) 1/3 of the whole area was damaged c) 2/3 was damaged d) more than 2/3 was damaged e) cells were totally damaged

In terms of survival percentage, vacuum and doses (1 and 2x10<sup>16</sup> ions/cm<sup>2</sup>) did not affect growth of the explants, but the higher dose at 4x10<sup>16</sup> ions/cm<sup>2</sup>, the survival percentage reduced by 20% and increased to 60% at 6x10<sup>16</sup> ions/cm<sup>2</sup>. At the maximum dose, 8x10<sup>16</sup>, the explants failed to grow. Considering from the damage on the surface of the receptacle explants, in the natural control there was no damage at all, however under only vacuum there was a slight damage. The damage to the cells at the surface of the explants increased as the dose increased (Table 5).

**Table 5** The survival percentages of the receptacles after being bombarded with various doses of ion beams and the degree of damage on the explant surface.

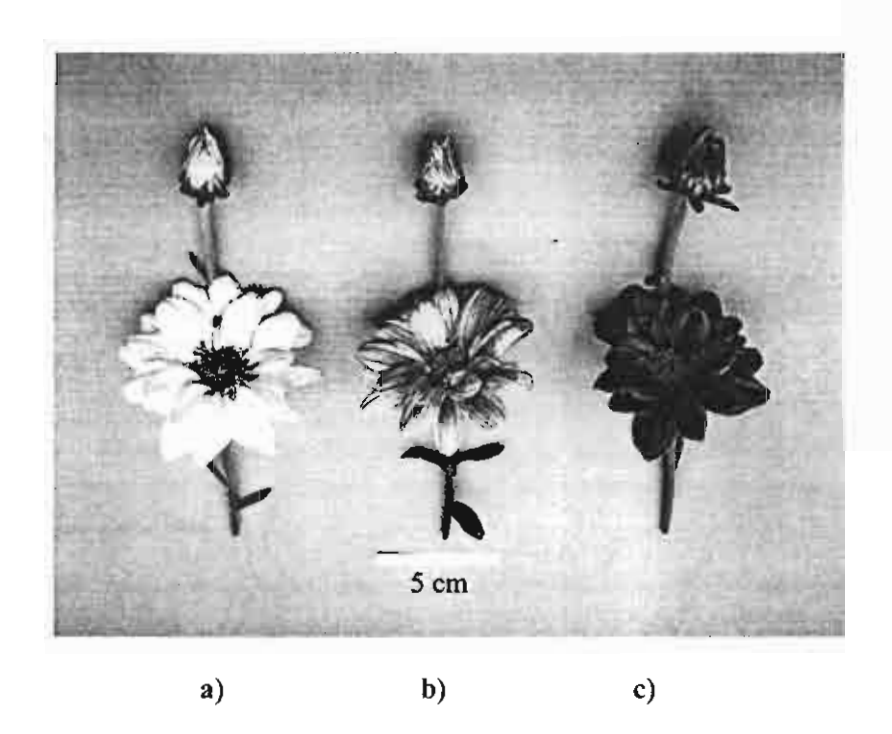
Dose		Sur	Survival rate		Intensity of cell explant surface damage								
$(ions/cm^2,60)$	Replication	r			A		В		,	D		]	E
KeV)		No.	%	No.	%	No.	%	No.	%	No.	%	No.	%
Control	10	10	100	10	100	0	0	0	0	0	0	0	0
Vacuum													
control	10	10	100	7	70	3	30	0	0	0	0	0	0
1x10 <sup>16</sup>	10	10	100	5	50	5	50	0	0	0	0	0	0
2x10 <sup>16</sup>	10	10	100	4	40	3	30	2	20	1	10	0	0
4x10 <sup>16</sup>	10	8	80	3	30	3	30	2	20	0	0	2	20
6x10 <sup>16</sup>	10	4	40	0	0	1	10	0	0	3	30	6	60
8x10 <sup>16</sup>	10	0	0	0	0	0	0	0	0	0	0	10	100

#### 3.3.2. Mutation induction

As the experiment was carried out during the long day photoperiod (March to July), so artificially long night condition was artificially given. One mutant was found where the flower colour change from pink to bronze. The rest were paler, darker or variegated ray florets, the details were presented in Table 6 and Figure 23.

**Table 6** Number of chrysanthemum plants showing various colour intensities compared to the original pink and one colour mutant.

D	N6	Nf		(	Changi	ng in	colour	intens	ity		Cal	Colour	
Dose (ions/cm <sup>2</sup> , 60 KeV)	No. of plants tested	No. of plants	Similar to control		Paler		Darker		Variegated		mutation		
ou Kev)	lested	flowered	No.	%	No.	%	No.	%	No.	%		%	
Control	15	9	9	100	0	0	0	0	0	0	0	0	
Vacuum													
control	143	88	87	98.9	1	1.1	0	0	0	0	0	0	
1x10 <sup>16</sup>	223	138	87	63.0	3	2.2	46	33.3	2	1.5	0	0	
2x10 <sup>16</sup>	113	54	39	72.2	0	0	12	20	3	5.6	0	0	
4x10 <sup>16</sup>	227	158	115	72.8	2	1.3	33	20	7	4.4	1	0.6	
6x10 <sup>16</sup>	52	44	39	88.6	0	0	3	0	2	4.6	0	0	
8x10 <sup>16</sup>	0	0	0	0	0	0	0	0	0	0	0	0	



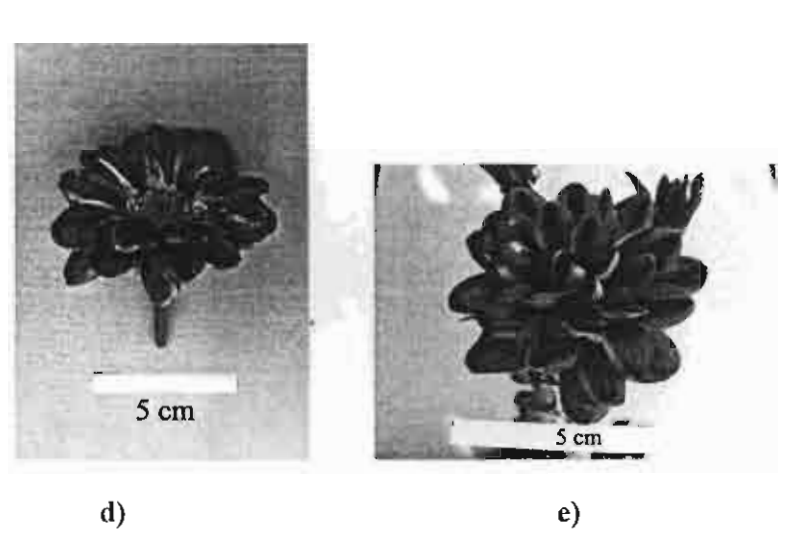


Figure 23 Changing in flower intensity and colour a) paler than control b) control c) darker than control d) variegated e) colour mutation from pink to bronze

#### Conclusion

After three years, the research team was able to demonstrate as follows

- 1. How to prepare the samples to be irradiated in order to avoid dehydration due to vacuum condition of the ion generating machine.
- 2. Low energy ion beam was able to induce mutations in flowering crops.
- 3. Mutation induced was the stable ones which indicate the genetical effect of ion beam.
- 4. Publications will soon be followed because the research team received the confirmation data of the early results on the third year.
- 5. One of each of master and doctoral degree students have been working on this project and will continue running their researches until they finish their studies.

57

# **Chapter IIII Output and Outcome**

# 4.1 Technology

- 4.1.1 Low energy ion beam induced mutation in Thai rice.
- 4.1.2 A target holder for ion bombarding rice seeds

# 4.2 KDML 105 rice mutants

Five KAML 105 rice mutant lines

Rice Label	Phenotypic variation
BKOS6	<ul> <li>Photoperiod insensitive</li> <li>Early flowering</li> <li>Short in stature</li> <li>Reddish- dark brown to black in leaf sheath</li> <li>Dark brown to black in seed coat (hull)</li> <li>Black rice seeds (brown rice)</li> </ul>
TKOS4	<ul> <li>Photoperiod insensitive</li> <li>Early flowering</li> <li>Low tillering capacity</li> <li>Low % filled-spikelets</li> <li>Low number panicles/plant</li> <li>Tall variety</li> </ul>
PKOS1	<ul> <li>Photoperiod insensitive</li> <li>Big and long panicles</li> <li>high % filled spikelets</li> <li>High number of seeds in panicle</li> <li>Short in stature</li> </ul>
PKOS2	Photoperiod insensitive - Big and long panicles - high % filled spikelets - High number of seeds in panicle - Short in stature
PKOS3	Photoperiod insensitive - Big and long panicles - high % filled spikelets - High number of seeds in panicle - Short in stature

#### 4.3. Publications

- 4.3.1. L.D. Yu, T. Vilaithong, B. Phanchaisri, P. Apavatjrut, S. Anuntalabhochai, P. Evans, I.G. Brown. Ion Penetration Depth in Plant Cell Wall. *Nuclear Instruments and Methods*, B206(2003)586-590.
- 4.3.2. Pimchai Apavatjrut, Chiara Alisi, Boonrak Phanchaisri, Liangdeng Yu, Somboon Anuntalabhochai and Thiraphat Vilaithong. Induction of Exogenous Molecule Transfer in Plant Cells by Ion Beam Bombardment. ScienceAsia, Vol. 29, No. 2 (2003), 99-107.
- 4.3.3. T. Vilaithong, L.D. Yu, P. Apavatjrut, B. Phanchaisri, S. Sangyuenyongpipat, S. Anuntalabhochai, I.G. Brown. Heavy Ion Induced DNA Transfer in Biological Cells. *Radiation Physics and Chemistry*, 71/3-4 (2004) pp. 927-935.
- 4.3.4. S. Sangyuenyongpipat, T. Vilaithong, L.D. Yu, R. Yimnirun, P. Singjai and I.G. Brown. Development of In-Situ Atomic Force Microscopy for Study of Ion Beam Interaction with Biological Cell Surface. *Solid State Phoenomena*, 107(2005) 47-50.
- 4.3.5. S. Sangyuenyongpipat, L.D. Yu, T. Vilaithong, A. Verdaguer, I. Ratera, D.F. Ogletree, O.R. Monteiro and I.G. Brown. Metal Ion Bombardment of Onion Skin Cell Wall. *Nuclear Instruments and Methods* B, 227(2005)289-298.
- 4.3.6. S. Sangyuenyongpipat, L.D. Yu, T. Vilaithong and I.G. Brown. Ion Bombardment Induced Formation of Micro-craters in Plant Cell Envelopes. *Nuclear Instruments and Methods* B, (2006), in press.

#### 4.4 Book

4.4.1. L.D. Yu, T. Vilaithong, I.G. Brown (English Translators). *Introduction to Ion Beam Biotechnology*. Translator, originally authored by Yu Zengliang in Chinese, Springer Science & Business Media, New York, 2006.

#### 4.5 Presentations

- 4.5.1. T. Pusadee, L.D. Yu, T. Vilaithong, S. Anuntalabhochai. Genomic Mutation Induced by Low-energy Ion Beam in Rice (Oryza sativa var. Induca) KDML105. Presented to the National Conference on Genetics and Sustainable Development, 5-7 June 2003, Narasuan University, Pitsanulok, Thailand.
- 4.5.2. S. Sangyuenyongpipat, L.D. Yu, T. Vilaithong, I.G. Brown. Ion Beam Bombardment of Biological Tissue. Oral presentation to the 56<sup>th</sup> Annual Gaseous Electronics Conference, October 21-24, 2003, NASA Ames Research Center, San Francisco, California, USA

- 4.5.3. S. Anuntalabhochai, R. Chandej, B. Phanchaisri, L.D. Yu, S. Promthep, S. Jamjod, and T. Vilaithong. Mutation Induction in Thai Purple Rice by Low Energy Ion Beam. Oral presentation and published in the *Proceedings* of the 9<sup>th</sup> Asia Pacific Physics Conference, Hanoi, Vietnam, October 25-31, 2004, Session 10: Applied Physics, 10-24C.
- 4.5.4. L.D. Yu, S. Sangyuenyongpipat, S. Annuntalabhochai, B. Phanchaisri, T. Vilaithong and I.G. Brown. Effects of Low-energy Ion Beam Bombardment on Biological Cell Envelopes, presented to the 14th International Conference on Surface Modification of Materials by Ion Beams, September 4-9, 2005, Kusadasi, Turkey, and to be published in Surface and Coatings Technology (2006).
- 4.5.5. B. Phanchaisri, R. Chandet, L.D. Yu, T. Vilaithong, S. Jamjod, S. Anuntalabhochai. Low-energy ion-beam-induced mutation in Thai jasmine rice (Oryza sativa indica, KDML 105), presented to the 14th International Conference on Surface Modification of Materials by Ion Beams, September 4-9, 2005, Kusadasi, Turkey, and to be published to Surface and Coatings Technology (2006).
- 4.5.6. S. Mahadtanapuk, L.D. Yu, T. Vilaithong, and S. Anuntalabhochai. Mutation of *Bacillus Licheniformis* by Low-energy Ion Beam, presented to the 14th International Conference on Surface Modification of Materials by Ion Beams, September 4-9, 2005, Kusadasi, Turkey, and to be published in Surface and Coatings Technology (2006).
- 4.5.7. L.D. Yu, S. Sangyuenyongpipat, C. Sriprom, C. Thongleurm, C. Tengsirivattana, R. Suwanksum, and T. Vilaithong. A Specialized Bioengineering Ion Beam Line, to be presented and submitted to the 15<sup>th</sup> International Conference on Ion Beam Modification of Materials (IBMM 2006), Taormina, Sicily, Italy, September 18-22, 2006.
- 4.5.8. Somjai Sangyuenyongpipat, Liangdeng Yu, Thiraphat Vilaithong, Ian G. Brown. *In-situ* Atomic Force Microscopy for Microcrater-like Structure Observation of Plant Cell Envelope, to be presented and submitted to the 15<sup>th</sup> International Conference on Ion Beam Modification of Materials (IBMM 2006), Taormina, Sicily, Italy, September 18-22, 2006.

#### 4.6 Conference and Workshop

"The Second International Workshop on Particle Beam & Plasma Interaction on Material" and "The Second Asia Symposium on Ion & Plasma Surface Finishing" were held during 25-27 November 2004 in Chiang Mai in the frame work of the Thailand Research Fund Senior Scholar Awards and the Royal Golden Jubilee program.

The proceeding was published in a special issue of journal Solid State Phenomena Vol. 107 (October 2005) 1-160.

#### 4.7 Award

- 4.7.1 National Research Council Award in 2004 for Distinguished Research Work on Ion Beam Induced DNA Transfer
- 4.7.2 Our presentation entitled "Investigation of Mutation in Purple Glutinous Rice Induced by Low Energy Ion Beam," was awarded the best 10 posters at the 14<sup>th</sup> International Conference on Surface Modification of Materials by Ion Beams held during September 4 9, 2005 in Kusadasi, Turkey.

#### 4.8 Students

# 4.8.1 Ph.D. graduate

Ms. Somjai	Sangyeunyongpipat	(Physics)
Ms. Supuke	Mahadtanapuk	(Biology)
4.8.2 M.S. gra	duate	
Ms. Suphannee	Promthep	(Biology)

4.8.3 B.S.

Mr. Chartra Ladpala (Biology)
Ms. Chintana Wongta (Biology)

#### 4.9 Public Relation

The Press conference on the success of induction mutation in Thai jasmine rice (KDML 105) by ion beam technique was held on the 24<sup>th</sup> of June in 2005 by the President Chiang Mai University.





# Appendix Reprints and Abstracts.



## Available online at www.sciencedirect.com



Nuclear Instruments and Methods in Physics Research B 206 (2003) 586-590

www.elsevier.com/locate/nimb

### Ion penetration depth in the plant cell wall

L.D. Yu a,\*, T. Vilaithong a, B. Phanchaisri b, P. Apavatjrut c, S. Anuntalabhochai d, P. Evans e, I.G. Brown f

Fast Neutron Research Facility, Department of Physics, Faculty of Science, Chiang Mai University, Chiang Mai 50200, Thailand
 Institute for Science and Technology Research and Development, P.O. Box 111, Chiang Mai University, Chiang Mai 50200, Thailand
 Department of Horticulture, Faculty of Agriculture, Chiang Mai University, Chiang Mai 50200, Thailand
 Department of Biology, Faculty of Science, Chiang Mai University, Chiang Mai 50200, Thailand
 Physics Division, ANSTO, Menai, NSW 2234, Australia
 Lawrence Berkeley National Laboratory, University of California, Berkeley, CA 94720, USA

#### Abstract

This study investigates the depth of ion penetration in plant cell wall material. Based on the biological structure of the plant cell wall, a physical model is proposed which assumes that the wall is composed of randomly orientated layers of cylindrical microfibrils made from cellulose molecules of C<sub>6</sub>H<sub>12</sub>O<sub>6</sub>. With this model, we have determined numerical factors for ion implantation in the plant cell wall to correct values calculated from conventional ion implantation programs. Using these correction factors, it is possible to apply common ion implantation programs to estimate the ion penetration depth in the cell for bioengineering purposes. These estimates are compared with measured data from experiments and good agreement is achieved.

© 2003 Elsevier Science B.V. All rights reserved.

PACS: 61.80.Az; 61.80.Jh; 61.82.Pv; 87.50.Gi

Keywords: Ion penetration depth; Plant cell wall; Ion implantation; Ion beam bioengineering

#### 1. Introduction

Fundamental studies on mechanisms of ion beam induced transfer of exogenous macromolecules such as deoxyribose nucleic acid into plant and bacterial cells [1,2] have led to investigations on the ion penetration depth in the cell envelope. It has recently been observed from experimental facts [3] that the measured ion range in the cell wall is much greater than the one calculated for a solid that is assumed to have the same chemical composition as the cell wall. Furthermore, abnormally deep penetration (some 100-fold or greater deeper than those calculated) of ions in biosamples has been reported [4]. The reason has been qualitatively explained to be due to the special porous and inhomogeneous structure of the cell wall [1,5]. Recent studies on ion beam effects on plant and bacterial cell envelopes have revealed that only ions with appropriate energies and fluences can result in suitable penetration and radiation damage to bring about successful exogenous macromolecule transfer into the cell and simultaneously

<sup>\*</sup>Corresponding author. Tel.: +66-53-94-3379; fax: +66-53-22-2776

E-mail address: yuld@fnrf.science.cmu.ac.th (L.D. Yu).

maintain cell viability [2,6]. Therefore, a quantitative study on ion penetration depth in the cell wall becomes necessary. We have carried out such a study to predict the effective ion penetration depth, which defines the depth (below the original cell-wall surface) that the dominant portion of the implanted ions can normally penetrate (thus any unpredictable abnormality is ruled out).

#### 2. Experimental

Specimens of monolayers of the fresh onion outermost cell layer stripped from medium sheets of the bulb scale and prepared on Si substrates were implanted with Ar ions at energies from 25 to 130 keV mostly to a fluence of  $2 \times 10^{15}$  ions/cm<sup>2</sup>. Specimens of thin layers of Curcuma embryo cells were implanted with 30-keV Ar ions. Details on the ion implantation conditions refer to our previous publication [6]. After ion implantation, the specimens were subjected to standard biosample-preparation for transmission electron microscopy (TEM) observation. Some of the Si-substrates were subsequently analyzed using Rutherford backscattering spectrometry (RBS) to detect the presence of Ar.

#### 3. Results and discussion

Fig. 1 shows TEM microphotographs of crosssections of the onion skin cell walls. A monolayer of the cells consists of upper wall (Fig. 1(A)) and lower wall (Fig. 1(B)), and the total fresh cell wall thickness of the monolayer is estimated to be about 2600 nm. In Fig. 1(C), the lighter areas are the radiation damage regions (due to inhomogeneity of the hard cuticle thin layer on the cell-wall surface, the damaged area is not homogeneously distributed). The average thickness of the lighter areas is measured to be about 200 nm for the case of 25-keV Ar-ion implantation to the fluence of  $2 \times 10^{15}$  ions/cm<sup>2</sup>. If the ion range is assumed to correspond to the damage range, the ion range in our cell wall is about 200 nm. The Ar-ion range in this case is calculated to be about 40 nm using the PROFILE-code [7] program. Fig. 2 shows a TEM

micrograph of cross-section of a 30-keV Ar-ion implanted Curcuma embryo cell wall. The fresh cell wall thickness is seen about 550 nm. The light area has a thickness roughly about 450 nm. The mean range and the range straggling of 30-keV Ar ions in the cell wall are calculated to be about 55 and 10 nm respectively. The differences between the observed and calculated results are significant. We have established a model of the plant cell wall to interpret the difference.

The plant cell wall is a discontinuous structure, consisting of nanosized cellulose microfibrils [8,9]. A cellulose microfibril, made from cellulose molecules, is about 3.5 nm in diameter in most higher plants with the microfibrils cross-linked in a net style with about a 5-nm spacing in between [8]. The primary chemical structure of cellulose is C<sub>6</sub>H<sub>12</sub>O<sub>6</sub> [9] (Fig. 3). The cellulose material occupies about 7/17 = 3.5/(3.5+5) of the linear thickness of the fresh cell wall. Since a fresh plant cell completely shrinks in the vacuum condition [10], in the modeling, the cell wall is represented as a shrunk closely packed solid model. The model (Fig. 4) is composed of many microfibril layers, which overlap one by one in random orientation, as illustrated in Fig. 4(A). Each layer consists of many microfibrils that are closely arrayed in parallel. Each microfibril is assumed to be a long circular column with about 3.5 nm in diameter, composed of planar chains of cellulose molecules (Fig. 4(B)) in the chemical structure of C<sub>6</sub>H<sub>12</sub>O<sub>6</sub>. The mass density of the dried cell wall material is experimentally determined to be 1.05 g/cm<sup>3</sup>.

As the average number of the bonds of each atom in a molecular unit is 2, the interatomic equipotential surface is no longer spherical. We construct the equipotential surface of two cylindrically symmetrical ellipsoids in the central symmetry with the atom itself at the center. The potential has two variables, r and  $\theta$ , where  $\theta$  is the angle between the cylindrical symmetry axis and the vector  $\mathbf{r}$ , and they are assumed to have a linear relationship as  $r = -2\theta/\pi + 1$ . If the interatomic potential between two atoms is taken as a Coulomb potential, it is assumed to have the form as  $V(r,\theta) \propto (\pi/2 - \theta)/r$ .

We assume that changes in the stopping process of a low-energy ion in the cell wall is dominated by

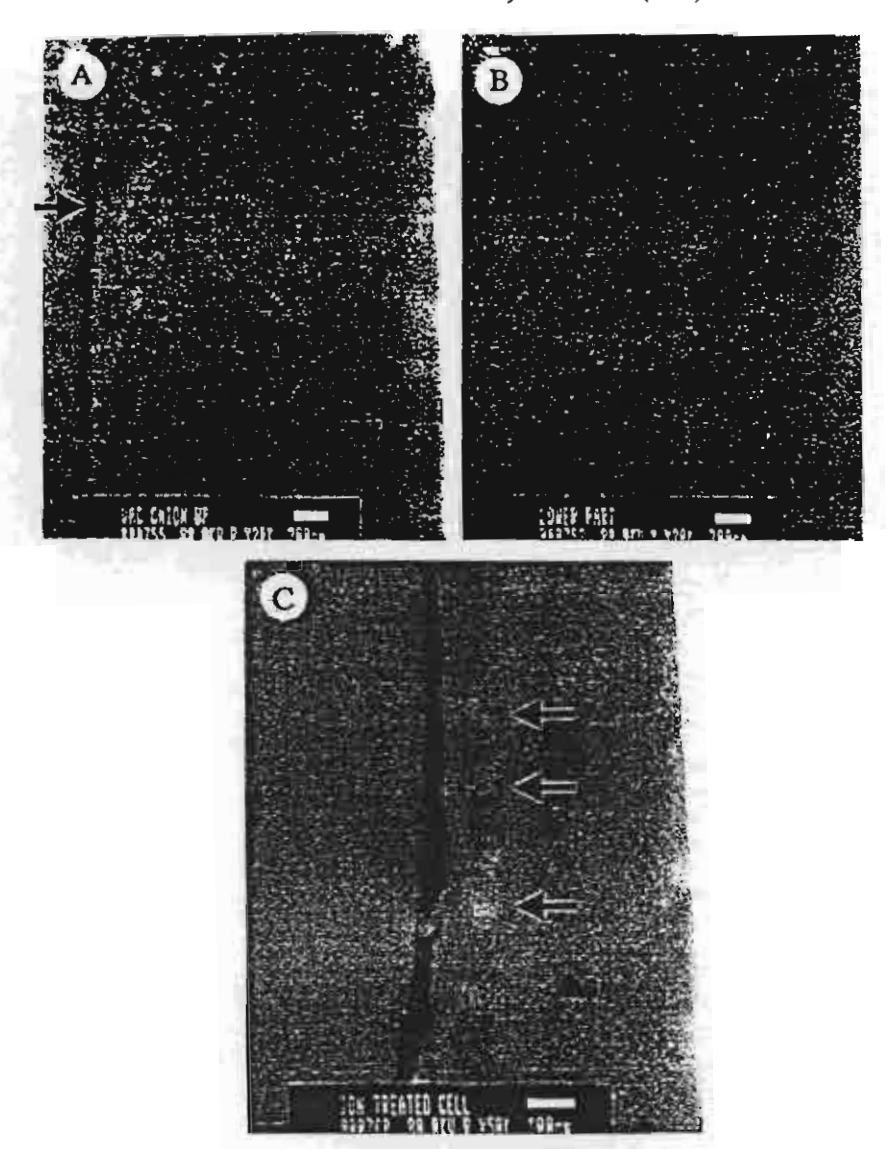


Fig. 1. TEM micrographs of the cross-sections of onion skin cell wall. (A) Fresh upper part: the arrow indicates the cuticle. (B) Fresh lower part. (C) 25-keV Ar-ion implanted upper part, fluence:  $2 \times 10^{15}$  ions/cm<sup>2</sup>; the arrows indicate the deep region of radiation damage.

nuclear stopping. When interactions between those atoms in equilibrium are passed between an energetic ion and a rest atom for the effect of scattering and subsequent energy loss [11], the interaction potential is assumed to follow directly the interatomic potential between atoms in equilibrium. From the simplified calculation of the nuclear stopping [12] using the Coulomb potential, we

obtain  $(-dE/dx)_{elas} \propto 4\pi (Z_1Z_2e^2)^2$ . This can be rewritten as  $(-dE/dx)_{elas} \propto 4\pi (Z_1Z_2e^2/r)^2r^2 \propto 4\pi r^2V_c^2 \propto A_s$ , where  $A_s$  is the surface area of the equipotential sphere and  $V_c$  is the Coulomb potential. The surface area of the two ellipsoids is  $2\pi^2/3$  (r is taken as 1). The ratio between the surface areas of the two ellipsoids and the sphere is  $\pi/6 \cong 0.52$ . Therefore, the stopping cross-section

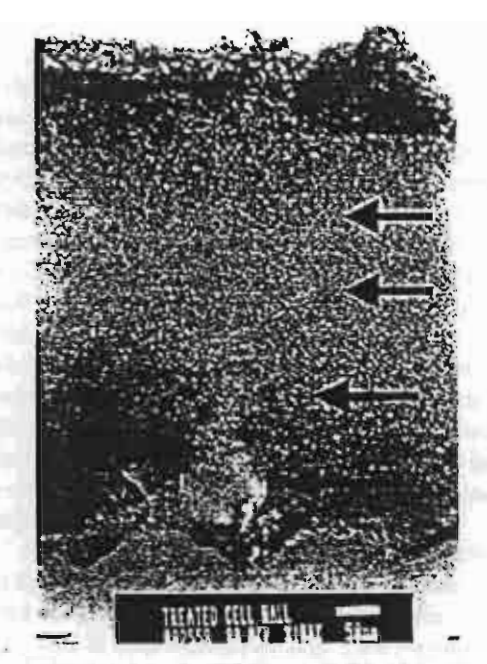


Fig. 2. TEM micrograph of the cross-section of the *Curcuma* embryo cell wall implanted by 30-keV Ar ions to a fluence of  $2 \times 10^{15}$  ions/cm<sup>2</sup>. The bottom side is the external surface of the cell wall. The arrows indicate the damaged region.

Fig. 3. Chemical structure of a unit of the cellulose molecule. The broad dashed lines represent van der Waals bonding with atoms in neighboring units.

of the cell wall atom is approximately 0.52 times that of the same atom in a matrix with homogeneously distributed atoms. Hence the ion range in the cell wall should be 1/0.52 = 1.91 of that in a matrix with homogeneously distributed atoms.

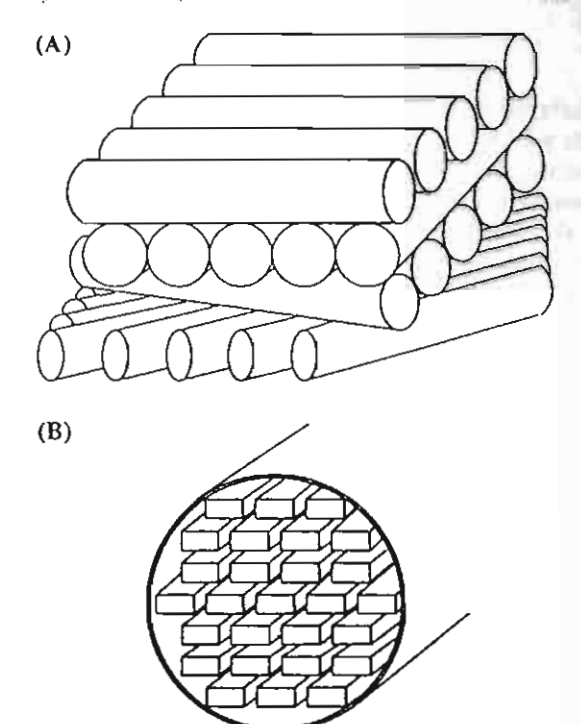


Fig. 4. Microscopic physical model of the cell wall. (A) The wall is made of random-oriented layers of closely packed cylindrical microfibrils. The columns represent microfibrils. (B) Inside each microfibril are chains of cellulose molecules in which the atoms reside in the same plane. The strips represent the cellulose molecule chains.

Furthermore, for the case of a cylindrical microfibers, four corner areas outside the circular crosssection are lost compared with the full area of the square that contains the circle. Thus, the atom number density of the modeled cell wall, N<sub>m</sub>, is less than that of the fully space-filled or homogeneous solid cell wall material, N. The ratio  $N_m/N$  is equivalent to the ratio between the circle area of the column cross-section and the square area to be  $\pi/4$ . Therefore, the ion range in the modeled cell wall is  $4/\pi$  of that in the homogeneous solid cell wall material. In a summary, the total correction factor for the range is  $1.91 \times 4/\pi = 2.43$ . Since the range straggling is proportional to the range [11], the range straggling in the modeled cell wall gets the same correction factor.

There is another factor due to sputtering. In the model, the surface of every microfiber layer of the

cell wall is not flat but curved. Thus the ion beam impinges on this curved surface at different angles, which in turn result in different angle-dependent surface sputtering yields. For 30-keV Ar-ion bombardment of the cell wall material, the sputtering yields as a function of incident angle are calculated using the PROFILE-code and the ratio between the average yield and the 0° yield is 1.43. In our recent study on ion beam sputtering of the cell envelope, a fivefold sputtering yield has been obtained [10]. Combining both results mentioned above, we derive an average sputtering yield of the modeled cell wall to be about seven times that of a flat-surface solid cell wall. The surface thickness loss due to sputtering of the cell wall is thus ~seven times that calculated for the flat-surface solid cell wall material.

For the onion cell wall, if the calculated ion range, 40 nm, is multiplied by the factor of 2.43 and then the factor of 17/7, the range in the fresh cell wall is then about 240 nm. This result is fairly close to the measured value of 200 nm. Because of the hard cuticle stopping ions more effectively, the measured range is less than the calculated. Also due to the hard cuticle, the sputtering of the onion skin surface is negligible (Fig. 1), thus the calculation does not take sputtering into account. For the Curcuma embryo cell, if the calculated ion range and straggling are multiplied by 2.34 and then 17/7, the total effective range in the fresh cell wall is about 390 nm. The sputtering loss is converted from the PROFILE-calculated 11 nm to about 80 nm using the factor of 7. Therefore, the total 30-keV Ar penetration depth in the fresh cell wall is about 470 nm. This result is reasonably close to the observed value 450 nm.

RBS did not detect the presence of Ar in any of the Si substrates analyzed. The sensitivity of RBS is about  $1-2 \times 10^{14}$  Ar/cm<sup>2</sup>, which represents the maximum amount of Ar that could be present in the Si substrates. Thus no more than 10% of the implanted Ar ions could have completely penetrated the 2600-nm cell wall. This indirectly demonstrates that the effective ion penetration depth in the cell wall is within our estimated value range and is not as large as the previously reported 100-fold or more.

#### 4. Conclusion

We established the physical model of the plant cell wall, derived correction factors of 2.43 for the range and straggling and 7 for the sputtering to the calculated values, and confirmed their correctness with the experiment. Using these correction factors, it is possible to apply conventional ion implantation simulation programs to estimate the ion penetration depth in the cell wall for bioengineering purposes.

#### Acknowledgements

We wish to thank C. Alisi for her very helpful discussion and suggestions. This work was supported by The Thailand Research Fund.

#### References

- Z.L. Yu, J. Yang, Y. Wu, B. Cheng, J. He, Y. Huo, Nucl. Instr. and Meth. B 80-81 (1993) 1328.
- [2] S. Anuntalabhochai, R. Chandej, B. Phanchaisri, L.D. Yu, T. Vilaithong, I.G. Brown, Appl. Phys. Lett. 78 (2001) 2393.
- [3] Z.L. Yu, C. Shao, J. Yang, J. Anhui Agric. Univ. 21 (3) (1994) 260.
- [4] R.J. Wang, Y.Y. Xia, Y.G. Mu, M.W. Zhao, Y.C. Ma, X.D. Liu, J.H. Zhang, J.T. Liu, Z.L. Yu, Chin. Phys. Lett. 18 (2001) 208.
- [5] J.M. Xue, Y.G. Wang, S. Yan, W.J. Zhao, Surf. Coat. Technol. 128-129 (2000) 139.
- [6] T. Vilaithong, L.D. Yu, C. Alisi, B. Phanchaisri, P. Apavatirut, S. Anuntalabhochai, Surf. Coat. Technol. 128-129 (2000) 133.
- [7] PROFILE Code Software, Version 3.20, Implant Science, Wakefield, MA 01880-1246, USA, 1995.
- [8] B. Alberts, D. Bray, J. Lewis, M. Raff, K. Roberts, J.D. Watson, Molecular Biology of the Cell, Garland Publishing, New York & London, 1992, p. 1137.
- [9] D. Voet, J.G. Voet, Biochemistry, John Wiley & Sons, New York, 1990, p. 254.
- [10] L.D. Yu, B. Phanchaisri, P. Apavatjrut, S. Annutalabhochai, T. Vilaithong, I.G. Brown, Surf. Coat. Technol. 158-159 (2002) 146.
- [11] M. Nastasi, J.W. Mayer, J.K. Hirvonen, Ion-Solid Interactions, Fundamentals and Applications, Cambridge University Press, Cambridge, Great Britain, 1996.
- [12] N. Bohr, Mat. Fys. Medd. Dan. Vid. Selsk. 18 (8) (1948).



## Induction of Exogenous Molecule Transfer into Plant Cells by Ion Beam Bombardment

Pimchai Apavatjrut<sup>a</sup>, Chiara Alisi<sup>b</sup>, Boonrak Phanchaisri<sup>b</sup>, Liangdeng Yu<sup>c</sup>, Somboon Anuntalabhochai<sup>d</sup> and Thiraphat Vilaithong<sup>c</sup>

- a Department of Horticulture, Faculty of Agriculture, Chiang Mai University, Chiang Mai, Thailand.
- Institute for Science and Technology Research and Development, Chiang Mai University, Chiang Mai, Thailand.
- c Fast Neutron Research Facility, Department of Physics, Faculty of Science, Chiang Mai University, Chiang Mai, Thalland.
- <sup>a</sup> Department of Biology, Faculty of Science, Chiang Mai University, Chiang Mai, Thailand.
- \* Corresponding author, E-mail: aglppvtj@chlangmai.ac.th

Received 22 Oct 2001 Accepted 28 Oct 2002

Assumed Although the technology of ion-beam-induced gene transfer into either plant or bacterial cells has been successfully established, relevant mechanisms have not been understood. This work aimed to study the process of induction and thus to develop applications of ion beam bioengineering. Cells of various plant tissues were bombarded in vacuum with argon and nitrogen ion beams at energies of 15-30 keV with fluences ranging from  $5 \times 10^{14} - 3 \times 10^{16} \text{ions/cm}^2$ . The ion bombardment effects on tissue viability and neutral red dye molecule transfer into the cells through the cell envelope were investigated. The results showed that the characteristics of the tissue survival from the ion bombardment and penetration of the dye molecules into the cells through the cell envelope depended on ion species, energy and fluence. For 30-keV argon-ion bombardment at a fluence of  $2 \times 10^{15}$  ions/cm², the dye molecules entered the cells without fatal injury, whereas under other conditions, the dye either did not enter the cells or stained the nuclei. On the cell envelope surface, ion-bombardment-induced crater-like structures were observed. Calculations indicated that exogenous molecule transfer into living plant cells can be achieved by ion beams with appropriate physical parameters such that the ion range and the radiation damage range lie within the solid cell wall thickness

KEYWORDS: exogenous molecule transfer, ion beam bombardment, plant cells, cell envelope, cell wall. **ABBREVIATIONS:** Ar, argon; Au, gold; BA, Benzyladenine; GA<sub>3</sub>, Gibberellic acid; MS, Murashige and Skoog; N, nitrogen; NAA, α-Naphthaleneacetic acid; NR, Neutral Red; SEM, Scanning Electron Microscopy; TEM, Transmission Electron Microscopy; VW, Vacin and Went; W, tungsten.

#### INTRODUCTION

Ion beam technology has been widely applied in the fields of physics and materials science. The technology is typified by ion bombardment, a physical process in which energetic charged particles are accelerated by an electric field and transported to a target into which they penetrate, introducing foreign atoms, electric charge, and radiation damage in the near surface region.1 Heavy ion beams have recently been used to bombard biological materials for genetic modification purposes, particularly for the mutation of plants and bacteria<sup>2-6</sup>, in which the DNA structure is modified by relatively high energy (~102-103 keV) ion beam irradiation. More recently, attempts have been made to use relatively low energy (a few 10 keV) ionbeam bombardment for the direct transfer of exogenous macromolecules such as DNA and vital dye into biological cells. Yu et al 7 reported the successful

GUS and CAT gene transfer into the suspension cells and mature rice embryos following the 20-30-keV argon (Ar)-ion bombardment. Hase et al 8 developed tobaccopollen-mediated gene transfer using carbon ion beam bombardment. We have described our experiments in transferring Trypan blue (a vital dye) into Curcuma embryos induced by bombardment with argon ion beam.9 There is intrinsic difference between the irradiation and bombardment for DNA modification processes. In ion-beam mutagenesis a large number of cells are irradiated and DNA modifications are randomly induced in the nucleus, of which the desired ones are subsequently selected out.3 In ion-beam-induced DNA transfer only the cell envelope is bombarded in order to allow a subsequent transfer of whole DNA into the internal cell region. 7 A recent report 10 described the interaction of energetic ions with bacterial cells, inducing direct DNA transfer into E. coli, indicating that ion beams with an energy such that the ion range is

approximately equal to the cell envelope thickness, at a certain range of fluence, are able to create suitable conditions for DNA transfer through the bacterial cell envelope without irreversible damage. Although the technology of ion-beam-induced gene transfer into either plant or bacterial cells has been successfully established, relevant mechanisms have not been understood. Some mechanisms have been proposed, such as pathways created by ion bombardment, enhanced permeability from ion beam etching, and charge exchange resulting from ion implantation<sup>7</sup>, but none of them has been well supported experimentally.

Here we report in more detail our systematic and comprehensive studies on the induction of exogenous molecule transfer into plant cells by heavy ion bombardment in order to explain how the induction occurs, and the mechanisms involved in creating passages or channels through the cell envelope and enhancing its permeability. A vital dye, neutral red (NR), was used not only as the cell-injury-testing signal but also as the exogenous molecules to be transferred. The information obtained from the dye molecule transfer and physical changes on the plant cell envelope resulting from ion-beam-cell-surface interaction provides a necessary basis for induction of DNA transfer by ion beams.

#### MATERIALS AND METHODS

#### Plant tissues

Table 1 shows a list of the plant species, mostly horticultural ones, and tissue culture-derived explants used in this study. The explants were rehydrated in sterile distilled water for 30 min, thereafter cultured onto artificial media [Murashige and Skoog (MS) 11 + NAA and kinetin each at 0.5 mg/l for items 1 and 16 (Table 1), White12 for items 2 and 6-8, MS+NAA and kinetin each at 1.0 mg/l for items 3 and 4, MS + BA 1 mg/l for items 5 and 17, Vacin and Went (VW) 13 + 20% coconut water for items 9-14, and MS supplemented with BA, GA, and NAA at 1, 0.1 and 0.01 mg/l, respectively, for items 15, 18 and 19] kept at 28±1 °C under continuous light approximately at 13 µmol/m<sup>2</sup>/ s for 15 days. The fresh onion outermost cell layer from its bulb scale (uncultured) was also used in this study. Pieces of fresh tissue specimens, about 2-4 mm in size, were fixed onto a petri dish using sterile autoclaved tape, and divided into two groups, one to be exposed to the ion beam for bombardment and the other, nonexposed group, as a vacuum-treated control. Some fresh tissues were also used as controls to compare the vacuum and low-temperature effects on the samples. Four tissue pieces of each species were employed in each treatment such that four replicates per fluence were applied. Each experiment was repeated at least three times

#### Ion beam bombardment

The ion bombardment was carried out using the 150-kV mass-analyzed heavy ion implantation facility at Chiang Mai University. <sup>14,15</sup> In this machine, ions were produced by a radio-frequency ion source, electrostatically extracted and accelerated, magnetically mass-analyzed and focused, and finally transported to the target chamber where a special bio-sample holder was installed (Fig 1). Ar and nitrogen (N) ions were used with energies of 15, 20 and 30 keV at fluences of 0.5, 1,2,4,10,15, and  $30 \times 10^{15}$  ions/cm². Because the term "dose" has different meanings within the ion-implantation and biological-irradiation communities, here we avoid the term completely and use "fluence" to refer to the ion-bombardment intensity.

The whole beam line including the target chamber (Fig 1a) and the sample holder (Fig 1b) was constructed from stainless steel. The sample holder was designed to hold a standard petri dish (9 mm in size) which could expose four different tissue targets to the ion beam. Pulsed beam modes were adopted with the beam periodically sweeping across the exposure holes of the sample holder. The beam fluence (f) was determined from the target beam current (I) and the bombardment time (t) as  $\int \infty It$ . In order to measure the beam current correctly, an electron suppression tube was mounted in front of the holder shutter and biased to -200 V to suppress the emitted secondary electrons from the metal shutter surface due to ion beam bombardment. The beam current densities were varied from 3 to 10 µA/cm2. The fluence of each pulse irradiating the target was about 3-5×1012 ions/cm2. During ion bombardment, the pressure in the target chamber was kept around 10-3 Pa by a turbomolecular pump, and the temperature of the target in such an environment was estimated to be about 0°C. During each experiment, the tissue specimens were under these conditions for about 1.5-2 hours.

#### Neutral Red dye transfer

After ion beam bombardment, the tissues were immediately rehydrated in sterile distilled water for 30 min. The NR vital dye with a molecular weight of 300 Da 16 was chosen to be introduced into the bombarded plant cells and also to rapidly determine the ion-bombardment effect on structural modifications of the cell wall and the cell survival. 16 The rehydrated tissues were placed on a glass slide, stained with the NR solution (1 mg/ml in phosphate buffer 50 mM, pH 7.5) and observed under a light microscope.

## Scanning and transmission electron microscopy observation of the cell wall

The ion-bombarded and control specimens were observed by scanning electron microscopy (SEM) and

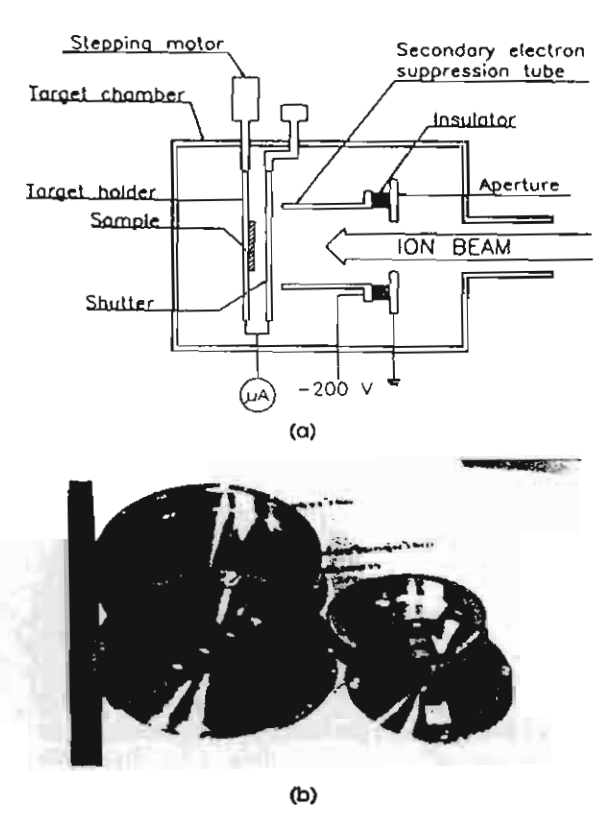


Fig 1. (a) Schematic of the ion-beam target chamber. (b) Photograph of the sample holders (in two different sizes).

transmission electron microscopy (TEM) using the JEOL 840 A scanning electron microscope and JEOL 1200 EX II transmission electron microscope respectively

#### RESULTS AND DISCUSSION

#### Vacuum effect on cell survival

Since the ion beam treatment under high vacuum condition caused water loss and created a lowtemperature environment for the tissues, the effect on the cell survival due to these harsh conditions was therefore first tested separately from the ion bombardment effects. Before the ion bombardment experiment, the effect due to pressure of about 10.3 Pa (which led to a specimen temperature of about 0 °C or lower) on the tissues was tested. SEM micrographs in Fig 2 show the difference in shape between the fresh control (Fig 2a) and vacuum treated cells (Fig 2b). The significant shrinking of the cells in vacuum demonstrated the loss of water in the cells. However, the vacuumconditioned cells were found to survive after they were returned to the natural environment. The cell turgor caused by vacuum was restored in cell appearance after an incubation of 30 minutes in sterile distilled water (Fig 3, a-c). Furthermore, growing tests for the plant species and tissues subjected to appropriate ion bombardment in vacuum showed growths or survival steady states for almost all of the plants, as shown in Table 1. These facts indicated that the vacuum and low

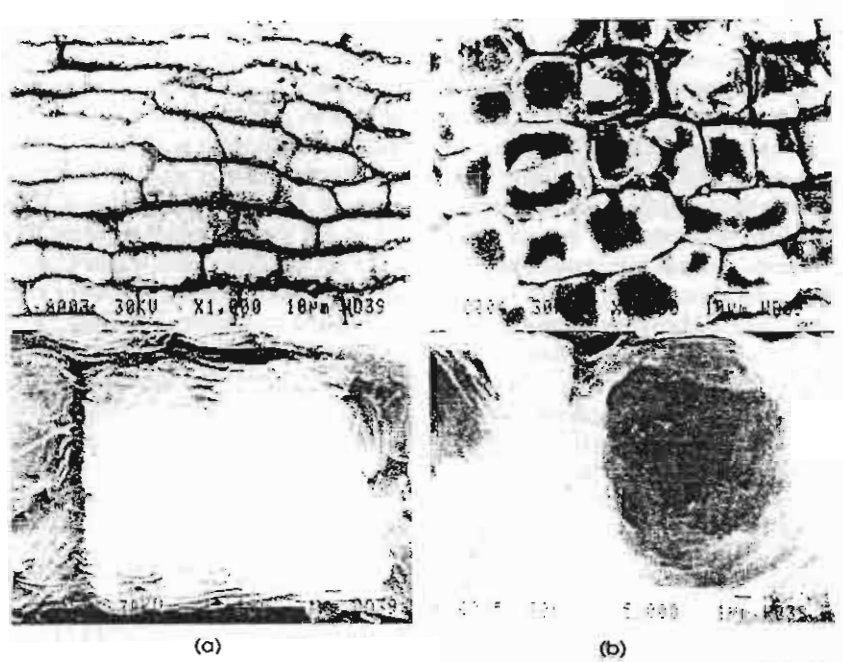


Fig 2. SEM photographs of an example of the vacuum effect of water loss from Curcuma embryo cells: (a) fresh control and (b) vacuum treated (10 <sup>3</sup> Pa, 2 hrs), in different magnifications. Scale: width of each photograph in the upper row is 110 μm, and that in the lower row is 22 μm. The arrow in (b) indicates the cell being magnified.

Table 1. Plant species and tissues used in the study, and their survival and in vitro growth states 15 days after Arion bombardment at 30 keV to a fluence of 2x10<sup>15</sup> lons/cm² in vacuum (pressure of 10<sup>-3</sup> Pa).

tem	Plant species	Tissue	Survival and growth state
1	Dendranthema Hybrids	leaf	grown/developed
2	Zea mays	leaf, embryo*	grown/developed
3	Eurycles ambolnensis	leaf base	grown/developed
4	Hippeastrum Hybrids	leaf base	steady state
5	Gladiolus Hybrids	leaf base	dead
6	Cucurbita moschata	embryo	steady state
7	Curcuma sp.	embryo*	steady state
8	Zingiber sp.	embryo*	steady state
9	Cymbidium fracyanum	protocorm	grown/developed
10	Dendroblum cruentum	protocorm	steady state
11	D.albosanguineum	protocorm	grown/developed
12	Ascocentrum curvifolium	protocorm	grown/developed
13	Paphlopedilum sp.	protocorm	grown/developed
14	Gnetum gnemon	lateral bud	grown/developed
15	Fragaria vesca	lateral bud	grown/developed
16	Tacca sp.	lateral bud	steady state
17	Globba sp.	lateral bud	grown/developed
18	Broussonetia papyrifera	stem	grown/developed
19	Maesa ramentacea	stem	steady state

<sup>\*:</sup> whole naked embryos were used.

temperatures for the operating period (1.5-2 hours) did not affect the viability of the cells. Thus the vacuum effect was negligible and final results would be only attributed to ion bombardment.

#### Ion bombardment effects Survival of plant cells

As shown in Table 1, after Ar-ion bombardment, almost all of the species and tissues could grow or survived at a steady state, except for Gladiolus. Ion beam effects on embryo germination and growth of the embryos bombarded under different conditions, ie ion species and fluence, were compared with the vacuumtreated control.9 The naked corn embryos in tissue culture could still germinate after 30-keV Ar- or 15keV N-ion bombardment at fluences of 5 × 1014, 1 × 1015 and 2×1015 ions/cm2, but with the growth retarded by up to about 50% (Table 2). Germination and growth did not occur for fluences higher than 1×1016 ions/cm2 at the above-mentioned energies of the ions, or for any fluences at energies higher than 20 keV when N ions were used (data not shown). The results indicated that under appropriate ion bombardment conditions (for a certain ion species, with proper energy and fluences), ion bombardment did not affect survival of the treated plant cells.

#### Microscopic modification of cell envelope

TEM photographs (Fig 4) show that at fairly high fluences, ion bombardment caused severe and extensive damage to the cell envelope (Fig 4b) and death of the cell, as demonstrated by the dye staining of the nucleus (also see Fig 6d). Suitably low fluence ion bombardment created modification of the outer layer of the cell envelope without complete damage (Fig 4d). The partial damage and thinning of the cell envelope are due to ion sputtering and etching, and the extent of this kind of damage has been found to depend on ion energy and fluence. Generally, bombardment with high-energy and high-fluence ion beam resulted in extensive damages to the cell envelope. A comparison between the cell envelope surfaces of the vacuumtreated control and the ion-bombarded specimens is shown in Fig 5. The ion-bombarded cell envelope surface was featured by blistering, exfoliation and cavity formation (Fig 5a), whereas the vacuum-treated control surface was very smooth (Fig 5b). Close examination of the damaged surface revealed some dispersed craters, which were large and deep. The results indicated that ion bombardment modified the cell envelope structure and was able to create appropriate damage under certain conditions.

Table 2. Average heights (in cm) of the seedling grown from the naked corn embryos in tissue culture 7 days after ion bombardment.

Fresh control	Vacuum-freated	Ion-beam	Ion Fluence (ions/cm²)			
	control	bombardment	5x1014	1x10 <sup>15</sup>	2x1015	1x1016
7.0	6.7	15-keV N ions	3.5	2.9	3.0	1.2
		30-keV Ar ions	2.9	3.0	2.9	1.0



Fig 3. Light-microscopic photographs of an example of the effect of vacuum on guard cells from Dendranthema leaf: (a) fresh control, (b) vacuum-treated control (at 10 ' Pa for 2 hrs), and (c) the vacuum-treated control after 30 min of rehydration in distilled water. Scale width of each photograph is 60 μm.

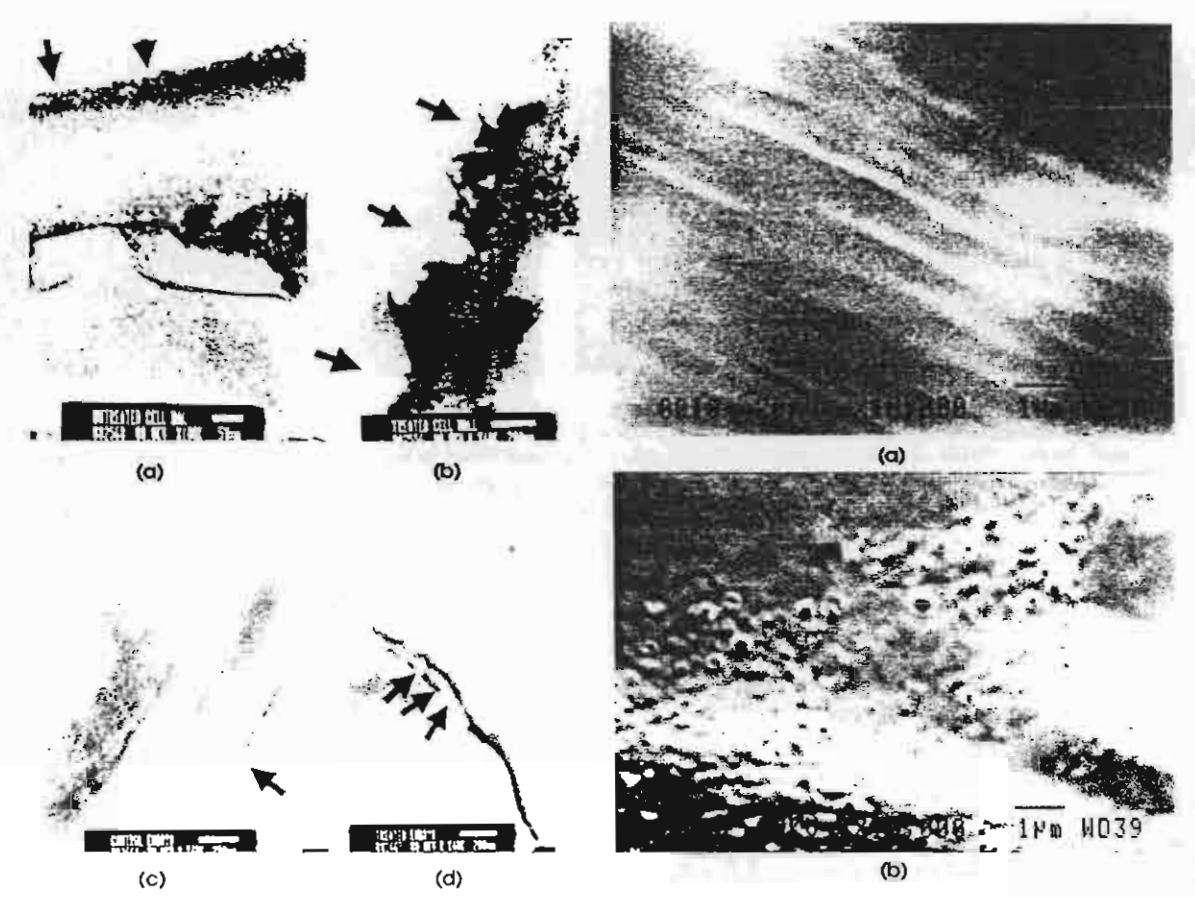


Fig 4. TEM photographs of the Curcuma embryo cell envelopes of (a) the vacuum-treated control, (b) the Ar-ion-bombarded (30 keV, 2x10<sup>15</sup> ions/cm²) cell, (c) the vacuum-treated control, and (d) the Ar-ion-bombarded (30 keV, 1x10<sup>15</sup> ions/cm²) cell. The arrows indicate the outside of the cell envelope. The scales are as indicated by the bars in the photographs

Fig 5. SEM photographs of examples of ion bombardment effect on the cell envelope morphology: (a) vacuum-treated control of the onion monolayer cell envelope surface, and (b) onion monolayer cell envelope surface bombarded by 30-keV Ar ions to a fluence of 2x10<sup>11</sup> ions(m). The scale is as indicated by the bars in the photographs

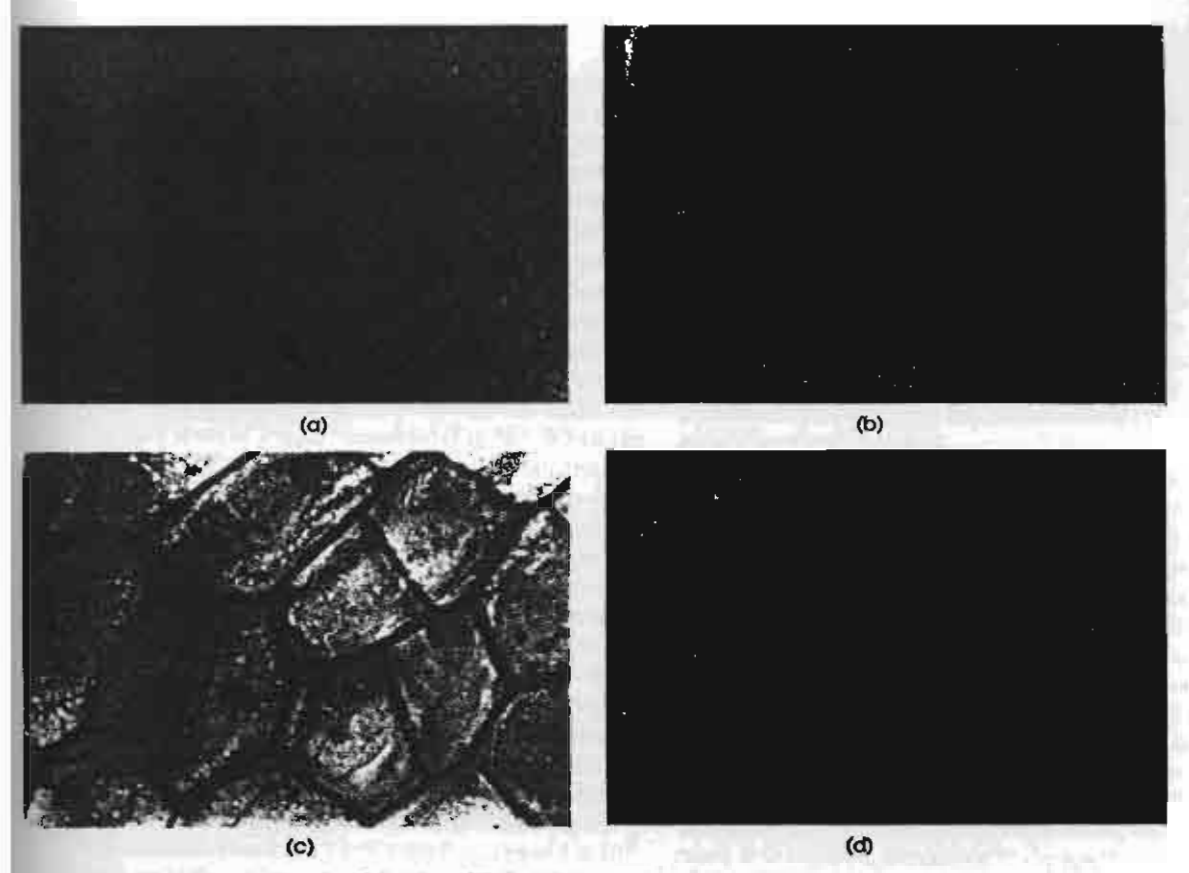


Fig 6. Light-microscopic photographs of the Neutral Red vital dye staining of 30-keV Ar-ion bombarded Curcuma embryo cells: (a) vacuum-treated control, (b) with a fluence of 1x10<sup>15</sup> ions/cm², (c) with 2x10<sup>15</sup> ions/cm², and (d) with 4x10<sup>15</sup> ions/cm². Scale: width of each photograph is 80 μm. In (c), tiny dye particles were initially moving around, then gradually aggregating into bigger spheres. Finally these spheres gathered into rather large dark areas, which were thought to be vacuoles.

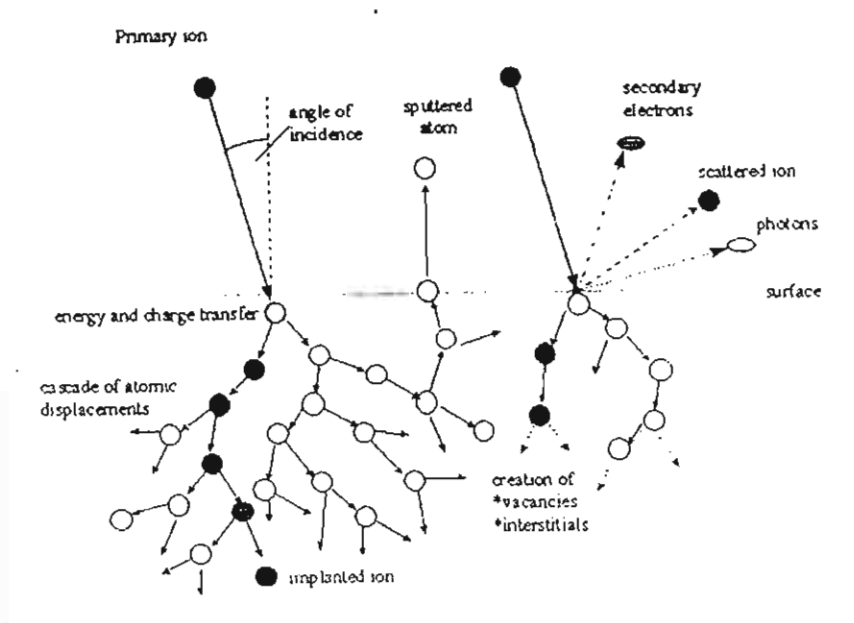


Fig 7. Schematic of basic interactions between incident energetic ions and a solid.

#### Dye penetration

Fig 6 shows that the 30-keV Ar-ion bombardment induced NR penetration in Curcuma embryo cells. Normally, intact or uninjured plant cells can prevent the vital dye from entering the cells, while injured but still alive cells accumulate the dye in their vacuoles and then exhaust the exogenous molecules out of the cells via the process called exocytosis. Dead cells, on the other hand, will be stained by the dye.16 Here we observed that the NR dye could not enter the cells of the non-bombarded embryo (Fig 6a), it could enter the cell wall and accumulated in the apoplast of the cells that were bombarded with 30-keV Ar-ion beam at a fluence level of  $1 \times 10^{15}$  ions/cm<sup>2</sup> (Fig 6b). When the fluence was increased to 2 × 1015 ions/cm2, the dye could enter inside the cells, where they streamed and circulated in the cytoplasm (Fig 6c), implying that the cells were functional and alive. At a higher fluence of 4×1015 ions/cm2, the cell envelope surface was severely damaged and the dye accumulated in the nuclear areas (Fig 6d), indicating that the cells did not survive. Ion bombardment using different ion species and dyes, such as N-ion and Trypan blue dye (molecular weight of 1000 Da17) was found to have the same effect on the dye molecule transferring into the cells, ie the penetration of the exogenous molecules is closely related to the ion energy and fluence. For example, Nion bombardment at 15 keV with fluences of  $1 \times 10^{15}$ and 2×1015 ions/cm2 was found to be ineffective to the dye penetration into the cells, but caused cell death at 30 keV with the same fluences. The experimental results suggested that after appropriate ion bombardment the dye could enter the plant cells without irreversible damage.

## Mechanisms for Neutral Red transfer into the plant cells

The ion bombardment is thought to create "entrance" through the cell envelope for the penetration of the dye molecules into the cells. Both previous literatures 18,19 and our experiments have demonstrated that the energy of the ion beams should be suitably low in order to obtain positive results. Low-energy ions naturally have short ranges. For example, the mean projected range of 30-keV Ar ions in water is calculated to be 63 nm. No However, the thickness of common cell walls varies from about 100 nm to many micrometers. How can penetration of low-energy ions through the cell wall occur?

The fact is that the plant cell wall, which composes the main part of the plant cell envelope, is not in a continuous structure but consists of bundles of cellulose microfibrils. From the primary structure of cellulose  $^{21}$ , its chemical formula is  $C_6H_{12}O_6$ . A cellulose microfibril is about 3.5 nm in diameter in most higher plants, and

the microfibrils are cross-linked in a net style with about a 5-nm space in between. <sup>21</sup> So, it is deduced that only about 3.5/(3.5+5)=7/17 of the thickness of the cell wall is packed with structural material (this fully-solid cell wall is termed the compressed cell wall). From electron microphotography, the thickness of the cell wall of the experimented tissues was estimated to vary from 250 to 400 nm (Fig 4a). Hence, the thickness of the compressed cell wall was about 100-165 nm. When the cell was placed in the vacuum chamber, the fluid among the microfibrils in the cell wall was pumped out and the cell wall shrank (Fig 2). Therefore, during ion bombardment, ions only interacted with atoms of the solid structural materials.

Based on the data above, simulations of the interactions between the ions and the cell wall material (Fig 7) using PROFILE20 and TRIM23 programs were performed to predict the ion and radiation damage ranges in cellulose. The mean ranges of 30-keV Arions at a fluence of 1 × 1015/cm2 and the induced radiation damage in the plant cell wall material are around 50-60 nm. The ions and the damage basically distribute within the compressed cell wall region (about 100 nm), mostly near the top surface of the cell wall. This indicates that no damage occurs to the plasma membrane, and consequently there are no effects on the cell viability. As the fluence increases, surface sputtering should be taken into account. According to the special structure of the cell wall mentioned above, the sputtering effect is extremely heterogeneous at the cell wall surface. This is confirmed by the TEM (Fig 4) that at some locations the cell wall surface is etched more severely by sputtering. Because the sputtering yield is linearly proportional to the ion fluence<sup>24</sup>, at a fluence of 2×10<sup>15</sup> ions/cm2 NR could enter inside the cell wall and keep the cell alive. At a higher fluence of  $4 \times 10^{15}$  ions/cm<sup>2</sup>, ions might completely penetrate the cell wall that had been thinned by sputtering and hence cause fatal damage to the cell wall, plasma membrane and organelles inside the cell, resulting in the staining of the nuclei.

Thus, ion beams of energies and fluences, which have maximum ranges of ions and radiation damage around the thickness of the compressed cell wall (which means no significant damage to the plasma membrane) and produce surface sputtering effects and inner atomic collision cascades for solids (Fig 7), could affect the porous biological tissues in a similar way. The cellulosepectin skeleton that constitutes the cell wall can be weakened and even pierced at some significantly weakened locations by extensive damage due to atomic collision cascades, and thus forming the crater-like structures. Because there has been experimental evidence of penetration of exogenous macromolecules (eg Trypan Blue dye with the molecular weight of 1000

Da° and DNA with 3.3 kb¹°) into cells induced by ion beams, it is inferred that the crater size should be sufficiently great for the movement of those exogenous molecules. This has been supported by our microscopic observation as described in the part of ion bombardment effect on the cell wall structure. The crater-like structures therefore constitute new molecule-exchange channels for exogenous macromolecule (such as DNA) transfer.

Gene transfer into cells has been induced by microparticle bombardment.25 The technique, termed biolistics, uses DNA-covered heavy-metal (eg Au or W) microparticles, 1-4 µm in diameter, shot from a pressured-air gun to bombard the target cell at an ultrasonic velocity (eg 430 m/s). Thus, the induction mechanisms are completely different between the techniques of microparticle bombardment and ion beam bombardment. The former transfers gene by directly introducing the gene attached on the particles which now penetrate inside the cell and locate in either cytoplasm, or organels, or nucleus. The latter transfers gene by first creating pathways on the cell envelope that is bombarded by ion beams and subsequently incubating the cell in a gene medium. The energy of a microparticle (eg Au, 1 µm in diameter, at a velocity of 430 m/s) is around an order of 10<sup>-8</sup> J, whereas the energy of an ion (eg Ar, at 30 keV) is in the range of 10-15-10-14 J. As a result, the microparticle pierces the cell envelope and enters inside the cell, but the ion basically only interacts with the cell envelope. Therefore, ion bombardment is thought to be safer for the cell survival due to the controllable ion species, energy and fluence so as to control the interaction extent, and gene is transferred more naturally.

#### CONCLUSION

Induction of exogenous molecule transfer into the living plant cells by ion beam bombardment in vacuum occurs when physical damage in the cell envelope is created by appropriate ion bombardment such that the ion range and radiation damage range lie within the compressed cell wall thickness. Certain types of damage structures can form channels for the exogenous molecules to transfer through the cell envelope.

#### **ACKNOWLEDGEMENTS**

We wish to thank Dr IG Brown for many valuable discussions and suggestions in preparing this manuscript. We thank P Vichaisirimongkul, R Charoennugul, and P Chitanan for their assistance in mechanical and technical work. This work was supported by the Thailand Research Fund.

#### REFERENCES

- Nastasi M, Mayer JW and Hirvonen JK (1996) lon-solid Interactions: Fundamentals and Applications. Cambridge University Press, New York.
- Schneider E, Kost M, and Schafer M (1990) Inactivation cross section of yeast and bacteria exposed to heavy ions of low energy (< 600 keV/u). Radiat Prot Dosim 31, 291-5.</li>
- Yu Z, Deng J, He J, Huo Y, Wu Y, Wang X, and Liu G (1991) Mutation breeding by ion implantation. Nucl Instr and Meth B59/60, 705-8.
- Wei Z, Xie H, Han G, and Li W (1995) Physical mechanisms of mutation induced by low energy ion implantation. Nucl Instr and Meth B95, 371-8.
- Tanaka A, Watanabe H, Shimizu T, Inoue M, Kikuchi M, Kobayashi Y, and Tano S (1997) Penetration controlled irradiation with ion beams for biological study. Nucl Instr and Meth B129, 42-8.
- Yu Z (2000) Ion beam application in genetic modification. IEEE Trans on Plasma Sci 28, 128-32.
- Yu Z, Yang J, Wu Y, Cheng B, He J, and Huo Y (1993) Transferring Gus gene into intact rice cells by low energy ion beam. Nucl Instr and Meth B80/81, 1328-31.
- Hase Y, Tanaka A, Narumi I, Watanabe H, and Inoue M (1998) Development of pollen-mediated gene transfer technique using penetration controlled irradiation with ion beams. JAERI-Review 98-016, 81-3.
- Vilaithong T, Yu LD, Alisi C, Phanchaisri B, Apavatjrut P, and Anuntalabhochai S (2000) A study of low-energy ion beam effects on outer plant cell structure for exogenous macromolecule transferring, Surf and Coat Technol 128-129, 133-8.
- Anuntalabhochai S, Chandej R, Phanchaisri B, Yu LD, Vilaithong T, Brown IG (2001) Ion beam induced deoxyribose nucleic acid transfer. Appl Phys Lett 78, 2393-5.
- Murashige T and Skoog F (1962) A revised medium for rapid growth and bioassays with tabacco tissue cultures. Physiologia Pl 15, 473-97.
- White PR (1963) The Cultivation of Animal and Plant Cells. Ronald Press, New York.
- Vacin E and Went F (1949) Some pH changes in nutrients solutions. Bot Gaz 110, 605-13.
- 14. Yu LD, Suwannakachorn D, Intarasiri S, Thongtem S, Boonyawan D, Vichaisirimongkol P, Vilaithong T (1995) Ion beam modification of materials program at Chiang Mai University. In: Proceedings of the 9th International Conference on Ion Beam Modification of Materials (Edited by Williams JS, Elliman RG and Ridgway MC), pp 982-5. Elsevier Science BV, Amsterdam.
- 15. Vilaithong T, Suwannakachorn D, Yotsombat B, Boonyawan D, Yu LD, Davydov S, Rhodes MW, Intarasiri S, et al (1997) lon implantation in Thailand (1) development of ion implantation facilities. ASEAN J on Sci and Technol for Devel 14, 87-102.
- Gahan PB (1984) Plant Histochemistry and Cytochemistry, p.126. Academic Press, London.
- Saunders JA and Matthews BF (1995) Pollen electrotransformation in tobacco. In: Plant Cell Electroporation and Electrofusion Protocols (Edited by Nickoloff JA), pp 81-7. Humana Press, New Jersey.
- Yu Z, Qiu L and Huo Y (1991) Progress in studies of biological effect and crop breeding induced by ion implantation. J of Anhui Agricultural College 18, 251-57 (in Chinese with the English abstract).
- Yu Z and Huo Y (1994) Review in low energy ion biology. J of Anhui Agricultural University 21, 221-5 (in Chinese with the English abstract).

- 20 PROFILE code software, Version 3.20 (1995) Implant Sciences Corp, Wakefield, MA, USA.
- 21 Alberts B, Bray D, Lewis J, Raff M, Roberts K, Watson JD (1992) Molecular Biology of the Cell, 2nd ed. p.1137. Garland Publishing Inc., New York.
- 22 Voet D and Voet JG (1990) Biochemistry, p.254. John Wiley & Sons, New York.
- 23 Ziegler JJ and Biersak JM (1990) TRIM-1991 program code, see, for instance, the web site <a href="http://www.research.ibm.com/uniteams/">http://www.research.ibm.com/uniteams/</a>
- 24 Nelson RS (1973) The physical state of ion implanted solids. In: Ion Implantation (Edited by Dearnaley G, Freeman JH, Nelson RS, Stephen J), pp 154-254. North-Holland Publishing Company. The Netherlands.
- Publishing Company, The Netherlands.

  25. Klein TM, Wolf ED, Wu R and Sanford JC (1987) High velocity microprojectiles for delivering nucleic acids into living cells. *Nature* 327, 70-3.



Available online at www.sciencedirect.com

SCIENCE (D) DIRECT

Radiation Physics and Chemistry 71 (2004) 927-935

**Radiation Physics** Chemistry

www.elsevier.com/locate/radphyschem

### Heavy ion induced DNA transfer in biological cells

- T. Vilaithong<sup>a,\*</sup>, L.D. Yu<sup>a</sup>, P. Apavatjrut<sup>b</sup>, B. Phanchaisri<sup>c</sup>, S. Sangyuenyongpipat<sup>a</sup>, S. Anuntalabhochai<sup>d</sup>, I.G. Brown<sup>c</sup>

\* Fast Neutron Research Facility, Department of Physics, Faculty of Science, Chiang Mai University, Chiang Mai 50200, Thailand Department of Horticulture, Faculty of Agriculture, Chiang Mai University, Chiang Mai 50200. Thailand <sup>c</sup> Institute for Science and Technology Research & Development, Chiang Mai University, Chiang Mai 50200, Thailand <sup>d</sup> Department of Biology, Faculty of Science, Chiang Mai University, Chiang Mai 50200, Thailand

Lawrence Berkeley National Laboratory. University of California, Berkeley, California 94720, USA

#### Abstract

Low-energy ion beam bombardment of biological materials for genetic modification purposes has experienced rapid growth in the last decade, particularly for the direct DNA transfer into living organisms including both plants and bacteria. Attempts have been made to understand the mechanisms involved in ion-bombardment-induced direct gene transfer into biological cells. Here we summarize the present status of the application of low-energy ions for genetic modification of living sample materials.

© 2004 Elsevier Ltd. All rights reserved.

Keywords: Low-energy heavy ion; Ion bombardment; DNA transfer; Biological cells

#### 1. Introduction

Towards the end of the eighties, enlightened by ion implantation modification of material's surface, attempts were made to apply the low-energy ion implantation technique to living biological materials. Induced mutation of rice by 30-keV nitrogen ions was reported for the first time (Yu et al., 1989). A new highly interdisciplinary field, low-energy ion beam bioengineering, was initiated (Yu et al., 1991) and has commanded increasing interest. Since then, ion implantation as a new genetic modification method has been widely applied to breeding of crops and microbes (Yu and Huo, 1994). In 1988, the etching effect of ion beams on the cell wall was discovered, which subsequently led to the process of ioninduced gene transfer in rice (Yu et al., 1993). For a decade researches and applications in the field of lowenergy ion-beam-induced exogenous macromolecule transfer into biological cells have been rapidly developed and particularly active in China, Japan and Thailand (Yu. 2000). In this paper, the development and present status of the technology of low-energy ion-beaminduced gene transfer in living biological organisms are reviewed.

#### 2. Principle of ion-beam-induced gene transfer in biological cells

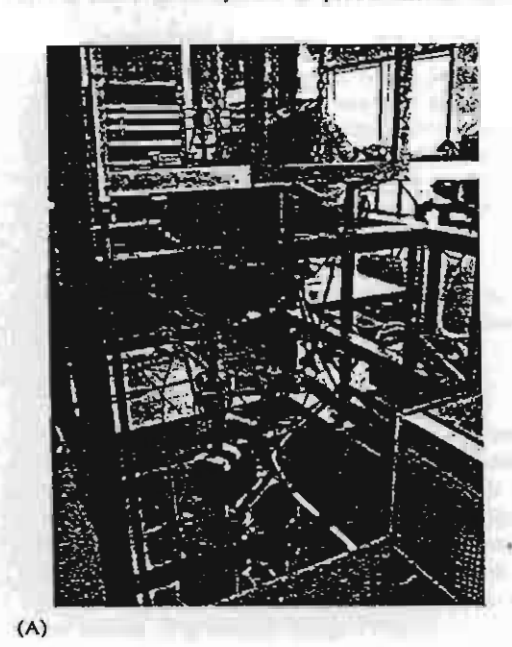
Gene transfer refers to the delivery of genetic information carriers from outside a cell, (the receptor) into it, crossing the cell envelope by whatever method, biological, physical, or chemical means, to realize expressions (at the levels of cell, organs, and whole system) and heritage under the new genetic background. Owing to their simplicity and effectiveness, a number of physical methods have been invented and employed for the gene transfer purpose, such as electroporation (Weaver, 1996), particle gun or microinjectile bombardment (Klein et al., 1987), microinjection and macroinjection, microlaser, and ultrasonication (Yu, 1999). All

<sup>\*</sup>Corresponding author. Tel.: +66-53-943379; fax: +66-53-

E-mail address: thirapat@fnrf.science.cmu.ac.th (T. Vilaithong).

of these methods perforate the cell wall substantially but do not severely damage the cell itself to provide exogenous genes with passages to enter the receptor cell.

The ion beam method is based on the same principle as that in other applications. It requires an ion beam installation, which normally consists of an ion source, an electric field, an ion beam transport system, and a target chamber. Such an installation can either be an integrated apparatus or a beam line facility with the components separately equipped (Lu et al., 1991; Nastasi et al., 1996). For the convenience of housing a biosample the holder is placed horizontally and so a vertical accelerator system is preferred, as shown in



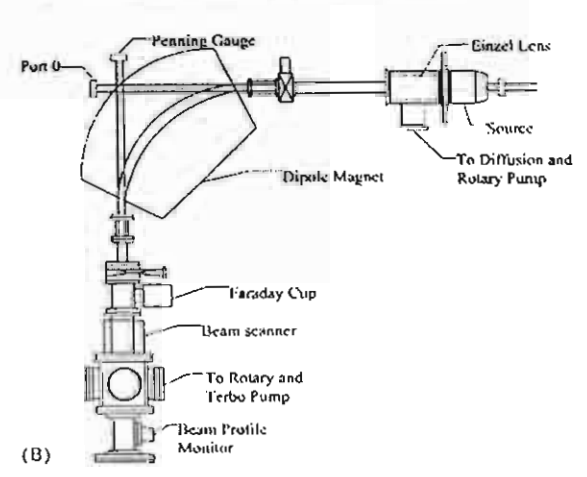


Fig. 1. A typical ion beam bioengineering facility installed at Chiang Mai University. (A) Photograph, and (B) schematic diagram (side view).

Fig. 1 (Sangyuenyongpipat et al., 2002). Both internal and external environments of the installation should meet bioclean requirements (Yu et al., 1993; Sangyuenyongpipat et al., 2002). In a conventional machine ions produced in the ion source are accelerated by the electrostatic field to gain a certain energy, then transported, preferably mass-analyzed by electric or magnetic fields and finally introduced into the target chamber to bombard the sample. Conventionally, the process is conducted in a vacuum environment. For treatment of biological cells to induce gene transfer, the ion energy can be relatively low, normally a few ten keV, and the pressure is about the orders of  $10^{-4}$ - $10^{-3}$  Pa. The cells at the target location are bombarded by the energetic ions to a fluence normally in the range of 1015-10<sup>16</sup> ions/cm<sup>2</sup>. During ion bombardment, the physical processes, due to the interaction between ions and the living cells, are in principle the same as that occurring in common solids, such as surface sputtering or etching, ion stopping and implantation, atomic displacement and charge introduction (Yu et al., 1993; Nastasi et al., 1996). After ion beam bombardment, DNA transfer is carried out by incubating a mixture of the DNA and the ion-bombarded cells (Yu, 1999; Anuntalabhochai et al., 2001). On an experimental level those DNAs, which have easily expressed-marker (or property) genes, are normally chosen to be used for quick and easy detection of the transferred DNA. The transferred DNA molecular size is measured to confirm that the transferred DNA indeed comes from the exogenous original (Anuntalabhochai et al., 2001).

In the following sections, we describe ion-beaminduced gene transfer starting with the simple case of general exogenous macromolecule transfer, then the gene transfer into plant cells, and finally, the most complicated case, the DNA transfer into bacterial cells.

## 3. Ion-beam-induced exogenous vital dye molecule transfer into plant cells

In the experiments, cells of various kinds of plant tissues, most of which were horticultural plants, were bombarded in vacuum with argon and nitrogen ion beams at energies of  $15-30\,\text{keV}$  with fluences ranging from  $5\times10^{14}$  to  $3\times10^{16}\,\text{ions/cm}^2$ . The ion bombardment effects on tissue viability, damaging of the cell wall, and trypan blue (TB) and neutral red (NR) dye molecule transfer into the cells through the cell envelope, were investigated (Fig. 2) (Vilaithong et al., 2000; Apavatjrut et al., 2003).

The results showed that the characteristics of the tissue survival, the degree of damage to the cell wall and penetration of dye molecules into the cells through the cell envelope, depended on ion species, energy and fluence. For example, the height of naked corn embryos

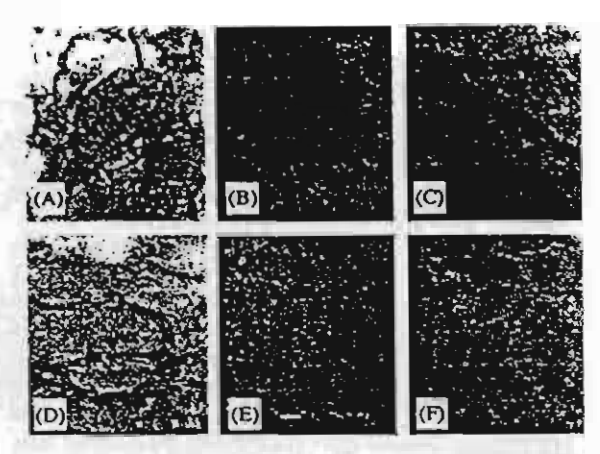


Fig. 2. Optical microphotographs of trypan blue staining of 30-keV Ar-ion bombarded and unbombarded corn embryo cells: (A) fresh control, (B) vacuum control, (C) at the fluence of  $5 \times 10^{14} \, \text{ions/cm}^2$ , (D) at the fluence of  $1 \times 10^{15} \, \text{ions/cm}^2$ , (E) at the fluence of  $2 \times 10^{15} \, \text{ions/cm}^2$ , and (F) at the fluence of  $4 \times 10^{15} \, \text{ions/cm}^2$ . The bar in the photo indicates  $5 \, \mu \text{m}$  (C, D, E, F from Vilaithong et al., 2000).

that were bombarded with 15-keV nitrogen ions or 30keV argon ions grown in tissue culture was found to be linearly proportional to the ion fluence:

Height = 
$$C - \alpha f$$
,

where C is the control height, a is a proportional coefficient and f is the ion fluence. This relationship is well applicable for fluences from 1 x 1014 to 1 × 1016 ions/cm2 of low-energy (a few tens of keV) ions. Microscopical examinations of the cell wall revealed that for a certain ion species, the damage to the cell wall was increased with the ion energy at a certain fluence and the ion fluence at a certain energy (Vilaithong et al., 2000; Apavatjrut et al., 2003). Correspondingly, the dye molecule transfer was shown to occur in accordance with the damage degree to the cell wall (Vilaithong et al., 2000; Apavatjrut et al., 2003). For instance, for 30-keV argon-ion bombardment at a fluence of 2 × 1015 ions/ cm2, the dye molecules entered the Curcuma embryo cells without causing severe damage. However, under other conditions such as lower or higher fluences, or lower or higher energies, the dye either did not enter the cells or stained the nuclei (Fig. 2).

All these results indicate that exogenous molecule transfer into living plant cells can be achieved by ion beams that have appropriate physical parameters to cause suitable radiation damage within the cell wall.

#### 4. Ion-beam-induced gene transfer into plant cells

Ion-beam-induced gene transfer was first achieved in plant cells. The first internationally reported success was

of transferring GUS (B-glucuronidase) and CAT (chloramphenical acetyltransferase) genes into rice cells by low energy ion beam (Yu et al., 1993). Intact suspension cells and ripe embryos of rice seeds were selected as the receptors, and plasmid DNA consisting of GUS and CAT genes were used as the exogenous genetic materials. Ar ions at 20-30 keV were employed to bombard the samples at fluences ranging from  $1 \times 10^{15}$ to 4 x 1015 ions/cm2 for the cells and 1 x 1016 to 2 × 10<sup>16</sup> ions/cm<sup>2</sup> for the embryos in a sterile vacuum environment. After ion bombardment, the samples were put into a solution containing the plasmid DNA (GUS and CAT genes). The drawing DNA's receptors were incubated in a liquid or solid incubation medium for several weeks. The fluorescence activities of GUS and CAT were detected for the incubated samples. The results showed that the fluorescence intensities of the ion-bombarded cells and embryos were 3-12 times higher than that of the control (in vacuum), as shown in Fig. 3. This evidence indicated that the genes had indeed been transferred into the receptors modified by the ion beams.

Following this work, ion-beam-induced gene transfer was achieved in other plant cells. The pCH gene was transferred into dry pollen of Nicotiana tabacum L. induced by carbon out-beam bombardment in atmosphere (Hase et al., 1998). Transferring gene into pollen was more difficult than in naked cells as pollen is covered with two layers of envelope, outer pollen exine and inner cell membrane. This was also the first time that an out-beam technique for ion bombardment of living biological materials was attempted. Further, the transferring of real plant genes into other plant seeds induced by ion beams was conducted. This work would be more difficult since seeds have thick and hard covers. Pumpkin (Cucubita maxima Duch) DNA was transferred into watermelon (Citrullus lanatus) seeds induced

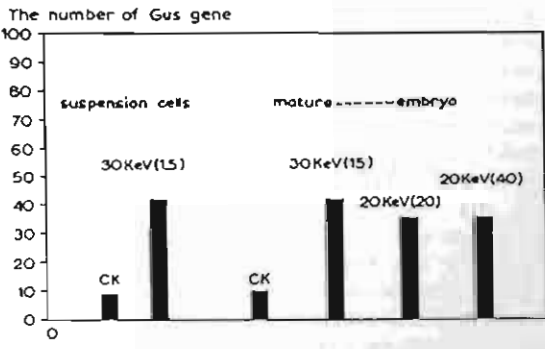


Fig. 3. Fluorescence counts of Gus genes transferred into the intact cells and embryos of rice seeds bombarded by Ar ion beam. The numbers in the brackets indicate the ion fluences in the unit of 10<sup>15</sup> ions/cm<sup>2</sup>. CK: the control in vacuum (Yu et al., 1993).

by 25-keV N-ion bombardment with a fluence of  $7.8 \times 10^{16}$  ions/cm<sup>2</sup> (Wang et al., 2002). Total DNA of cabbage was transferred into arabidopsis thaliana seeds induced by 30-keV Ar-ion bombardment with a fluence of  $1.5 \times 10^{17}$  ions/cm<sup>2</sup> (Bian et al., 2002). It is significant to note that in both gene transfers, the genetic modifications were maintained in next generations.

Transferring gene segments is not the ultimate objective as plenty of genetic information may be lost. Rather, exploration of the transfer of vital naked large DNA molecules or gene groups is always the direction of technological development. The working principle is the same as before, but the systems used are more important. The receptors should be able to accept highly effectively exogenous gene groups and stably inherit the gene to the next generations. The donors should have excellent characteristics consistent with the breeding purpose (Yu, 1999). In an experiment, rice was the receptor while DNA was directly extracted and prepared from young corn leaves. The embryos of the rice seeds were firstly bombarded with 35-keV Ar ions at a fluence of 1.0 × 1016 ions/cm2. Then the DNA solution was smeared onto the bombarded embryos, and the seeds were bombarded again with the same Ar-ion beam but at a fluence of 5 x 10<sup>15</sup> ions/cm<sup>2</sup>. The twice-ion-bombarded seeds were soaked into the corn-DNA SSC solution for DNA transfer. The results showed that corn characteristics were continuously expressed in the rice even to the Mg generation (Yu, 1999).

#### 5. Ion-beam-induced DNA transfer into bacteria

Following successes in gene transfer in plant cells, research interests were extended to gene transfer into bacteria. The bacterial cell envelope is more complicated and subtle than that of the plant cell. For example, the cell envelope of E. coli contains a rather thin cell wall, but a relatively thick complex outer membrane, as well as other structures such as a thin periplasmic space and a thin plasma membrane (Voet and Voet, 1990). Another difficulty exists in the ability of living bacteria to survive in vacuum much lower than that of dry seeds. Therefore, technical parameter control should be more precise in working on bacteria than on plants. The first published report on successful ion-beam-induced DNA transfer in bacteria was on transferring in E. coli (Anuntalabhochai et al., 2001). In this experiment, Ar- and N-ion beams were used to bombard the bacteria E. coli strain DH5a in a vacuum with an energy of 26 keV and fluences in the range 0.5-4 × 10<sup>15</sup> ions/cm<sup>2</sup>. Three DNA plasmids, pGEM2, pGEM-T easy and pGFP, carrying different marker genes, were subsequently transferred (separately) into the appropriately Ar-ion-bombarded bacteria and successfully expressed (Fig. 4). The effects on the plasmid DNA size, ion fluence and incubation time of the DNA transfer were studied. The results showed that at a fluence of about  $2 \times 10^{15}$  Ar-ions/cm<sup>2</sup> the smaller the DNA and the longer the incubation time, the easier the DNA transfer could be (Phanchaisri et al., 2002). This study indicates that ion beams with an energy such that the ion range is approximately equal to the cell envelope thickness, at a certain range of fluence, are able to generate pathways for macromolecule transfer through the envelope without irreversible damage (Anuntalabhochai et al., 2001).

#### 6. Discussions on mechanisms

Several attempts have been made to understand the mechanisms involved in the ion-beam-induced gene transfer into living cells. The essential mechanisms for gene transfer induced by any method can be, in the final analysis, attributed to either physical or chemical effects. It has been proposed (Yu, 1999) that ion beam bombardment plays both the role of enhancing probabilities for the gene to transfer and providing additional driving forces to the transferring process.

#### 6.1. Surface sputtering

Ion beam has a sputtering effect on the cell surface much the same as on conventional solid materials. An ion with an energy of several-tens of keV has a very strong sputtering action on the biological cell surface (Yu, 1999), which is effectively stripped off layer by layer. As the cell wall is a multi-layer, multi-phase, porous structure, the stripping effect eventually results in the perforation of the cell wall. Both experimental observations and theoretical investigations have revealed a considerably higher degree of surface sputtering and hence, higher sputtering yields by low-energy ion beam on the cell envelope compared with conventional solid surfaces.

Fig. 5 shows the transmission electron microscopic (TEM) photographs of the cross sections of the Curcuma embryo cell envelopes bombarded with 30-keV Ar-ion beam compared with that of the control, unbombarded embryo. The cell surface of the control looks smooth whereas the surfaces of the ion-bombarded cells exhibit apparent damage which becomes more severe with increasing ion fluence. The thickness loss due to sputtering, which is proportional to the sputtering yield, can be estimated from the damaged cell envelope thickness. The equivalent thickness loss is measured to be about 200 nm for the cell bombarded at a fluence of  $1 \times 10^{15}$  ions/cm<sup>2</sup>. This is significantly greater than the 6 nm calculated using ion implantation programs for the solid phase of the cell wall material. The sputtering yield of a biological-wall-equivalent material, C<sub>3</sub>H<sub>7</sub>O<sub>2</sub>N, was experimentally measured (Yu, 1999). The result showed

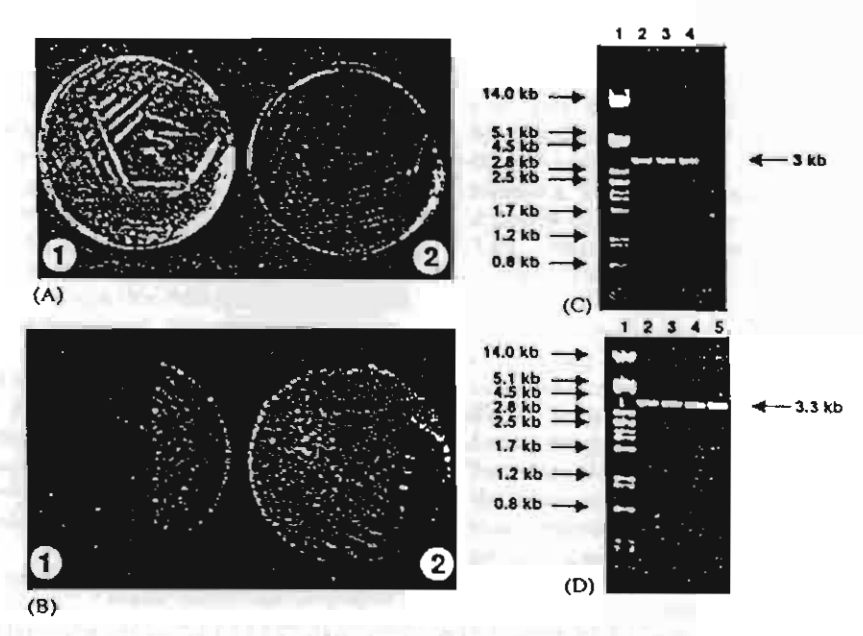


Fig. 4. Analysis of transferred pGEM-T easy and pGFP plasmids in ion-bombarded E. coli strain DH5x. (A)  $\beta$ -galactosidase activity in LB media added with X-gal and IPTG. The E coli without pGEM-T easy (1), and with the transferred pGEM-T easy (2), cultured in LB<sup>+</sup> and LB<sup>+</sup>, respectively. (B) Expression of green fluorescent protein in E. coli. The E. coli without pGFP (1), and with the transferred pGFP (2), plated on LB<sup>+</sup> and LB<sup>+</sup>, respectively, visualized under UV light. (C) Measurement of molecular size of pGEM-T easy in gel electrophoresis. The transferred pGEM-T easy was digested with restriction enzymes Pst1 (lane 2), and EcoR1 (lane 3). The original pGEM-T easy digested with Pst1 is in lane 4. A standard molecular-size marker is shown in lane 1. (D) Measurement of molecular size of pGFP in gel electrophoresis. The transferred pGFP was digested with restriction enzymes Pst1 (lane 2), EcoR1 (lane 3), and Xba1 (lane 4). The original pGFP digested with Pst1 is in lane 5. A standard molecular-size marker is shown in lane 1 (Anuntalabhochai et al., 2001).

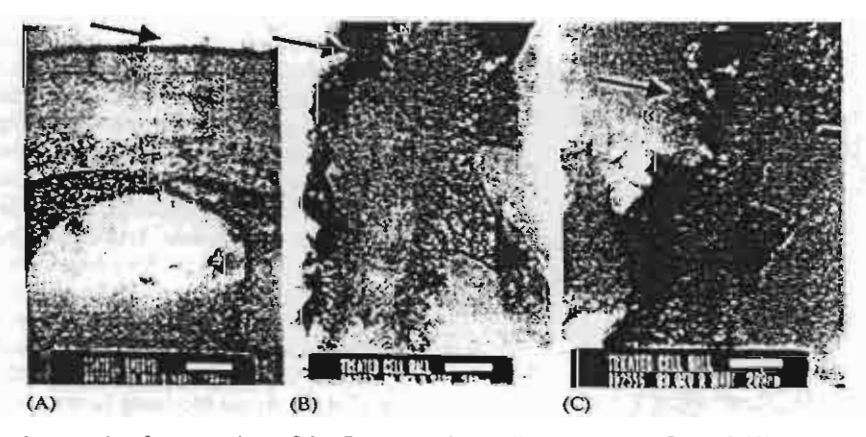


Fig. 5. TEM microphotographs of cross sections of the *Curcuma* embryo cell envelopes. (A) Control; (B) Ar-ion bombarded at 30 keV with a fluence of  $1 \times 10^{15}$  ions/cm<sup>2</sup>; (C) Ar-ion bombarded at 30 keV with a fluence of  $2 \times 10^{15}$  ions/cm<sup>2</sup>. The scale is as indicated on the photographs. The arrows point the external surface of the cell envelope (Vilaithong et al., 2000; Apavatjrut et al., 2003).

that the sputtering yield was 3-4 orders in magnitude higher than that calculated using classical ion-solid interaction theory. Remodeling of the plant cell wall, which is composed of the cellulose C<sub>6</sub>H<sub>12</sub>O<sub>6</sub>-compound,

in association with computer program simulation, also revealed a ten-fold higher sputtering yield for the ion-bombarded cell wall compared with that predicted by direct program calculation (Yu et al., 2002). The

consequence is that the cell envelope can be significantly thinned by the ion beam. The important fact is that an ion beam with a relatively low fluence, which will not cause severe damage to the cell, can make the cell envelope sufficiently thin to increase the permeability thereby enabling exogenous gene transfer to take place.

Experiments were performed to demonstrate the enhancement of the permeability of the cell envelope after ion bombardment. Changes in electro-conductivity were measured for the ripe rice embryos before and after 30-keV N-ion bombardment (Yu, 1999). The mean permeability of four groups of the unbombarded samples was  $4.3 \times 10^{-6}$  ppm. For the samples bombarded with a fluence of  $3 \times 10^{16}$  ions/cm<sup>2</sup>, the mean permeability was  $1.73 \times 10^{-5}$  ppm which was four times higher. For the samples bombarded with a fluence of  $6 \times 10^{16}$  ions/cm<sup>2</sup>, it was  $3 \times 10^{-5}$  ppm which was 7.2 times that of the control.

#### 6.2. Ion penetration depth in the cell wall

The thinned cell envelope, or the enhanced permeability that facilitates exogenous gene transfer, does play a certain role in the mechanism responsible for the macromolecules to enter the cell. Yet, there must exist gateways in the cell envelope, which should be large enough to allow the gene to pass through. Here we consider two possibilities. The cell envelope originally has some channels for exchanging living substances between inside and outside the cell. These channels may open up more as the thickness of the cell envelope decreases due to sputtering; this allows the gene to pass through. The second possibility may be due to the direct formation of structural pathways or channels in the cell envelope induced by ion bombardment. For the first possibility, studying the ion beam sputtering of the cell surface can lead to a knowledge of how thin the cell envelope can be. For the second possibility, the ion penetration depth in the cell envelope must be firstly investigated. Any structural change in the target material due to ion bombardment is a consequence of ion-bombardment-induced radiation damage as well as ion implantation in the material. Normally, the extent of the radiation damage is closely related to the implanted ion penetration depth (Nastasi et al., 1996).

The thickness of normal plant cell envelopes is in an order of several hundreds of nanometer, while a common ion with an energy of, say, 30 keV has a project range in an order of 100 nm in material such as water (which is sometimes used as a bio-equivalent or -close material). The question is then how such ions can penetrate the entire cell envelope and create structural changes or appropriate damage through the cell envelope.

There have been many experimental observations that demonstrate an abnormal penetration depth of implanted ions in biological materials, which is considerably greater than that predicted by calculations using conventional ion implantation theory (Yu, 1999). A basic explanation is that the plant cell envelope, in which the cell wall is the major component, is a very porous structure. Therefore, the apparent thickness of the cell envelope is much greater than its effective thickness. This explanation has recently been quantitatively studied (Yu et al., 2003). Based on the biological structure of the plant cell wall, a physical model has been proposed, which assumes that the wall is composed of randomly orientated layers of cylindrical microfibrils made from cellulose molecules of C<sub>6</sub>H<sub>12</sub>O<sub>6</sub>, as shown in Fig. 6. From this model, multiplication factors of 2.43 for ion range and straggling, and 7 for sputtering yield have been determined to allow calculations of both of these parameters from the conventional ion implantation programs. Using these correction factors, it is possible to apply common ion implantation programs to estimate the ion penetration depth as well as the radiation damage extent in the cell for bioengineering purposes. These estimates have been compared with measured data and good agreement is achieved (Yu et al., 2003). In practice, the ion projectile range in the homogeneous solid cell wall material, cellulose of  $C_6H_{12}O_6$  ( $\rho = 1.05 \text{ g/cm}^3$ ), and the sputtering yield of the surface for a given ion species at a given energy are first determined using classic ion implantation programs. The calculated ion range and the sputtering yield

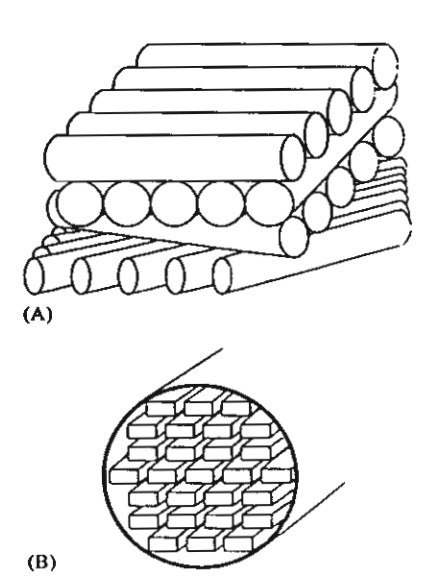


Fig. 6. Microscopic physical model of the plant cell wall. (A) The wall is made of random-oriented layers of closely packed cylindrical microfibrils. The columns represent microfibrils. (B) Inside each microfibril are chains of cellulose molecules in which the atoms reside in the same plane. The strips represent the cellulose molecule chains (Yu et al., 2002).

are then multiplied by the factors of 2.43 and 7, respectively, to give the modified range and sputtering yield. A multiplication of the sum of the ion range and straggling with the factor of 2.43 can result in an estimate of the ion maximum penetration depth in the cell wall. The modified ion range or maximum penetration depth is then multiplied by a factor of 17/7, the ratio between the apparent thickness of the cell wall and the effective thickness of the compact solid cell wall material (Yu et al., 2003), to obtain the apparent penetration depth in the cell wall. The thickness of the surface sputtering loss is calculated using the modified sputtering yield together with the ion fluence. The sum of the apparent penetration depth and the thickness of the sputtering loss results in the final estimate of the ion penetration depth in the cell wall. Since normal plant cell envelopes are composed mainly of the cell wall, the ion penetration depth in the cell wall is then approximately the penetration depth in the cell envelope. In vacuum almost all of the liquids are pumped out from the cells (Yu et al., 2002), therefore, during ion implantation, the major stopping source to the ions is then the cell wall or envelope. Thus, the estimate of the ion penetration depth in the cell wall is also an estimate for large biological sample such as tissues and organisms.

The study of the ion penetration depth in the cell envelope has shed some light on the ion beam parameters for successful ion-beam-induced macromolecule transfer. When the ion bombardment parameters, such as the ion species, energy and fluence, are such that the apparent maximum ion penetration depth in the cell envelope is approximately equal to the cell envelope thickness, ion beams are able to cause damage which partially enables macromolecule transfer through the cell envelope.

#### 6.3. Formation of pathways in the cell envelope

The appropriate ion penetration depth in the cell envelope does not provide a complete picture of the mechanism responsible for ion-beam-induced exogenous macromolecule transfer in the cells. Ion beam bombardment induces the formation of special structures on the cell surface. The earliest observation was on the cultured rice suspension cells that were bombarded with 30-keV nitrogen ions (Yu et al., 1993). When the ion fluence was increased to 5 x 1014 ions/cm2, some small and big holes were observed. Since then more evidence has been found on the ion-beam-induced formation of special surface microstructures including micro-holes and micro-craters in both plant and bacterial cell envelopes. Ions of N, Ar, Cl. Fe and Xe were used to bombard onion skin and E. coli strain DH5\alpha cells at energies around 10-30 keV to fluences in the range of  $0.5-4 \times 10^{15}$  ions/cm<sup>2</sup>. Normally, when the ion fluence was higher than 1 x 1015 ions/cm2, micro-craters or holes or pimples were observed on the sample surfaces with scanning electron microscopy (SEM) (Yu et al., 2002; Phanchaisri et al., 2002; Apavatjrut et al., 2003) (also Fig. 7). These structures have been seen to be sufficiently big and even perforate the cell envelope. However, at this point it cannot be concluded that the formation of these microstructures is a general phenomenon induced by ion bombardment. Further studies are required to shed more light on the formation of micro-holes and micro-craters.

### 6.4. Driving force for transferring exogenous DNA into the cell

Formation of pathways in the cell envelope is a prerequisite for gene transfer, but does not guarantee that exogenous macromolecules can certainly enter the cell; there must be driving forces and whether the driving force actively or passively makes exogenous gene be transferred is a question worthy of discussion here.

Generally speaking, the driving force can be either physical or chemical. Diffusion may be the first consideration in physics. Since in normal operations, the concentration of exogenous gene is considerably low, diffusion of the gene into the cell should be insignificant,

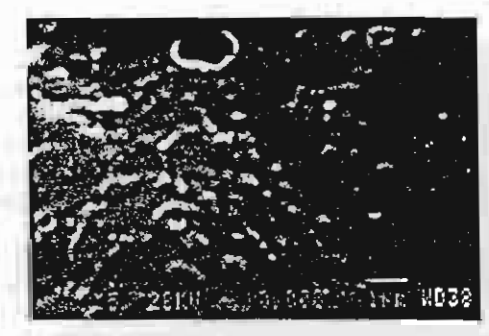




Fig. 7. SEM microphotographs of Ar-ion bombarded onion skin cell surface (the energy of 25 keV and the fluence of  $1 \times 10^{15}$  ions/cm<sup>2</sup>). Left: lower magnification, right: higher magnification. Micro-craters or holes and pimples are seen.

thus, playing a minor role. Another possibility to be considered is the charge exchange effect (Yu, 1999). As previously mentioned, ion bombardment introduces charges on the target. Thus, the charge exchange between the charged particles and the biological object surface can induce change in the electric polarization of the biological molecule, such as negativity becoming positivity. Experiments have observed the slowing down of the electrophoretic mobility of the ion-beam-bombarded rice suspension cells, indicating ion-beam-induced reduction of the negative electric charge in the cells (Yu et al., 1993). Although the change in electric polarization cannot be macroscopically measured, since the cell is a very poor electric conductor, local electric polarization may be changed particularly at the locations irradiated by positive charges. Thus, it is possible that, due to accumulated ultra positive charges, the ionbombardment-formed pathways become electrically positive. This generates an electrostatic attractive force to the electrically negative exogenous DNA that is going to be transferred into the cell so that DNA can be taken in. Even though the local electric polarization is not changed at the gene transferring pathways, due to a decrease in the receptor negativity, a decrease in the short-distance electrostatic expulsion between two electro-negative points is also beneficial to conducting in the gene.

#### 7. Summary and outlook

Low-energy ion beam bombardment induced exogenous gene transfer in plant and bacterial cells is a recently developed bioengineering technique. The principle, processes, and mechanisms of the method have been reviewed. The basics of applying this method for successful gene transfer is that the ion beam parameters should be controlled in such a way that the apparent ion penetration depth in the cell envelope is approximately equal to the cell envelope thickness. This is so that appropriate radiation damage can be induced to form special microstructures in the cell envelope to act as pathways for gene transfer. The mechanisms involved have not yet been thoroughly clarified and experimentally demonstrated. For example, what are the real pathways responsible for the gene transfer, how are the pathways formed, and what are the real driving forces to transfer the gene? Applications of this technique are to be expanded to serve effectively and profitably for developments of agriculture and biotechnological

Applying ion beam to induce gene transfer into the cells certainly has its shortcomings. The existing low-energy ion beam system operates in vacuum, therefore, for highly water-contained receptors of gene transferring, severe loss of water and freezing cause a decrease in the survival rate. Sterilized micro-environment in the target chamber can partly solve this problem (Yu et al., 1993), but then the requirement for professional handling skill is too high. This problem is expected to be solved as ion beam technology is developed further.

#### Acknowledgements

The authors thank Yu Zengliang for many fruitful discussions and permission to quote from his unpublished work. This study has been supported by the Thailand Research Fund.

#### References

- Anuntalabhochai, S., Chandej, R., Phanchaisri, B., Yu, L.D., Vilaithong, T., Brown, I.G., 2001. Ion-beam-induced deoxyribose nucleic acid transfer. Appl. Phys. Lett. 78, 2393-2395.
- Apavatjrut, P., Alisi, C., Phanchaisri, B., Yu, L.D., Anuntalabhochai, S., Vilaithong, T., 2003. Induction of exogenous molecule transfer into plant cells by ion beam bombardment. Sci. Asia 29, 99-107.
- Bian, P., Qin, G., Huo, Y., Wang, Y., 2002. Mutation analysis of arabidopsis thaliana transferred by total DNA of cabbage. Proceedings of the First International Symposium on Ion Beams: Biological Effects and Molecular Mechanisms, July, Wulumuqi, China, pp. 170-173.
- Hase, Y., Tanaka, A., Narumi, I., Watanabe, H., Inoue, M., 1998. Development of pollen-mediated gene transfer technique using penetration controlled irradiation with ion beams. JAERI Rev. 98-016, 81-83.
- Klein, T.M., Wolf, E.D., Wu, R., Sanford, J.C., 1987. High velocity microprojectiles for delivering nucleic acids into living cells. Nature 327, 70-73.
- Lu, R.L., Zhu, X.L., Yu, Z.L., Den, J.G., 1991. Preliminary study on effects of nitrogen cation beam on in vitro and in vivo DNAs. J. Anhui Agric. Coll. 18 (4), 294-297.
- Nastasi, M., Mayer, J.W., Hirvonen, J.K., 1996. Ion-Solid Interactions, Fundamentals and Applications. Cambridge University Press, Cambridge, Great Britain.
- Phanchaisri, B., Yu, L.D., Anuntalabhochai, S., Chandej, R., Apavatjrut, P., Vilaithong, T., Brown, I.G., 2002. Characteristics of heavy ion beam bombarded bacteria E. coli and induced direct DNA transfer. Surf. Coat. Technol. 158-159, 624-629.
- Sangyuenyongpipat, S., Yu, L.D., Tondee, N., Wattanavatee, T., Vilaithong, T., Thongleurm, C., Phanchaisri, B., Brown, I.G., 2002. Biological ion implantation facility, presented to the 29th IEEE International Conference on Plasma Science, May 26-30, Banff, Alberta, Canada.
- Vilaithong, T., Yu, L.D., Alisi, C., Phanchaisri, B., Apavatjrut, P., Anuntalabhochai, S., 2000. A study of low-energy ion beam effects on outer plant cell structure for exogenous macromolecule transferring. Surf. Coat. Technol. 128-129, 133-138.

- Voet, D., Voet, J.G., 1990. Biochemistry. Wiley, New York, p. 262.
  Wang, H., Gao, X., Guo, J., Wu, L., Huang, Q., Yu, Z., 2002.
  Genetic tranformation of watermelon with pumpkin DNA by low energy ion beam mediated introduction. Proceedings of the First International Symposium on Ion Beams: Biological Effects and Molecular Mechanisms, July, Wulumuqi, China, 165-169.
- Weaver, J.C., 1996. Electroporation Theory, Concept and Mechanisms, from Methods in Molecular Biology. In: Nickoloff, J.A. (Ed.), Plant Cell Electroporation and Electrofusion Protocols, Vol. 55. Humana Press Inc, Totowa, NJ, pp. 3-28.
- Yu, Z.L., 1999. Introduction to Ion Beam Biotechnology. Anhui Science and Technology Press, Hefei, China.
- Yu, Z.L., 2000. Ion beam application in genetic modification. IEEE Trans. Plasma Sci. 28 (1), 128-131.
- Yu, Z.L., Huo, Y.P., 1994. Review in low energy ion biology. J. Anhui Agric. Univ. 21 (3), 221-225.

- Yu, Z.L., Wu, X.D., Dong, J.G., Han, J.J., Zhao, J., 1989.
  Primary studies of mutational mechanism for rice induced by ion implantation. Anhui Agric. Sci. 16 (1), 12-16.
- Yu, Z.L., Qiu, L.J., Huo, Y.P., 1991. Progress in studies of biological effect and crop breeding induced by ion implantation. J. Anhui Agric. Coll. 18 (4), 251-257.
- Yu, Z.L., Yang, J., Wu, Y., Cheng, B., He, J., Huo, Y., 1993.
  Transferring Gus gene into intact rice cells by low energy ion beam. Nucl. Instrum. Methods B. 80, 1328-1331.
- Yu, L.D., Phanchaisri, B., Apavatjrut, P., Anuntalabhochai, S., Vilaithong, T., Brown, I.G., 2002. Some investigations of ion bombardment effects on plant cell wall surfaces. Surf. Coat. Technol. 158-159, 146-150.
- Yu, L.D., Vilaithong, T., Phanchaisri, B., Apavatjrut, P., Anuntalabhochai, S., Evans, P., Brown, I.G., 2003. Ion penetration depth in the plant cell wall. Nucl. Instrum. Methods B 206, 586-590.

## Development of *In-Situ* Atomic Force Microscopy for Study of Ion Beam Interaction with Biological Cell Surface

S. Sangyuenyongpipat<sup>1,a</sup>, T. Vilaithong<sup>2,b</sup>, L.D. Yu<sup>3,c</sup>, R. Yimnirun<sup>4,d</sup>,
P. Singjai<sup>5,e</sup>, and I.G. Brown<sup>6,f</sup>

1,2,3 Fast Neutron Research Facility, Department of Physics,
 Chiang Mai University, Chiang Mai 50200, Thailand
 4,5 Department of Physics, Faculty of Science
 Chiang Mai University, Chiang Mai 50200, Thailand

<sup>6</sup> Lawrence Berkeley National Laboratory,

Berkeley, California 94720, USA

'somjai@fnrf.science.cmu.ac.th, bthiraphat@fnrf.science.cmu.ac.th, cyuld@fnrf.science.cmu.ac.th,

<sup>d</sup>RattikornYimnirun@yahoo.com, <sup>e</sup>singjai@chiangmai.ac.th, <sup>f</sup>igbrown@lbl.gov

Keywords: In-situ AFM, Ion bombardment, Vibration isolation system.

#### Abstract

The interaction between ion beam and biological cells has been studied to apply ion-beam-induced mutation to breeding of crops and gene transfer in cells. Formation of micro-craters has been observed after ion bombardment of plant cells and they are suspected to act as pathways for exogenous macromolecule transfer in the cells. A technique of *in-situ* atomic force microscopy (AFM) in the ion beam line is being developed to observe ion bombardment effects on cell surface morphology during ion bombardment. A commercial AFM is designed to place inside the target chamber of the bioengineering ion beam line at Chiang Mai University. In order to allow the ion beam to properly bombard the sample without the risk of damaging the scanning tip and affecting normal operation of AFM, geometrical factors have been calculated for tilting the AFM with 35 degree from the normal. In order to avoid vibrations from external sources, mechanical designs have been done for a vibration isolation system. Construction and installation of the *in-situ* AFM facility to the beam line have been completed and are reported in details.

#### 1. Introduction

Ion implantation is a well-known surface modification tool. Ion bombardment into living biological cells is an interesting field of application of ion beam technology to biology. Important applications have included ion-beam-induced mutation breeding of crops and gene transfer in cells, which have been a great deal of practical successes in China and some other countries [1-5]. Recently, there have been reports on transfer of DNA into both plant cells [3,6] and bacterial cells

brought about by ion bombardment of cells under appropriately chosen beam parameters of ence and energy. However, mechanisms involved in ion-beam-induced DNA transfer are not yet clear. It is supposed that certain pathways in the cell envelope for exogenous macromolecule rester must be created by ion beam bombardment. Formation of microcrater-like structures on the face of onion skin cell wall has been observed after the material is bombarded by ion beam [10] of they may act as the pathways. Real time observation using Atomic Force Microscopy (AFM) is to clarify when and how the micro-craters form. An *in-situ* AFM for observation of micrometric formation induced by ion beam bombardment has been designed, constructed and installed at the standard many Mai University. Here we report our designing ideas in details.

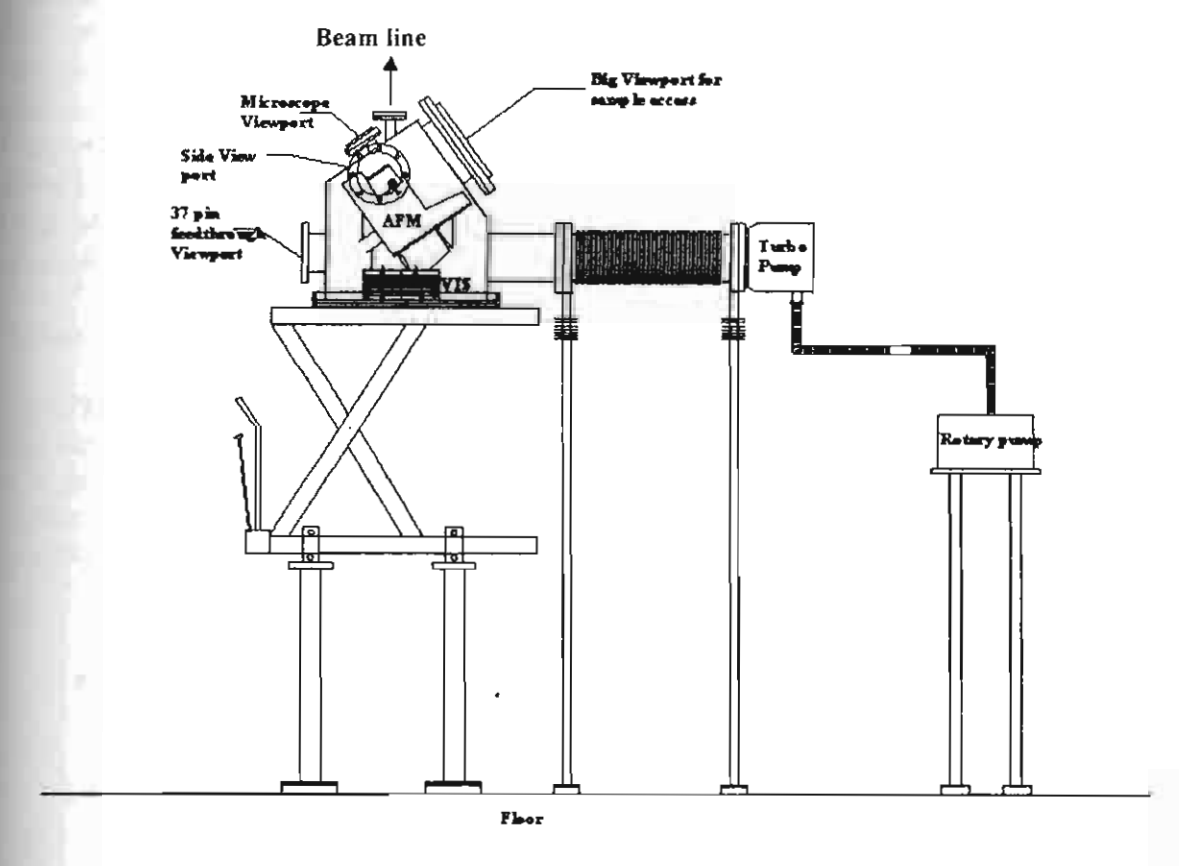


Figure 1. Schematic of the in-situ AFM facility.

#### Description of the Setup

The setup consists of an *in-situ* AFM chamber, a commercial AFM, a damping system, a unping system and supports, as shown in Fig. 1. The chamber is installed in the vertical beam line the target terminal of the ion bombardment facility. Its dimensions are approximately 550 mm in tight and 450 mm in diameter. It is made mainly from stainless steel. The whole commercial AFM SPM 9500-J2 from Shimadzu) is seated on a superlene support inside the chamber. The support eat is made in a special shape, which allows the AFM to tilt by 35 degree from the normal. Under the support seat there is a vibration isolation system capable of damping high frequency vibrations as explained below). There are two view ports on the top of the chamber for facilitating tanipulation of the sample and assistance in operation of the AFM. Two other ports oppositely at two sides of the chamber provide the operator with manual adjustment of the AFM. The bottom of the chamber is vertically translatable, serving as the main gate of the chamber.

#### Vibration isolation system

Any vibration seriously affects the resolution during scanning. Sources of vibration may be the roum pump and external vibrations from the environment. The vibration from the pump is at a subfrequency level. A method based on the model proposed by Oliva [11] has been adopted to mate this vibration from the instrument. Our vibration isolation system (VIS) is composed of cen stages. Each stage of the six of the seven is a metal plate with 220 mm in diameter and 8 mm thickness. There are 3 short pieces of VITON O-ring with 5.33 mm in diameter and 5 mm in 10 mg/h, located separately by 120° in a circle between two plates. The size of the O-ring piece has chosen after several experiments using various diameters and lengths. The seventh plate, which is the heaviest, is on the top of the six-plates array. In designing, we measured the stiffness and damping constant of the VITON for different cases. The present VITON stiffness and the 10 mping constant measured are 6.17×10<sup>4</sup> N/m and 58 Ns/m, respectively. These values were used the atheoretical simulation on the behavior of the Transfer Function of the VIS that was proposed 10 kano [12]. Fig. 2 shows the results of the simulation, which assumes an external input noise 11 mg/h and 2 decrease of this noise amplitude down to 1×10<sup>-12</sup> m (-120 dB). From 12, we obtain a cut-off frequency of 78 Hz for this condition.

#### Ulon beam isolation

The AFM, as shown in Fig. 3, has a top cover and the scanning tip right beneath the cover, both which do not allow the ion beam bombard the sample vertically. Therefore, the AFM must be and A geometrical calculation determined a tilting angle of 35 degree from the normal to be coropriate enough for avoiding beam hitting both cover and tip as well as keeping the microscope by working.

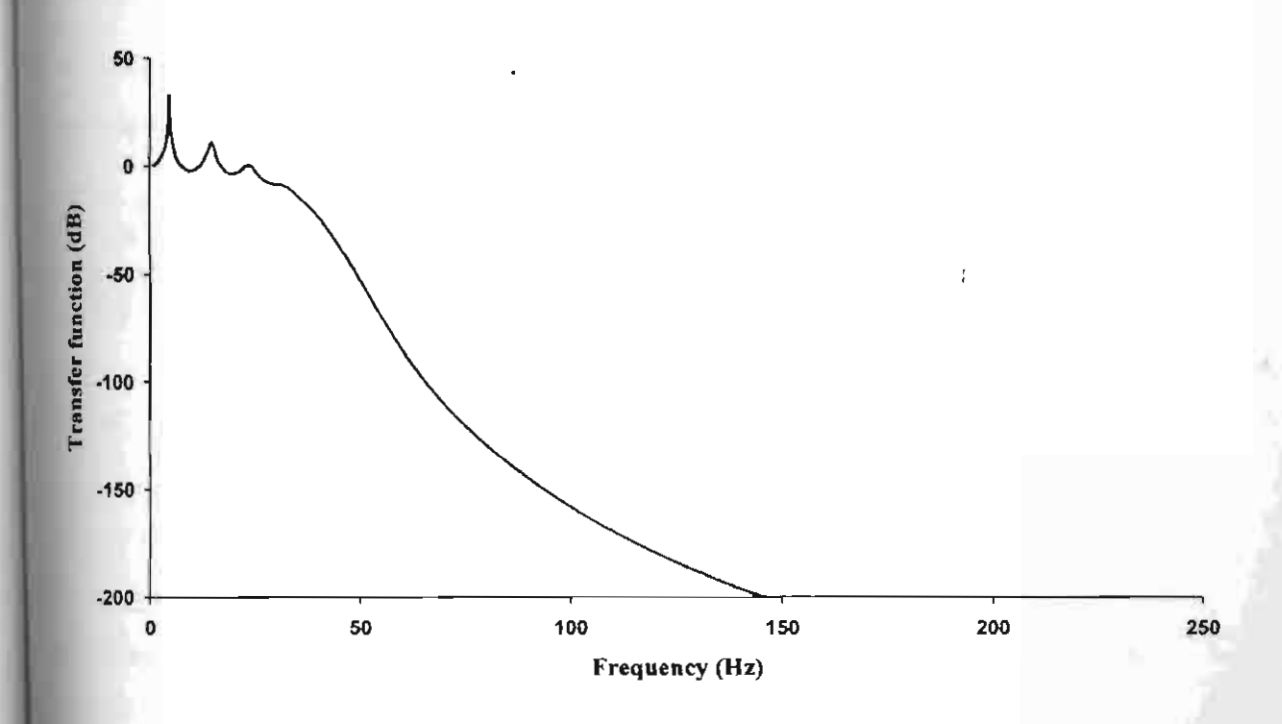


Figure 2. Transfer function plot for the seven-stages VIS in the AFM design.

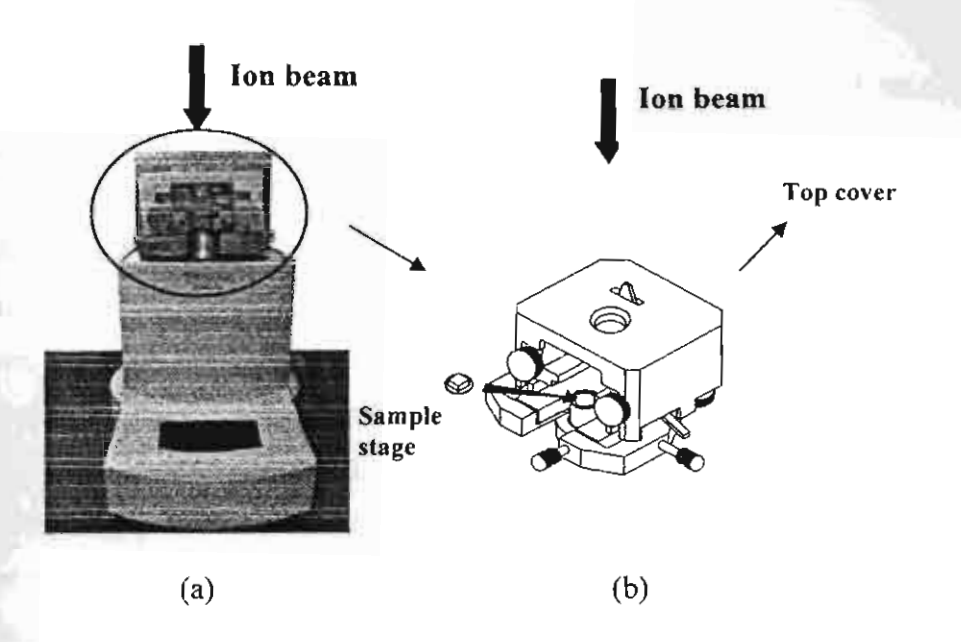


Figure 3. The commercial AFM (SPM9500-J2) from Shimadzu. (a) A photograph of the front view, and (b) the 3-D schematic of AFM's head.

#### Conclusion

An *in-situ* AFM facility has been designed to observe formation of micro-craters in the objectal cell envelopes during ion beam bombardment. The designing involves calculations for a mion isolation system composed of seven stages consisting of metal plates and VITON O-ring and tilting of the AFM by 35 degree from the normal. The *in-situ* AFM chamber has been attacted and installed to the bioengineering ion beam line, and installation of the whole system been completed.

#### Gnowledgements

This work was supported in part by the US Department of Energy under Contract Number 5AC03-76SF00098 and the Thailand Research Fund. S.S. is indebted to the Royal Golden program (Thailand) for supporting studies at the Lawrence Berkeley National Laboratory of Graduate School, Chiang Mai University.

#### Herences

- Chen Yuanru, Mo Shangwu and Qiu Shuhua, Nucl. Instrum. Meth. Phys. Res. B Vol. 23 (1987), p.344.
- Yu Zengliang, Deng Jianguo, He Jianjun, Huo Yuping, Wu Yuejin, Wang Xuedong and Lui Guifu, Nucl. Instrum. Meth. Phys. Res. B Vol. 59/60 (1991), p. 705.
- Yu Zengliang, Yang Jianbo, Wu Yuejin, Cheng Beijiu, He Jiangun and Huo Yuping, Nucl. Instrum. Meth. Phys. Res. B Vol. 80/81 (1993), p. 1328.
- Lengliang Yu, IEEE Trans. Plasma Sci. Vol. 28 (2000), p. 128.

- If F.Z. Cui and Z.S. Luo, Surf. Coat. Technol. Vol. 112 (1999), p. 278.
- Y. Hase, A. Tanaka, I. Narumi, H. Watanabe and M. Inoue, JAERI Rev. Vol. 98-016 (1998), p. 81.
- T. Vilaithong, L.D. Yu, C. Alisi, B. Phanchaisri, P. Apavatjrut and S. Anuntalabhochai, Surf. Coat. Technol. Vol. 128/129 (2000), p. 133.
- S. Anuntalabhochai, R. Chandej, B. Phanchaisri, L.D. Yu, T. Vilaithong and I.G. Brown, Appl. Phys. Lett. Vol. 78 (2001), p. 2393.
- B. Phanchaisri, L.D. Yu, S. Anuntalabhochai, R. Chandej, P. Apavatjrut, T. Vilaithong and LG. Brown, Surf. Coat. Technol. Vol. 158/159 (2002), p. 624.
- S. Sangyuenyongpipat, T. Vilaithong, L.D. Yu, A. Verdaguer, I. Ratera, D.F. Ogletree, O.R. Monteiro and I.G. Brown, Nucl. Instru. and Meth. B, Vol. 227 (2005), p. 289.
- A. I Oliva, M Aguilar and Victor Sosa, Meas. Sci. Technol. Vol. 9 (1999), p. 383.
- M. Okano, K. Kajimura, S. Wakiyama, F. Sakai, W. Mizutani, and M. Ono, J. Vac. Sci. Technol. A 5(6), Nov/Dec(1987), p. 3313.



Available online at www.sciencedirect.com





Nuclear Instruments and Methods in Physics Research B 227 (2005) 289-298

www.elsevier.com/locate/nimb

#### Metal ion bombardment of onion skin cell wall

S. Sangyuenyongpipat a,\*, T. Vilaithong a, L.D. Yu a, A. Verdaguer b, I. Ratera b, D.F. Ogletree b, O.R. Monteiro b, I.G. Brown b

<sup>a</sup> Fast Neutron Research Facility, Department of Physics, Chiang Mai University, Chiang Mai 50200, Thailand
<sup>b</sup> Lawrence Berkeley National Laboratory, Berkeley, California 94720, USA

Received 10 May 2004; received in revised form 24 August 2004

#### **Engract**

lon bombardment of living cellular material is a novel subfield of ion beam surface modification that is receiving powing attention from the ion beam and biological communities. Although it has been demonstrated that the technic is sound, in that an adequate fraction of the living cells can survive both the vacuum environment and energetic a bombardment, there remains much uncertainty about the process details. Here we report on our observations of monskin cells that were subjected to ion implantation, and propose some possible physical models that tend to support the experimental results. The ion beams used were metallic (Mg, Ti, Fe, Ni, Cu), mean ion energy was typically keV, and the implantation fluence was in the range 10<sup>14</sup>–10<sup>16</sup> ions/cm<sup>2</sup>. The cells were viewed using Atomic Force becoscopy, revealing the formation of microcrater-like structures due to ion bombardment. The implantation depth models was measured with Rutherford backscattering spectrometry and compared to the results of the TRIM, T-DYN 14 PROFILE computer codes.

1004 Elsevier B.V. All rights reserved.

40.5 41.75.Ak; 61.82.Pv; 61.80.Jh; 87.50.Gi

#### Introduction

Ion implantation into inorganic materials is a Indeveloped surface modification tool that has

Corresponding author. Tel.: +66 53 943 379x136; fax: +66

bmail uddress: somjui@fnrf.science.cmu.ac.th (S uenyongpipat). found application in a wide variety of research and industrial fields. Ion implantation into living biological tissue is a new but rapidly evolving field of application of ion beam technology. One important application to which the approach has been successfully put is the mutation breeding of various kinds of crop seeds, a field that has seen a great deal of practical success in China [1–5]. The action and effects of ion beam irradiation on

##583X/\$ - see front matter © 2004 Elsevier B.V. All rights reserved.

belogical material have been considered from fundamental perspectives also [6-9]. Olough it has been demonstrated that the techwe is sound, in that an adequate fraction of biving cells can survive both the vacuum enviment and energetic ion bombardment [1-9], remains much uncertainty about the process Among the kinds of ion beam induced bioand effects that have been reported is the transof DNA into both plant cells [3,10] and seterial cells [11-13] brought about by ion bomand ment of cells under appropriately chosen am parameters of fluence and energy. This sigmeant result has not yet been fully explained, in the observations seem to imply a model in which the cell envelope is perforated by ion bominduent, allowing subsequent transport of exomous macromolecules through the cell wall and the interior cell region [12]. When the ion mee is approximately equal to the cell envelope Mikness and the bombardment fluence is ademute, a nathway for the transfer of large molethrough the cell envelope may be formed. If damage to the cell wall is not too severe (i.e. wion fluence not too great) the cell wall may wible to recover and the cell to live and propae in the culture medium into which it is momptly reintroduced after the wwo ion bombardment process. It remains a to provide a strong, experimentally-justified, shysical model to explain in detail the mechanisms woved in ion beam induced DNA transfer.

For carrying out basic studies of the effect of m beam bombardment of biological cell wall sterial, onion skin is a target material that has me attractive features. Onion skin cells are large and fat - the transverse cell dimensions are of ormal 100 am, and a thin membrane of onion skin meadily be mounted so as to expose a more-last flat and uniform continuum of cell envelope the bombarding ion beam. The material is easily maded and simply prepared for the experiment. The skin has been selected for investigation in membrane previous ion bioengineering investigations that the stribed here.

A complicating feature that plagues all biologi-

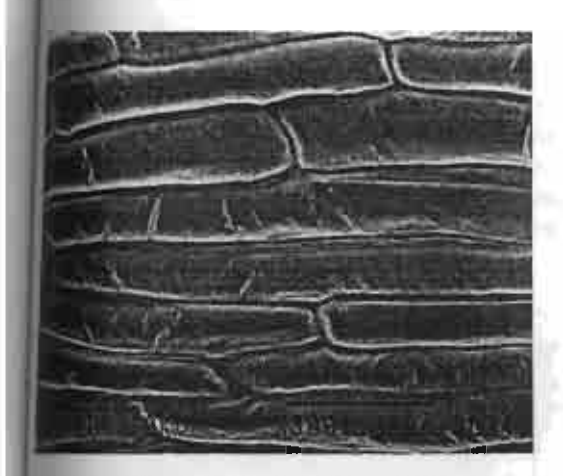
here is the circumstance that, in general, the implied depth of penetration of the ion beam into the cell wall material is greater by a large factor (an order of magnitude or greater) than is theoretically predicted using the textbook-known cell wall composition. On the other hand, it is clear from detailed analysis and also from the most casual visual inspection that the cellular material (the onion skin membrane) is severely dehydrated after exposure to the vacuum. Thus, neglecting temporarily the question of the larger effects of cell dehydration, we might provisionally suppose that the anomalously high apparent ion penetration depth could be a consequence of the removal by vacuum evaporation of a large amount of the cell material (water), leaving behind only a kind of scaffolding. Our model would then be of a cell wall whose line density (atoms/cm<sup>2</sup>) has been severely reduced, thus allowing an ion penetration depth that is comparable to the cell wall thickness, and a cell that is re-hydrated and alive after it has been reintroduced to an aqueous culture medium subsequent to the ion bombardment.

We report here on some observations we have made of the effects of metal ion bombardment on onion skin cells, including AFM imaging of the cell wall after exposure to vacuum and after ion bombardment, and a comparison of the measured and calculated depth profiles of ions implanted into the cell wall. First the experimental conditions are briefly summarized, followed by a description of the results obtained. The significance and implications of the measurements are discussed.

#### 2. Experimental

#### 2.1. Sample preparation

Thin layers of onion epidermis were prepared from ordinary yellow onions. The onion was cut and the third layer from the outer shell obtained. From the middle part of this layer, a thin skin of onion epidermis was peeled and attached to a flat holder using carbon tape. A low magnification SEM photograph of onion epidermis prepared in this way is shown in Fig. 1. A surface of large, flat



Low magnification scanning electron microphotograph multiplesmis as prepared for ion bombardment, showing and flat onion skin cells.

both be seen with cell wall material exposed for bombardment normal to the substrate.

#### In bombardment

or bombardment of onion skin was carried out hal Chiang Mai and at Berkeley. The CMU3 heam facility [16] at Chiang Mai University III) is a dedicated facility designed specifically bombardment of living material. It makes use Danfysik Nielson-type ion source to produce ans of gaseous or metallic ions with energy up 30keV at beam current up to hundreds of stroamperes. The terminal is equipped with a sweeper and a beam profile monitor. The met chamber is located in a clean room and alrapid access and quick pump-down so as to mize sample time in the vacuum for maximum Wability. Gaseous ion species including N and rwth energy 20-30 keV have been investigated CMU [12-15]; here we limit our attention to me-In species. The Berkeley ion beam facility ema vacuum arc ion source to form broad and of metal ions with energy up to ~100 keV. Incility has been described in detail elsewhere For the work described here, the Berkeley ally was used to carry out ion implantation into skin using the metal ion species Mg, Ti, Fe, hand Cu at a mean ion energy of 30 keV and fluin the range  $10^{14}$ – $10^{16}$  ions/cm<sup>2</sup>.

#### 2.3. Characterization and observation techniques

Samples were observed microscopically using both scanning electron microscopy (SEM) and atomic force microscopy (AFM). SEM was done using a JEOL JSM-840A and AFM using a Bioscope III Microscope from Veeco Inc. with an inverted microscope (Axiovert M35 of Carl Zeiss) to position the tip exactly on the cell to be scanned. We scanned using tapping mode with tips from Nanosenors (NCH-100) with a force constant of 42 N/m. The Ti ion implanted sample was characterized by Rutherford backscattering spectrometry (RBS) using 1.95 MeV He<sup>+</sup> ions at an analyzing beam current of 10nA to a total fluence of about  $1 \times 10^{14}$  ions/cm<sup>2</sup> with a beam spot size of about I mm in diameter to measure the Ti depth profile. The detector was a Si surface barrier detector located at a scattering angle of 165°. The sample was glued to an Al plate using conducting silver paint and mounted on a two-axis goniometer which could tilt the sample from 0° to 65°.

#### 3. Results and discussion

#### 3.1. Sample dehydration

The dehydration that occurs when the samples are placed in vacuum has been quantified by mass loss measurements and by AFM of the surface, as a function of time for which the onion epidermis is exposed to vacuum. Mass loss measurements are complicated by the fact that the dehydrated samples, upon removal from the vacuum system and re-exposure to room air, rapidly re-hydrate, with an associated increase in mass. Thus the mass loss data should be taken as only semi-quantitative. Nevertheless, even with this uncertainty, we find that the mass loss due to water evaporation in vacuum is substantial indeed. Even for the shortest time for which the onion skin samples were maintained in vacuum, 5 min or less, the mass loss was approximately 85%. This value did not increase when the exposure to vacuum was longer, out to periods of several hours. We conclude that for all the ion beam bombardment experiments, the samples are fully dehydrated. Examples of AFM

ricrographs of the onion skin cell wall material after various periods of time in vacuum are shown Fig. 2. The development of severe "grooves" or convolutions is clearly evident. The degree of convolution can be quantified by an AFM roughness measurement; note however that the roughness riameter measured in this case is not random

surface irregularity but is dominated by the "grooved" surface structure. The measured surface roughness increases markedly with the time period for which the sample was in vacuum. These data are summarized in Table I. We conclude that cell dehydration is accompanied by the development of surface convolution.

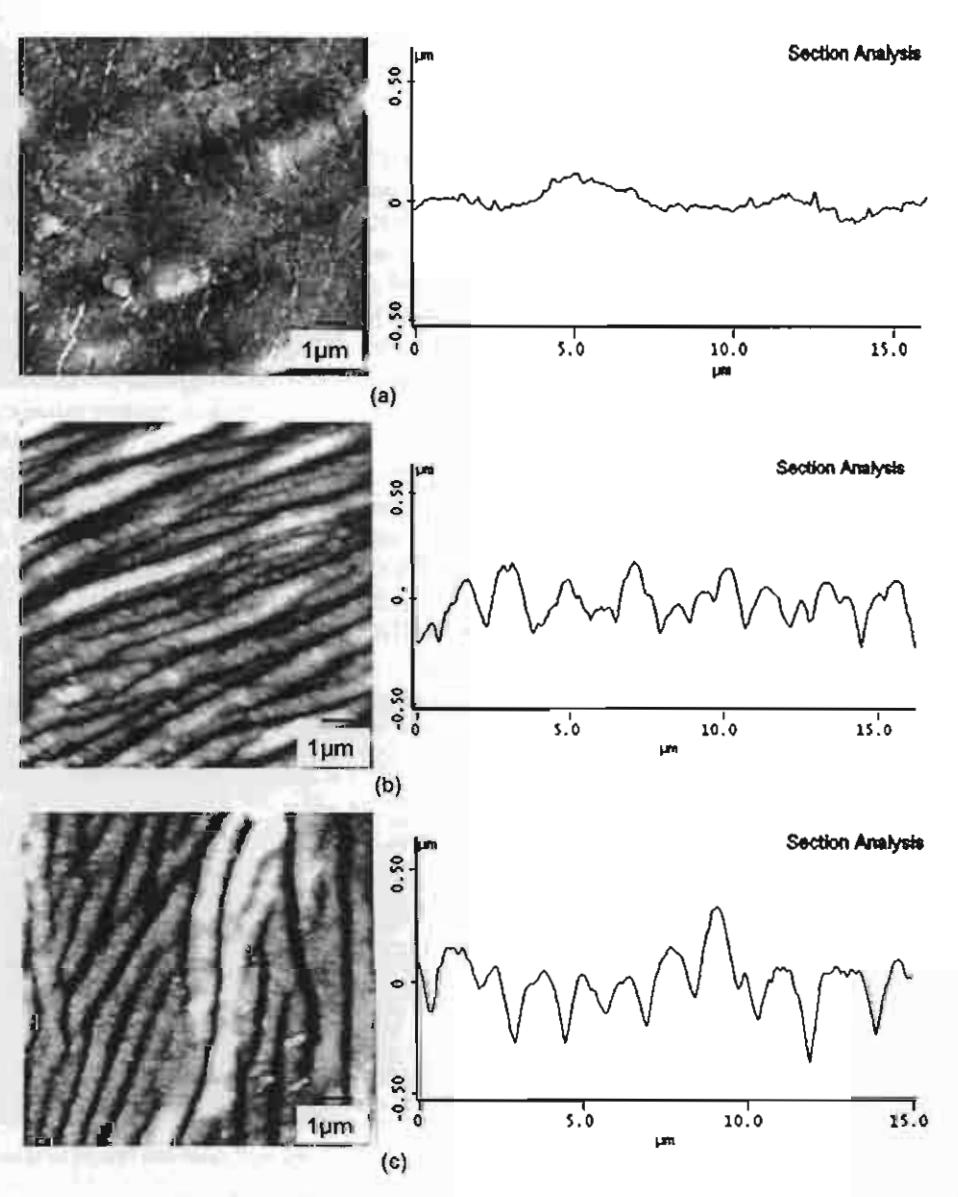


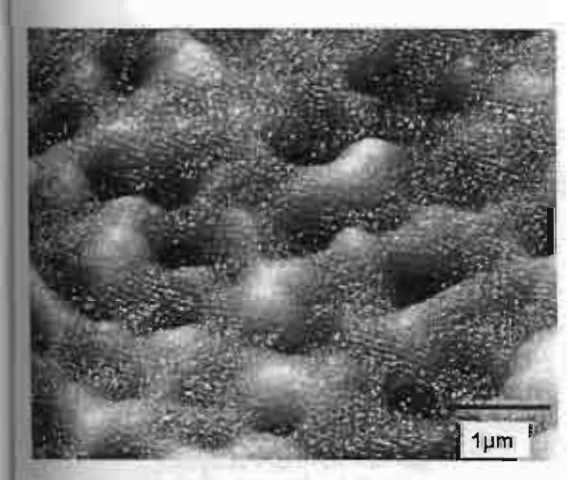
Fig. 2. AFM images of onion skin surface, and section analysis showing surface roughness, (a) after 1 min exposure to vacuum, (b) after 1 h exposure to vacuum and (c) after 12h exposure to vacuum.

half f mm cell wall surface roughness (rms) measured by AFM man analysis as shown in Fig. 2, as a function of exposure med the onion cells to high vacuum

m in vacuum	Roughness (rms) (nm)		
((frish)	29 ± 5		
ın	26 ± 7		
Time to the same t	51 ± 9		
	65 ± 13		
	66 ± 5		

#### 2. Formation of microcraters

A primary effect that is observed when onion is ion beam bombarded is the formation of perocrater-like structures on the surface of the cell material. This phenomenon has been observed experiments carried out both at the Chiang Mai m beam facility, as previously reported [14] and to at the Berkeley ion beam facility. The microtures are observed for approximately the same im beam parameter regime (energy and fluence) as which DNA transfer can be brought about for bombarded bacterial cells [11-13], thus compting the speculation that the microcraters my provide channels or pathways for transfer of regenous macromolecules into the cell interior. samples of the kind of structure formed are flown in Fig. 3. Importantly, note that the AFM



3). AFM image of typical microcrater structures formed on man skin cell wall surface by ion beam bombardment. In a particular case the ion species was Fe, ion energy was 21xV, fluence was 1 × 10<sup>15</sup> ions/cm<sup>2</sup>.

observations indicate that microcraters are not the result of vacuum alone – the formation of microcraters requires ion bombardment. The features shown are quite typical and have been observed for a great many (of order one hundred) ion bombardment experiments. The diameter of the microcrater rim lies in the broad range from several hundred nm to 1 µm. An important part of our ongoing research is to understand the formation mechanism of the microcraters, and to acquire evidence to support or negate the idea that the microcraters provide the mechanism (channels) for DNA transfer. At the present time we can say:

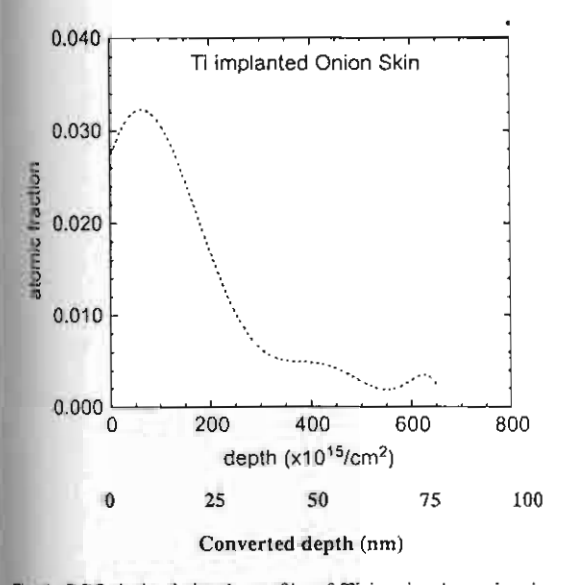
- Microcraters are formed only when the onion epidermis is ion beam bombarded; they are not formed simply by placing the samples in vacuum.
- The ion beam energy (~25-30 keV) and fluence range (roughly 1-5 × 10<sup>15</sup> ions/cm<sup>2</sup>) for which microcraters are formed are similar to the energy and fluence range for which DNA transfer is observed. However, we have not yet explored the parameter space in full detail.
- Microcraters are formed when the ion beam species is gaseous (N, Ar) and also when it is metallic (Mg, Ti, Fe, Ni, Cu and others).

The mechanical interaction between energetic ions and plant cell envelope has been discussed to some extent and some speculations have been proposed [3,9,14]. Highly severe ion sputtering of the cell envelope drastically peels off top layers and opens pathways for following incident ions to bombard more easily the deeper inner structure of the envelope. Due to the extreme inhomogeneity of the cell envelope inner structure, the ions penetrate more easily into those less dense zones and result in higher-degree atomic displacement cascades. Subsequently, simultaneous ion sputtering removes the displaced atoms from these zones at a greater rate. Thus, at these zones there are more possibilities to form crater-like structures. Another possibility is that the ion beam most easily sputters material that fills in the net structure of the cell envelope framework and leaves pores. When ion beam etching breaks the net framework, the cell

wall collapses at that location to form large holes

#### 3.3. Ion range in the cell wall

The results of RBS characterization of ion b in bombarded onion epidermis are shown in Fig. 4. For this experiment the implantation was carried out using a Ti ion beam at 30 keV energy. Since we do not know the mass density of the cell wall material we can give neither an absolute depth scale to the profile (the depth unit remains in 1015 atoms/cm2, an area density, which can be converted to the absolute depth scale when divided by the mass density) nor an accurate value of implantation fluence, but can say only that the RBSmeasured fluence is of order 1×10<sup>16</sup> ions/cm<sup>2</sup>, and that the Ti depth profile has the general shape that is expected. We use Ti to investigate the depth profile from the results of RBS characterization to compare with TRIM and T-DYN simulations. Note also that, as pointed out above, the implanted substrate material is far from a flat surface, but on the contrary has surface bumps and grooves of transverse dimension microns and of



Fe 4. RBS-derived depth profile of Ti ion implantation into min. skin cell wall. Ion energy was  $30 \, \text{keV}$ , and the measured library  $\sim 1 \times 10^{16} \, \text{ions/cm}^2$ . The converted depth is made under an assumption that the cell envelope mass density is 1 g/cm<sup>3</sup>.

longitudinal dimension about the same. The effect of this severe surface irregularity on the RBS measurement is not known in detail, but we should nevertheless interpret the measured profile shape with some caution.

We have simulated the implantation profile using the well-known codes TRIM [19,20], T-DYN [21,22] and PROFILE [23]. The TRIM (Transport and Range of Ions in Matter) code is essentially a low-fluence ion implantation simulation in that it does not correct for changes in the composition of the solid with increasing fluence nor for the effects of sputter removal of surface material as the implantation proceeds, while T-DYN (dynamic TRIM) and PROFILE include these effects. Because the detailed properties of the substrate material are not at all well known. the results obtained from the simulations need to be taken with caution. The composition of the cell envelope and its density in high vacuum are unknown. As shown in Section 3.1, there is a significant loss in mass of onion skin in vacuum. This reduction in mass is due to loss of water, and certainly corresponds to a simultaneous decrease in density although we do not know to what extent. Density and composition are key input parameters for the simulations.

The following assumptions were made in our simulations. The cell wall (target material) compo-

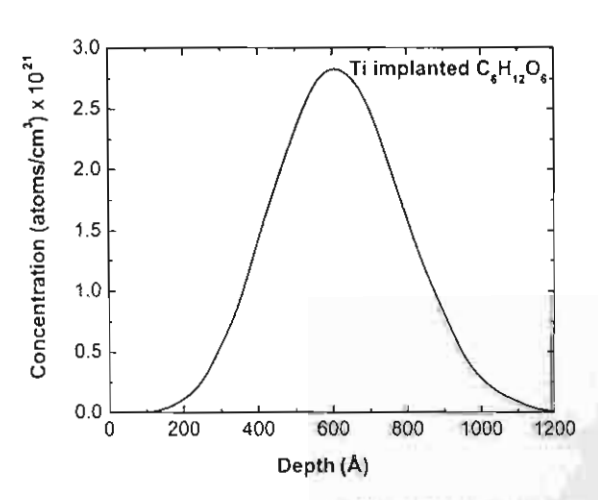


Fig. 5. TRIM-calculated depth profile for 30 keV Ti ions implanted into substrate of composition C:H:O with atomic ratios 1:2:1 and mean density 1 g/cm<sup>3</sup>.

was taken to be C, H and O in atomic ratio H, and the cell wall density was assumed to be ptm<sup>3</sup>. These parameters remain constant during te TRIM simulation, whereas in the T-DYN and ROFILE calculations the target composition ranges with time due to the addition of Ti and sputtering of surface material.

The Ti concentration profiles calculated using the three codes are shown in Fig. 5-7. Fig. 5 shows the TRIM results. The profile is typical of low flume implantation profiles in that the shape is quite Gaussian, with no Ti concentration at the surface. The ion range is 620 Å and the straggling is 180 Å. The most striking difference between the RBS-

measured profile and the TRIM profile is the relatively high Ti concentration at the surface for the experimental data. It is well known from a great many investigations involving implantation into inorganic materials that profiles of the kind shown in Fig. 4 (high concentration of the implanted species at and near the surface) are seen when the implanted fluence is high, typically  $\sim 10^{17} \, \mathrm{cm}^{-2}$  or more. The reason for this effect is sputter removal of surface layers as the implantation proceeds; in a sense, previously-implanted profiles move closer to the surface as the surface is ion etched away. Although this is conventionally thought of as a "high fluence effect" for the case of inorganic

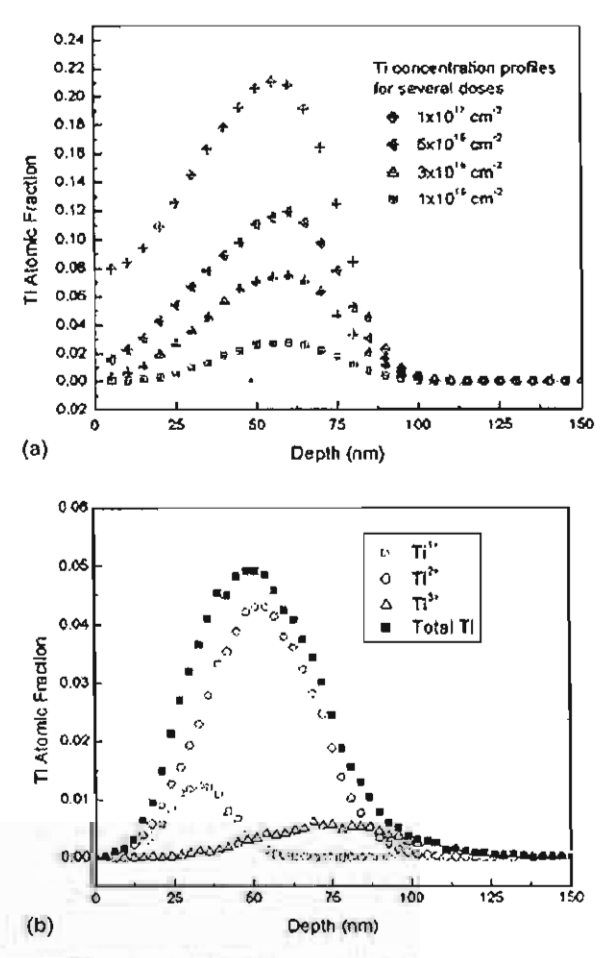
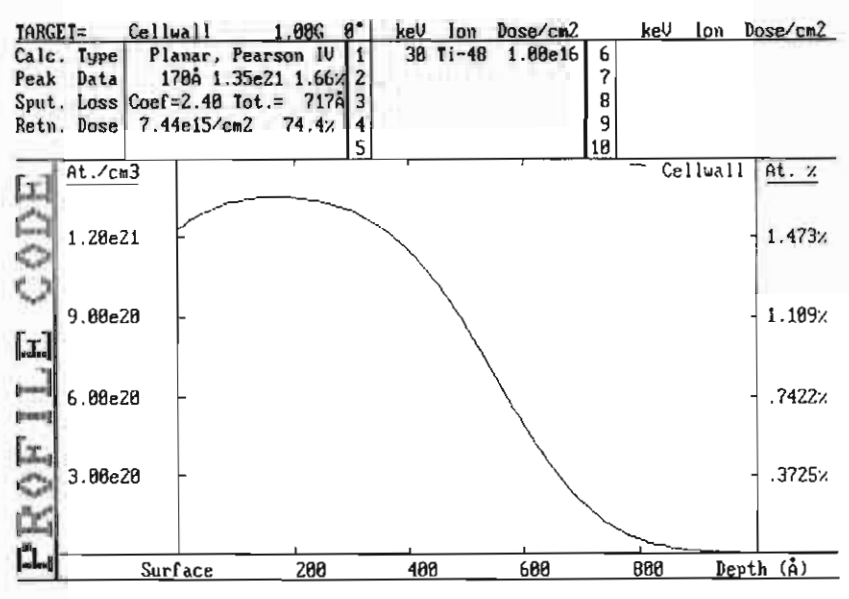


Fig 6. T-DYN-calculated depth profile for Ti ions implanted into substrate of composition C:H:O with atomic ratios 1:2:1 and mean limity 1 g/cm<sup>3</sup>. (a) Mean ion energy 30 keV, for various incident fluences as indicated by the legends. (b) Incident fluence  $2 \times 10^{16}$  ions/m<sup>2</sup>, for a beam with complex energy structure.



1. 7. PROFILE-calculated depth profile for Ti ions at  $30 \,\text{keV}$  with a fluence of  $1 \times 10^{16} \,\text{ions/cm}^2$  implanted in the substrate of studies of the cell wall which has the chemical compound of  $C_6H_{12}O_6$  with a mean mass density of  $1 \,\text{g/cm}^3$ .

larget materials, it is more fundamentally a "high puttering effect". While the TRIM code does tot include this effect, the T-DYN and PROFILE todes do, and thus while we do not expect to see melevated surface concentration for the TRIM inculation, we do expect to see it for the latter w calculations. Results of T-DYN calculations shown in Figs. 6(a) and (b). Fig. 6(a) shows rofiles for a Ti ion energy of 30 keV and for varwas implantation fluences. The surface concentraon is seen to increase with fluence as expected, ut at a slower rate than is necessary to provide second fit to the RBS profile. In searching for an xpanation for this, we calculated the T-DYN stofile using a more exact description of the Ti on beam energy structure produced by the MEV-A ion source. As described in detail elsewhere 117,18], the Ti ion beam has a charge state specfrom containing components Ti+, Ti2+ and Ti3+ proportions 11:75:14, and thus an ion energy petrum with the same proportions. Fig. 6(b) hows the implantation profiles for the three sepaale energy components and their sum, for a mean menergy of 30 keV and a fluence of 2 × 10<sup>16</sup> ions/ We see that the difference in profile due to the attenergy structure is small, and does not provide an explanation for why the calculated surface concentration is lower than measured. Finally, Fig. 7 shows the Ti concentration depth profile as calculated using the PROFILE code. The profile shape displays a high surface concentration, in fact more so than is called for in order to provide a good fit to the RBS data. Note most importantly that the PROFILE calculation was carried out for the case where the target material was taken to be a C<sub>6</sub>H<sub>12</sub>O<sub>6</sub> compound, as opposed to a C:H:O mixture of proportions 1:2:1, with the effect that the sputtering rate of the target material due to the incident ion bombardment is considerably greater than otherwise. This difference implies that high sputtering yields from the cell wall material result from ion bombardment induced molecular or cluster sputtering rather than individual atomic sputtering which is common for inorganic materials. A PROFILE calculation for the case when the target is taken to be a mixture yields a depth profile similar to that given by the TRIM and T-DYN codes. We thus hypothesize that the high surface concentration of Ti as measured by RBS is due to enhanced sputtering (ion etching) of the organic C<sub>6</sub>H<sub>12</sub>O<sub>6</sub> cell wall material. If the mass density of the onion cell envelope is assumed to be 1 g/cm<sup>3</sup>

as used for simulations, the depth scale of the RBS measured Ti ion profile can be converted to the rate of nm, as shown in Fig. 4 (as a mean atomic weight of the substrate material,  $C_6H_{12}O_6$ , is 7.5,  $10 \times 10^{15}$  atoms/cm<sup>2</sup> is now corresponding to 2.5 nm). It is found that the profile peak is at about 10-15 nm. This is in good agreement with the PROFILE result.

High surface sputtering of living biomaterials, much higher than is usual for typical inorganic solis and including sputtering of large molecular fragments, has been observed by others [2,3] also. The effects of ion beam bombardment of cellular biomaterials extend to a much greater depth than can be explained by the conventional model. Thus for example ion implantation into rice seeds at noderate ion energy has led to gene transfer, a rejuli that can only be explained by assuming an implantation range of many microns. The model of ion bombardment of the cell wall that suggests uself is one in which (i) the cell wall contains many channels and voids, regions from which the water has been removed and replaced by vacuum, leavng a skeletal scaffolding structure; (ii) ion sputtering is severe, releasing not only atomic sputtered particles but also large clusters and molecular deb-15. Thus the effective ion penetration range is much greater than naively expected, and 'the antation profile shows a shape consistent with high sputtering.

#### 4. Conclusion

We have reported on some observations of the effects of ion bombardment of onion skin cells by 30keV metal ions at ion implantation fluence of up to about 10<sup>16</sup> ions/cm<sup>2</sup>. Atomic Force Microscopy revealed the formation of microcrater-like structures with rim dimension typically several hundred nanometers; we speculate that the microcraters might provide channels for the transfer of exogenous macromolecules (such as DNA) through the cell wall into the cell interior. The RBS-measured implanted ion depth profile was compared to several computer simulations, and the similarities and differences seen can be interpreted as being due to severe sputtering of the cell wall material.

#### Acknowledgements

This work was supported in part by the U.S. Department of Energy under Contract Number DE-AC03-76SF00098 and the Thailand Research Fund. S.S. is indebted to the Royal Golden Jubilee program (Thailand) for support at Lawrence Berkeley National Laboratory; I.R. is grateful to the Generalitat de Catalunya (Spain) for a Nanotec postdoctoral grant; and A.V. is grateful to the Ministerio de Ciencia y Tecnología (Spain) for a postdoctoral grant.

#### References

- [1] Y. Chen, S. Mo, S. Qiu, Nucl. Instr. and Meth. B 23 (1987) 344.
- [2] Z. Yu, J. Deng, J. He, Y. Huo, Y. Wu, X. Wang, G. Lui, Nucl. Instr. and Meth. B 59-60 (1991) 705.
- [3] Z. Yu, J. Yang, Y. Wu, B. Cheng, J. He, Y. Huo, Nucl. Instr. and Meth. B 80-81 (1993) 1328.
- [4] Z. Yu, IEEE Trans. Plasma Sci. 28 (2000) 128.
- [5] F.Z. Cui, Z.S. Luo, Surf. Coat. Technol. 112 (1999) 278.
- [6] J. Kiefer, M. Brend'amour, U. Stoll, Nucl. Instr. and Meth. B 107 (1996) 292.
- [7] A. Tanaka, H. Watanabe, T. Shimizu, M. Inoue, M. Kikuchi, Y. Kobayashi, S. Tano, Nucl. Instr. and Meth. B 129 (1997) 42.
- [8] J. Xue, Y. Wang, F. Liu, S. Wang, S. Yan, W. Zhao, Surf. Coat. Technol. 128–129 (2000) 139.
- [9] Z.L. Yu, Introduction to Ion Beam Biotechnology (L.D. Yu, T. Vilaithong, I.G. Brown, Trans.) Kluwer Academic Publishers, New York, in press.
- [10] Y. Hase, A. Tanaka, I. Narumi, H. Watanabe, M. Inoue, JAERI Rev. 98-016 (1998) 81.
- [11] T. Vilaithong, L.D. Yu, C. Alisi, B. Phanchaisri, P. Apavatjrut, S. Anuntalabhochai, Surf. Coat. Technol. 128-129 (2000) 133.
- [12] S. Anuntalabhochai, R. Chandej, B. Phanchaisri, L.D. Yu, T. Vilaithong, I.G. Brown, Appl. Phys. Lett. 78 (2001) 2393.
- [13] B. Phanchaisri, L.D. Yu, S. Anuntalabhochai, R. Chandej, P. Apavatjrut, T. Vilaithong, I.G. Brown, Surf. Coat. Technol. 158-159 (2002) 624.
- [14] L.D. Yu, B. Phanchaisri, P. Apavatjrut, S. Anuntalabhochai, T. Vilaithong, I.G. Brown, Surf. Coat. Technol. 158– 159 (2002) 146.
- [15] L.D. Yu, T. Vilaithong, B. Phanchaisri, P. Apavatjrut, S. Anuntalabhochai, P. Evans, I.G. Brown, Nucl. Instr. and Meth. B 206 (2003) 586.
- [16] S. Sangyuenyongpipat, L.D. Yu, N. Tondee, K. Wattanavatee, T. Vilaithong, C. Thongleurm, B. Phanchaisri, S. Anuntalabhochai, I.G. Brown, The 29th International

Conference on Plasma Science, Banff, Alberta, Canada, 26-30 May 2002; IEEE Conference Record - Abstracts, Cat. No. 02CH37340, p. 310.

T.G. Brown, M.R. Dickinson, J.E. Galvin, X. Godechot, R.A. MacGill, Nucl. Instr. and Meth. B 55 (1991)

III. G. Brown, Rev. Sci. Instr. 65 (1994) 3061.

13 See the website: http://www.srim.org/.

- [20] J.F. Ziegler, J.P. Biersack, U. Littmark, The Stopping and Range of Ions in Solids, Pergamon Press, New York, 1984.
- [21] J.P. Biersack, Nucl. Instr. and Meth. B 27 (1987) 21.
- [22] J.P. Biersack, S. Berg, C. Nender, Nucl. Instr. and Meth. B 59-60 (1991) 21.
- [23] Implant Sciences Corp., USA, see the website http:// www.implantsciences.com/products/semi\_apps/profile.html.



#### Available online at www.sciencedirect.com

SCIENCE DIRECT.

Nuclear Instruments and Methods in Physics Research B 242 (2006) 8-11



# Ion bombardment induced formation of micro-craters in plant cell envelopes

S. Sangyuenyongpipat a,\*, L.D. Yu a, T. Vilaithong a, I.G. Brown b

\* Fust Neutron Research Facility, Department of Physics, Faculty of Science, Chiang Mai University, Chiang Mai 50200, Thailand

b Lawrence Berkeley National Laboratory, Berkeley, CA 94720, USA

Available online 4 November 2005

100

beam bombardment of biological material has been recently applied for gene transfer in both plant and bacterial cells. A consistent mechanism for this significant result has not yet been developed. A fundamental question about the mechanism is the position of pathways due to ion bombardment that are responsible for the gene transfer. We have carried out investigations of the flow-energy bombardment by both gaseous and metallic ion species of onion skin cells on their surface microstructure. Our mital results reveal evidence demonstrating that the formation of micro-crater-like structures on the plant cell envelope surface in phenomenon consequent to ion bombardment, no matter what ion species, under certain ion beam conditions. The micro-crater about 0.1–1 µm in size (diameter) and a few tens of nanometers in depth. The micro-crater formation process seems to be also the chemical composition of and rapid water evaporation from the cell envelope, but is associated with the special micro-of the cell wall.

Published by Elsevier B.V.

M.82.Pv; 61.80.Jh; 87.50.Gi

on hombardment; Micro-crater; Plant cell envelope; Gene transfer; Onion skin

#### mduction

u beam bombardment of biological organisms has mently applied for gene transfer in both plant and riel cells [1-4]. In this application, a low-energy ion typically in tens of keV range, bombards biological perforate the cell wall, through which exogenous clocules can be introduced into the cell interior in equent post-bombardment biological processing llowever, a consistent physical mechanism for this interest has not yet been developed. Questions inderstood include how the exogenous DNA macrocles enter the cell, whether the molecules are directly interest through pathways in the cell envelope, whether

and how ion bombardment creates the pathways, and the nature of the pathway structure and geometry. Thus, we have investigated the effects of ion bombardment on plant cell envelopes from a more fundamental perspective.

# 2. Experiment

Thin layers of onion epidermis were prepared from ordinary fresh yellow onions. The onion was cut and the third layer from the outer shell removed. From the middle part of this layer, a thin skin of onion epidermis was peeled and attached to a flat holder using carbon tape.

Ion bombardment was carried out using either the bioengineering ion beam line at Chiang Mai University [5] or the metal vapor vacuum arc (MEVVA) ion source metal ion implanter at Berkeley [6]. A broad range of ion species was used for bombardment, including gaseous N, Cl, Ar and Xe, metals Mg, Ti, Fe, Ni and Cu. The average ion

mannding author. Tel.: +66 53 943379; fax: +66 53 222776.

Taddress: somjai@fnrf.science.emu.ac.th (S. Sangyuenyongpi-

\*\*\* see front matter © 2005 Published by Elsevier B.V. #### 2005.08.200

gr was about 20–30 keV, and the ion fluence was type  $1.2 \times 10^{15}$  ions/cm<sup>2</sup>; for some ion species (such as Ar) fluence was varied from  $1 \times 10^{13}$  to  $2.5 \times 10^{15}$  ions/cm<sup>2</sup>. Indee and very dry onion skin were also used as targets powering time than 100 methods.

After ion bombardment, the samples were removed the vacuum chamber and promptly observed micromicroscopy (SEM) and the force microscopy (AFM).

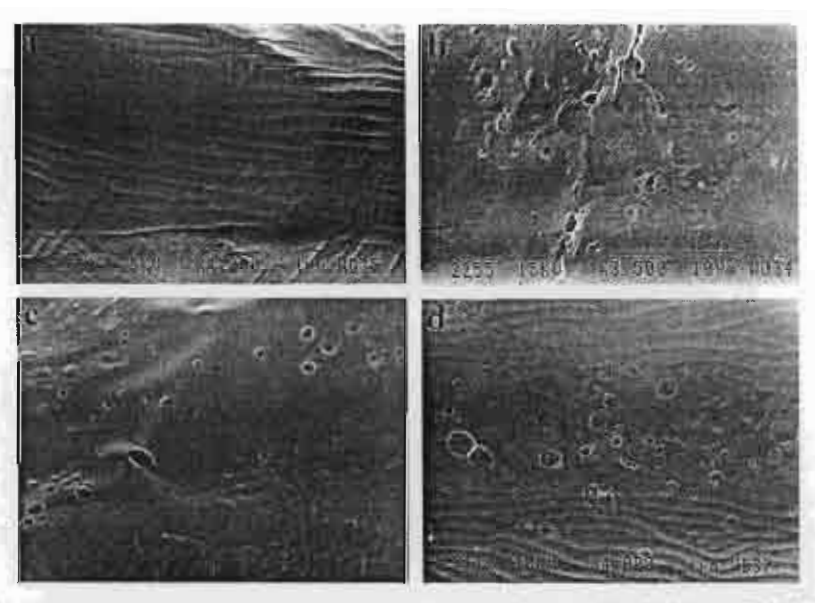
#### Results and discussion

SEM and AFM observations of the ion-bombarded wes found formation of micro-crater-like structures the cell envelopes. We have previously reported finding formation of micro-craters in the plant cell wall meed by N, Ar and some metal ion bombardments [7-From this experiment, it is found that ion-bombardnt-induced formation of micro-crater-like structure in eplant cell envelope is a general phenomenon, no matter on species is used. Fig. 1 shows examples of SEM stographs of the onion skin cell surfaces bombarded giseous ion species such as Cl and Xe, or metal ions ch as Mg. Fig. 2 shows AFM observation of Fe-ionmbarded onion cell surface. From the figures, the erage size of the craters is estimated to be about a halfcrometer to one micrometer (Figs. 1 and 2(a)), seemingly depending on the size or mass of the ion (see also Table The mean depth of the craters is measured to be about d 60 nm (Fig. 2(b)). The micro-craters were distributed homogeneously on the cell surface, at some locations ore densely distributed while at other locations less so.

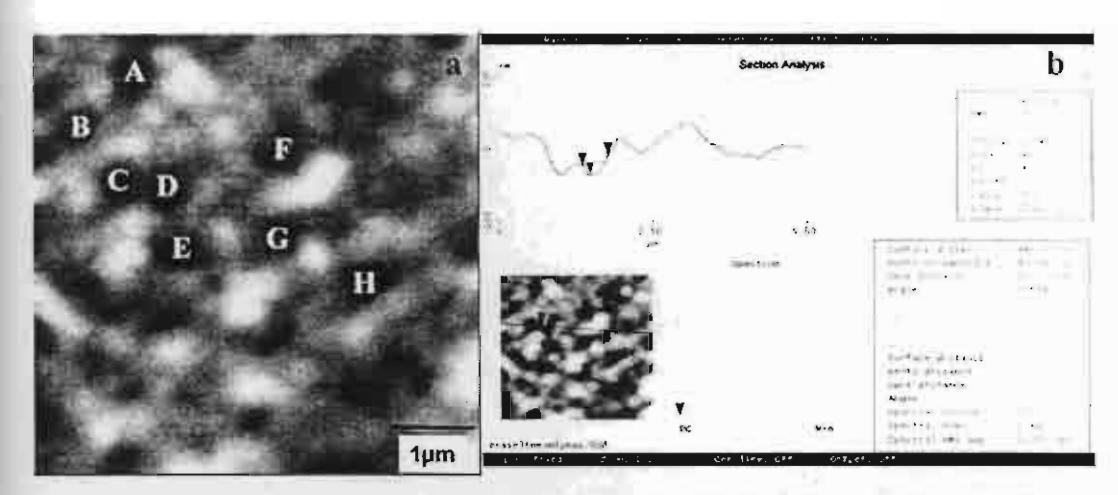
Ion fluence dependence of the formation of the micro-craters was studied. Fig. 3 shows SEM photographs of the onion skin cell surfaces bombarded with various Ar-ion fluences. At a fluence of  $1\times10^{13}\,\mathrm{ions/cm^2}$ , no micro-craters were observed on the cell surface (compared with that in Fig. 1(a)). But, starting from a fluence of  $1\times10^{14}\,\mathrm{ions/cm^2}$  up to a fluence of  $2.5\times10^{15}\,\mathrm{ions/cm^2}$  (our previous results have shown that a fluence of  $3\times10^{15}\,\mathrm{ions/cm^2}$  causes burning or severe damage of the cells), ion bombardment could induce formation of the micro-crater-like structures. With increasing fluence, it was increasingly easier to observe micro-craters, i.e. the micro-craters could be seen at more locations or areas on the cell surface.

The ion energies were chosen according to our previous experience and studies [10,3,11] such that the ion penetration depth should be approximately equal to the effective thickness of the biological cell envelope in order to induce exogenous macromolecule transfer. The result of the fluence dependence implies that at the appropriate ion energy, fluences appropriately high may create a sufficient chance for exogenous macromolecules to transfer into the biological cells.

Mechanisms for the ion-bombardment-induced formation of micro-crater-like structures were also investigated. Cellulose material, whose molecules have the same chemical composition,  $C_6H_{12}O_6$ , as that of the plant cell wall which is composed of micro-cellulose fibers [12], was bombarded under the same ion beam conditions as used for the onion cells. A comparison between the control and the ion-bombarded surfaces, as shown in Fig. 4, shows minimal meaningful differences in the surface structure. This result implies that ion-bombardment-induced formation of



1. SEM photographs of onion cell surface: (a) vacuum (unbombarded) control, and bombarded by (b) Mg ions (20 keV), (c) Xe ions (30 keV) and (d) ions (25 keV), with fluences of 1 × 10<sup>35</sup> ions/cm<sup>2</sup>.



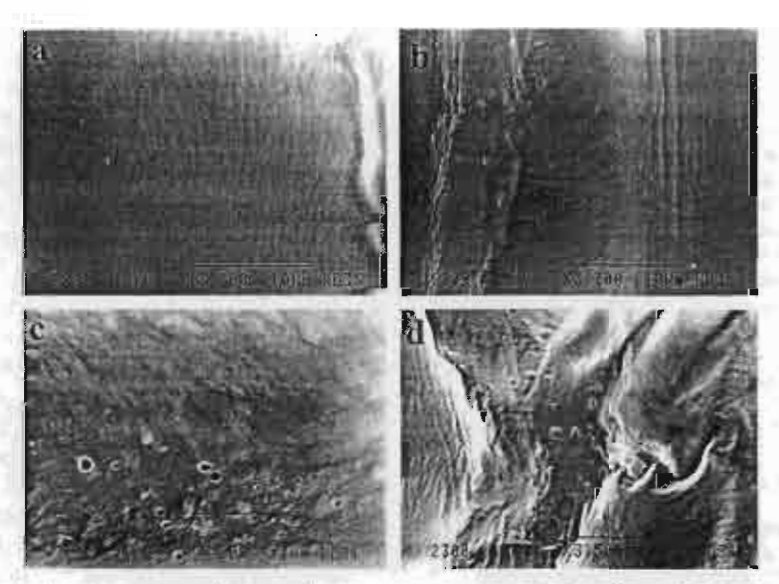
AFM micrograph of typical micro-crater structures formed on the onion skin cell wall surface by Fe-ion bombardment at 25 keV with a fluence of ons/cm<sup>2</sup> (a) Top view (the letters label the micro-craters for measuring the crater size as shown in Table 1); (b) section analysis for measuring the flue craters.

micro-crater size and depth as measured from Fig. 2

m position	Width of crater (nm)	Depth of crater (nm)	
	468.75	69.8	
	390.63	46.1	
	410.16	57.85	
	429.69	55.43	
	468.75	53.75	
	468.75	53.93	
	429.69	56.92	
	527.34	115.89	
mat :	449.22	63.709	

not due to the material chemical composition. Very

beam conditions. Micro-crater-like structures can be clearly seen on the ion-bombarded cell surface in contrast to the control, as shown in Fig. 5. This result rules out the possibility that the formation of the micro-craters is caused by rapid water evaporation induced by ion beam heating. Therefore, the formation can be only attributed to the special structure of the cell envelope, particularly of the cell wall [11,12]. The inhomogeneous distribution of the micro-craters on the cell surface implies that the formation of the structures is not a direct consequence of ion bombardment, but instead may be a secondary effect of ion bombardment. One mechanism which has been discussed [13] is very possible. Ion beam bombardment most easily sputters substances that fill in the net structure of the cell envelope framework and leaves pores. When ion beam



SEM photographs of 25-keV Ar-ion-bombarded onion cell surfaces with fluences of (a)  $1 \times 10^{13}$  ions/cm<sup>2</sup>, (b)  $1 \times 10^{14}$  ions/cm<sup>2</sup>, (c)  $1 \times 10^{15}$  ions/ (d)  $2.5 \times 10^{15}$  ions/cm<sup>2</sup>.

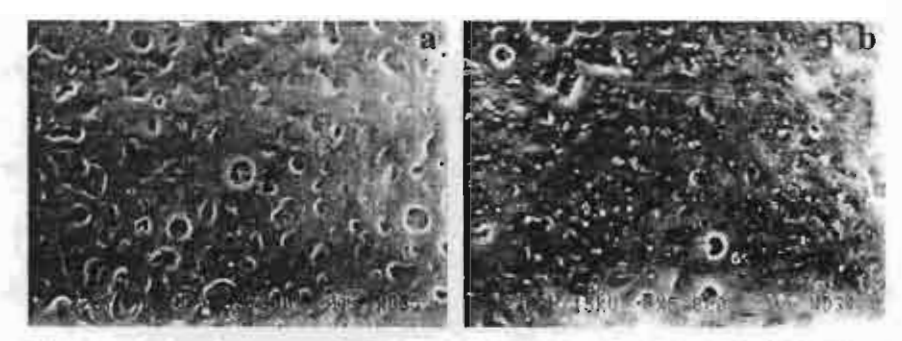


Fig. 4. SEM photographs of cellulose surface: (a) control and (b) Ar-ion-bombarded (25 keV, 1 × 1015 ions/cm2).



SEM photographs of dry onion skin surfaces: (a) control and (b,c) Ar-ion-bombarded (25 keV, 1 × 1015 ions/cm²) surfaces at different locations.

ching breaks the net framework, the cell wall collapses at location to form large holes.

# Conclusion

The formation of micro-crater-like structures in the ant cell envelope is a general phenomenon induced by n bombardment, no matter what ion species, under cermion beam conditions such as ion beam energy and fluace range. The reason for micro-crater formation seems melated to the material chemical composition of and pid water evaporation from the cell envelope; instead, relates to the special microstructure of the cell wall. Evice is insufficient and to be further explored is in the topos of whether the ion-bombardment-induced micro-craters indeed the pathways or channels for exogenous DNA tanafer into biological cells, and if they are, how DNA is tanaferred through these channels.

# knowledgements

We wish to thank A. Verdaguer, I. Ratera, D.F. Oglece, O.R. Monteiro, N. Pasaja and the staff of the electron puroscope laboratory of the Chiang Mai University Laharaj Hospital, for their invaluable contributions to ion implantation, SEM and AFM observations. One us (S.S.) is grateful to the Royal Golden Jubilee program or a fellowship grant. This work was supported by the hailand Research Fund.

#### References

- Y. Zengliang, Y. Jianbo, W. Yuejin, C. Beijiu, H. Jiangun, H. Yuping, Nucl. Instr. and Meth. B 80/81 (1993) 1328.
- [2] Y. Hase, A. Tanaka, I. Narumi, H. Watanabe, M. Inoue, JAERI Rev. 98-016 (1998) 81.
- [3] S. Anuntalabhochai, R. Chandej, B. Phanchaisri, L.D. Yu, T. Vilaithong, I.G. Brown, Appl. Phys. Lett. 78 (2001) 2393.
- [4] B. Phanchaisri, L.D. Yu, S. Anuntalabhochai, R. Chandej, P. Apavatjrut, T. Vilaithong, I.G. Brown, Surf. Coat. Technol. 158/159 (2002) 624.
- [5] S. Sangyuenyongpipat, L.D. Yu, N. Tondee, K. Wattanavatee, T. Vilaithong, C. Thongleurm, B. Phanchaisri, S. Anuntalabhochai, I.G. Brown, presented to the 29th International Conference on Plasma Science, Banff, Alberta, Canada, 26–30 May 2002; IEEE Conference Record Abstracts, Cat. No. 02CH37340, p. 310.
- [6] I.G. Brown, M.R. Dickinson, J.E. Galvin, X. Godechot, R.A. MacGill, Nucl. Instr. and Meth. B 55 (1991) 506.
- [7] L.D. Yu, B. Phanchaisri, P. Apavatjrut, S. Anuntalabhochai, T. Vilaithong, I.G. Brown, Surf. Coat. Technol. 158/159 (2002) 146.
- [8] P. Apavatjrut, C. Alisi, B. Phanchaisri, L. Yu, S. Anuntalabhochai, T. Vilaithong, ScienceAsia 29 (2003) 99.
- [9] S. Sangyuenyongpipat, T. Vilaithong, L.D. Yu, A. Verdaguer, I. Ratera, D.F. Ogletree, O.R. Monteiro, I.G. Brown, Nucl. Instr. and Meth. B 227 (2005) 289.
- [10] T. Vilaithong, L.D. Yu, C. Alísi, B. Phanchaisri, P. Apavatjrut, S. Anuntalabhochai, Surf. Coat. Technol. 128/129 (2000) 133.
- [11] L.D. Yu, T. Vilaithong, B. Phanchaisri, P. Apavatjrut, S. Anuntalabhochai, P. Evans, J.G. Brown, Nucl. Instr. and Meth. B 206 (2003) 586.
- [12] D. Voet, J.C. Voet, Biochemistry, John Wiley and Sons, New York, 1990.
- [13] Y. Zengliang, L.D. Yu, T. Vilaithong, I.G. Brown (Transls.), Introduction to Ion Beam Biotechnology, Springer Science and Business Media Inc., New York, 2006.

# การชักนำให้เกิดการกลายพันธุ์ โดยไอออนบีมพลังงานต่ำในข้าว (Oryza sativa var.

indica KDML105)

(Genomic Mutation Induced by Low Energy Ion Beam in Rice (Oryza sativa var. indica) KDML105)

ค่อนภา ผุสดี Yu Liangdeng 2 ถิรพัฒน์ วิลัชทอง และ สมบูรณ์ อนันคลาโภชัย Tonapha Pusadee 1 Yu Liangdeng 2 Thiraphat Vilaithong 2 and Somboon Anuntalabhochai 1

# บทคัดย่ถ

ไอออนบีมพลังงานต่ำถูกนำมาชักนำให้เกิดการกลายพันธุ์ในข้าว(Oryza sativa var. indica)KDML 105 ชนิดของไอออนที่เลือกใช้คือ อาร์กอนไอออน (Ar<sup>2</sup>) โดยทำการระดมยิงคัพภะ ของข้าวที่พลังงาน 75, 100 และ 120 keV จำนวนไอออน 10<sup>15</sup> – 10<sup>17</sup> ions/cm<sup>2</sup> บันทึกอัตราการ งอกและอัตราการรอดชีวิตของข้าวภายหลังการระดมยิง ตรวจสอบผลการชักนำการกลายพันธุ์ ด้วยเทคนิค HAT-RAPD การทดลองพบว่าที่พลังงาน 75 keV จำนวนไอออน 1x10<sup>16</sup> ions/cm<sup>2</sup> สามารถชักนำให้เกิดการกลายพันธุ์ในข้าวได้

#### Abstract

Low energy argon ion (Ar<sup>+</sup>) beam was applied to induce mutation in embryo of rice (Oryza sativa var. indica)KDML105. Ar<sup>+</sup> was chosen to bombard the embryo at 75, 100 and 120 keV with fluences of  $10^{15} - 10^{17}$  ions/cm<sup>2</sup> in range. After bombardment, germination and survival ability of bombarded embryo were observed. And genomic mutation was analyzed by HAT-RAPD technique in rice seedling. The mutation was detected at 75 keV with fluences of  $1x10^{16}$  ions/cm<sup>2</sup>. Introduction

lon beam biotechnology is a newly founded interdisciplinary field between applied nuclear physics and biology, where physical ion beam are utilized for biological engineering or processing. Application of the ion beam has been recently extended to field biology and agriculture (Vilaithong et al., 2000) for induction of mutation (Y and gene transfer (Anuntalabhochai et al., 2001). Low energy ion beam implantation as a way of mutation breeding has been characterized by a higher mutation rate and wider mutation spectrum with lower damage to organism. Since 1997, it has been widely applied to industrial and agricultural purposes (Yu et al. 2000) providing better economic and social benefit for these application (Li et al. 2002). In the aspect of

<sup>1</sup> กาควิชาชีววิทยา คณะวิทยาศาสตร์ มหาวิทยาลัยเชียงใหม่ เชียงใหม่ 50200 Department of Biology, Faculty of Science, Chiang Mai University, Chiangmai 50200 Thailand. 2 หน่วยเทคโนโลยีใอออนบีม ภาควิชาฟิสิกส์ คณะวิทยาศาสตร์ มหาวิทยาลัยเชียงใหม่ เชียงใหม่ 50200

# Ion Beam Bombardment of Biological Tissue.

S. Sangvuenyongpipat, L. D. Yu, T. Vilaithong, (Dept. of Physics, Chiang Mai University, Thailand), B. Phanchaisri, (Institute for Science and Technology R&D, Chiang Mai University, Thailand), S. Anuntalabhochai (Dept. of Biology, Chiang Mai University, Thailand), I. G. Brown (Lawrence Berkeley National Laboratory, Berkeley, CA)

While ion implantation has become a well-established technique for the surface modification of inorganic materials, the ion bombardment of cellular tissue has received little research attention. A program in ion beam bioengineering has been initiated at Chiang Mai University, and the ion beam induced transfer of plasmid DNA molecules into bacterial cells (*E. coli*) has been demonstrated. Subsequent work has been directed toward exploration of ion beam bombardment of plant cells in an effort to understand the possible mechanisms involved in the DNA transfer. In particular, ion beam bombardment of onion cells was carried out and the effects investigated. Among the novel features observed is the formation of "microcraters" – sub-micron surface features that could provide a pathway for the transfer of large molecules into the interior cell region. Here we describe our onion skin ion bombardment investigations.

Orally presented to the 56<sup>th</sup> Annual Gaseous Electronic Conference, October 21-24, 2003, NASA Ames Research Center, San Francisco, California USA

#### MUTATION INDUCTION IN THAI PURPLE RICE BY LOW-ENERGY ION BEAM

# Anuntalabhochai<sup>a</sup> S., Chandej<sup>b</sup> R., Phanchaisri<sup>c</sup> B., Yu<sup>d</sup> L.D., Promthep<sup>a</sup> S., Jamjod<sup>e</sup> S., and Vilaithong<sup>d</sup> T.

"Department of Biology, Faculty of Science, Chiang Mai University, Chiang Mai 50200, Thailand 
bDepartment of Biology, Faculty of Science, Mae Jo University, Chiang Mai 50210, Thailand 
Institute for Science and Technology Research and Development, Chiang Mai University, Thailand 
Department of Physics, Faculty of Science, Chiang Mai University, Chiang Mai 50200, Thailand 
Department of Agronomy, Faculty of Agriculture, Chiang Mai University, Chiang Mai 50200, Thailand

About 1200 seeds of Thai purple rice were bombarded by low-energy nitrogen ions accelerated by 60 kV with ion fluences of 1, 4 and 8x 10<sup>16</sup> ions/cm<sup>2</sup>. Consequently, the bombarded seeds were germinated for 5 days, and then rice seedlings were transferred to grow in soil until ripening stage. Two mutants were observed only in rice plants bombarded with the fluence of 1x10<sup>16</sup> ions/cm<sup>2</sup>. Leaf blade and stem sheath of the mutants were green. In order to determine genetic modification in the mutant genomes, HAT-RAPD (High Annealing Temperature-RAPD) was chosen for DNA investigation. Of 10 primers three primers named OPK14, OPH15 and OPL01 detected genetic variation between the mutant and control. An additional DNA band was detected by OPK14 at the molecular weight of 600 bp in both mutants. The DNA fragment was subcloned and sequenced. The analysis revealed that the DNA fragment encoding partial sequence of protein (designated OSP450) belonging to members of P450 plant protein family.

#### 1. INTRODUCTION

Mutation breeding has played an important role in crop improvement. A variety of mutagenic agents has been documented including X-rays, gamma rays, neutrons, UV light, chemical mutagens and recent ion beam bombardment. Regarding to relatively high energies (102 - 103 keV) of ion beams, they have been used to bombard biological materials for genetic modification purposes, particularly for mutation (Yu et al., 1991; Wei et al., 1995; Tanaka et al., 1997 and Yu, 2000), in a number of plant species, for instance, maize and rice (Mei et al., 1994; Yu et al., 1991), wheat (Morishita et al., 2003), rose and chrysanthemum (Yamaguchi et al., 2003), carnation (Okamura et al., 2003). To evaluate genetic variation in plant genomes, DNA-based techniques, in particular Random Amplification of Polymorphic DNA (RAPD), is one of a powerful techniques. RAPD technique is simple and generally performed at low annealing temperature (35 - 38 °C; Cho et al., 1995). But, this condition has greatly hindered in its reaction such as low reproducibility and high sensitivity. Anuntalabhochai et al., (2000) and Atienzae et al., (2000) reported that increasing the annealing temperature above 46 °C in the reaction resulting in high resolution and reproduction as well as high degree of polymorphism. And it was named HAT-RAPD (high annealing temperature RAPD; Anuntalabhochai et al., 2000). This technique succeeded in detecting genetic mutation in several plant species including jasmine rice whose mutation was induced by Ar-ion beam bombardment (Pusadee et al., 2003).

Thai purple rice is native to Thailand. It has a typical rice shape, unique color (deep purple) and exotic taste (sweet flavor). It is glutinous rice which is a major type of cultivated rice with longstanding cultural importance in Thailand, Laos and Cambodia. (Golomb,1976; Roder et al.,1996). Typically, the purple sticky rice is reserved for use in festival foods and desserts. Anthocyanins are responsible for the purple-red pigmentation of the vegetative and floral organs in a number of plant species including Thai purple rice. They are believed to assist in pollinator attraction, fruit dispersal and possible UV protection.

The objective of this study was to use N-ion beam bombardment to induce genomic mutation in Thai purple rice and detect the mutation by HAT-RAPD marker.

# Material and methods

#### Rice strain

Seeds of Thai purple rice (Oryza sativa indica strain Purple ) is provided from Agronomy

Department, Agriculture Faculty, Chiang Mai University and the Rice Research Station, San Pah Tong, Chiang Mai, Thailand.

#### Ion bombardment

Dry seeds of Thai purple rice were placed individually in holes of a specially designed sample holder (Figure 1), which was made from copper for excellent thermal transportation and in a disk shape with a size of 10 cm in diameter and 1 cm in height. On the holder there were about 400 holes, each of which was about 5-mm deep and 1-mm wide in order to hold an individual rice seed. The coat of each seed at the embryo part was removed to expose the embryo. The seeds were placed in such a way that the embryos were facing to the ion-beam incident direction. The prepared seeds with the holder were then installed in a vacuum chamber of a high-beam-current ion implanter (Figure 1) at Fast Neutron Research Facility, Chiang Mai University, Nitrogen ion beam mixed with both atomic (N) and molecular (N2) ions was used to bombard the seeds at an accelerating voltage of 60 kV (therefore, the energies of nitrogen ions were 30 and 60 keV) with fluence of 1, 4 and 8 × 10<sup>16</sup> ions/cm<sup>2</sup> (Table 1). About 400 rice seeds were bombarded in each fluences. The operating pressure in the chamber was at an order of 10<sup>-6</sup> Torr. Water cooling was deliberately applied at the sample holder to prevent overheating of the seeds due to the ion beam bombardment. To further reduce the ion beam heating, the bombardment was operated in a pulse mode with beam exposure time and close time of 10 seconds respectively.

(b)

Figure 1. Photographs of the ion beam facility. (a) The high-current ion implanter at Chiang Mai University,
(b) the target holder with Thai purple rice seeds for ion beam bombardment.

After bombardment the seeds were sown on moistened filter papers at room temperature under day light condition. The rice seeds at day 5 with large cotyledons were determined as germination stage, and then they were transplanted to soil where they were cultivated under natural condition. Seedling developed with 3 leaves at the 15th day (after germination) was scored as surviving rice

samples. The control was unbombarded seeds but kept in the bombardment environment.

DNA extraction

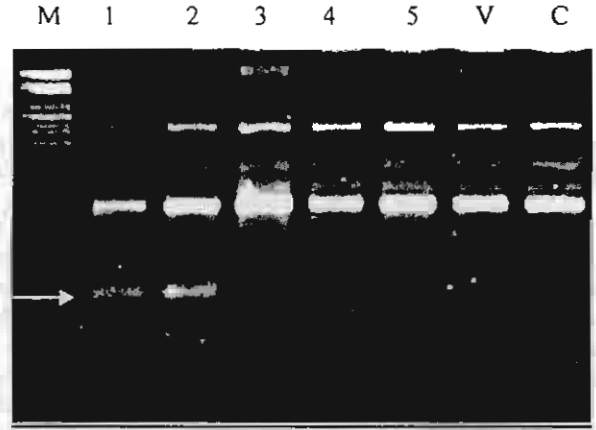


Figure 2. Result of HAT-RAPD analysis of genomic mutation of Thai purple rice plants using primer OPK14. Lane 1 – 5: genomic DNA of purple rice samples induced by N-ion beam bombardment with an accelerating voltage of 60 kV and a fluence of 1x10<sup>16</sup> ions/cm<sup>2</sup>. M: λ/Pst 1 marker, V: vacuum control, and C: control. The arrow indicates the additional bands at 600 bp presented in the mutants.

Table 1. N-ion bombardment conditions and percentages of germination and survival of Thai purple rice.

Accelerating voltage (kV)	Fluence (ions/cm <sup>2</sup> )	Number of seeds	Percentage of germination (number of germination seedling)	Percentage of survival (number of survival seedling)	Number of mutants detected
60	1 x 10 <sup>16</sup>	400	98.75 (395)	41.25 (165)	2
	4 x 10 <sup>16</sup>	400	98.50 (394)	40.00 (160)	-
	8 x 10 <sup>16</sup>	400	98.22 (386)	19.34 (76)	-

Table 2. Sequence of 10 primers used and condition of HAT-RAPD.

Primer	Sequence	HAT-RAPD reaction	
OPK 14	CCCGCTACAC		
OPL01	GGCATGACCT	94°C 2 min	
OPH15	AATGGCGCAG		
OPH11	CTTCCGCAGT	94° 30 sec	
OPC09	CTCACCGTCC	46°C 30 sec	
OPT18	GATGCCAGAC	72°C 45 sec	
OPT19	GTCCGTATGG		
OPT20	GACCAATGCC	30 cycles	
OPW09	GTGACCGAGT	1	
OPW10	TCGCATCCCT	72°C 5 min	
OPW11	CTGATGCGTG		
OPAS10	CCCGTCTACC		

DNA extraction followed the method of Doyle and Doyle (1990) with minor modifications. About 0.1 g ground powder of leaf sample was mixed with 700  $\mu$ L of CTAB extraction buffer [4% (w/v) CTAB, 1.4M NaCl, 20mM EDTA, 100mM Tris-HCl pH 8.0, 1% (w/v), and 0.1% (v/v)  $\beta$ -mercaptoethanol]. The sample was vortexed and incubated at 60 °C for 60 min, then centrifuged at

12,000 rpm for 5 min. The supernatant was extracted once with equal volume of chloroform: isoamyl alcohol (24: 1, v/v), consequently, precipitated with equal volume of cool isopropanol. After resuspension of DNA precipitation, DNA solution was treated with 5 units of RNase ONE<sup>TM</sup> ribonuclease (Sigma-Aldrich, St. Louis) and finally the DNA was precipitated again by equal volume of precool isopropanol.

#### **HAT-RAPD** protocol

Amplification of the DNA was carried out following in a 0.2 mL PCR tubes, (Sorenson<sup>TM</sup> Bioscience Inc.) in a total volume of 20 μL. Each reaction volume contained 1 μL of 20-ng DNA template, 1x buffer (10 mM Tris-HCl pH 8.0, 50 mM KCl, 0.1% TritonX-100), 2.0 mM MgCl<sub>2</sub>, 200 μM of each dNTP, 0.5 unit *Taq* Polymerase (Promega, Madison, WI) and 2-3.5 pmol of arbitrary primers (Operon Technologies, Almeda, California, USA). A list of the primers is presented in Table 2. The reaction mixture was performed in a thermocycler (GeneAmp PCR System 2400, Perkin-Elmer, Foster City, CA). The PCR amplification was performed using the method described by Anuntalabhochai et al., (2000) as follows: 2 min at 94°C, followed by 30 cycles of 30 sec at 94°C, 30 sec at 46-48°C, 45 sec at 72°C and terminating with 5 min at 72°C. The amplification products were separated by electrophoresis at 60V/cm in 1.4% agarose gels with 1x TBE buffer.

#### DNA sequencing

DNA fragment was sequenced using manual sequencer model Sequi-GenGT Sequencing Cell Power PAC 300 (Biorad) and Silver Sequecing kit (Promeca). The protocol followed the manufacture instruction.

#### 2. RESULTS AND DISCUSSION

#### Effect of ion beam on germination and survival of purple rice seedling

Since ion bombardment was carried out under low-temperature and vacuum environment, the rice seeds in experiment might be affected for their survival (Vilaithong et al., 2000).

The percentages of germination and survival of purple rice are shown in Table 1. Apparently the seed germination was not effected by N-ion bombardment at all fluences. The percentages of seed germination at three fluences (1, 4 and  $8 \times 10^{16} \text{ ions/cm}^2$ ) were 98.75%, 98.50%, and 98.22%, respectively.

On the contrary, seedling survival was effected by N ions at all fluences. The survival of rice seedling was decreased with increasing of N ion fluences (Table 2). Ishii et al., (2003) and Wu and Yu (2001) also reported this relationship between ion fluences and plant survival. However, the survival at N-ion fluences of 1 and  $4 \times 10^{16}$  ions/cm² was not significantly different (40.25% and 40%). This might be possible that all N ions could not interact with entire cells in target seeds properly. Yamagushi et al., (2003) also found this evidence in auxiliary buds of roses irradiated with certain helium ion fluences, indicating that under appropriate ion bombardment conditions (for certain ion species), ion bombardment did not effect survival of plant species (Apavajarut et al., 2003).

#### Analysis of bombarded rice mutants

At M1 stage, two mutants were detected in rice plants bombarded with the ion beam at fluence of 1x 1016 ions/cm2 at 5 days after germination. Green pigment was observed in leaf blade and stem sheath of mutants. Usually the pigment was deep purple in those tissues. However, pigment of rice panicle at the ripening stage was purple, indicating that biosynthesis of the pigment in those tissues was under genes from different loci. Wu and Yu (2001) showed that ion implantation was effective in inducing mutation in wheat and their cytological analyses revealed chromosome aberration such as chromosome bridges and lagging. Since Pusadee et al., (2003) demonstrated that HAT-RAPD marker could detect genomic mutation of jasmine rice induced mutation by Ar-ion bombardment, total DNA from leaves of the mutants and the control was extracted to serve as DNA templates for HAT-RAPD analysis. Ten arbitrary nucleotide primers from Operon Technologies Inc. (Table 2) were chosen for PCR reaction. These primers yielded a total of 85 polymorphic bands with molecular weight ranging from 300 - 1000 kb. Of ten primers, three primers, named OPK14, OPL01 and OPH15, generated 19 bands distinguished between the mutants and the control. Interestingly OPK14 primer provided an additional DNA band at the same molecular size around 600 bp in both mutants (Figure 2, lane 1 and 2 ), indicating the occurrence of genetic change in their genomes. Subsequently, this DNA fragment was chosen to be subcloned into pGemTeasy vector then transformed into E. coli. One of positive clone, named pOSP450, was selected for sequencing.

This DNA sequence was 555 bp and contained partial polypeptide of 42 amino acids (designated OSP450). The polypeptide was aligned in all proteins available in Genbank database (http://us.expasy.org/tools/blast/). Sequence analysis revealed that this OSP450 protein belonged to members of cytochrome P450 with the highest identity (92%) to cytochrome P450 protein of *Oryza sativa* japonica. The cytochrome P450 is the largest family of plant proteins. These proteins catalyze most of the oxidation steps in plant secondary metabolism resulting in complex reaction in plant cells. Some P450s are involved in the modification of the basic anthocyanin structure found in all plant species. Anthocyanins, the largest subclass of plant flavoniod, are pigment primarily responsible for most of the red, purple and blue colors seen in plant and have a variety of bioactivities of medical interest (Bourne and Willams, 2000). Moreover, a number of genes encoding enzymes involved in anthocyanin synthesis in plants have been cloned and characterized (Morant *et al.*, 2003).

#### 3. CONCLUSION

N-ion beam bombardment was applied to induce mutation in Thai purple rice seeds. There was no correlation between N ion fluences, survival and mutation detection in Thai purple rice in the bombardment conditions applied. HAT-RAPD reaction could detect genomic mutation between the mutants and the control. Amino acid sequence analysis revealed that the OSP450 protein found in the mutant showed high identity to cytochrome P450 of plant proteins.

# **ACKNOWLEDGEMENT**

This work was supported by the Thailand Research Fund.

#### REFERENCES

- Anuntalabhochai, S., Chandej, R., Chiangda, J., and Apavatjrut, P. (2000). Genetic diversity within Lychee (Litchi chinensis Sonn.) based on RAPD analysis. Acta Horticulturae 575: 253-259.
- [2] Anuntalabhochai, S., Chandej, R., Phanchaisri, B., Yu, L.D., Vilaithong, T. and Brown, I.G. (2001). Ion-beam-induced deoxyribose nucleic acid transfer. Applied Physics Letters 78(16), 2393-2395.
- [3] Atienzar, F., et al. (2000). Optimized RAPD analysis generates high quality genomic DNA profiles at high annealing temperature. BioTechniques 28, 52-54.
- [4] Bourne, J.B. and Willams, C.A. (2000). Advances in flavoniod research since 1992. Phytochemistry 55: 481-504.
- [5] Chitrakon, S. (1998). Jasmine, Juamati and Patents (in Thai) Rice Research Institute, Ministry of Agriculture, Thailand. P.6.
- [6] Cho, Y. C., Chung, T.Y., Park, Y.H. and Suh, H.S. (1995). Genetic polymorphisms and phylogenetic relationships of Korean red rice (weedy rice in Oryza sativa L.) based on randomly amplified polymorphic DNA (RAPD) markers. Korean Journal of Breeding 27(1): 86-93.
- [7] Doyle, J.J. and Doyle, J.L. (1990). A rapid DNA isolation procedure for small quantities of fresh leaf tissue. Phytochem. Bull. 19: 11-15.
- [8] Golomb, L. (1976). The origin, spread and persistence of glutinous rice as a staple crop in mainland Southeast Asia. J. Southeast Asian Stud. 7:1-15.
- [9] Hirono, Y., Smith, H.H., Lyman, J.T., Thomson, K.H., and Baum, J.W. (1970). Ralative biological effectiveness of heavy ions in producing mutations, tumours and growth inhibition in the crucifer plant, Arabidopsis. Radiation Research 44: 204-223.
- [10] Ishii, K., Yamada, Y., Hase, Y., Shikazano, N., and Tanaka, A. (2003). RAPD analysis of mutants obtained by ion beam irradiation to hinoki cypress shoot primordial. *Nucl. Instr. and Meth.* B206: 570-573.
- [11] Li, Y.F., Huang, Q., and Yu, Z. (2002). Analysis of N<sup>+</sup> induced α-DNA mutation by RAPD. The Proceedings of the Third National Conference of Ion Beam Bioengineering and the First International Symposium on Ion Beam: Biological Effects and Molecular Mechanism, 27<sup>th</sup> July 3<sup>rd</sup> Aug. 2002, Wulumuqi, China. 95 97.
- [12] Maekawa, M., Hase., Y., Shikazono, N., and Tanaka, A. (2003). Induction of somatic instability in stable yellow leaf mutant of rice by ion beam irradiation. Nucl. Instr. and Meth. B206: 579-585.
- [13] Mei, M., Deng, H., Lu, Y., Zhuang, C., Lui, Z., Qiu, Q., Qiu, Y., and Yang, T.C. (1994). Mutagenic effects of heavy ion radiation in plants. Advance in Space Research, 14(10): 363-372.
- [14] Morishita, T., Yamaguchi, H., Degi, K., Shikazono, N., Hase, Y., Tanaka, A., and Abe, T. (2003). Dose

- response and mutation induction by ion beam irradiation in buckwheat. Nucl. Instr. and Meth. B106: 565-569.
- [15] Okamura, M., Yasuno, N., Ohtsuka, M., Tanaka, A., Shikazazono, N., and Hase, Y. (2003). Wide variety of flower-color and -shape mutants regenerated from leaf cultures irradiated with ion beams. *Nucl. Instr.* and Meth. B206: 574-578.
- [16] Pusadee, T., Liangden, Y., Vilaithong, T., and Anuntalabhochai, S. (2003). Genomic mutation induced by low energy ion beam in rice (Oryza sativa var. indica) KDML 105. Presented to the National Conference in Gnetics and Sustanable Development, 5-7 June, 2003, Pitsanulok, Thailand.
- [17] Rodder, W., Keoboulapha, B., Vannalath, K., and Phouaravanh, B. (1996). Glutanous rice and its importance for hill farmers in Loas. Econ. Bot. 50: 401-408.
- [18] Tanaka, A., Tano, S., Chantes T., Yokota, Y., Shikazono, N., and Watanabe, H. (1997). A new Arabidopsis mutant induced by ion beams affects flavonoid synthesis with apotted pigmentation in testa. Genes Gen. Syst. 72, 141-148.
- [19] Vilaithong, T., Yu, L.D., Alisi, C., Phanchaisri, B., Apavatjarut, P., and Anuntalabhochai, S. (2000). A study of low-energy ion beam effects on outer plant cell structure for exogenous macromolecule transferring. Surface and Coating Technology 128-129:133-138.
- [20] Wei, Z., Xei, H., Han, G. (1994). Physical mechanisms of mutation induced by low energy ion implantation. Nucl. Instr. and Meth. B95: 371-378.
- [21] Wu, L., Pehrson, G.R., Xu, A., Waldren, C.A., Yu, Z., and Hei, T.K. (1999). Target cytoplasmic irradiation with alpha particles induces mutations in mammalian cells. *Proc, Natl. Acad. Sci. USA* 4(10): 1325-1329.
- [22] Wu, L. and Yu, Z. (2001). Radiobiological effects on low-energy ion beam on wheat. Radiat. Biophysics 40: 53-57.
- [23] Xiangin, W., Jianwei, H., Chunlin, S., and Zenglian, Y. (1998). Study on damage of molecular structure of solid uracil induced by low energy argon ions implantation. Acta Biophys. Sinica 14(2).
- [24] Yamaguchi, H., Nagatomi, S., Morishita, T., Degi, K., Tanaka, A., Shikazono, N., and Hase, Y. (2003). Mutation induced ion beam irradiation in rose. *Nucl. Instr. and Meth.* B206: 561-654.
- [25] Yu, Z., Deng, J., He, J,m Huo, Y., Wu, Y., Wang, X., and Liu, G. (1991). Mutation breeding by ion implantation. Nucl. Instr. and Meth. B59/60: 705-708.
- [26] Yu, L. (1993). in: Research on biological effects induced by ion implantation in China, Atomic Energy Press, Beijing. 1.
- [27] Yu, Z., Yang, J., Wu, Y., Cheng, W., He, J., and Huo, Y. (1993). Transferring GUS gene into intact rice cells by low energy ion beam. Nucl. Instr. and Meth. B80/81: 1328-1331.
- [28] Yu, Z., Shao, C., and Yang, J. (1994). Low energy ion beam mediated DNA delivery into rice cells. J. Anhui. Agric. Univ. 21(3): 330-335.
- [29] Yu, Z. (2000). Ion beam application in genetic modification. IEEE Transaction on Plasma Science 28(1): 128-132.
- [30] Yu, Z. (2002). Study on low energy heavy ion biology and its application undertaken in China. The Proceedings of the Third National Conference of Ion Beam Bioengineering and the First International Symposium on Ion Beams: Biological Effects and Molecular Mechanisms, 27<sup>th</sup> July - 3<sup>rd</sup> August 2002, Wulumuqi, China. 1-5.
- [31] Morant, M., Bak S., Moller, B.L, and Werck-Reichhart, D. (2003). Plant cytochrome P450: tools for pharmacology, plant protection and phytoremediation. Cur. Opin. Biotechnol. 14: 1-12.

Effects of Low-energy Ion Beam Bombardment

on Biological Cell Envelopes

L.D. Yu<sup>a</sup>\*, S. Sangyuenyongpipat<sup>a</sup>, S. Anuntalabhochai<sup>b</sup>, B. Phanchaisri<sup>c</sup>, T. Vilaithong<sup>a</sup>,

<sup>a</sup> Fast Neutron Research Facility, Department of Physics, Faculty of Science,

<sup>b</sup> Molecular Biology Lab, Department of Biology, Faculty of Science,

<sup>c</sup> Institute for Science and Technology Research and Development.

Chiang Mai University, Chiang Mai 50200, Thailand

and I.G. Brown<sup>d</sup>

<sup>d</sup> Lawrence Berkeley National Laboratory, Berkeley, California 94720, USA

Low-energy ion beam biotechnology has recently been rapidly developed worldwide. This is an important expansion of studies on ion beam modification of solid materials, tremendously different and complex from the latter. Among the novelties, we have focused our interest onto ion beam bombardment effects on the plant and bacterial cell envelopes and tried to figure out mechanisms involved in ion beam induced gene transfer. Through a comprehensive investigation, we have discovered ion-beam-induced formation of nanocrater-like structures in the cell envelope, a general phenomenon of ion beam bombardment of the cells, and the structures may act as pathways for exogenous macromolecule transfer. We have also quantitatively obtained abnormally great penetration depth and sputtering of ions in the cell envelope. All of these results will be significantly beneficial to ion beam processing of biological cells.

Keywords: Ion beam bombardment, Nanocrater, Cell envelope, Gene transfer

\*Corresponding author: Postal address: FNRF, Department of Physics, Faculty of Science,

Chiang Mai University, Chiang Mai 50200, Thailand.

Fax: +66 53 222776. Tel.: +66 53 943379. Email: yuld@fnrf.science.cmu.ac.th

1

#### 1. Introduction

Ion beam technology applied to modification of materials has been successfully developed for about three decades [1]. Since the middle of 1980s when biological effects of low-energy ion beam implantation in plant cells were discovered [2], ion beam materials modification has been expanded to biology and a highly interdisciplinary new subject, ion beam biotechnology [3], has been established and rapidly developed worldwide. The technology uses low-energy (in orders of  $10 - 10^3$  keV) ion beams to bombard biological organisms for broad applications on mutation breeding, gene transfer, heavy ion therapy, life origin study, radiation hazard evaluation and biological structure analysis. Compared with ion beam interaction with conventional solids, ion beam bombardment of living materials has significant differences and complexities:

- Biological organisms are living, and ion beam treatment should not kill them.
- Fresh cells contain a large amount of water, which essentially evaporates in vacuum,
   and the evaporation causes differences in the target status from that in normal atmosphere.
- Biological material structures are highly porous and inhomogeneous, and ions
  penetrate and sputter abnormally more than for normal condensed materials.
- The functioning structures of organisms are very complicated and different ion-beam treated locations have different responses, and hence in order to get a certain response, ion beam should be precisely controlled to target the location.
- Biological organisms are extremely sensitive to ion irradiation, will actively respond
  to the irradiation and thus highly produce secondary effects, which can greatly affect
  consequences of ion beam bombardment.
- Organisms have recovery ability, and ion beam radiation damage may be repaired and thus ion beam effects may disappear in a certain time period.

 Different parts of an organism may have communications and an ion-beam treated location may produce unexpected effects.

All of these are great challenges but also attractions to scientists. In developing ion beam biotechnology, we have focused our interests onto ion interaction with biological cell envelopes. The cell envelope here means the total outer cell structural material that encases the cell, consisting of the cell wall, plasma membrane and outmost coat for plant and bacterial cells. The cell envelope is the first and also the main material for ions to interact with when they are bombarding biological organisms in vacuum, and the interaction is able to lead to important applications such as induction of gene transfer in the cells [4,5] and mutation of plants [6]. From the physics point of view, mechanisms involved in the transfer and physical parameters dominating the mutation are still fairly unclear. In this report we summarize progresses that we have recently made in the study of ion beam bombardment effects on the cell envelopes and answers to the unclear questions that we have obtained up to now.

# 2. Experiments

Ions of gaseous species such as N, Ar, Cl and Xe and metals such as Mg, Al, Ti, Fe, Ni, Cu and Au at an average ion energy about 15-30 keV with fluences typically around 1 to  $2 \times 10^{15}$  ions/cm<sup>2</sup> were used to bombard biological samples such as plant cells of onion skin, corn embryo, *Curcuma* embryo and bacterial cells of *Escherichia coli* (*E. coli*). The ion implanters used were a special bioengineering ion beam facility at Chiang Mai University and a MEVVA-source ion implanter at Berkeley. Post-ion-bombardment biological and physical analyses were carried out to observe features of the cells using scanning electron microscopy (SEM), transmission electron microscopy (TEM) and atomic force microscopy (AFM), and survival of the cells using vital dye staining, and to measure the ion range using Rutherford backscattering spectrometry (RBS). The experimental details refer to our previous

publications [4,7-10]. Molecular dynamics simulation (MDS) was also carried out using HyperChem [11] and AMBER8 [12] to simulate ion bombardment of cellulose, the basic substance of the plant cell wall.

#### 3. Results and Discussion

# 3.1 Vacuum Effect

It was observed and measured that the fresh cells almost totally lost their containing water after they were exposed to vacuum for a short time period [5]. The water loss was due to the low-pressure-accelerated rapid evaporation, which also caused a rapid temperature decrease for the cells. Therefore, the cells in the vacuum chamber suffered severe shrinkage and freezing (Fig. 1). All these harsh conditions affected the cell survival but a part of the cells could still be alive (Fig. 2). The vacuum effect on the cell indicates that the cell envelope remains as the major structural material in the ion bombardment environment while the inner substances of the cell are less significant when we study ion interaction with the matter of the cells. Vacuum effect checking is important, because when ion beam bombardment effects are studied, the vacuum effect should not be included.

# 3.2 Ion Beam Bombardment Effect on Cell Survival

The ion energy and fluences were chosen in the experiments such that the ion implantation range could be similar to the cell envelope thickness. Under these conditions, the ion beam bombardment effect on the cell survival was checked. It was found that ion beam bombardment could make cells surviving only under appropriate energy and fluence conditions, beyond which the cells would not survive (Fig. 3). Ion beam bombardment retarded growth of the cells (Fig. 4).

# 3.3 Abnormally Great Ion Range and Sputtering

It has been found that ion penetration range and sputtering yield in the cell envelope are abnormally greater than results calculated or simulated by conventional theoretical considerations. Successful DNA transfer and mutation induced by ion beams imply that the ions should pierce the cell envelope to create pathways for DNA molecule transfer and hit the cell nucleus inside for mutation. Typical cell envelopes have a thickness about several hundred nanometers (see Fig. 5a). But, the ion range of a 30-keV nitrogen ion in water is about 150 nm (simulated by TRIM [13]). Therefore, the real ion range in the cell envelope is supposed to be abnormally greater. This abnormality has been indeed observed in the experiments and it shows that the ion penetration depth in the cell envelope is about a few times that calculated with an assumption of the envelope being the compact solid cell wall material [8]. Furthermore, abnormally high ion sputtering yield of the cell envelope has also been observed [10]. As shown in Fig. 5, the sputtering loss of the Curcuma embryo cell envelope surface caused by 30-keV Ar-ion bombardment with a conventionally low fluence at an order of 10<sup>15</sup> ions/cm<sup>2</sup> is considerably high, about more than 100 nm depending on the fluence. But calculations (by PROFILE code [14]) based on the assumption of the envelope being the compact solid cell wall material show the sputtering loss should be only about 10 nm.

In order to interpret both observed abnormally great ion range and sputtering, we have established a material structure model for the cell wall which is the dominant part of the cell envelope [8]. The real cell wall is a discontinuous structure consisting of nanosized cellulose microfibrils, made from cellulose molecules in a chemical structure of  $C_6H_{12}O_6$ , in a size of 3.5 nm in diameter (for most of high plants) and cross-linked in a net style with about a 5-nm spacing in between [15,16] (Fig. 6a). The physical model of the cell wall, as shown in Fig. 6, is therefore a compact solid, which has a linear thickness of 7/17 that of the real cell wall, consisting of 3.5-nm-diameter microfibrils arranged in parallel in a plane but oriented in

random for different planes; each microfibril is composed of chains of cellulose molecules in the chemical structure of  $C_6H_{12}O_6$ ; and the mass density of the modeled cell wall is about 1.05 g/cm<sup>3</sup> (close to that of water). From this model it can be known that the average number of bonds of each atom in a molecule is 2, thus the stopping power is deduced to be about 1/2, the ion range about 2.5 times, and the sputtering yield about 7 times that of a matrix with homodistributed atoms of the same elements [8]. Calculations of the ion penetration depth based on this model yield good agreements with measured results (Fig. 7).

# 3.4 Formation of Nanocrater Structure

Besides studying the ion behavior in the cell envelope, we have also investigated ion bombardment effects on the morphology of the cell envelope surface. This study is owing to the interest in mechanisms involved in gene transfer induced by ion beams. When exogenous macromolecules are transferred into the cell, they must pass certain pathways through the cell envelope. Although there originally exist biological channels in the cell wall for exchanging substances across the cell envelope, these channels are too small for large molecules such as DNA to pass through. Evidence also shows that without ion beam bombardment, cells cannot automatically transfer exogenous macromolecules into them. This fact demonstrates that ion beam bombardment must create or induce some pathways for the transferring.

We have found from our experiments that ion bombardment can induce formation of nanocrater-like structures on the cell envelope under certain ion beam conditions such as ion beam energy and fluence range, which is a general phenomenon, no matter what ion species and what cells are used [9] (Fig. 8). Molecular dynamics simulation (MDS) of 25-keV Fe<sup>2+</sup> ions bombarding a cellulose structure demonstrates possible formation of nanocraters in the target, as shown in Figure 9. The created structures are featured with an inhomogeneous distribution, implying the formation not to be a direct ion beam effect but an indirect

consequence of ion bombardment, and large sizes with several hundreds of nm in diameter and several tens of nm in depth (measured from both SEM and AFM images), implying possibilities for the structures to act as DNA transferring pathways. Further investigations are ongoing to explore whether the ion-bombardment-created nanocrater-like structures really play a role in DNA transfer.

#### 4. Conclusion

Effects of low-energy ion beam bombardment on the biological cell envelope have been studied and known to include:

- Ion beams dominantly interact with the cell wall material with negligible effects on other substances of the cell envelope.
- Under appropriate beam conditions, cells survive.
- Ion penetration range and sputtering in the cell envelope are abnormally greater than
  calculated or simulated results when the material is considered as a homogeneous
  compact solid.
- Ion-beam-bombardment can create nanocrater-like structures, which may act as pathways for DNA transfer.

Applications of these effects include ion-beam induced mutation and gene transfer, which will lead to genetic modification of biological organisms.

# Acknowledgements

We wish to thank researchers and students at Chiang Mai University and Lawrence Berkeley National Laboratory for experimental assistance. This work was supported by the Thailand Research Fund.

# References

- [1] M. Nastasi, J.W. Mayer, J.K. Hirvonen, Ion-Solid Interactions, Fundamentals and Applications (Cambridge University Press, Cambridge, Great Britain, 1996).
- [2] Z.L. Yu, L.J. Qiu, Y.P. Huo, J. Anhui Agricultural College, 18(4) (1991) 251-257.
- [3] Z.L. Yu originally authored, and L.D. Yu, T. Vilaithong and I. Brown translated, Introduction to Ion Beam Biotechnology (English Edition, Springer, New York, 2005) in press.
- [4] S. Anuntalabhochai, R. Chandej, B. Phanchaisri, L.D. Yu, T. Vilaithong, I.G. Brown, Appl. Phys. Lett. 78 (2001) 2393-2395.
- [5] B. Phanchaisri, L.D. Yu, S. Anuntalabhochai, R. Chandej, P. Apavatjrut, T. Vilaithong, I.G. Brown, Surf. & Coat. Technol. 158-159 (2002) 624-629.
- [6] S. Anuntalabhochai, R. Chandej, B. Phanchaisri, L.D. Yu, S. Promthep, S. Jamjod, T. Vilaithong, Proceedings of the 9<sup>th</sup> Asia Pacific Physics Conference (9<sup>th</sup> APPC), Hanoi, Vietnam, October 25 31, 2004, in press.
- [7] T. Vilaithong, L.D. Yu, C. Alisi, B. Phanchaisri, P. Apavatjrut, S. Anuntalabhochai, Surf.& Coat. Technol. 128-129 (2000) 133-138.
- [8] L.D. Yu, T. Vilaithong, B. Phanchaisri, P. Apavatjrut, S. Anuntalabhochai, P. Evans, I.G. Brown, Nucl. Instr. and Meth. B206 (2003) 586-590.
- [9] S. Sangyuenyongpipat, T. Vilaithong, L.D. Yu, A. Verdaguer, I. Ratera, D.F. Ogletree,O.R. Monteiro, I.G. Brown, Nucl. Instr. and Meth. B227 (2005) 289-298.
- [10] L.D. Yu, B. Phanchaisri, P. Apavatjrut, S. Anuntalabhochai, T. Vilaithong, I.G. Brown, Surf. and Coat. Technol. 158-159 (2002) 146-150.
- [11] Hypercube, Inc., see the website of http://www.hyper.com.
- [12] D.A. Pearlman, D.A. Case, J.W. Caldwell, W.R. Ross, T.E. Cheatham, III, S. DeBolt,D. Ferguson, G. Seibel and P. Kollman. Comp. Phys. Commun. 91 (1995) 1-41. Also

- see the website of http://amber.scripps.edu.
- [13] TRIM, see <a href="http://www.srim.org">http://www.srim.org</a>; J.F. Ziegler, J.P. Biersack, U. Littmark, The Stopping and Range of Ions in Solids (Pergamon Press, New York, 1984).
- [14] PROFILE Code Software, Version 3.20, Implant Sciences, Wakefield, MA 01880-1246, USA, 1995.
- [15] B. Alberts, D. Bray, J. Lewis, M. Raff, K. Roberts, J.D. Watson, olecular Biology of the Cell (Garland Publishing, New York & London, 1992) p.11137.
- [16] D. Voet and J.G. Voet, Biochemistry (John Wiley & Sons, New York, 1990) p.254.

9

# List of figure captions

Figure 1. SEM micrographs of corn embryo cells. (a) Fresh, and (b) in vacuum.

Figure 2. Measured mass loss and survival rate of onion cells exposed to vacuum.

**Figure 3.** Trypan-blue (TB) staining of 30-keV Ar-ion bombarded corn embryo cells. A: fresh control, B: vacuum control, C:  $5 \times 10^{14}$  ions/cm<sup>2</sup>, D:  $1 \times 10^{15}$  ions/cm<sup>2</sup>, E:  $2 \times 10^{15}$  ions/cm<sup>2</sup>, F:  $4 \times 10^{15}$  ions/cm<sup>2</sup>. TB only stains dead parts of the cell, and staining of the cell nuclei indicates death of the cells.

Figure 4. Growth of naked corn embryos after 15-keV N-ion bombardment. A: fresh control, B: vacuum control, C:  $5\times10^{14}$  ions/cm<sup>2</sup>, D:  $1\times10^{15}$  ions/cm<sup>2</sup>, E:  $2\times10^{15}$  ions/cm<sup>2</sup>, F:  $1\times10^{16}$  ions/cm<sup>2</sup>.

Figure 5. TEM micrographs of the cross sections of the *Curcuma* embryo cell envelopes before (a) and after 30-keV Ar-ion bombardment at  $1 \times 10^{15}$  ion/cm<sup>2</sup> (b) and  $2 \times 10^{15}$  ions/cm<sup>2</sup> (c), respectively. The arrows indicate the externals of the cells.

Figure 6. The physical model of the cell wall. (a) An electron micrograph of the real cell wall structure, and (b) the model, where A: microfibrils, B: a microfibril, and C: the chemical structure of a cellulose molecule.

Figure 7. Distribution of implanted Ti ions (at 30 keV with a fluence of 1×10<sup>16</sup> ions/cm<sup>2</sup>) in the cell envelope of the onion skin cell. (a) RBS-measured profile, and (b) PROFILE-code calculated profile based on the cell wall model.

Figure 8. SEM micrographs of biological cell surface morphology. (a) Unbombarded onion skin cell surface, (b) 20-keV Mg-ion bombarded onion skin cell surface at a fluence of  $1\times10^{15}$  ions/cm<sup>2</sup>, (c) unbombarded *E. coli* cell surface, and (d) 25-keV Ar-ion bombarded *E. coli* cell surface at a fluence of  $1\times10^{15}$  ions/cm<sup>2</sup>.

Figure 9. Molecular dynamics simulation result of the cellulose structure after Fe<sup>2+</sup> bombardment for 0.01024 ps. The velocity scale is 1/10 the actual velocity (energy: 25 keV).

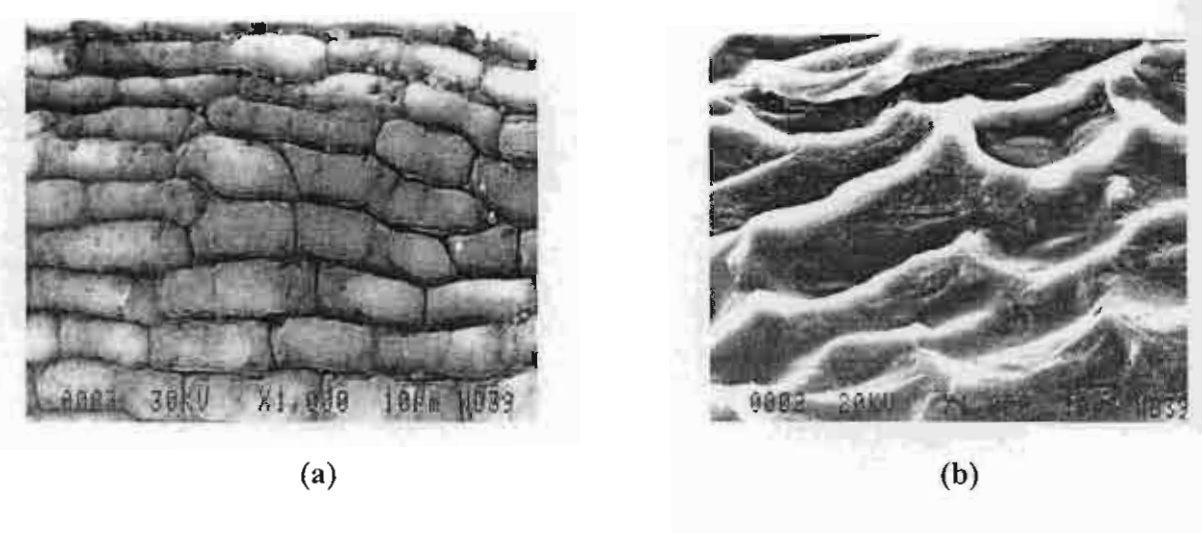


Figure 1

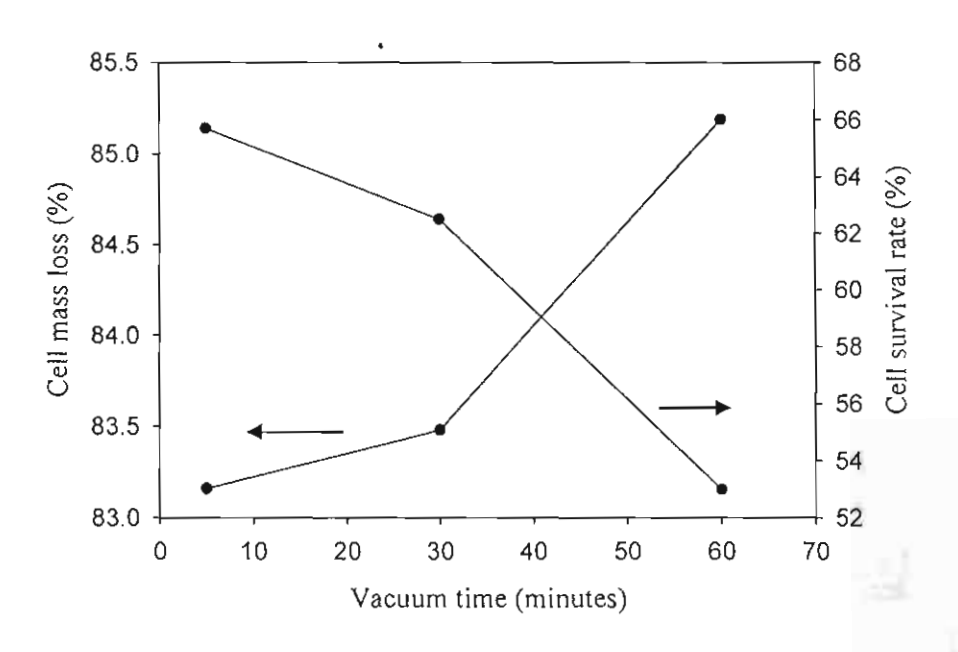


Figure 2

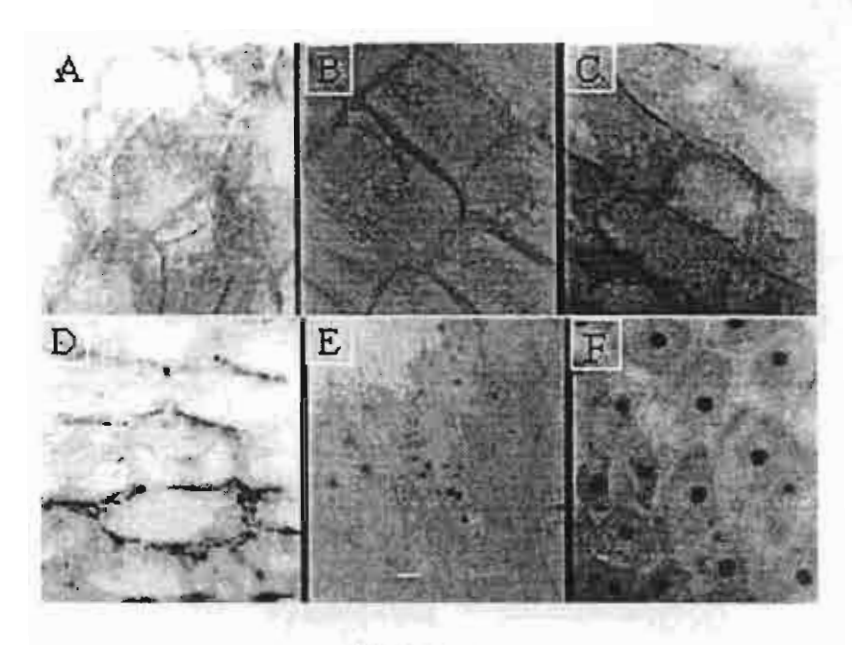


Figure 3

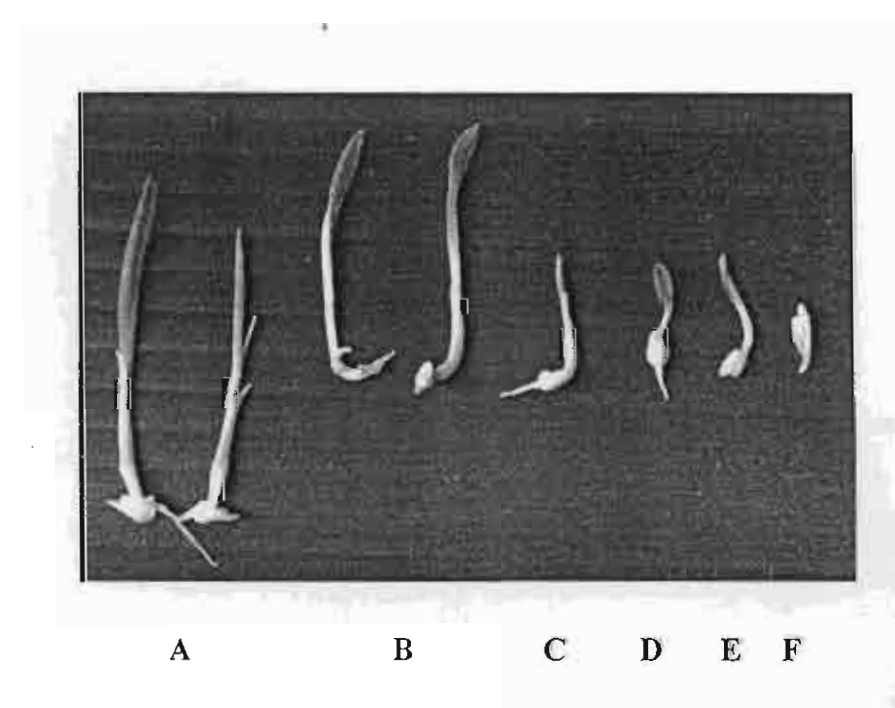
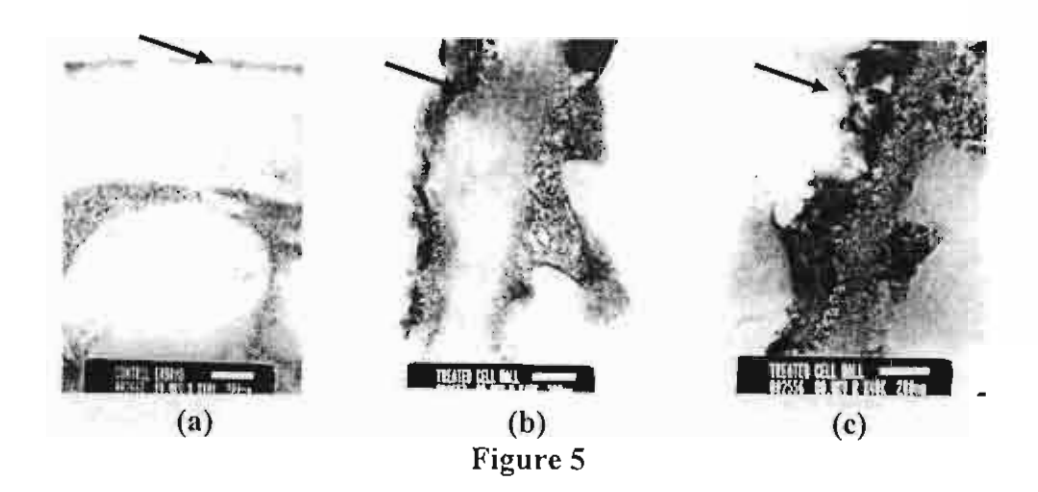
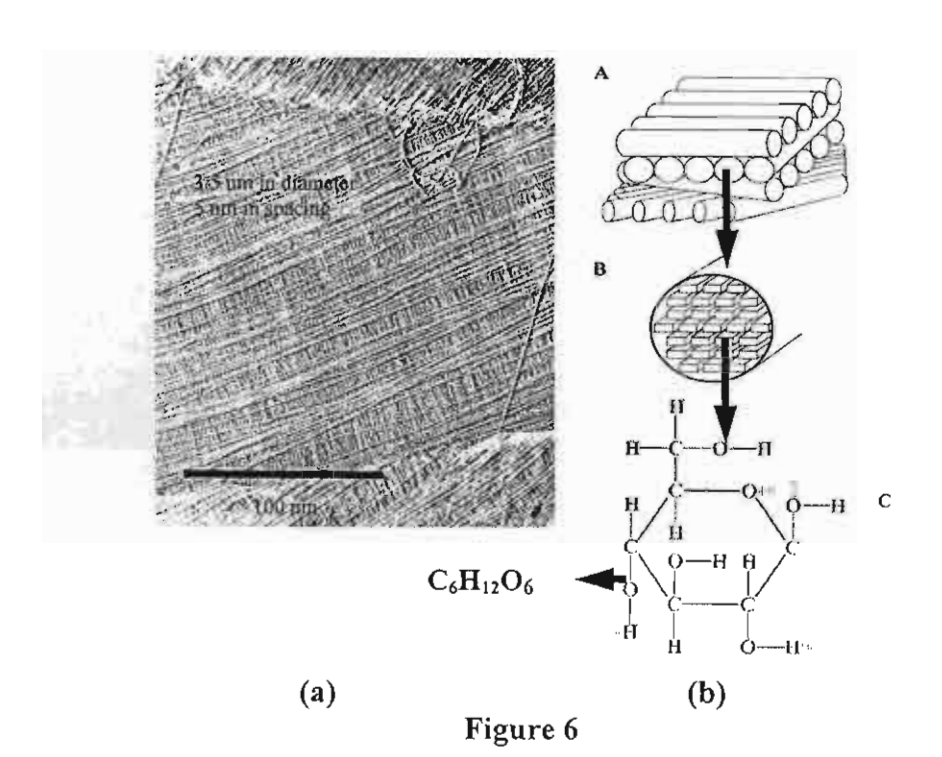
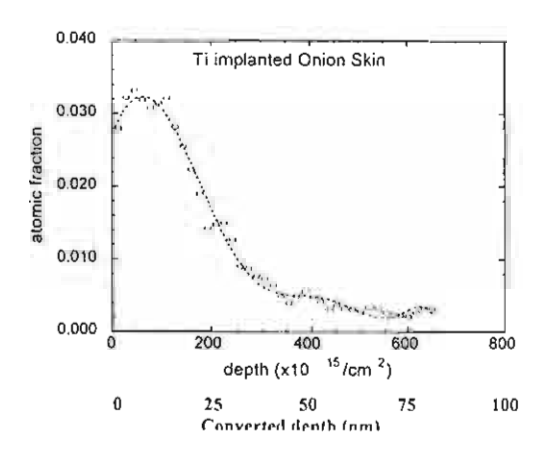
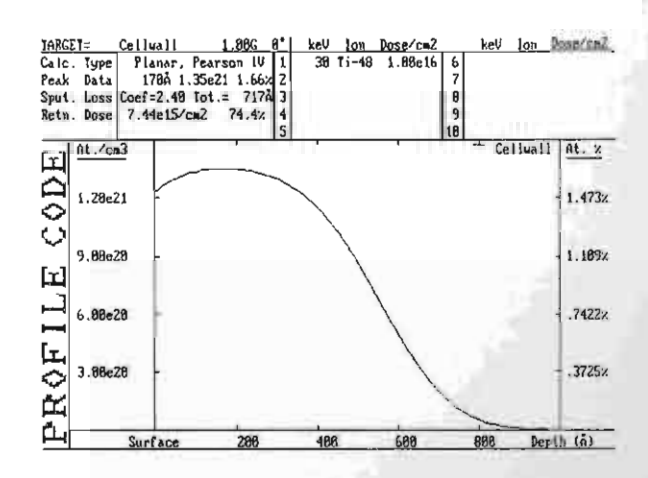


Figure 4









(a) (b)

Figure 7

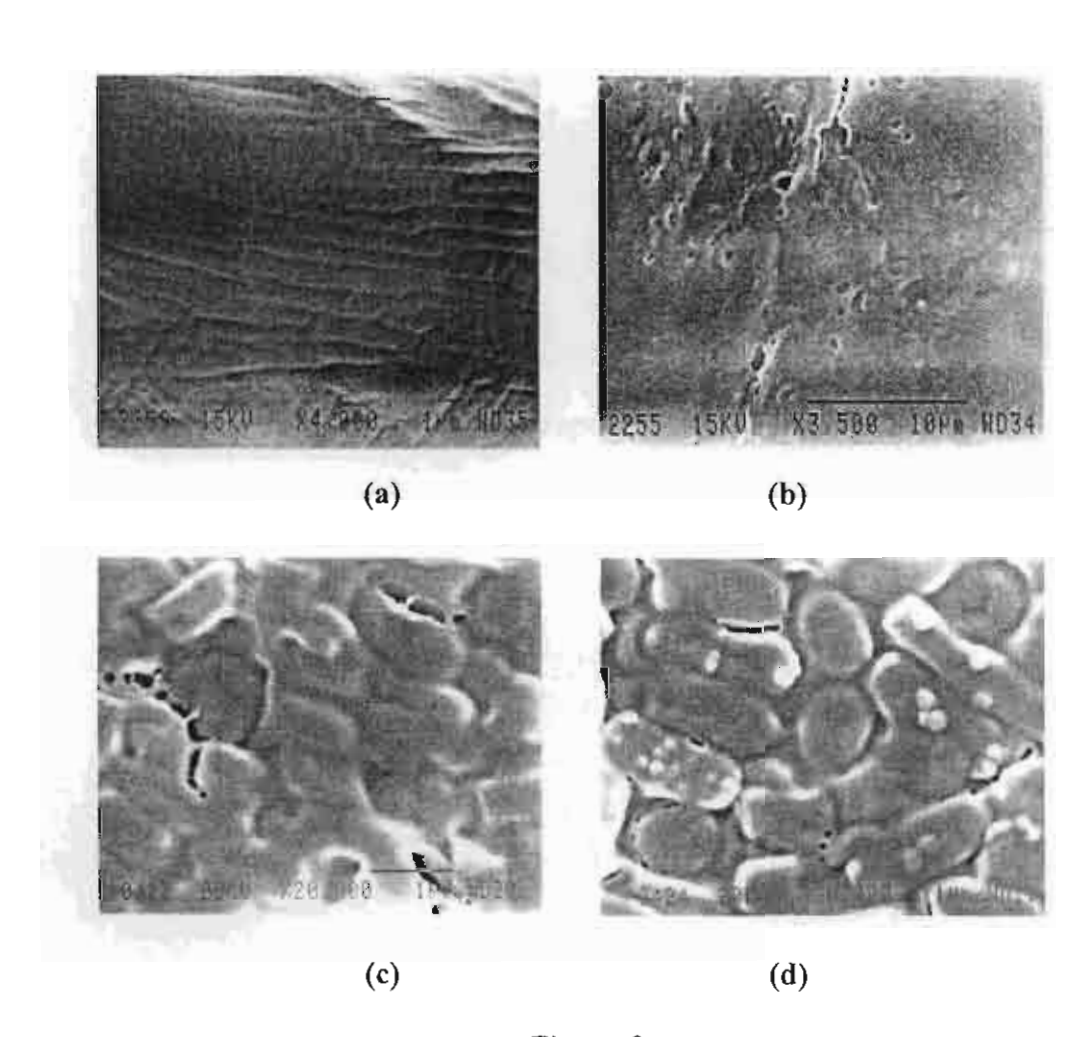


Figure 8

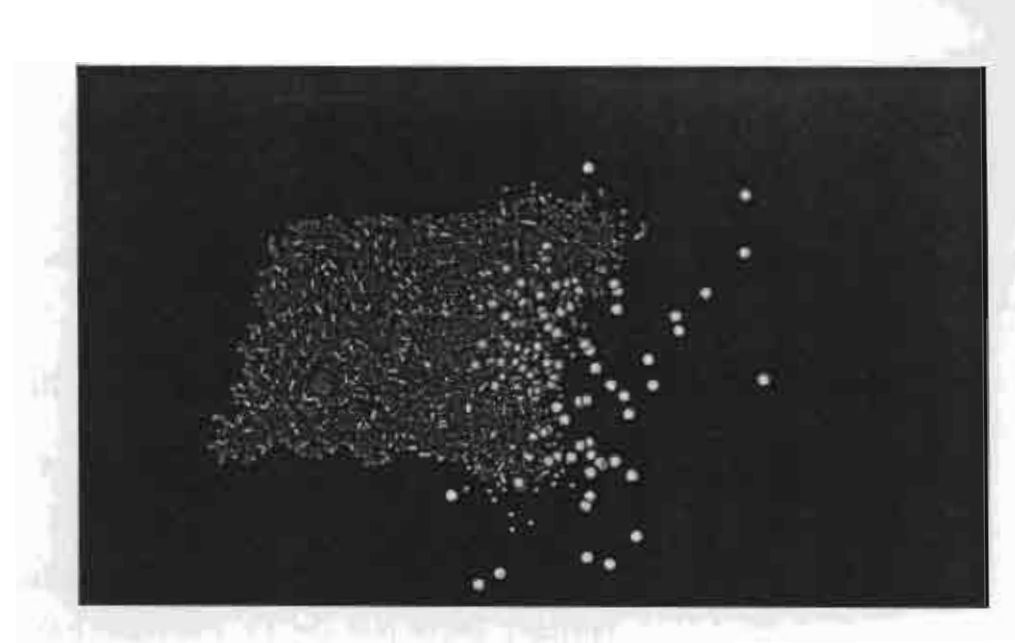


Figure 9

A paper submitted and accepted to be published in Surface and Coatings Technology

# Low-energy ion-beam-induced mutation in Thai jasmine rice (*Oryza sativa* L. cv. KDML 105)

B. Phanchaisri <sup>a</sup>, R. Chandet <sup>b</sup>, L.D. Yu <sup>c</sup>, T. Vilaithong <sup>c</sup>, S. Jamjod <sup>d</sup>, S. Anuntalabhochai <sup>e</sup>

Chiang Mai University, Chiang Mai 50200, Thailand

Maejo University, Chiang Mai 50290, Thailand

Chiang Mai University, Chiang Mai 50200, Thailand

Chiang Mai University, Chiang Mai 50200, Thailand

Chiang Mai University, Chiang Mai 50200, Thailand

# Abstract

Low-energy ion beam bombardment at energy levels in the range of 60-125 keV and ion fluences (dose) of  $1 \times 10^{16} - 5 \times 10^{17}$  ions/cm² was chosen for mutation induction in Thai jasmine rice (*Oryza sativa* L. cv. KDML 105) at Chiang Mai University. One of the rice mutants designed BKOS6 was characterized. The rice mutant was obtained from KDML105 rice embryos bombarded with N<sup>+</sup> + N<sub>2</sub><sup>+</sup> ions at an energy level of 60 keV and ion fluence of  $2 \times 10^{16}$  ions/cm². Phenotypic variations of BKOS6 were short in stature, red/purple color in leaf sheath, collar, auricles, ligule, and dark brown stripes on leaf blade, dark brown seed coat and pericarp. The mutant's reproductive stage was found in off-season cultivation (March-July). HAT-RAPD (High Annealing Temperature-Random Amplified Polymorphic DNA) was applied for analysis of genomic variation in the mutant. Of 10 primers, two primers detected two additional DNA bands at 450 bp and 400 bp. DNA sequencing revealed that the 450 bp and the 400 bp fragments were 60 % and 61% identity to amino acid sequence of flavanoid 3'hydroxylase and cytochrome P450 of *Oryza sativa japonica*, respectively.

<sup>&</sup>lt;sup>a</sup> Institute for Science and Technology Research and Development,

<sup>&</sup>lt;sup>b</sup> Department of Biology, Faculty of Science,

<sup>&</sup>lt;sup>c</sup> Fast Neutron Research Facility, Department of Physics, Faculty of Science,

<sup>&</sup>lt;sup>d</sup> Department of Agronomy, Faculty of Agriculture,

<sup>&</sup>lt;sup>e</sup> Department of Biology, Faculty of Science,

# Mutation of Bacillus licheniformis by Low Energy Ion Beam

S. Mahadtanapuk (e,b) , L.D. Yu°, T. Vilaithong°, S. Anuntalabhochai<sup>b</sup>

Antracnose, caused by the fungus Collectrotrichum sp., is one of an important disease affecting flowers. The use of natural antagonists in biological control has recently applied. In these study, *Bacillus licheniformis* isolated from hot spring Chiang Mai province showed its activity to suppress conidia germination of the fungus and reduce symptom causing by the disease in planta. Low energy ion beam was applied to induce mutation in B. *licheniformis* N-ions were chosen to bombard the bacteria under the vacuum condition at energy of 28 keV with fluence range of 1-10x 10<sup>15</sup> ions/cm<sup>2</sup>. One of a mutant with loosing its antagonistic property was obtained. Polymorphic bands were detected between the bombarded bacteria and wild type by HAT-RAPD technique. These DNA bands will be investigated for further analysis in gene involving in its antipathogenicity.

.

<sup>&</sup>lt;sup>a</sup> Econimic Plants Genome Research and Service Center, Department of Biology, Faculty of Science, Chiang Mai University, Chiang Mai 50200, Thailand

<sup>&</sup>lt;sup>b</sup>Department of Biology, Faculty of Science, Chiang Mai University, Chiang Mai 50200, Thailand

<sup>&</sup>lt;sup>c</sup>Fast Neutron Research Facility, Department of Physics, Faculty of Science, Chiang Mai University, Chiang Mai 50200, Thailand

# A specialized bioengineering ion beam line

L.D. Yu\*, S. Sangyuenyongpipat, C. Sriprom, C. Thongleurm, R. Suwanksum,
N. Tondee and T. Vilaithong

Fast Neutron Research Facility, Department of Physics, Faculty of Science,
Chiang Mai University, Chiang Mai 50200, Thailand

# I.G. Brown

Lawrence Berkeley National Laboratory, Berkeley, California 94720, USA

#### H. Wiedemann

Applied Physics and SSRL, Stanford University, Stanford, CA 94305, USA

# \*Corresponding author:

Name:

L.D. Yu

Postal address:

Fast Neutron Research Facility, Department of Physics, Faculty

of Science, Chiang Mai University, Chiang Mai 50200, Thailand

Telephone:

+66 53 943379

Fax:

+66 53 222776

E-mail:

yuld@fnrf.science.cmu.ac.th

Abstract

A specialized bioengineering ion beam line has recently been completed at

Chiang Mai University to meet rapidly growing needs of research and application

development in low-energy ion beam biotechnology. This beam line possesses special

features: vertical main beam line, low-energy (30 keV) ion beams, double swerve of the

beam, a fast pumped target chamber, and an in-situ atomic force microscope (AFM)

system chamber. The whole beam line is situated in a bioclean environment, occupying

two stories. The quality of the ion beam has been studied. It has proved that this beam

line has significantly contributed to our research work on low-energy ion beam

biotechnology.

PACS code: 85.40.Ry, 87.50.Gi

Keywords: ion beam, bioengineering, ion beam bioengineering (or biotechnology), ion

beam line, atomic force microscope (AFM).

2

# 1. Introduction

Ion beam bioengineering (IBBE), or more exactly termed as low-energy ion beam bioengineering, is a fairly new subject, established and developed for only less than two decades. The IBBE technology was invented and proposed by Prof. Yu Zengliang, Chinese Academy of Sciences, China, in late 1980s' (e.g. [1,2]). The technology has been extensively developed in China, Japan (e.g. [3]) and USA (e.g. [4]) and recently drastically expanded to laboratories worldwide. The IBBE research program was initiated at Chiang Mai University (CMU), Thailand in late 1990s', and rapidly developed in late years [e.g. 5,6,7].

IBBE is such a technology that uses energetic ion beams (a few tens of keV being enough) to bombard biological organisms in vacuum to induce mutation breeding and gene transfer for increasing applications of biological living materials as well as to detect characteristics of localized biological organisms for basic life studies [8]. Living biological organisms are subjected to low pressure (about  $10^{-4} - 10^{-3}$  Pa) and ion beam irradiation for the treatment. In the bombardment, ions penetrate through the coats of the organisms and the cell envelopes and may finally interact with the cells to induce changes in physics, chemistry and biology. The interaction takes place in a nano-scale but effects may last generations and even for ever. Ion beam interaction with living biological organisms is so different from that with solid materials. The latter has been studied for many decades and thus related physics is clear and simpler compared with the former, which is considerable complex [9]. Therefore, IBBE, a highly interdisciplinary subject, which involves physics, biology, agriculture, chemistry, and medical science, is full of research interests.

In order to carry out IBBE experiments, an ion accelerator is necessary. Although an ordinary conventional ion implanter can be in principle useable, some special requirements should be addressed for more effective and professional treatments [8]. As mentioned above, the energy of the accelerator is not necessarily high since low-energy ion beam effects on biology have been discovered, thus the facility can be greatly cost-reduced. It is better to make the beam line vertical for convenient holding of biological samples in horizontal. The pumping ability should be high enough to prevent the living biosamples from long-time vacuum exposure caused death. The inner and external environments of the equipment should be maintained as clean and sterile as possible to prevent unexpected biological contamination. For studies of particular aspects of biological effects, accessory instruments may be associated with the beam line.

At the laboratory of Fast Neutron Research Facility (FNRF), CMU, we have developed two ion implanters for IBBE research and applications. One is a modified traditional ion implanter normally for industrial service, but the other is a specialized IBBE beam line which has recently been totally completed. This paper describes in detail the latter.

### 2. The Beam Line

The bioengineering ion beam line, as shown in Figure 1, is comprised of a Nielsen-type high-temperature ion source including a 30-kV extraction/acceleration unit and an Einzel focusing lens, a mass analyzing magnet, an NEC Faraday cup, a double-magnet beam steering system including a beam scanning magnet, a target chamber, a

beam profile monitor, and an in-situ atomic force microscope (AFM) system. The ion source (Danfysik model 910) is able to produce various ion species from gas, solid, metal and nonmetal source materials. The beam current can be up to hundreds of microampere. The source system contains an integrated extraction electrode and an Einzel-lens setup. Without an acceleration unit, ions can be extracted with the maximum voltage of 30 kV. The 90° mass-analyzing magnet is able to select any ion species in principle. The magnet is supported and fixed in vertical by a four-post steel framework capable of being adjusted (shifted) in position both horizontally and vertically. The beam line after the mass analyzing magnet is vertical in order to accommodate convenient horizontal holding of biosamples which are normally very difficult to hold in vertical because of their irregular and various shape and size. The Faraday cup and beam profile monitor are used to measure the beam current and density distribution along the beam line. The double-magnet beam steering system consisting of two beam sweeping magnets bends the ion beam twice in a small angle. The second magnet also acts as a beam sweeper. Neutral particles may not be a serious problem to ion beam modification of normal solid materials, but indeed a great disturbance to sensitive biosamples. Conventionally avoiding the neutral particles is simple, just using a small beam bending device, either electrostatic or magnetic. However, if only one magnet is used, although the neutral particles are avoided, the beam in our facility no longer vertically enters the target chambers, particularly the in-situ AFM chamber, which is designed to definitely require the beam to vertically enter. The target chamber is deliberately made small, about 20 cm in diameter and 20 cm in height for fast pumping to reduce the risk for biosamples staying in vacuum too long. In routine operations, the target chamber can be pumped from the atmosphere to the working pressure of an order of 10<sup>-3</sup> Pa within 10 minutes. Inside the chamber there is a horizontally moveable sample holder, controlled by a stepping motor, which holds a standard biological petri dish where the bio-sample is placed. Cooperation of the sample holder translation and beam scanning makes a bombarding area of 5 cm × 5 cm in maximum. An automatically controlled halogen-lamp heating system is installed to maintain the biosample temperature for experiments on living organisms. Below the target chamber is the beam profile monitor, a NEC product, where a bent needle rotates across the beam to measure the beam density distribution in two dimensions. After the beam monitor is the in-situ AFM system chamber for real-time surface observation of biosamples. Detailed descriptions on the AFM system are given elsewhere [10]. In brief, a commercial AFM setup is placed inside the chamber in a certain tilting angle to allow the well-collimated ion beam to bombard the sample without hitting any parts of the microscope and with a damping system to avoid external vibration disturbances. Both tilting angle and damping system were carefully designed in geometry and mechanics. There is a convenient control board to control the operational parameters of the ion source, gas inlet, mass analysis, and beam bending and scanning, the measurement of the beam current, and the manipulation of the target holder. The bioengineering ion beam line facility is entirely housed in an ion-beam-bioengineering compartment inside the ion beam building of FNRF. The compartment is composed of three bio-clean rooms occupying two floors. The main room, on the 2<sup>nd</sup> floor, housing the 30-kV massanalyzed vertical ion implanter, is for control and operation of the machine. The second one situated on the 1st floor houses the beam line parts such as the target chamber and the AFM chamber, biological sample preparation and testing equipment, such as the bio-hazard laminar flow, CO2 incubator, and air cleaner. The third room next to the first room on the 2<sup>nd</sup> floor is used for bio-sample analysis and equipped with scientific apparatus such as pH meter, autoclave set, laboratory centrifuge, light microscope, inverted light microscope and magnetic stirrer, as well as computers.

# 3. Results

The beam emittance of the beam line was measured using relevant theory and method [11] to study the beam optics and quality. The emittance of the ion source could be determined from the measured emittance using beam transportation matrix theory [11,12] (Figure 2), and then the best beam position, or the target position, to be applied was determined by beam optics designing from the data of the ion source (Figure 3).

At the target position, the beam intensity distribution was investigated for precise control of beam bombardment of biological samples. If the beam current density of the beam spot at the target is assumed to be a Gaussian distribution in two dimensions as shown in Figure 4a, the beam current line density in one dimension, e.g. y, is then

$$I(y) = 2 \int_{0}^{r} i_{0} \exp(\frac{-x^{2}}{2\Omega^{2}}) \exp[\frac{-y^{2}}{(r^{2} - x^{2})} \times (\ln 20 - \frac{x^{2}}{2\Omega^{2}})] dx,$$
 (1)

where  $i_0$  is the maximum current density at the beam spot center, r is the beam spot radius, and  $\Omega$  is the standard deviation of the Gaussian distribution of the beam current density. In our calculation, the Gaussian boundary beam current density is assumed to be 1/20 of that at the center. It is supposed to have a rectangular beam sweeping area  $a \times r$ , where a is the length of the long leg, with x as the long-leg

coordinate and y as the short-leg coordinate. The ion dose rate, the dose falling into an element area  $\Delta x \times \Delta y$ , at the position (x, y) of the swept area is then

Dose rate 
$$(x, y) = \frac{2i_0 \int_0^r \exp(\frac{-x'^2}{2\Omega^2}) \exp[\frac{-y^2}{(r^2 - x'^2)} \cdot (\ln 20 - \frac{x'^2}{2\Omega^2})] dx' \cdot \Delta x}{e}$$

$$\times \frac{1}{\left[\frac{(d^{2} + x^{2})^{1/2}}{\cos(\tan^{-1}\frac{x}{d})}\right] \cdot 4\gamma \tan^{-1}\frac{a}{d}},$$
 (2)

where d is the distance between the beam scanner and the center of the beam swept rectangular area, and  $\gamma$  is the frequency of the beam sweeping. Using formula (2) we calculated the bean intensity distribution in a restricted scanning area 27 mm  $\times$  6 mm as shown in Figure 4b. Measured beam band in the beam swept area at the target position was compared with the calculated result and good agreement was obtained (Figure 4c). It has been found that if the beam density distribution is approximately in a Gaussian type with a moderate standard deviation, the ion dose distribution at a restricted target area can be considered nearly uniform. This has allowed us to set up appropriate parameters to control the corporation between the beam sweeping and the target holder translation for homogeneous ion bombardment.

Ion beam bioengineering or biotechnology research and application experiments have actively been carried out with the bioengineering ion beam facilities at FNRF, CMU. Plentiful results have been obtained in mutation, gene transfer and observation of

ion-bombarded cell envelopes, as previously reported (e.g. [9,13,14]). Figure 5 shows a recent result of *in-situ-AFM*-observed micro/nano-crater formation on plant cell envelopes induced by ion bombardment, confirming our previously reported results obtained by using conventional methods.

# 4. Summary

The specialized ion beam line for bioengineering research and application has been completed at Chiang Mai University. The beam line is featured with low energy, vertical applied beam line, versatile ion source, double beam-bending, *in-situ* AFM, fast pumping, accurate beam control and bioclean environment. Experimental results achieved have proved the beam line successful.

# Acknowledgement

This work was supported by The Thailand Research Fund.

# References

[1] Yu Zengliang, Qiu Lijian, Huo Yuping, J. of Anhui Agricultural College (in Chinese), 18-4(1991) 251-257.

[2] Yu Zengliang, Deng Jianguo, He Jianjun and Huo Yuping, *Nucl. Instr. and Meth.* B59/60(1991)705-708.

- [3] R. Tanaka, Proc. 5th Japan-China Joint Symp. on Accel. for Nucl. Sci. and Their Appl., Osaka, Japan (1993) 201.
- [4] Tom K. Hei, Chang Q. Piao, James C. Willey, Sutter Thomas and Eric J. Hall, Carcinogenesis 15(1994)431-437.
- [5] T. Vilaithong, L.D. Yu, C. Alisi, B. Phanchaisri, P. Apavatjrut, S. Anuntalabhochai.
  A Study of Low-Energy Ion Beam Effects on Outer Plant Cell Structure for Exogenous Macromolecule Transferring. Surface and Coatings Technology, 128-129(2000)133-138.
- [6] S. Anuntalabhochai, R. Chandej, B. Phanchaisri, L.D. Yu, T. Vilaithong, I.G. Brown. Ion-Beam-Induced Deoxyribose Nucleic Acid Transfer. *Applied Physics Letters*, Vol.78, No.16(April 16, 2001)2393-2395.
- [7] L.D. Yu, T. Vilaithong, B. Phanchaisri, P. Apavatjrut, S. Anuntalabhochai, P. Evans, I.G. Brown. Ion Penetration Depth in Plant Cell Wall. *Nuclear Instruments and Methods*, B206(2003)586-590.
- [8] L.D. Yu, T. Vilaithong, I.G. Brown (English translators and editors). *Introduction to Ion Beam Biotechnology*, English edition, originally authored by Yu Zengliang in Chinese. Springer Science & Business Media, New York, 2006.

- [9] L.D. Yu, S. Sangyuenyongpipat, S. Annuntalabhochai, B. Phanchaisri, T. Vilaithong and I.G. Brown. Effects of Low-energy Ion Beam Bombardment on Biological Cell Envelopes, accepted and to be published in *Surface and Coatings Technology* (2006).
- [10] S. Sangyuenyongpipat, L.D. Yu, T. Vilaithong, I.G. Brown. *In-situ* Atomic Force Microscopy for Microcrater-like Structure Observation of Plant Cell Envelope, presented and submitted to the same conference, i.e. The 15<sup>th</sup> International Conference on Ion Beam Modification of Materials (IBMM 2006), Taormina, Sicily, Italy, September 18-22, 2006.
- [11] H. Wiedemann. Particle Accelerator Physics, Springer-Verlag, Berlin, 1993.
- [12] N. Tondee, High Precision 30-kV Vertical Ion Implantation System, Thesis of Master of Science, Graduate School, Chiang Mai University, 2002.
- [13] S. Anuntalabhochai, R. Chandej, B. Phanchaisri, L.D. Yu, S. Promthep, S. Jamjod, and T. Vilaithong. Mutation Induction in Thai Purple Rice by Low Energy Ion Beam. Proceedings of the 9<sup>th</sup> Asia Pacific Physics Conference, Hanoi, Vietnam, October 25-31, 2004, Session 10: Applied Physics, 10-24C.
- [14] T. Vilaithong, L.D. Yu, P. Apavatjrut, B. Phanchaisri, S. Sangyuenyongpipat, S. Anuntalabhochai, I.G. Brown. Heavy Ion Induced DNA Transfer in Biological Cells. *Radiation Physics and Chemistry*, 71/3-4 (2004) pp. 927-935.

# **Figure Captions**

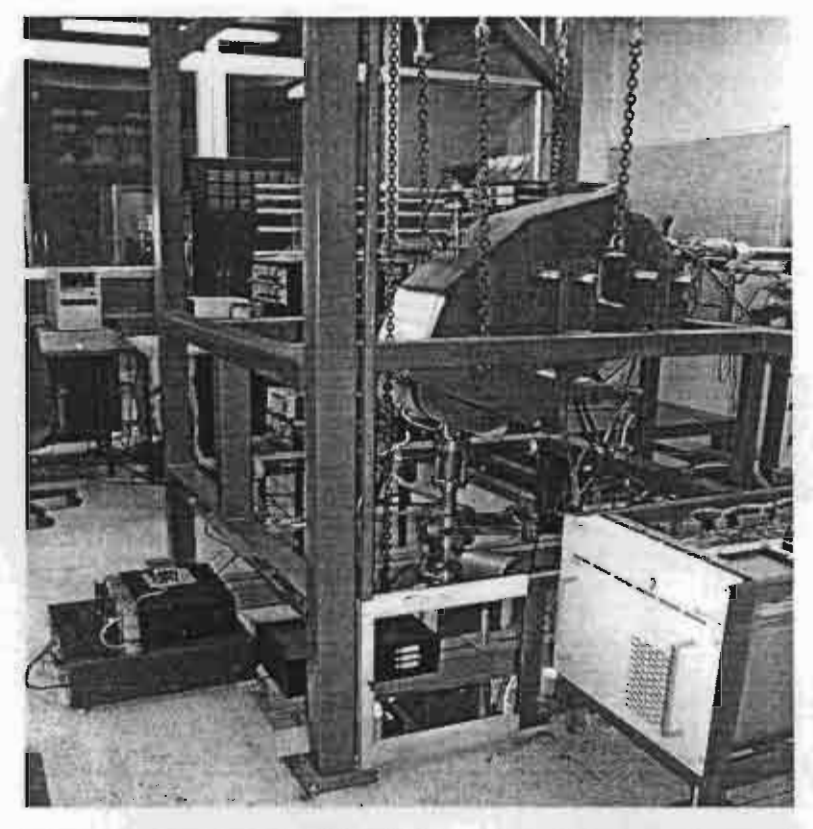
Figure 1. The bioengineering-specialized ion beam line system at Chiang Mai University. (a) Photographs of the beam line. Upper: the part upstairs. Lower: the part downstairs. (b) Schematic diagram (side view) of the entire beam line. Note that in the schematic diagrams the orientation of two magnets of the double beam steering system is drawn in 90° from the real one in order to show the beam transportation path.

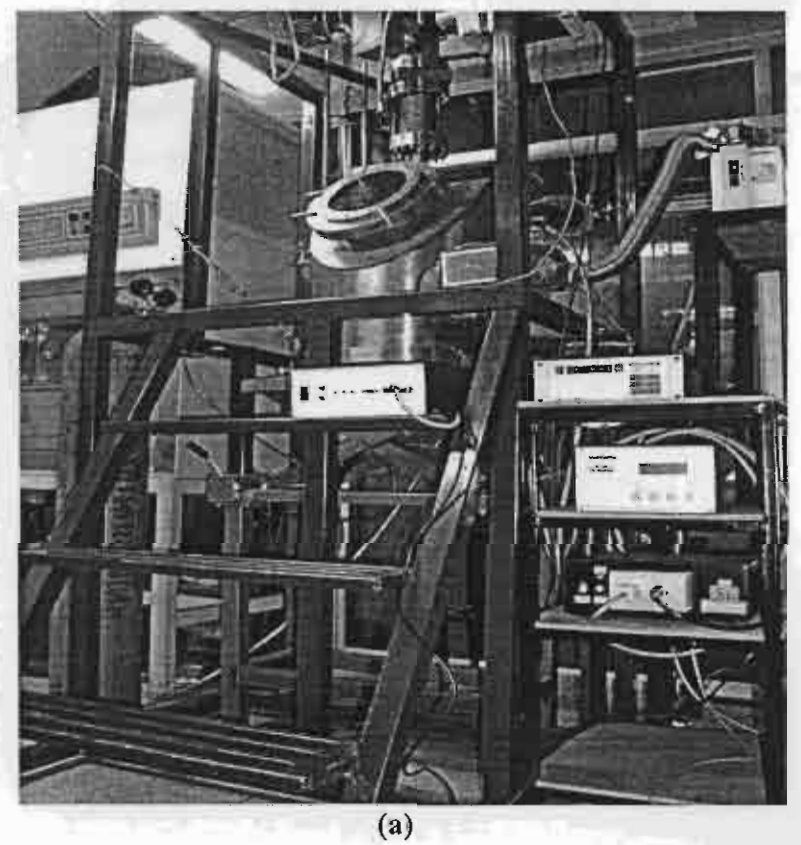
**Figure 2.** Beam emittance study. The positions marked are: P0 at the extraction, P1 at the entrance of the Einzel lens, P2 at the exit of the Einzel lens, and P3 at the measurement position, 20 cm from P2. The beam conditions for the measurement are 15-keV Ar ions with 11.75-kV focusing.

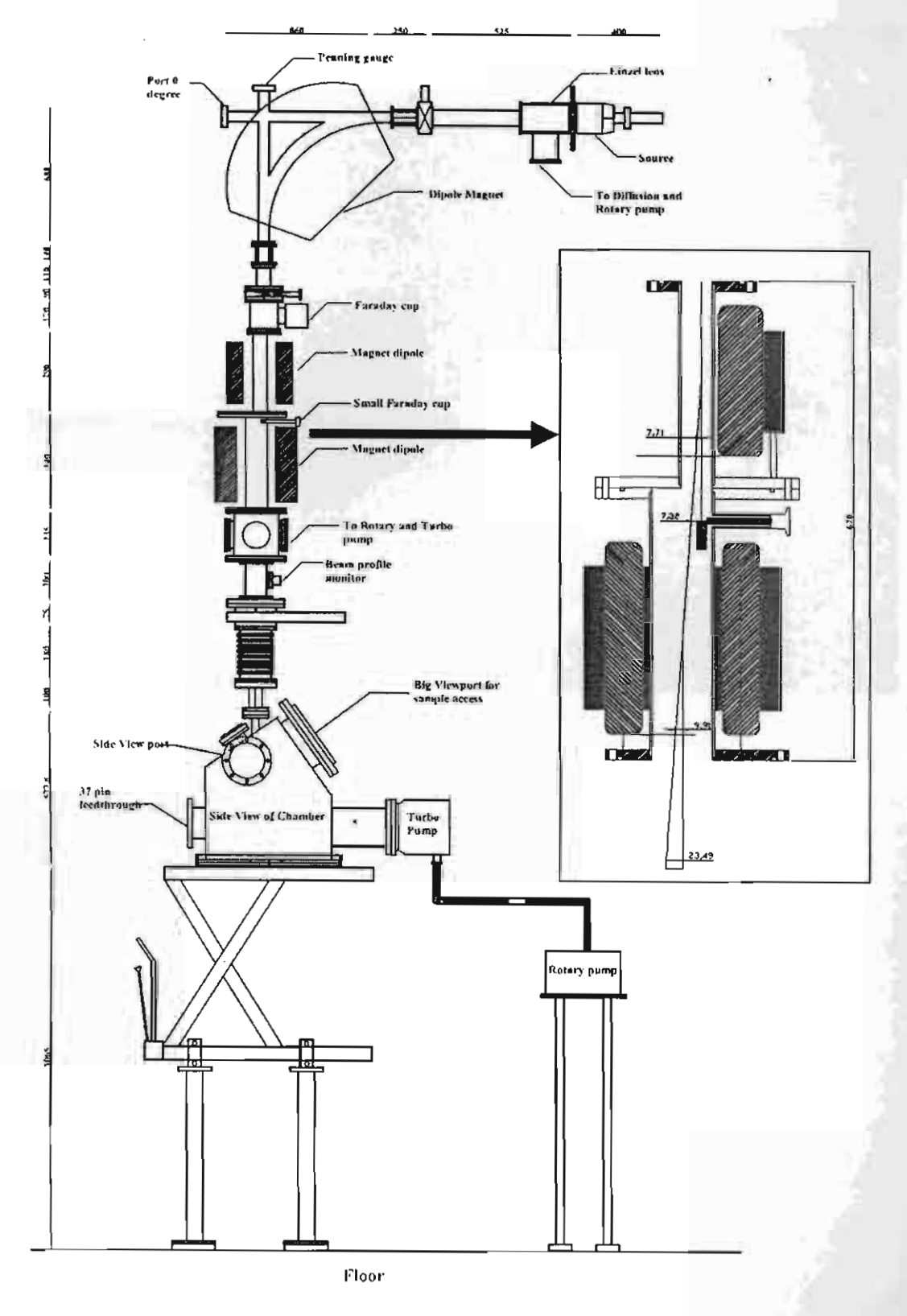
**Figure 3.** Beam envelope calculated using program Nectrace 2.2. The calculation conditions for this drawing are 15-keV Ar ions with 10-kV focusing. The best applicable beam position is found to be one meter from the exit of the mass analyzing magnet.

Figure 4. Study of the beam intensity distribution at the target. (a) Schematic of a two-dimensional Gaussian distribution of the beam current density of a beam spot. (b) Calculated result of a beam sweeping on a target area, assuming a Gaussian beam spot such as shown in (a). (c) Measured result.

**Figure 5.** The *in-situ-AFM*-observed onion cell envelopes. (a) Vacuum control. (b) 25-keV Ar-ion-bombarded cell surface, where micro/nano-craters are seen.







(b) Figure 1

Lifted chamber

Commercial AFM

Superlene tilting seat

Vibration isolation system stack

Chamber bottom

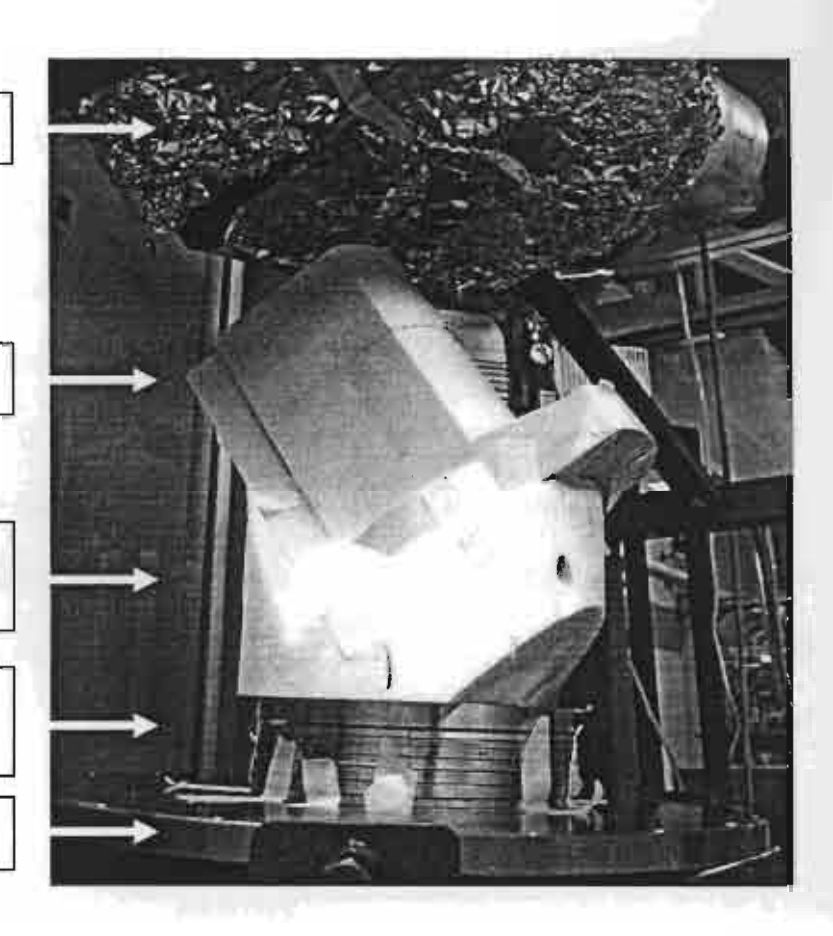


Figure 2

# In-Situ Atomic Force Microscopy for Microcrater-Like Structure Observation of Plant Cells

S. Sangyuenyongpipat<sup>a,b\*</sup>, C. Seprom<sup>a</sup>, L.D. Yu<sup>a</sup>, T. Vilaithong<sup>a</sup>, and I.G. Brown<sup>c</sup>

<sup>a</sup> Fast Neutron Research Facility, Department of Physics, Faculty of Science,

Chiang Mai University, Chiang Mai 50200, Thailand

<sup>b</sup> Department of Physics, P.O. Box 35 (FL), FIN-40014, University of Jyväskylä, Finland

<sup>c</sup> Lawrence Berkeley National Laboratory, Berkeley, California 94720, USA

\*Corresponding author: Postal address: Department of Physics, PO Box 35 (YFL), FIN-

40014, University of Jyväskylä, Finland. Fax: +358 14 260 2315. Tel.: +358 40 852 8302.

Email: nok265@hotmail.com

### Abstract

lon beam bioengineering is set up at Chiang Mai University (CMU). A specialized vertical beam line for bioengineering purpose has been installed. Recently, ion beams have induced direct transfer of plasmid DNA molecules into bacterial cells (*E. coli*). However, the understanding of fundamental mechanisms involved in ion interaction with biological organisms has not yet well developed. Onion skin cells are bombarded with Ar<sup>+</sup> ion, energy of 25 keV and fluence of 1-2 × 10<sup>15</sup> ions/cm<sup>2</sup>. The results reveal evidence of microcrater-like structure formed on the onion cell surface due to ion bombardment, under certain conditions. An *in-situ* atomic force microscopy (AFM) system has been designed and installed into the bioengineering ion beam line and relevant experiments are ongoing. The formation of microcrater-like structures maybe the pathway for transferring of exogenous macromolecules into biological cells if the ion penetration depth is approximately equal to the thickness of the biological cell envelope.

PACS: 61.82Pv, 61.80Jh, 82.37Gk, 87.50Gi,

Keywords: Ion bombardment, Microcrater, AFM, Plant cell envelope, Gene transfer, Onion

skin

1. Introduction

The mechanisms involved in ion beam induced DNA transfer into bacterial cells and plant

cells are not yet understood [1,2]. One important set of observations of the ion beam

bombardment process is the formation of micro-craters on the plant cell surface [3,4]. These

micro-craters could perhaps provide the explanation for DNA transfer into the cells. Real time

observations using AFM clarify when and how ion induced micro-craters formation. An in-situ

AFM has been designed, constructed and installed at CMU [5].

2. The 30-kV bioengineering ion beam facility

The ion beam facility at CMU is a designed facility specifically for bombardment of

living material [6]. Gaseous ion species including N and Ar with energy 20-30 keV have been

investigated at CMU [2,7,8]. This is a simple ion implanter consisting of a Danfysik 910 ion

source, a 30-kV extracting, a 90° mass-analysis magnet and the in-situ AFM chamber as

shown in Figure 1. The configuration of the commercial AFM with our vibration isolation

system (VIS) in the chamber, including collimator with Faraday cup and shutter, is shown in

Figure 2.

2

### 3. Experiments

The effect of ion bombardment on onion cell envelope can be observed using *in-situ* AFM. Examples of the kind of microcrater like structures formed are shown in Figure 3 and Figure 4. Importantly, note that the AFM observations indicate that micro-craters are not the result of vacuum alone (the formation of microcraters require ion bombardment). AFM images of typical microcrater structures formed on the onion skin cell wall surface are observed after ion beam bombardment. In this case, the ion species was Ar with energy 25 keV and fluence various from  $1-2\times10^{15}$  ions/cm<sup>2</sup>.

### 4. Results and Discussion

From Figure 3, it can be seen that the onion skin cell wall in vacuum, Figure 3b, is more dehydrated than in atmosphere, Figure 3a, because its surface structure is dominated by "grooves". The observations of onion skin cell wall after bombardment by Ar ion with fluence  $2x10^{15}$  ions/cm<sup>2</sup>, Figure 3d, shows more dense microcrater-like structure formation than for fluence1x10<sup>15</sup> ions/cm<sup>2</sup>, Figure 3c. The diameter of the microcrater rim lies in the broad range from several hundred nm to 1  $\mu$ m and the depth of craters is 100-150 nm.

Figure 4 shows the microcraters observed by the *in-situ* AFM in a very-near-in-situ condition, at which after ion bombardment of the onion skin sample, the chamber pressure was slightly increased to 10<sup>-3</sup> Torr for a good AFM imaging. From the figure, it is clearly seen the formation of microcraters, which are in sizes of 100-200 nm in diameter. With this fact, it can almost be concluded that microcraters are formed by ion bombardment only.

### 5. Conclusion

The results have shown clear evidence of microcraters formed on onion skin cells bombarded by 25 keV Ar ion with fluence 1-2x10<sup>15</sup> ions/cm<sup>2</sup>.

### Acknowledgements

I wish to thank the Royal Golden Jubilee program for a fellowship grant and this work was supported by the Thailand Research Fund. I am also very grateful to Prof. Dr. Harry J. Whitlow for travel support from the Academy of Finland Centre of Excellence in Nuclear and Accelerator Based Physics (Ref. 213503).

### References

- T. Vilaithong, L.D. Yu, C. Alisi, B. Phanchaisri, P. Apavatirut and S. Anuntalabhochai,
   Surf. Coat. Technol. 133 (2000) 128.
- [2] S. Anuntalabhochai, R. Chandej, B. Phanchaisri, L.D. Yu, T. Vilaithong and I.G. Brown, Appl. Phys. Lett. 78 (2001) 2393.
- [3] S. Sangyuenyongpipat, T. Vilaithong, L.D. Yu, A. Verdaguer, I. Ratera, D.F. Ogletree, O.R. Monteiro and I.G. Brown, Nucl. Instru. and Meth. B 227 (2005) 289.
- [4] S. Sangyuenyongpipat, L.D. Yu, T. Vilaithong, and I.G. Brown, Nucl. Instru. and Meth. B 242 (2006) 8
- [5] S. Sangyuenyongpipat, T. Vilaithong, L.D. Yu, R. Yimnirun, P. Singjai and I.G. Brown, Solid State Phenomena. 107 (2005) 47.
- [6] S. Sangyuenyongpipat, L.D. Yu, N. Tondee, K. Wattanavatee, T. Vilaithong, C. Thongleurm, B. Phanchaisri, S. Anuntalabhochai and I.G. Brown, presented to the 29<sup>th</sup> International Conference on Plasma Science, Banff, Alberta, Canada, May 26-30, 2002; IEEE Conference Record Abstracts, Cat. No. 02CH37340, p. 310.
- [7] L.D. Yu, B. Phanchaisri, P. Apavatjrut, S. Anuntalabhochai, T. Vilaithong and I.G. Brown, Surf. Coat. Technol. 158/159 (2002) 146.

[8] L.D. Yu, T. Vilaithong, B. Phanchaisri, P. Apavatjrut, S. Anuntalabhochai, P. Evans and I.G. Brown, Nucl. Instrum. Meth. Phys. Res. B. 206 (2003) 586.

### **Figure Captions**

**Figure 1.** Schematic diagram (sideview) of the bioengineering ion beam line at CMU. Note that in the schematic diagrams the orientation of two magnets of the double beam steering system is drawn in 90° from the real one in order to show the beam transportation path.

Figure 2. Configuration of in-situ AFM chamber for 2D (left) and 3D (right).

Figure 3. AFM micrographs of onion skin cell wall (a) in atmosphere (b) in vacuum (c) after bombarded by  $Ar^+$ , fluence  $1x10^{15}$  ions/cm<sup>2</sup> (d) after bombarded by  $Ar^+$ , fluence  $2x10^{15}$  ions/cm<sup>2</sup>. The scanned area is 5 x 5  $\mu$ m<sup>2</sup>.

Figure 4. AFM micrographs of onion skin cell wall bombarded by  $Ar^+$ , fluence  $2x10^{15}$  ions/cm<sup>2</sup> in vacuum with pressure  $1x10^{-3}$  Torr. The scanned area is  $7.5 \times 7.5 \mu m^2$ .

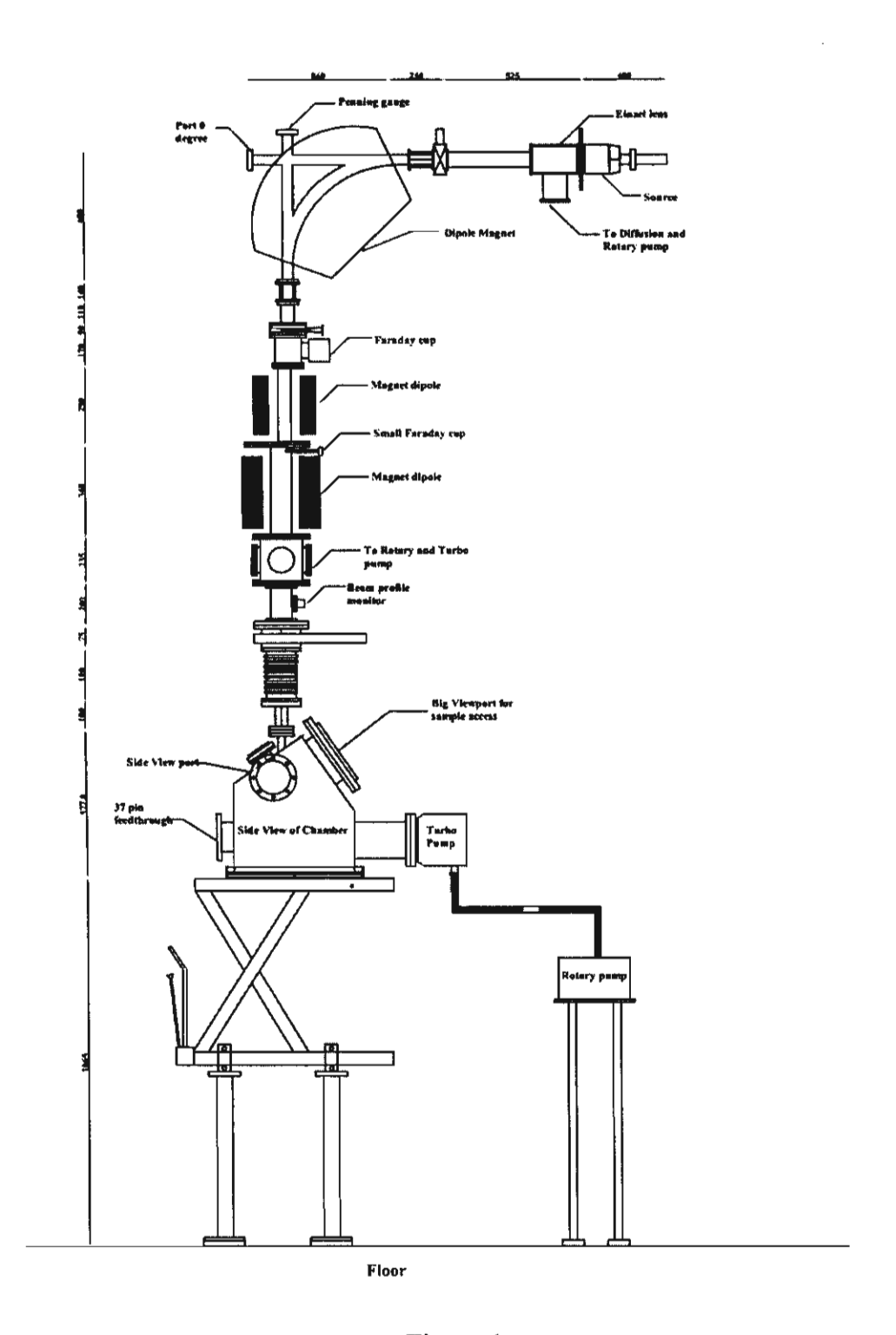


Figure 1

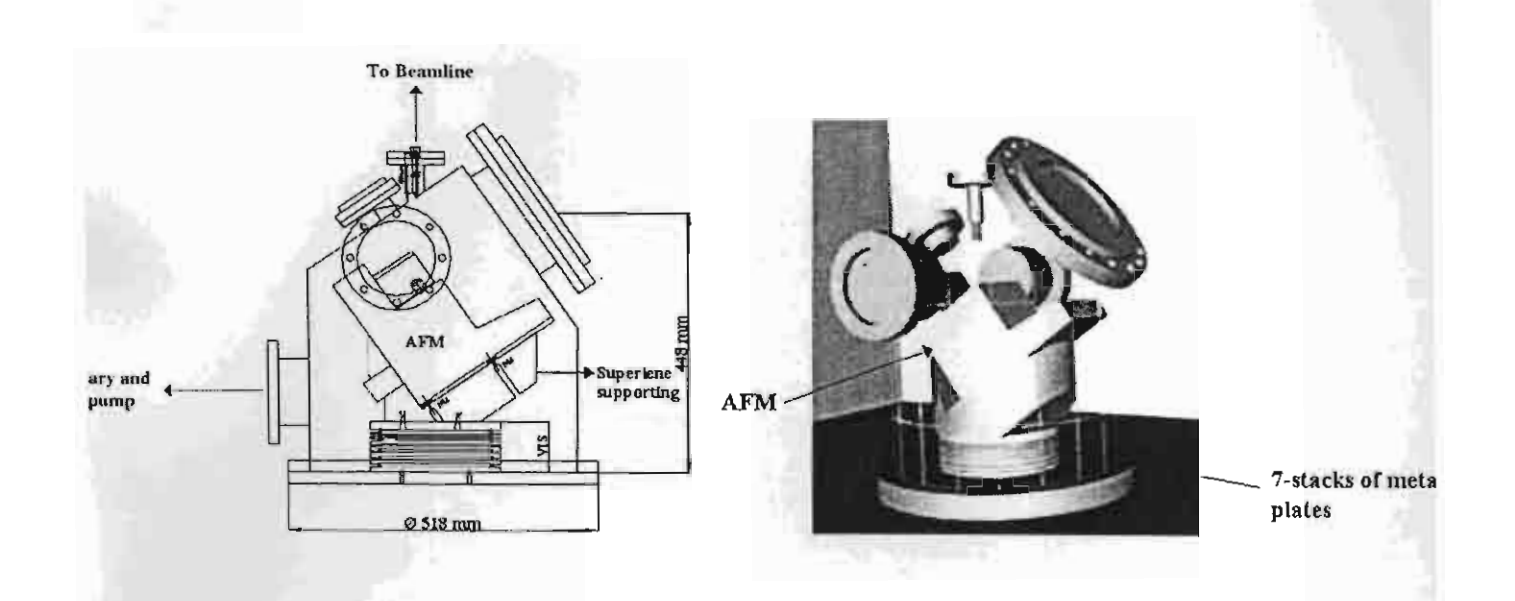


Figure 2

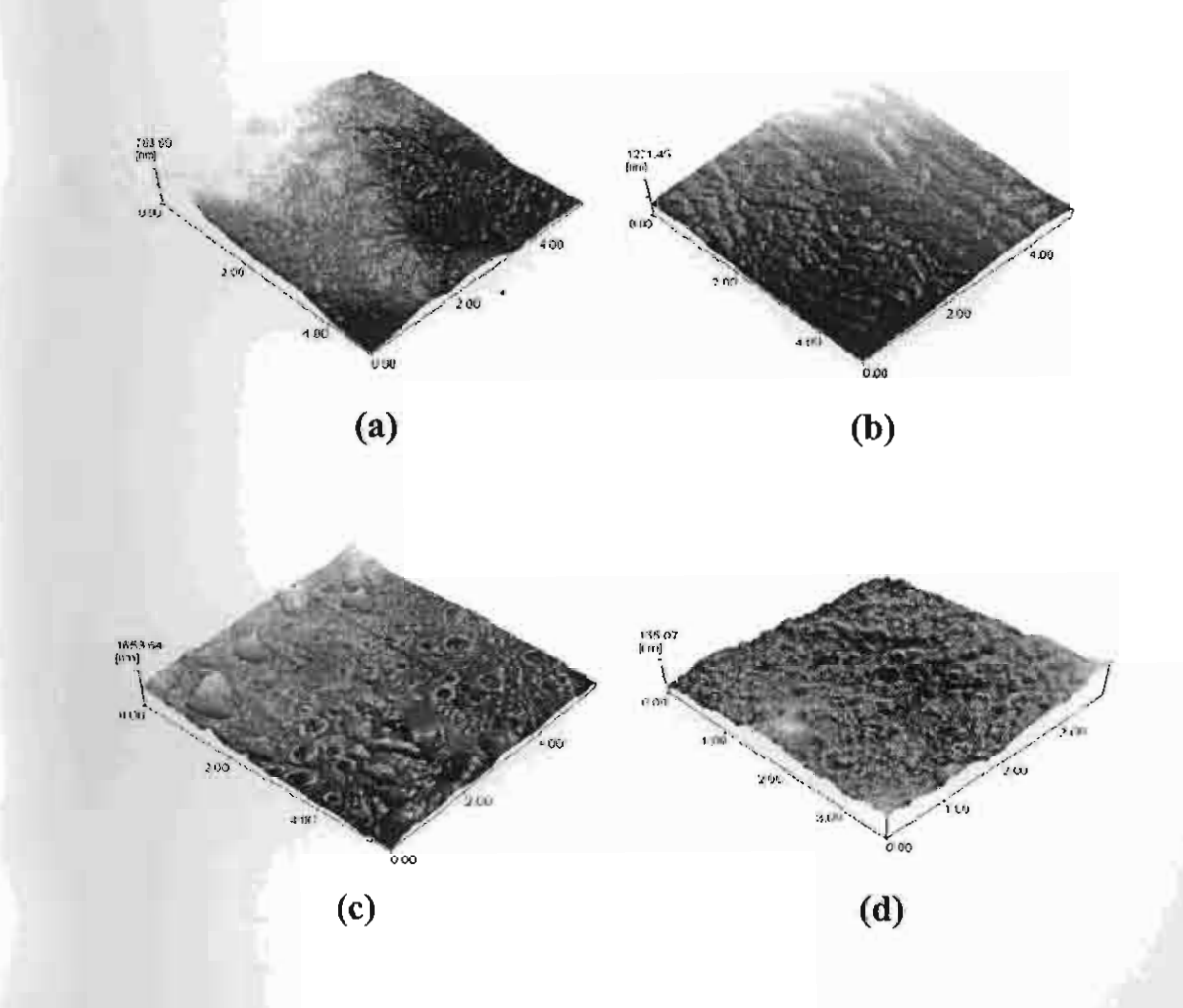


Figure 3

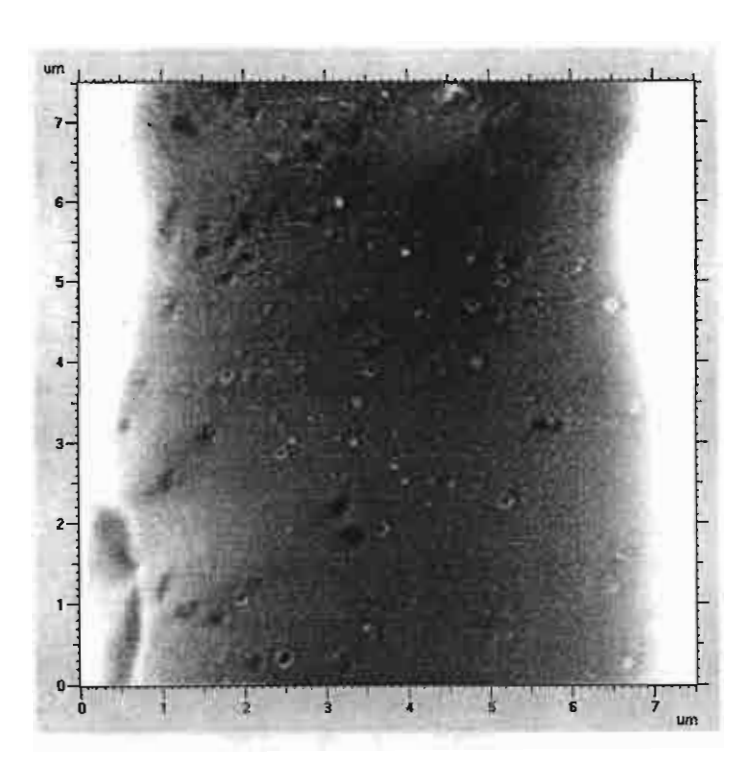


Figure 4



# สภาวิจุยแห่ยชาติ

ศาสตราจารย์ฉิรพัฒน์ วิฉัยทอง รองศาสตราจารย์สมบูรณ์ อนันคลาโภชัย ผู้ช่วยศาสตราจารย์พิมพ์ใจ อาภาวัชรูคมั่ มอบประกาศันยบทานี้ เพื่อประกาศเกียรผิดณ

อาจารย์เหลียงเคิง ยู นายบุญรักษ์ พันธ์ใชยศรี และ อาจารย์รัฐพร จันทร์เคช นิจานะฟิลักร์บรารบรักษาสามาลัย

รางาัก คิเยียม

र्वतक्ष्त्रंत्ये 2547

พุทธศึกราช 2548 เรื่อง "การตำผหากคืเอ็นเอเช้าผู้เชลล์แบคทีเรียโดยการจักนำด้วยถ่าไอออน"

सिर्वा न्या ३ क्या मध्य

(unavoughed fulled) Investment fulled fulled for the season of the seaso

Dat beinein

(คร.ประชัย เปียนสหบูรณ์) ประชานศึกาวิจัยแห่งชาติ



Poster presentation at SMMIB05, Kusadasi, Turkey.

Investigation of Mutation in Purple Glutinous Rice by Low Energy Ion Beam

- S. Promthep (a), T. Vilaithong (b), L.D. Yu (b), S. Jamjod (c), and S. Anuntalabhochai (a)
- (a) Department of Biology, Faculty of Science, Chiang Mai University, Chiang Mai 50200, Thailand
- (b) Fast Neutron Research Facility, Department of Physics, Faculty of Science, Chiang Mai University, Chiang Mai 50200, Thailand
- (c) Department of Agronomy, Faculty of Agriculture, Chiang Mai University, Chiang Mai 50200, Thailand

Application of low energy ion beam bombardment for induction mutation in purple glutinous rice were investigated. About 4800 seeds were bombarded by low energy nitrogen ion beam at energies and fluences in ranges 60-125 keV and 1-8 x 10<sup>16</sup> ions/cm<sup>2</sup> respectively. With increasing of the fluences reduced survival ability in the rice seeding. Two mutants with green leaf and stem sheath were detected at 80 keV and 4x10<sup>16</sup> ions/cm<sup>2</sup>. Twenty seeds of M<sub>2</sub> plants were cultivated and HAT-RAPD was chosen to determine genetic modification at DNA level. Three primers, named OPH15, OPX13, and OPW06, revealed genetic variation between M<sub>2</sub> mutant and wild type. All 20 M<sub>2</sub> plants exhibited different characteristic as following: stable green leaf blade and stem sheath, green leaf and purple stem sheaths, purple leaf and stem sheaths, white seed coats, and amylase content in starch granules of some mutant seeds.